



Swansea University
Prifysgol Abertawe



Swansea University E-Theses

Next generation polyurethanes for enhanced durability pre-finished architectural steel products.

Wray, Jenet

How to cite:

Wray, Jenet (2008) *Next generation polyurethanes for enhanced durability pre-finished architectural steel products..* thesis, Swansea University.

<http://cronfa.swan.ac.uk/Record/cronfa42649>

Use policy:

This item is brought to you by Swansea University. Any person downloading material is agreeing to abide by the terms of the repository licence: copies of full text items may be used or reproduced in any format or medium, without prior permission for personal research or study, educational or non-commercial purposes only. The copyright for any work remains with the original author unless otherwise specified. The full-text must not be sold in any format or medium without the formal permission of the copyright holder. Permission for multiple reproductions should be obtained from the original author.

Authors are personally responsible for adhering to copyright and publisher restrictions when uploading content to the repository.

Please link to the metadata record in the Swansea University repository, Cronfa (link given in the citation reference above.)

<http://www.swansea.ac.uk/library/researchsupport/ris-support/>

677

Next Generation Polyurethanes for Enhanced Durability Pre-Finished Architectural Steel Products

Jenet Wray

Thesis Submitted for the Degree of Engineering Doctorate

EPSRC Engineering Doctorate Centre for Steel Technology

University of Wales Swansea

Department of Materials Engineering

ProQuest Number: 10805425

All rights reserved

INFORMATION TO ALL USERS

The quality of this reproduction is dependent upon the quality of the copy submitted.

In the unlikely event that the author did not send a complete manuscript and there are missing pages, these will be noted. Also, if material had to be removed, a note will indicate the deletion.



ProQuest 10805425

Published by ProQuest LLC (2018). Copyright of the Dissertation is held by the Author.

All rights reserved.

This work is protected against unauthorized copying under Title 17, United States Code
Microform Edition © ProQuest LLC.

ProQuest LLC.
789 East Eisenhower Parkway
P.O. Box 1346
Ann Arbor, MI 48106 – 1346

Summary

This research has focussed on the photo-oxidation of polyurethane coatings with aim to identify formulations with enhanced durability. The stability of a coating against the effects of environmental ultraviolet (UV) light poses a challenge to coating manufacturers particularly since almost all coatings contain titanium dioxide (TiO_2) as a pigment. It is widely acknowledged that TiO_2 can become photoactivated by incident UV light, causing initiation of free radicals which under go reactions with the polymeric matrix and result in degradation of the coating.

Previous research has identified a novel accelerated weathering test that allows quantification of coating photo-oxidation by measurement of evolved carbon dioxide (CO_2) gas using a Fourier Transform Infrared (FTIR) spectrometer. The FTIR flat panel irradiation apparatus was used in conjunction with QUV A and xenon arc weathering in order to assess the durability of polyurethane coatings.

Out of a range of TiO_2 pigments Tronox R-KB-4 was the most stable for production of polyurethane coatings. It was found that alterations to the coating formulation, namely replacement of the standard durability polyester with one expected to improve UV durability did not provide the improvements anticipated. The polyurethane formulation containing a polyisocyanate cross-linker based on a combination of hexamethylene diisocyanate (HDI) and isophorone diisocyanate (IPDI) showed the best durability and most promise for improvement of commercial coatings.

The effects of additives commonly used in commercial polyurethane coatings were investigated. It was found that although the addition of coloured pigments and texturing agents commonly affected coating durability, the majority of increase in coating degradation was due to the unstable nature of organic matting and texturing agents.

Finally it was shown that the dispersion of a TiO_2 pigment within polymeric matrix can significantly affect its durability. Coatings containing poorly dispersed TiO_2 pigments showed a significant reduction in durability compared to those containing an optimum dispersion of TiO_2 .

Acknowledgements

I would like to acknowledge the financial support from Bayer Material Science, Corus Colors and the EPSRC throughout this research program. Huge thanks go to my academic supervisor Professor Dave Worsley for his continued support, encouragement and guidance, and for the time he has spent thinking about and working on this project with me. I would like to thank Hefin Ap-Llwyd-Dafydd for his enthusiasm, advice and extraordinary attention to detail throughout the project. To Paul Jones, thank you for your support, ideas and for putting up with my irrational stresses.

I am very grateful to all the people at Bayer Material Science in Leverkusen who have been involved in this project. I would particularly like to thank Dr Beate Baumbach for her direction, technical knowledge and for arranging the generous financial support that has helped this project immeasurably. Thanks to Bernadette Gerhartz-Quirin for her hard work on this project and for looking after me so well during my visits to Germany. Thanks also to Michael Fullenbach who taught me the art of paint formulation and helped to make the hundreds of samples without which, this project could not have happened.

I would like to thank Peter Davies for his training and technical support on the SEM. I also owe him a big thank you for loaning me numerous nitrogen cylinders when mine had gone ‘walkabout’ at inconvenient times. Thanks to Beverly Williams for the plentiful chats and words of advice, and for looking after and organising us on the Eng D.

Most of all I would like to thank my family for their continued support especially during the hard times. Special thanks to my parents Julie and Phil who have always encouraged and supported me and my brothers in whatever we do and for working so hard to make sure we are happy. I don’t tell you often enough how grateful I am and how much I love you both. To James, thank you for your unending encouragement, support and love, it really does mean the world to me. Finally, I would like to thank my friends for the laughter and good times that have made the last four years so enjoyable.

Chapter 1	1
Literature Review	1
1.1 Introduction to Pre-Finished Steel	2
1.1.1 The Coil Coating Process.....	3
1.1.1.1 Galvanising	4
1.1.1.2 Pre Treatment.....	5
1.1.1.3 Primer.....	5
1.1.1.4 Topcoat.....	6
1.1.2 Failure and Degradation of Organic Coatings	7
1.2 Polyurethanes	8
1.2.1 Polyisocyanates	9
1.2.2 Polyester Polyols.....	13
1.2.3 Dibutyltin Dilaurate (DBTL)	13
1.2.4 Texturing Agents.....	14
1.2.5 Melamine Cross-Linking Systems	15
1.3 Introduction to Photochemistry.....	16
1.3.1 Excitation of Electrons.....	17
1.3.2 Energy Transfer.....	18
1.3.2.1 Radiative Energy Transfer	19
1.3.2.2 Non-Radiative Energy Transfer	19
1.3.2.3 Transfer in Polymer Matrices.....	20
1.4 Polymer Degradation	21
1.4.1 Degradation Mechanisms.....	21
1.4.1.1 Formation of Free Radicals.....	23
1.4.2 Photo-Oxidation Mechanisms.....	26
1.4.2.1 Initiation	26
1.4.2.2 Propagation	27
1.4.2.3 Termination.....	30
1.5 Titanium Dioxide	31
1.5.1 Manufacturing Process of TiO ₂	32
1.5.1.1 The Sulphate Process	33
1.5.1.2 The Chloride Process	33
1.5.1.3 Surface Treatments.....	34
1.5.1.4 Grinding and Finishing	36
1.5.2 Characteristics	37
1.5.3 Photoactivity of TiO ₂	40
1.5.4 Photocatalysis by TiO ₂	42
1.5.4.1 Further Influences of TiO ₂ on Coating Degradation.....	44
1.6 Weathering and Accelerated Testing	46
1.6.1 Natural Exposure.....	47
1.6.1.1 Adjusted Angle Open Back Rack	48
1.6.1.2 Adjusted Angle Standard Black Boxes.....	49
1.6.1.3 EMMA/EMMAQUA (Equatorial Mount with Mirrors for Acceleration).....	50
1.6.2 Artificial Exposure	51
1.6.2.1 Xenon Arc	51
1.6.2.2 QUV A/QUV B.....	52
1.6.3 Physical Measures of Degradation.....	53
1.6.3.1 Loss of Coating Weight and Film Thickness.....	53

1.6.3.2	Gloss Loss and Chalking.....	53
1.6.3.3	Colour Retention.....	55
1.6.3.4	Crazing and Cracking.....	55
1.6.4	Chemical Tests used to Quantify Degradation.....	55
1.6.4.1	Infrared and Fourier Transform Infrared Spectroscopy.....	56
1.6.4.2	Tube Photoactivity Test Reactor ⁵⁵	59
1.6.4.3	The Flat Panel Reactor ⁵⁶	60
1.7	Conclusions and Aims.....	61
1.8	References.....	62
Chapter 2.....	67	
Experimental Techniques.....	67	
2.1	Coated Sample Preparation.....	68
2.1.1	Polyurethane and Polyester-Melamine Coating Formulation.....	68
2.1.1.1	White Pigmented Polyurethane Coatings.....	68
2.1.1.2	White Pigmented Polyester-Melamine Coatings.....	71
2.1.1.3	Commercial Colour Pigmented Polyurethane Coatings.....	73
2.1.1.4	Textured Polyurethane Coatings.....	74
2.1.2	Production of Polyurethane/Polyester-Melamine Coated Samples.....	74
2.1.3	Model PVC Coating Formulation.....	75
2.1.3.1	White Pigmented PVC Coatings.....	75
2.1.3.2	Colour Pigmented PVC Coatings.....	76
2.1.4	Production of PVC Coated Samples.....	77
2.2	Accelerated Weathering Techniques.....	78
2.2.1	The Fourier Transform Infrared Spectrometer (FTIR) Spectrometer.....	78
2.2.2	The Automatic Data Collection Program (Evolgas).....	79
2.2.3	The Irradiation Apparatus.....	82
2.2.3.1	The IR Gas Cell.....	83
2.2.3.2	The Flat Panel Reactor Cell.....	84
2.2.3.3	Calibration of the FTIR Flat panel Reactor Apparatus.....	86
2.2.4	Commercial Accelerated Weathering Methods.....	87
2.2.4.1	QUV A.....	88
2.2.4.2	Xenon Arc.....	88
2.2.4.3	Gloss Measurement.....	88
2.2.4.4	Colour Measurement.....	89
2.3	References.....	89
Chapter 3.....	91	
The Effect of Titanium Dioxide Photoactivity Grade on Polyurethane and Polyester-Melamine Photo-Oxidation.....	91	
3.1	Introduction.....	92
3.1.1	Aims.....	93
3.2	Experimental Techniques.....	93
3.2.1	Titanium Dioxide Pigments.....	93
3.2.2	The First Series Polyurethane and Polyester-Melamine Coatings.....	94
3.2.2.1	Polyurethane and Polyester-Melamine Coating Preparation.....	94
3.2.2.2	Production of Polyurethane/Polyester-Melamine Coated Samples.....	94
3.2.3	Assessing Pigment Photoactivity in the Fourier Transform Infrared (FTIR) Flat Panel Irradiation Apparatus.....	94
3.2.4	Assessing Coating Durability in Commercial Weathering Tests.....	95
3.3	Results and Discussion.....	96
3.3.1	Evolution of Carbon Dioxide.....	96

3.3.2	Weathering Results for the HDI based Polyurethane Coatings Formulated with the Standard Polyester Resin	97
3.3.2.1	CO ₂ Evolution Rates	97
3.3.2.2	QUV A Gloss Retention.....	99
3.3.2.3	Xenon Arc Gloss Retention	101
3.3.2.4	Standard Durability HDI Based Polyurethane Rankings	102
3.3.3	Weathering Results for the Polyester-Melamine Coatings Formulated with the Standard Polyester Resin.....	104
3.3.3.1	CO ₂ Evolution Rates	104
3.3.3.2	QUV A Gloss Retention.....	106
3.3.3.3	Xenon Arc Gloss Retention	106
3.3.3.4	Standard Durability Polyester-Melamine Rankings.....	107
3.4	Conclusions.....	110
3.5	References	112
Chapter 4	114
The Effect of Changes to the Polymer Resin on Coating Durability.....	114
4.1	Introduction.....	115
4.1.1	Aims	115
4.2	Experimental Techniques.....	116
4.2.1	Titanium Dioxide Pigments	116
4.2.2	The Second and Third Series Polyurethane and Polyester-Melamine Coatings.....	116
4.2.2.1	Polyurethane/Polyester-Melamine Coating Preparation	118
4.2.2.2	Production of Polyurethane/Polyester-Melamine Coated Samples.....	118
4.2.3	Assessing Coating Durability in the Fourier Transform Infrared (FTIR) Flat Panel Irradiation Apparatus	118
4.2.4	Assessing Coating Durability in Commercial Weathering Tests.....	119
4.3	Results and Discussion.....	120
4.3.1	Weathering Results for the HDI Based Polyurethane Coatings Formulated with the Adapted Polyester Resin.....	120
4.3.1.1	CO ₂ Evolution Rates	120
4.3.1.2	QUV A Gloss Retention.....	122
4.3.1.3	Xenon Arc Gloss Retention	123
4.3.1.4	'Improved' Polyurethane Ranking.....	127
4.3.2	Weathering Results for the Polyester-Melamine Coatings Formulated with the Adapted Polyester Resin	129
4.3.2.1	CO ₂ Evolution Rates	129
4.3.2.2	QUV A Gloss Retention.....	130
4.3.2.3	Xenon Arc Gloss Retention	131
4.3.2.4	'Improved' Polyester-Melamine Ranking.....	133
4.3.3	Weathering Results for the IPDI Based Polyurethane Coatings.....	134
4.3.3.1	CO ₂ Evolution Rates	134
4.3.3.2	QUV A Gloss Retention.....	135
4.3.3.3	Xenon Arc Gloss Retention	136
4.3.3.4	IPDI Based Polyurethane Ranking.....	137
4.3.4	Weathering Results for the HDI/IPDI Based Polyurethane Coatings.....	138
4.3.4.1	CO ₂ Evolution Rates	138
4.3.4.2	QUV A Gloss Retention.....	140
4.3.4.3	Xenon Arc Gloss Retention	140
4.3.4.4	HDI/IPDI Based Polyurethane Ranking	142

4.4	Conclusions	143
4.5	References	145
Chapter 5.....		146
The Effect of Coloured Pigmentation on Coating Photo-Oxidation		146
5.1	Introduction	147
5.1.1	Aims	147
5.2	Experimental Techniques.....	147
5.2.1	Colour Pigmented Coatings	147
5.2.1.1	Model Colour Pigmented PVC Coating Preparation	148
5.2.1.2	Production of PVC Coated Samples	149
5.2.1.3	Colour Pigmented Polyurethane Coating Preparation	150
5.2.1.4	Production of Polyurethane Coated Samples	150
5.2.2	Assessing Coating Durability in the Fourier Transform Infrared (FTIR) Flat Panel Irradiation Apparatus	150
5.2.3	Assessing Coating Durability in Commercial Weathering Tests.....	151
5.3	Results and Discussion.....	151
5.3.1	CO ₂ Evolution Rate Results for the Colour Pigmented Coatings	151
5.3.1.1	Model PVC Coatings Pigmented with Single Secondary Organic Colour Additions.....	151
5.3.1.2	Model PVC Coatings Pigmented with Single Secondary Inorganic Colour Additions.....	154
5.3.1.3	Model PVC Coatings Pigmented with Multiple Inorganic Coloured Pigment Blends	157
5.3.1.4	Polyurethane Coatings Pigmented with Inorganic Coloured Pigment Blends.....	160
5.3.2	Commercial Weathering of Polyurethane Coatings Pigmented with Inorganic Coloured Pigment Blends	162
5.3.2.1	QUV A Gloss Retention.....	162
5.3.2.2	Xenon Arc Gloss Retention	163
5.3.2.3	Colour Pigmented Polyurethane Rankings	164
5.4	Conclusions	166
5.5	References	167
Chapter 6.....		168
The Effect of Texturing Agent Additions on the Durability of Polyurethane Coatings.....		168
6.1	Introduction	169
6.1.1	Aims	169
6.2	Experimental Techniques.....	170
6.2.1	Textured Polyurethane Coatings	170
6.2.1.1	Textured Polyurethane Coating Preparation	171
6.2.1.2	Production of Textured Polyurethane Coated Samples	171
6.2.2	Assessing Coating Durability in the Fourier Transform Infrared (FTIR) Flat Panel Irradiation Apparatus	171
6.3	Results and Discussion.....	172
6.3.1	CO ₂ Evolution Rate Results from Textured Polyurethane Coatings	172
6.4	Conclusions	173
6.5	References	174
Chapter 7.....		175
The Effect of Titanium Dioxide Pigment Dispersion on Polymer Photo-Oxidation		175

7.1	Introduction.....	176
7.1.1	Aims.....	176
7.2	Experimental Techniques.....	177
7.2.1	TiO ₂ Pigmented Model PVC Coatings	177
7.2.1.1	TiO ₂ Pigmented PVC Coating Preparation.....	177
7.2.1.2	Production of PVC Coated Samples	177
7.2.2	Assessing Pigment Photoactivity in the Fourier Transform Infrared (FTIR) Flat Panel Irradiation Apparatus.....	178
7.2.3	UV/Vis Spectroscopy.....	178
7.3	Results and Discussion.....	178
7.3.1	CO ₂ Evolution from Model PVC Coatings Pigmented with Different Commercial TiO ₂ Grades.....	178
7.3.2	CO ₂ Evolution from Model PVC Coatings Pigmented with Various Dispersions of Kronos 2220 and Tronox R-KB-4	180
7.3.3	Dispersion Analysis of Coated Samples (SEM)	184
7.4	Conclusions.....	191
7.5	References.....	192
	Chapter 8.....	194
	Conclusions and Future Work.....	194

Chapter 1

Literature Review

1.1 Introduction to Pre-Finished Steel

The pre-finished steel industry has seen an enormous growth in demand for construction products over recent years, particularly in fast developing countries such as China and Russia. Pre-finished steel products have gained popularity in an ever increasing range of applications, the largest being the construction and domestic appliances industries. The approximate market share of organic coated strip steel products is shown in Figure 1.1.

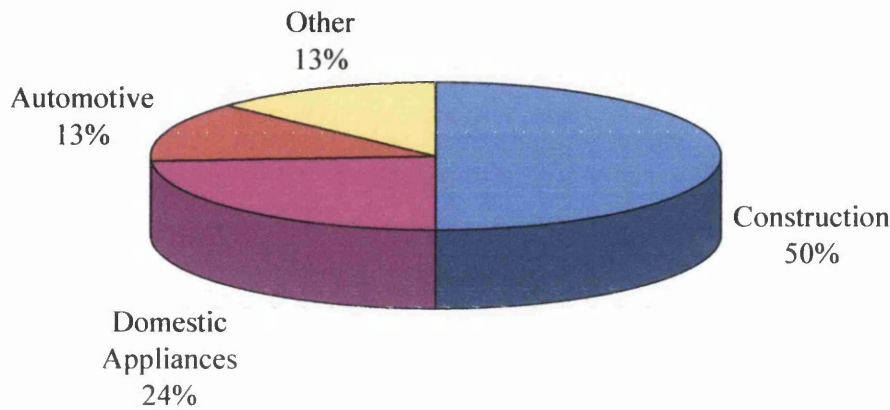


Figure 1.1 – Breakdown of End Use for Pre-Finished Steel Products

The primary purpose of coating application is to provide a barrier which isolates the steel substrate from aggressive corrosion agents that would rapidly cause oxidation. This is particularly important for construction and cladding industry as products are subjected to an exterior environment for their entire service life. These products are therefore continually subjected to corrosive environmental factors such as oxygen, water and more highly corrosive agents for example salt spray or pollutants when positioned in coastal or industrial locations.

The functionality of the coating in preventing corrosion and subsequent loss of structural integrity is significant however recently aesthetics have also become increasingly important. Due to the growth in use of pre-finished steel products in high-profile constructions such as those shown in Figure 1.2, the importance of the product remaining aesthetically pleasing and maintenance free for its service life is now greater than ever.

One major challenge with regard to both the aesthetic appearance of a coating and its integrity as a barrier to corrosion is the effect of environmental sunlight. Products intended for service in external environments will be exposed to ultraviolet

(UV) light for prolonged periods of time and therefore photo-oxidation is a very real possibility. Photo-oxidation can cause significant chemical and physical damage to the coating leading to impaired aesthetics and functionality as a corrosion barrier.

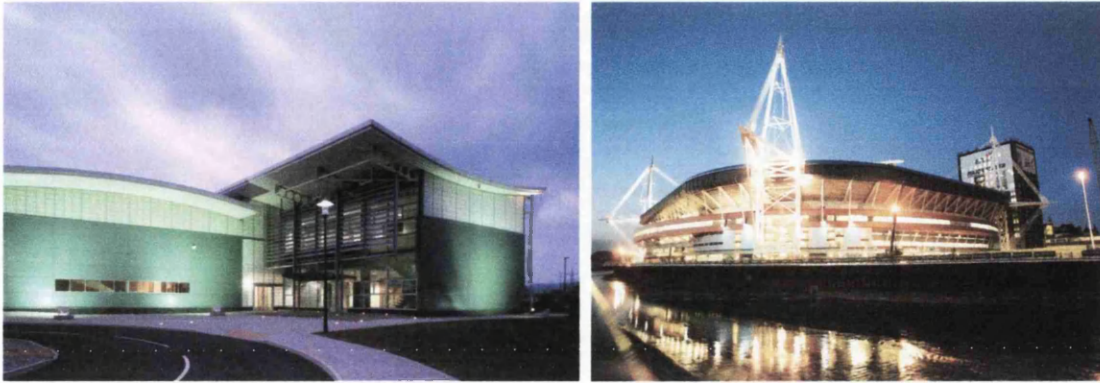


Figure 1.2 - Examples of the use of Pre-Finished Steel in Construction

The launch of Colorcoat HPS200[®] Ultra in April 2008 saw maintenance free-lifetime guarantees on pre-finished steel products extended to 40 years¹. Currently most coating guarantees range from 15-20 years² however continual research aims to increase the weathering resistance and provide longer guarantees for a maintenance free, aesthetically pleasing product. This has become increasingly challenging due to the variability of service environments. The development of these coatings now has to account for a wider range of factors.

1.1.1 The Coil Coating Process

The process used in the continuous coating of metal coils is often termed the reverse roll coating process due to the rotation of applicator rolls in a direction opposite to that of the strip³. The coil coating process allows the application of each coating layer of the pre-finished steel on a single processing line, a schematic diagram of the process is shown in Figure 1.3. The continuous automated nature of this process in the coating of metal substrate - most commonly steel, allows the production of a high quality coated product at speeds that would be otherwise impossible. The speed at which the coating line runs is dependent on the system in use, particularly the topcoat. It is however, not uncommon for a coil coating line to be run at speeds reaching 150m/min.

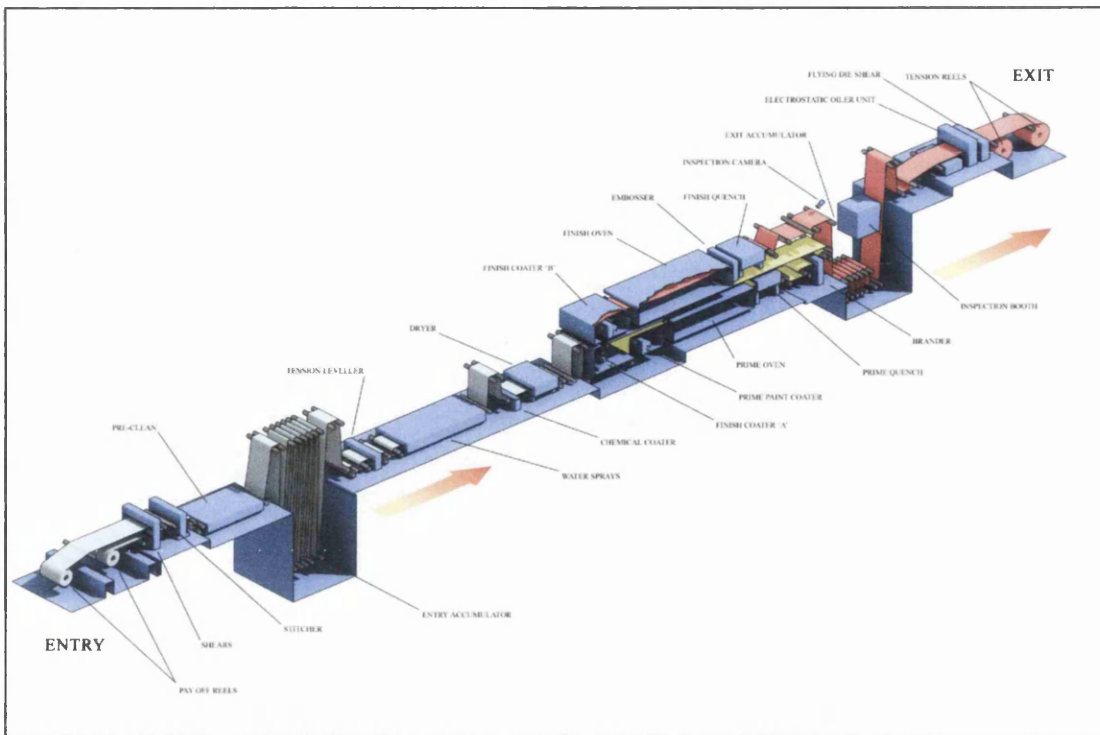


Figure 1.3 – The Coil Coating Process

1.1.1.1 Galvanising

It is necessary to cut the pre-finished steel to the size required by a consumer, thus creating an uncoated edge and resulting in exposure of the metal substrate. The exposed substrate is susceptible to oxidation and creates a preferential site for the occurrence of corrosion⁴. This is not only unsightly but also affects the integrity of the coating, thus increasing the likelihood of corrosion at other sites. In order to protect against cut edge corrosion the steel coils are zinc galvanised prior to painting to provide sacrificial corrosion protection to the steel substrate⁴.

Aluminium, although also more electronegative than iron (-1.67V vs. SHE) cannot provide sacrificial protection to the substrate due to the passivity it exhibits. Aluminium in contact with the atmosphere is quickly oxidised, forming a highly resistant protective oxide layer on its surface that prevents further corrosion. As a result aluminium cannot be used alone for galvanic protection of steel however its passivity has been exploited in the production of galvanising coatings to reduce corrosion of the zinc layer thus increasing the life of the protective coating.

The compositions of galvanising coatings range from pure zinc to zinc alloys containing up to 55wt% aluminium. The most commonly used in the coil coating process is Galvalloy, a Zn-4.8wt.%Al alloy. This coating has been found to provide

superior corrosion protection⁵ at cut edges via the sacrificial dissolution of zinc dendritic phases, while retaining its intrinsic corrosion protection via the formation of a protective aluminium oxide layer. This aluminium layer increases coating passivity and prevents excessive zinc dissolution, thus ensuring lasting integrity of the coating.

1.1.1.2 Pre Treatment

On entry into the coil coater the galvanised steel is alkali cleaned, followed by a hot water rinse to remove all excess alkali and surface impurities. It is then roller coated with a 1µm thick layer of pre-treatment and dried. In the case of most products for external applications a chemical conversion is carried out by a chromating process. Due to increasing regulations regarding chromate use pre-treatment with a phosphate it is becoming increasingly more common – in this case the substrate is subjected to a conditioning process prior to phosphating.

Application of a conversion coating serves a dual purpose, to further increase the corrosion resistance of the substrate by inhibiting the spread of underfilm corrosion and to modify⁶ the surface to improve primer and topcoat application. The continuously moving strip is coated with the chemical conversion coating by a roller coater and then heated to approximately 80°C to remove the water content from the coating.

1.1.1.3 Primer

The pre-treated substrate then proceeds to the priming stage where a layer of primer (between 5-30µm thick) is applied to enhance the corrosion resistance of the coated product and prepare the substrate surface for the finishing coat. The substrate then passes through the primer oven set at 400°C, on passing through the oven at line speed the substrate reaches a peak metal temperature (PMT) of ~220°C thus ensuring it is fully cured.

The primers used in the coil coating process are based on epoxy, polyester or acrylic resins pigmented with ~6 parts per hundred resin (PHR) of a sparingly soluble corrosion inhibitor such as strontium chromate or calcium chromate. These pigments are currently the most effective corrosion inhibitors available, however due to the tightening legislation regarding chromates their use is restricted. A great deal of research^{7, 8, 9, 10, 11, 12, 13} has been carried out on chromium-free corrosion inhibitors but is beyond the scope of this review.

1.1.1.4 Topcoat

The coil is then quenched and passed through to the finish coater where the topcoat is applied by a roller coating process. The application parameters and thickness of the topcoat is dependant on the formulation of the resin and added constituents. It is generally 25-100µm thick on the exterior surface and significantly thinner on the backing coat of the steel and is controlled by the distance between metering and coating rolls in relation to the line speed and coating viscosity.

The coated coil is then cured in the finishing oven which is often multi-staged and zone controlled, tailoring the temperatures to the coating system used. The total curing time is dependant on the topcoat used but is on average 25-35 seconds. If further processing such as embossing is required, then it is carried out on the cured coil prior to the final quenching and drying process. The finished coated material is then inspected for quality and recoiled.

Topcoats can be classified in various different ways; including composition, curing method, appearance and application to name but a few. The range of components used within the organic coating process is extensive, coating composition varies by manufacturer and formulations are kept secret within the coatings industry. Despite the lack of specific formulations it is clear that all coatings are comprised of several key components the main ones being a polymeric resin (which gives the coating its structure), a pigment (an insoluble material which provides opacity and colour) and solvent (which makes the coating fluid during application). Other more minor components include various additives or fillers¹⁴, lubricants, viscosity regulators, thermal stabilisers and UV absorbers, which are added to modify the coating properties.

In the coil coating process, it is possible to apply a top coat and backing coat simultaneously. In this case the strip must remain unsupported during the primer and finishing coat curing processes, this is achieved using a catenary oven system which maintains tension in the coil using bridle rolls. The backing coat system of organically coated steel is comprised of similar layers as the topcoat system. The galvanised substrate is coated with a pre-treatment and primer identical to that of the exterior coating, and a thin final layer of paint – which is frequently a different polymer system. The different layers of a pre-finished steel product are shown in Figure 1.4.

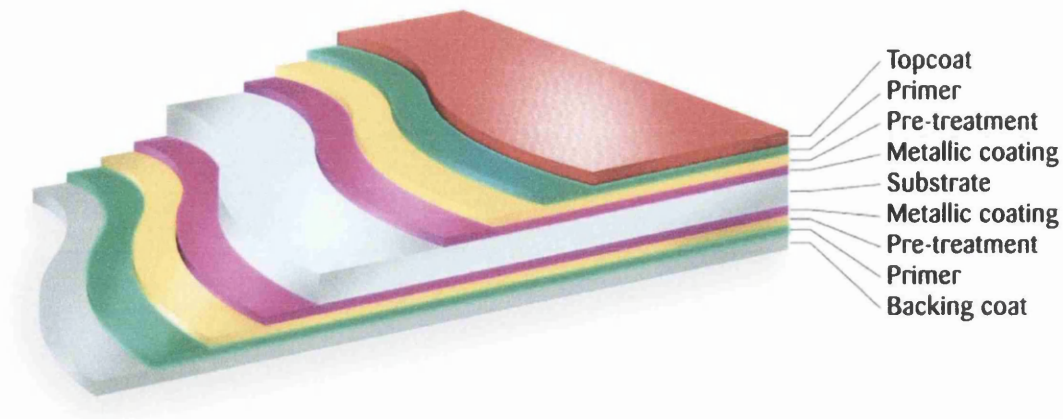


Figure 1.4 – Coating Layers of an Organically Coated Steel Product

The predominant variation between pre-finished steel products is the type of polymer used in the topcoat. The polymeric resin determines the additives, application, curing and inevitably final properties of the coating. There is a vast range of different resins available, each presenting a number of combinations for formulation, application and curing processes. There are currently four major resin systems marketed, PVC plastisol, polyester, polyurethane and PVDFs (often referred to as polyvinylidenedifluoride or PVF₂). Within each of these an even larger range of product variations such as metallic and colour shift are available, offering an innumerable range of both performance and aesthetic parameters².

1.1.2 Failure and Degradation of Organic Coatings

Organic coatings are applied to steel products to improve aesthetic appearance and provide corrosion resistance to the product. Failure of organic coatings can occur in a number of ways and the effects can range from being purely aesthetic to complete failure at which point the coating is no longer able to perform its intended task. There are two primary causes of coating failure, incorrect preparation and environmental stresses during service.

Incorrect preparation is a major cause of coating failure. Improper mixing, incorrect pigment volume concentration or solvent levels can all affect the integrity of the coating and lead to failure. The substrate is also a concern for production of pre-finished steel products. If the surface of the metal substrate is not smooth and is coated with only a thin layer of paint then de-wetting may occur, leaving areas of exposed metal susceptible to corrosion. The presence of contaminants on the substrate surface can also cause damage to the coating as they create a concentration gradient

which encourages diffusion of water through the coating. This phenomenon is known as osmotic blistering.

Any damage to the coating during forming or service that results in exposure of the substrate can lead to corrosion. This corrosion can undercut the paint, leading to the development of a highly corrosive differential aeration cell⁴. Undercutting of the organic coating is generally initiated by cut edge corrosion and can lead to further corrosion and failure of the coating.

Degradation of a coating as a result of exposure to ultraviolet (UV) light is a long-term effect of its service environment. The wavelength of UV light is such that it can cause excitation of certain materials - one such material is titanium dioxide (TiO₂) which is used as a pigment in almost all coatings. This excitation can lead to the formation of free-radicals which undergo reactions with the polymeric matrix causing degradation affecting both coating integrity and aesthetic appearance. Products are now expected to carry guarantees in excess of 20 years and although UV degradation is a relatively slow process it still proves a challenge for manufacturers. With the increasing number of high-profile buildings being constructed from pre-finished steel products, resistance to both the aesthetic and structural effects of UV degradation is becoming increasingly important.

1.2 Polyurethanes

This research has primarily focussed on polyurethane coatings for pre-finished steel products. The increased focus on improving product aesthetics and durability throughout the service life of the product has led to increased use of more robust and inherently stable polymers. Colorcoat Prisma[®] is a market leading polyurethane coated steel product from Corus Colours that offers technical and aesthetic superiority in comparison with many of the other pre-finished steel products available¹⁵. Polyurethane coatings offer outstanding colour and gloss retention and challenge more traditional coatings such as polyvinylidenedifluoride (PVDF).

Despite their increased use, polyurethane systems have not yet fulfilled their potential within the coatings market. They are still significantly more expensive than other coating systems and do not have the lifetime guarantees of the new generation PVC plastisol coatings. Currently Colorcoat Prisma[®] has a guarantee of up to 25 years¹⁵. The aim of this research has been to identify more stable polyurethane resins

in order to bring the guarantees more in line with the 40 years offered on the PVC plastisol HPS200® Ultra¹.

The generic term polyurethane covers a huge range of polymers comprising a urethane group and is misleading since it suggests a single polymeric structure. In reality there are a huge number of precursors available and therefore a correspondingly large number of possible polymeric structures and properties that fall into the polyurethane category^{16, 17, 18}.

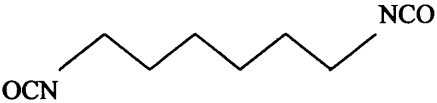
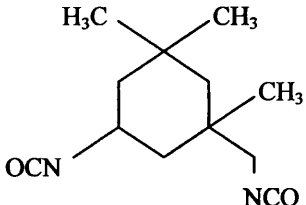
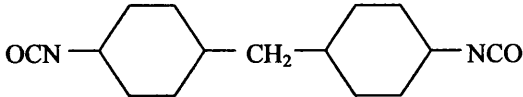
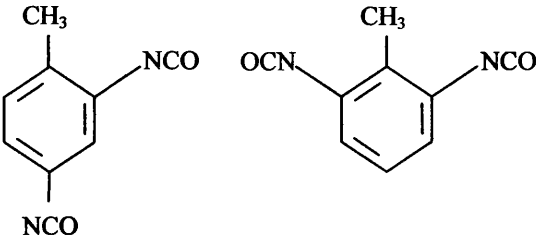
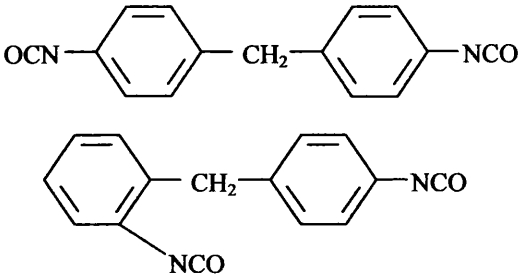
Modern polyurethane coatings are formed by the reaction of hydroxyl functional polyols such as polyester or polyether with isocyanate cross-linkers^{16, 17}, both of which influence the final properties of the coating. Descriptive names which more accurately describe the polymer structure such as polyesterurethane, polyetherurethane and polyurea-urethane although technically correct are complicated and thus often forsaken for the general term polyurethane¹⁸. This research has focussed on one component polyesterurethane coatings based on different combinations of polyester polyols and blocked polyisocyanate cross-linkers, and for the purpose of simplicity will be referred to as polyurethanes throughout.

1.2.1 Polyisocyanates

Most polyurethane coatings for the coil coating process are one component coatings cross-linked with blocked polyisocyanates. Monomeric diisocyanates (with the exception of MDI which has low vapour pressure) are classified as highly toxic and therefore their use is therefore restricted in coating raw materials. Higher molecular weight polyisocyanates are physiologically less dangerous than the lower molecular weight diisocyanates and therefore have replaced their use as raw coating materials.

Polyisocyanates are manufactured by polymerisation reactions of low molecular weight, highly reactive isocyanate species. Commercial polyisocyanate production uses a small selection of aromatic, aliphatic or cycloaliphatic based diisocyanates shown in Table 1.1. The commercial manufacturing process¹⁶ of polyisocyanates from diisocyanates is simplified in Figure 1.5. As opposed to their diisocyanate precursors, polyisocyanates have a functionality of greater than two, which is necessary to achieve the density of cross-linking required for adequate strength and resistance.

Table 1.1 – Diisocyanates used in Industrial Polyisocyanate Production

Diisocyanate	Structure
Hexamethylene diisocyanate (HDI)	
Isophorone diisocyanate (IPDI) (3-Isocyanatomethyl-3,5,5-trimethylcyclohexylisocyanate)	
Bis-(4- Isocyanatocyclohexyl)methane H ₁₂ MDI	
2,4- and 2,6-Toluene diisocyanate	
Diphenylmethane-4,4'- and/or -2,4'- diisocyanate (MDI)	

Rather than defined polyisocyanate compounds, the manufacturing process yields oligomer mixtures with a molecular weight distribution dependant on the degree of conversion of base diisocyanates. Both the polyisocyanates and diisocyanates will continue to react as long as there is surplus diisocyanate in the mixture, yielding higher and higher molecular structures. To prevent formation of high molecular weight, highly cross-linked polymerised structures only some of the isocyanate groups are reacted and the surplus removed by distillation. It is then possible to customise mean polyisocyanate functionality and viscosity within certain ranges.

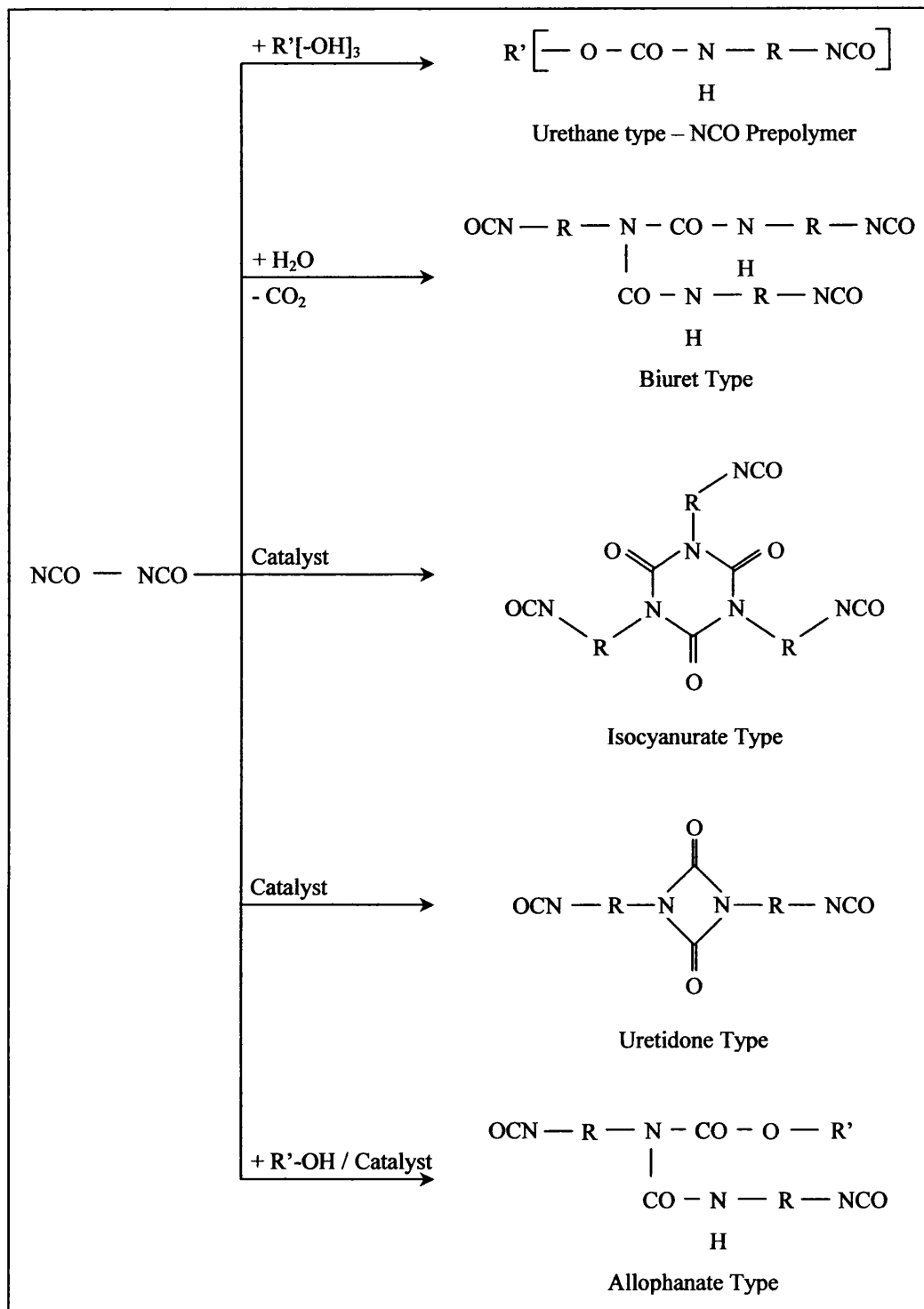


Figure 1.5 – A Simplified Illustration of the Manufacture of Polyisocyanates from Diisocyanates

One method of further reducing the physiological toxicity of polyisocyanates is via stabilisation of the functional NCO group with a blocking agent as shown in Figure 1.6. Blocking is carried out by the reaction of the functional groups of a polyisocyanate with a monofunctional group containing a reactive hydrogen

molecule¹⁹, for example ϵ -caprolactam, butanone oxime or diethylmalonate. This creates a stable resin¹⁶ that does not present the health risks associated with isocyanates.

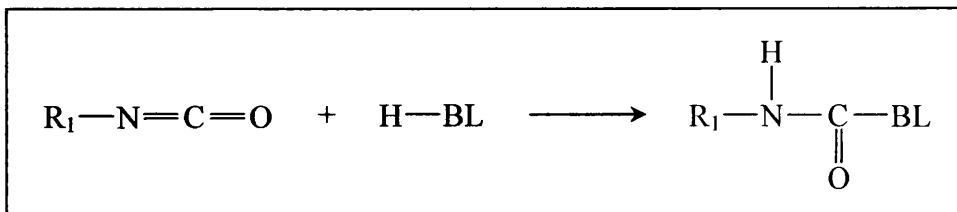


Figure 1.6 – Blocking of an Isocyanate

A further benefit of blocking polyisocyanates is the stability provided to the resin which allows greater ease of use in coating production. A blocked polyisocyanate can be combined with a polyol in advance of coating to produce a one component coating that is stable at room temperature. Without blocking the coating would have no storage stability, upon addition to the polyol the polyisocyanate would immediately begin to cross-link with the polyol resulting in hardening of the paint.

As with other polyurethane systems the polyisocyanate hardens the coating by cross-linking with the polyol. In one component systems where the polyisocyanate is blocked coatings have to be oven cured as the blocking agent is only released from the coating at sufficiently high temperatures (above $\sim 130^\circ\text{C}$). During curing the blocking agent splits from the polyisocyanate, leaving the functional NCO group free to undergo cross-linking reactions with the hydroxyl functional polyol as shown in Figure 1.7. The rate of reaction and amount of product differ widely between coating systems and are dependant on the nature of the base isocyanate species, blocking agents, the structure of the co-reactant and the addition of catalysts²⁰.

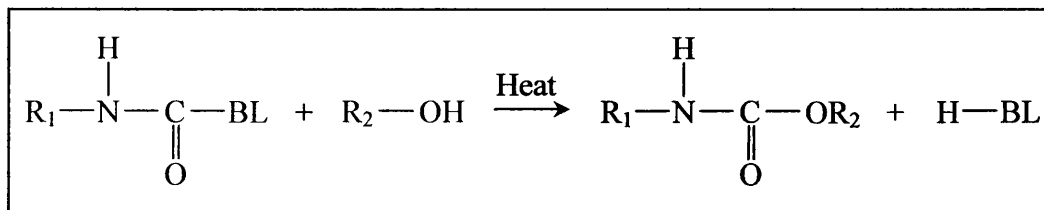


Figure 1.7 – Reaction between a Blocked Isocyanate and Hydroxyl-Functional Polyol

1.2.2 Polyester Polyols

The polyester polyols used in polyurethane coating formulation are produced by reaction of an acid with a difunctional alcohol. This is commonly known as an esterification reaction but can also be termed a step growth reaction – given that the reactions between one functional group and another build up the polyol in steps²¹. It has been previously discussed that the polyester polyols are required to be hydroxyl functional and for this reason the reaction is carried out in a stoichiometric excess of the alcohol¹⁸. The polycondensation reaction yields a mixture of low molecular weight polymers and by use of high temperatures and low pressures or inert gas streams is optimised¹⁶ to yield high molecular weight polyesters.

The most important¹⁶ polycarboxylic acids for the production of polyester polyols include the aromatic acids - phthalic acid and isophthalic acid, the aliphatic acids – adipic acids and maleic acid and the cycloaliphatic acids such as tetrahydrophthalic acid and hexahydrophthalic acid. The alcohols used include aliphatic alcohols such as ethane diol, 1,2-propane diol, 1,6-hexane diol, neopentyl glycol, and trimethylol propane and the cycloaliphatic alcohols such as 1,4-cyclohexane dimethanol.

The type of polyol used in a coating system is selected depending on its associated properties, which given the numerous possible precursors can vary significantly. Some examples of the possible variations between different polyester polyols include cost, rate of esterification and stability at high temperatures (important in one component systems due to the likelihood of discoloration during curing).

Generally speaking polyester polyols offer good solvent, graffiti and chemical resistance and very good weathering stability and colourfastness. This combination of properties - particularly those associative with weather stability, has made them the most commonly used polyols in the production of polyurethanes for coil coating applications¹⁶.

1.2.3 Dibutyltin Dilaurate (DBTL)

Although blocking increases the ease of handling and therefore functionality of isocyanate containing systems, addition of a blocking agent can cause thermal yellowing of the coating particularly if over cured. Blocked polyisocyanates are very stable as resin components and will only undergo cross-linking reactions at high temperatures and even then they are relatively heat stable. In order to obtain a fully-

cross-linked coating these resins require baking at very high temperatures for relatively long periods of time, which is risky in some coatings due to the likelihood of thermal yellowing.

In order to optimise the cross-linking reaction and reduce the temperature and time required to cure the coating catalysts are commonly added to the resins. Dibutyltin dilaurate (DBTL) is an organotin compound commonly used as a catalyst in the coatings industry to optimise the cross-linking reaction. The chemical structure of DBTL is shown in Figure 1.8 and is proposed²² to catalyse the cross-linking reaction via sequential complexation of alcohol and isocyanate to the tin. Addition of DBTL as a catalyst reduces the initial cross-linking temperature²¹ of the polyisocyanate by between 12°C and 46°C¹⁶, reducing the likelihood of thermal yellowing and over curing.

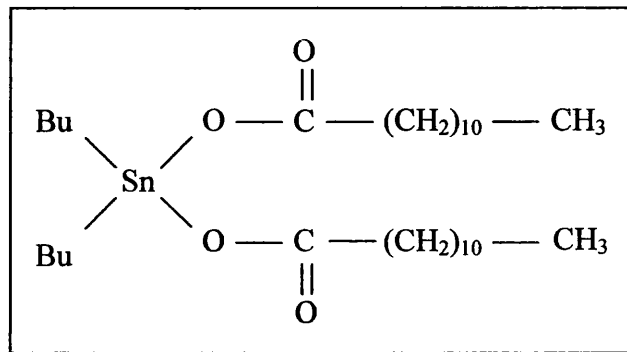


Figure 1.8 – Structure of Dibutyltin Dilaurate Catalyst

1.2.4 Texturing Agents

Texturing agents are incorporated into coatings primarily for aesthetic reasons, creating a range of products which are not restricted to high-gloss smooth coatings. Textured products are often preferable to smooth due to their ability to disguise minor imperfections in the coating which may be introduced during production or subsequent product use.

Colorcoat Prisma[®] is a very successful pre-finished steel product which has increased significantly in popularity over recent years. The textured polyurethane topcoat provides an excellent aesthetic appearance, which coupled with its relatively easy route of manufacture has made it a commercially valuable product. Polyamide beads are incorporated into Colorcoat Prisma[®] mainly for aesthetic reasons

however, the benefit is two-fold as they also provide reinforcement and abrasion resistance to the coating.

When incorporated into coatings with highly reactive components the polyamide beads can become integrally bonded within the coating resin. During the curing process the functional carbonamide [- CO – NH -] forms hydrogen bonds with reactive components, thus linking the molecular chains of the polyamide to the polymer resin²³. This bonding reinforces the coating and prevents the polyamide being rubbed out of the paint providing excellent abrasion resistance.

Chemical bonding between the polymer resin and polyamide beads is particularly good in polyurethanes due the reactivity of the polyisocyanates used to cross-link the coatings. In all cases, addition of polyamide beads to polyurethane produces a reinforced coating with good resistance to abrasion - something that is particularly important for intended for use in external architecture.

1.2.5 Melamine Cross-Linking Systems

One alternative to the use of polyisocyanates as a cross-linker in thermosetting coatings is hexamethoxymethylmelamine (HMMM). HMMM has been used in the production of polyester-melamine systems which have been tested alongside the polyurethane coatings throughout this thesis. The principal function of the melamine shown in Figure 1.9 is to cross-link the molecules of the polyester polyol in order to build a three-dimensional thermoset polymer network.

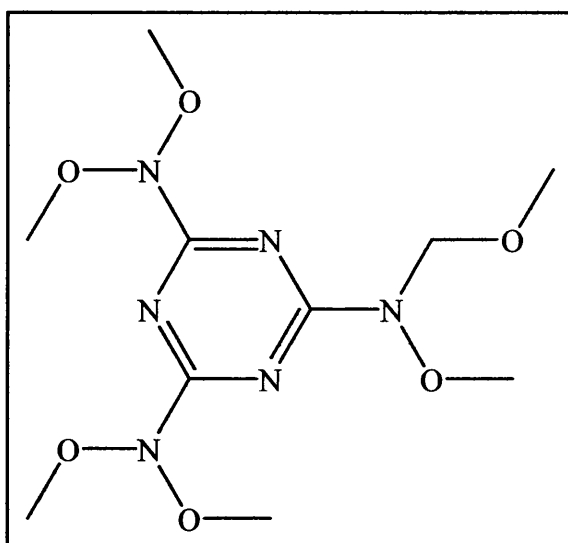


Figure 1.9 - Structure of Hexamethoxymethylmelamine (HMMM)

HMMM containing resins are formed by methylolation of melamine crystal with formaldehyde in presence of acid or alkali, followed by methylation in the presence of acid. It cannot be produced or isolated in its pure form, commercial production yields a polymeric mixture where the HMMM is present within the mixture as a monomer or as a low molecular-weight polymer. The exact proportions of HMMM contained in the mixture vary with manufacturing process but generally contain about 28-50% HMMM monomer and the balance methylated melamine-formaldehyde polymer²⁴.

Like the one component polyurethane coatings containing blocked polyisocyanates it is possible to combine the cross-linker and polyol resins systems prior to coating. The HMMM resin is stable at room temperature and only undergoes cross-linking reactions under high temperature curing conditions. HMMM forms stable cross links with polyester polyols, giving good solvent and chemical resistance and outdoor durability.

1.3 Introduction to Photochemistry

One of the biggest challenges faced by coating manufacturers is the effect of prolonged exposure to sunlight on the polymer. The ultraviolet (UV) component of sunlight can cause photo-oxidation of the polymer resulting in impaired performance and if allowed to continue, failure of the coating. For photo-oxidation to occur the polymer must first absorb UV irradiation which causes excitation and subsequent initiation of the chemical reactions that result in degradation. This occurs either by means of organic group or impurity in the polymer known as a chromophore.

Polymers are classified into two groups dependant on the nature of the chromophore responsible for UV absorption^{25, 26}. Type A absorb light heterogeneously through isolated impurities in the polymer, these impurities are often introduced during processing and can either be part of the polymeric chain or as a separate component, for example a pigment. Type B polymers absorb light homogeneously through chromophores present as repeat units integral to the polymer structure, for example aromatic groups. The initiation of photo-oxidation mechanisms associated with type A and B polymers will be discussed in further detail in Section 1.4.1.1.

1.3.1 Excitation of Electrons

The absorption of light by a chromophore does not itself cause a chemical reaction but rather promotes an electron from the valance band to a higher unoccupied orbital, producing an excited singlet state (S^*). It is these excited singlet states that can bring about the formation of free-radicals which are responsible for the occurrence of degradation reactions. For excitation to occur the absorbed photon must have an amount of energy greater than or equal to the difference between the ground state and first excited singlet state as shown in Figure 1.10.

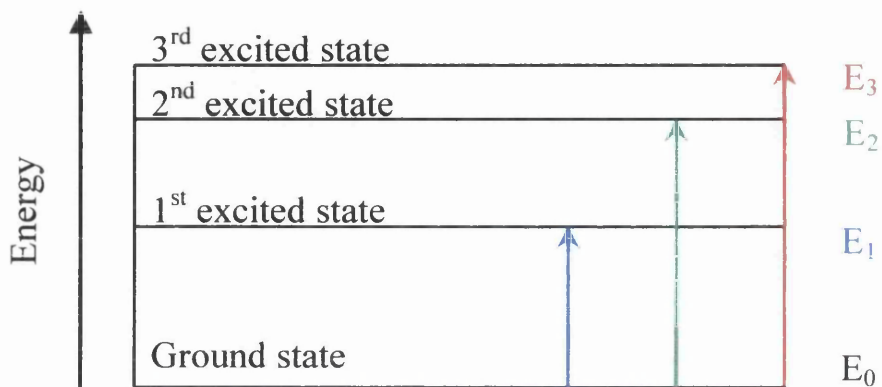


Figure 1.10 - Energy Levels of Excited States

$$E = \frac{hc}{\lambda}$$

E = Energy of the photon (kJmol^{-1})

h = Planks constant (Js)

c = Speed of light (ms^{-1})

λ = Wavelength of the light (m)

Equation 1.1 - Energy of a Photon

The energy of a photon can be calculated using Equation 1.1 and is inversely proportional to its wavelength. If the energy absorbed exceeds that needed for promotion of an electron to a higher energy state, but is lower than that required to promote to the next excited state the excess energy is lost through vibration within the molecule. Higher energy singlet states rapidly lose their energy thermally via internal conversion (IC) to the lowest excited singlet state (S_1). Following deactivation to the first excited singlet state the S_1 molecule can reduce its excess energy in a number of ways^{25, 27} as shown in Figure 1.11.

The excited singlet molecule (S_1) can undergo internal conversion back to its ground state, releasing its energy thermally or it may emit a photon of light – a process known as fluorescence. Many orders of magnitude less often they can undergo intersystem crossing (ISC) and produce an excited triplet state (T_1). These triplet states are much longer lived and likely to react chemically via bond cleavage however, if thermodynamically and kinetically possible the excited singlet state (S_1) can also undergo bond cleavage. It is during the bond cleavage reactions that free radicals are formed, thus initiating the oxidation reactions which are discussed in more detail in Section 1.4.2.

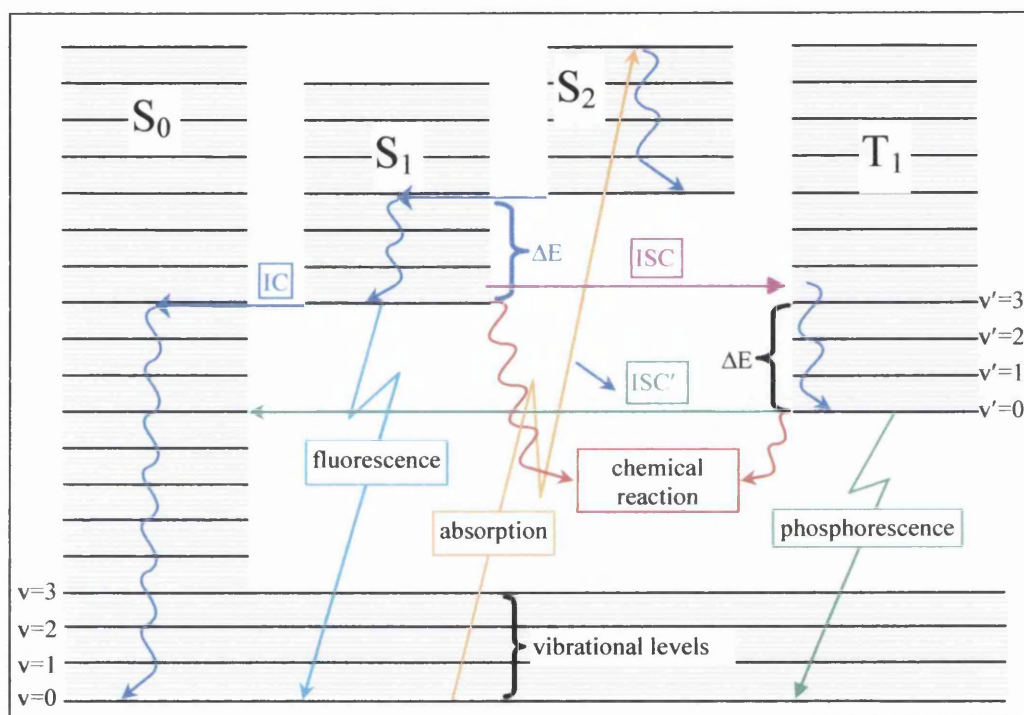


Figure 1.11 - Deactivation Pathways in the form of a Jablonski Diagram

1.3.2 Energy Transfer

Energy transfers can occur either intra-molecularly (within the molecule) or inter-molecularly (between two molecules), both the donor and acceptor molecules can be either simple molecular compounds or large macromolecules. The degree of energy transfer is affected a range of factors, including the distance between donor and acceptor, the relative orientations of the donor, spectroscopic properties of donor and acceptor, optical properties of the polymer matrix and the effect of collisions on the motion of the donor and the acceptor whilst the donor is excited. The transfer of

energy is never 100% efficient as during transfer some energy is lost as light or heat, and therefore the energy of the acceptor is therefore always lower than that of the donor molecule.

1.3.2.1 Radiative Energy Transfer

The emission of a photon from an excited molecule and the subsequent absorption of this photon by an acceptor molecule is radiative (or trivial) energy transfer. As energy transfer can only occur at wavelengths correspondent to both the emission and absorption spectra of the relative molecules the efficiency of this transfer is dependant on the degree of spectral overlap between the species shown in Figure 1.12. Radiative energy transfer is long range in nature – in comparison with the molecular dimensions of species involved and transfer occurs by means of an intermediate photon as opposed to direct interaction between donor and acceptor molecules (non-radiative transfer).

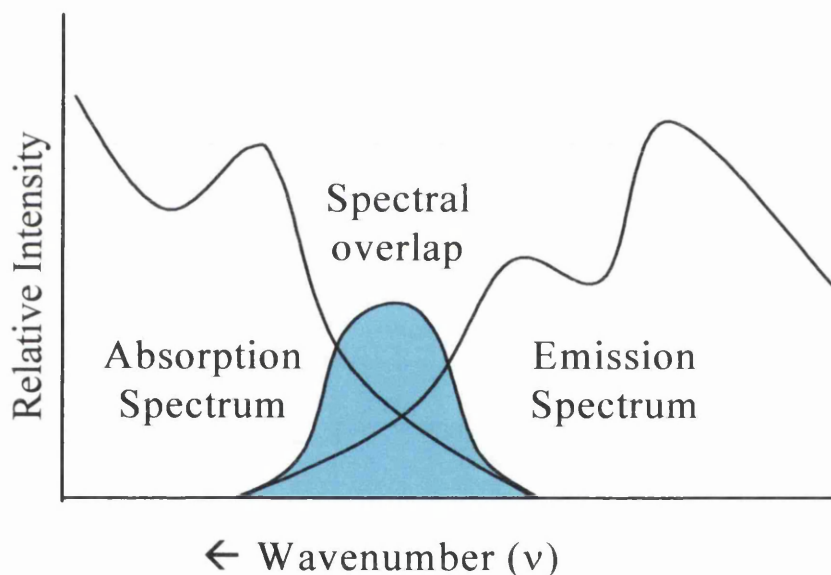


Figure 1.12 - Overlap of Absorption and Emission Spectra

1.3.2.2 Non-Radiative Energy Transfer

Non-radiative energy transfer occurs via interactions between the donor and acceptor molecules and can occur by one of two mechanisms. The first is a short range transfer that occurs when two molecules are in contact – that is to say that they have a distance of less than 1.5nm between them. At these distances the electron clouds overlap and therefore excited electrons can pass from one cloud to another.

The second is longer with a gap of 5 to 10 nm between molecules and involves transfer via dipole-dipole interactions known as resonance coulombic interaction.

1.3.2.3 Transfer in Polymer Matrices

Intermolecular energy transfer can occur in one of three ways, by transfer from small molecules within the matrix to molecular chromophores, transfer from polymeric chromophores to small molecular chromophores or transfer from one polymeric chain to another. Intra-molecular energy transfer occurs within the same polymeric molecule, energy can either be transferred between adjacent or near adjacent chromophores (locally) or across loops in the polymeric chain (long range) as illustrated schematically in Figure 1.13.

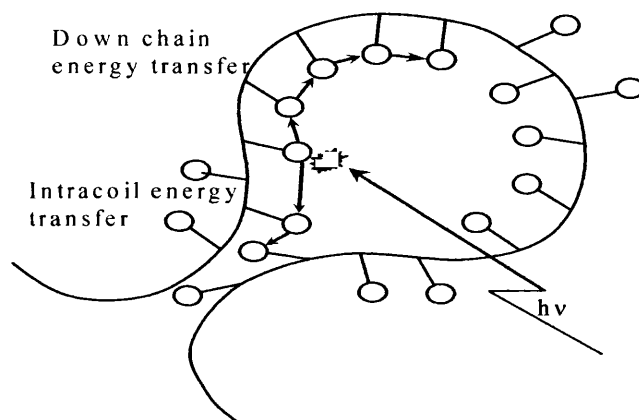


Figure 1.13 - Energy Transfer across a Polymer Chain Loop

It is possible for excitation to travel large distances^{28, 29} as transfer of excitation from one chromophore to the next can occur many times in a chain-like manner. If two triplet or two singlet states migrate close enough to one another then annihilation occurs, producing a highly excited triplet or singlet state as shown in Figure 1.14.

The highly excited triplet (T^{**}) and singlet (S^{**}) states can undergo deactivation and to lose their excess energy in one of two ways. Firstly, the triplet and singlet states can revert to their ground state by emitting a photon of light known as phosphorescence and fluorescence respectively as shown in Figure 1.11. Another possibility is that these states undertake chemical reactions and produce free radicals as shown in Figure 1.15, which can undergo reactions with the polymeric matrix resulting in degradation.

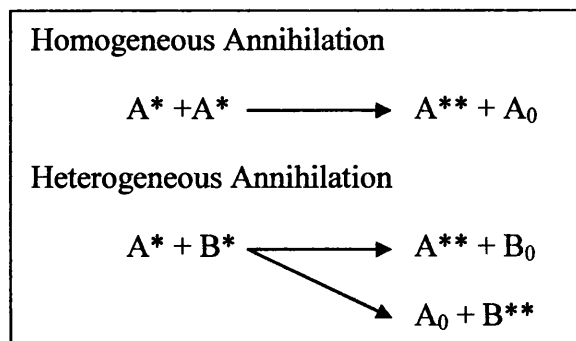


Figure 1.14 - Annihilation Processes of Excited States

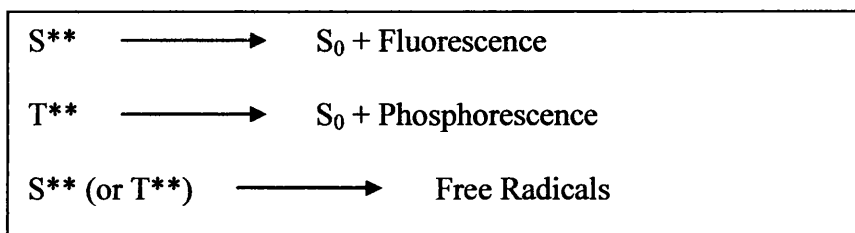


Figure 1.15 - Deactivation of Highly Excited Triplet and Singlet States

1.4 Polymer Degradation

Polymeric materials are generally considered to be relatively stable, however when exposed to environmental stresses chemical and/or physical changes can occur. The rate at which these changes occur is dependant on both polymer stability and environmental factors such as atmosphere - particularly the presence of oxygen, UV intensity and temperature. In the presence of oxygen exposure to environmental stresses can cause rapid chain scission of polymers at temperatures significantly lower than their melting points^{30, 31}.

1.4.1 Degradation Mechanisms

Regardless of initiation conditions it is acknowledged that all polymer degradation mechanisms involve the production and subsequent reactions of free radicals^{28, 32}. The mechanisms of thermal and UV induced degradation are very similar and only significantly differ in the initiation step and nature of the degradation products.

Photodegradation

Although photodegradation is often used to describe any instance of UV induced degradation, its direct definition is UV induced degradation in the absence of oxygen³³.

Photo-oxidation

The occurrence of UV induced polymer degradation in the presence of oxygen is technically termed photo-oxidation.

Photo-hydrolysis

This is the degradation of polymers by UV irradiation under conditions of high humidity.

Hydrolysis

This is the degradation of polymers by UV irradiation under conditions of high humidity.

Photolysis

This term relates to the degradation reactions resulting from light absorption by the polymer backbone as opposed to the functional groups or other irregularities.

Photo-thermal Degradation/Oxidation

This encompasses the UV induced degradation reactions that occur above ambient temperature but below that at which degradation can be considered entirely thermal.

Thermal Degradation

This term covers the polymer degradation mechanisms induced by exposure to high temperatures. The reaction mechanisms are specific to the polymer and tend to fall into one of the following categories:

Depolymerisation

The polymer chain splits into two separate chains comparable to the original polymer but of lower molecular weight. This is the mechanism by which polyurethanes thermally degrade³⁴.

Elimination

The products of elimination reactions tend to be of low molecular weight and show no direct relation to the initial polymer structure. One example of this mechanism is the dehydrochlorination of PVC to produce HCl.

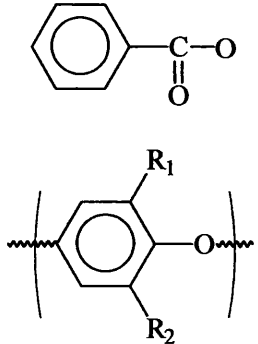
Substitution

These reactions result in the functional group of a polymer repeat unit being replaced by a different molecule. This can sometimes occur simultaneously with elimination reactions as substituted groups can react to form products similar to those of elimination.

1.4.1.1 Formation of Free Radicals

The focus of this thesis is the photo-oxidation of polymers, in particular polyurethanes based on aliphatic polyisocyanates. The stability of a polymer, particularly with regard to initiation is affected by the presence of chromophores. These are organic or inorganic species capable of absorbing a photon of light, resulting in excitation of an electron from ground to an excited state. This excitation can lead to the creation of free radicals which are responsible for photo-oxidation initiation, as discussed in Section 1.3.

Table 1.2 – Examples of Common Chromophores Present in Different Polymer Types

Type A Polymers	Example Chromophoric Groups	Example Polymers
Chromophores are present as extrinsic impurities and bring about heterogeneous changes. These can be introduced during polymerisation or processing and may even have been added as a separate component of the system e.g. pigments.	$\begin{array}{c} \text{---C=C---C=C---} \\ \text{---C---} \quad \text{---C=C---C---} \\ \parallel \quad \quad \quad \parallel \\ \text{O} \quad \quad \quad \text{O} \end{array}$ <p>POOH $\text{Ti}^{+4}, \text{Al}^{+3}, \text{Fe}^{+3}$</p> $\left[\text{P=H}^+ \text{---O}_2^- \right] \quad \left[\begin{array}{c} \text{---C=C---} \\ \\ \text{O}_2 \end{array} \right]$	<p>Poly(vinyl halides)</p> <p>Polyacrylics</p> <p>Poly(vinyl alcohols)</p> <p>Aliphatic esters</p> <p>Aliphatic polyurethanes</p>
Type B Polymers Chromophores are an integral part of the polymer structure. They can be part of the polymer backbone or attached as functional side groups of the polymer.		<p>Poly(ethyleneterephthalate)</p> <p>Poly(2,6-dialkyl-1,4-phenylene ether)</p> <p>Poly(ethersulphone)</p> <p>Aromatic polyurethanes</p>

Chromophores can be intrinsic or extrinsic to the polymer, introducing either homogenous or heterogeneous changes respectively. Examples of common chromophores and the polymers with which they are associated are illustrated in Table 1.2. Polymers are classified into two main types according to the nature of chromophores responsible for radical creation^{25, 26}.

Type A polymers absorb light through extrinsic chromophores that are present as isolated in-chain or end of chain impurities. Type B polymers absorb light through intrinsic chromophores that form part of the backbone structure of the polymer. The distribution of chromophores in type A and B polymers is illustrated in Figure 1.16.

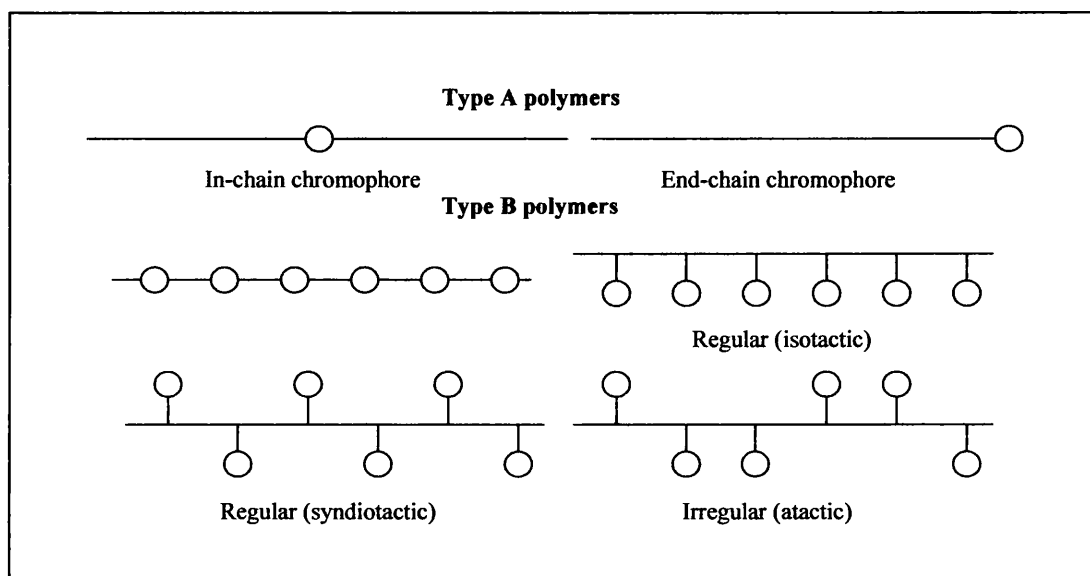


Figure 1.16- Formation of Chromophores on Type A and B Polymers

The absorption spectra of some typical polymers overlaid with the emission spectra of natural sunlight is shown in Figure 1.17 and illustrates a clear difference between type A and type B polymers. The absorption region of type A polymers lies well outside the natural spectra of sunlight while type B polymers absorb within the spectral range. Absorption of light by intrinsic chromophores in the backbone of type B polymers results in high susceptibility to degradation by sunlight compared to type A polymers.

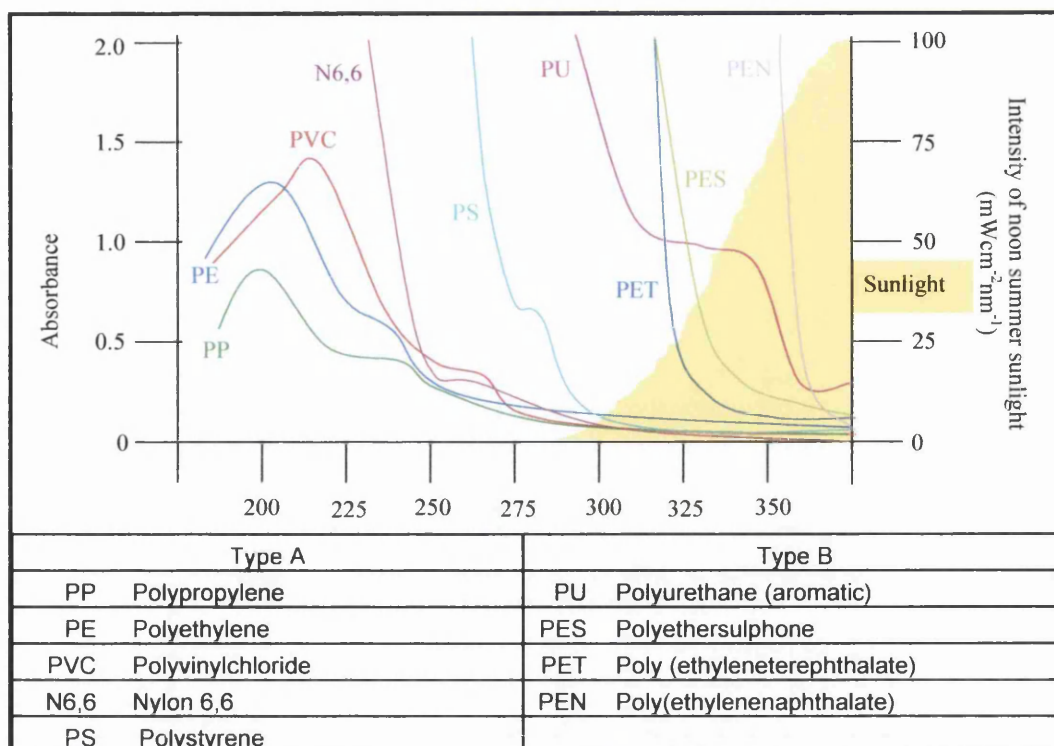


Figure 1.17 - Absorption Spectra of Some Common Polymers³⁵

Aromatic Polyurethanes

Polyurethanes based on aromatic polyisocyanates fall into the category of type B polymers. The aromatic species in the polymer cross-linker are highly absorptive in nature and rapidly initiate reactions that result in yellowing and chain scission of the polymer. Yellowing of aromatic polyurethanes is symptomatic of degradation and involves two mechanisms, a photo-Fries rearrangement shown in Figure 1.18 and the production of quinone-imide species^{25, 36}.

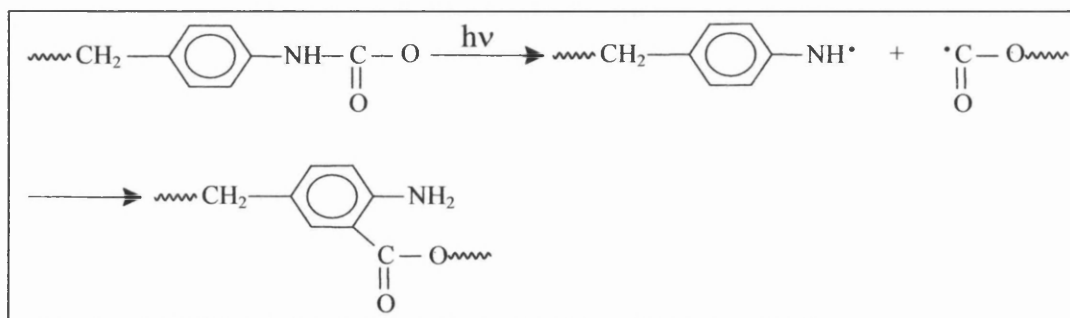


Figure 1.18 – The Photo-Fries Rearrangement Mechanism

The mechanisms of quinone-imide formation and photo-Fries rearrangement involve free radical reaction. The radicals formed during these processes can initiate

photo-oxidation reactions within the polymer, resulting in degradation. The highly absorptive nature of aromatic species coupled with the rapid progression of photo-oxidation reactions in these polymers greatly limits their suitability for external applications.

Aliphatic Polyurethanes

The focus of this thesis is photo-oxidation of polyurethanes cross linked with the aliphatic polyisocyanates Hexamethylene diisocyanate (HDI) and Isophorone diisocyanate (IPDI). These are type A polymers and the most probable cause of radical formation and subsequent reactions are extrinsic chromophores³⁷.

1.4.2 Photo-Oxidation Mechanisms

The mechanism of polymer photo-oxidation is autocatalytic and the initiation step is believed to involve hydroperoxides³⁸ and/or carbonyl groups²⁵. The three major steps involved in photo-oxidation are initiation, propagation and termination as described by the Bolland Gee auto-oxidation mechanism shown in Figure 1.19.

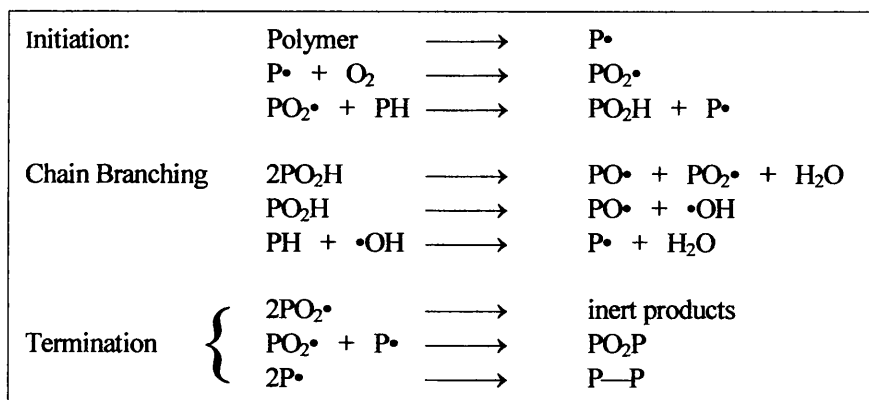


Figure 1.19 – The Bolland-Gee Auto-Oxidation Mechanism

1.4.2.1 Initiation

Polymer stability can be significantly affected by processing during manufacturing as these stages are often responsible for the introduction of chromophores. Excitation of a chromophore can create highly reactive free radicals (R•) which initiate the oxidation mechanisms illustrated in Figure 1.19. Free radicals are capable of abstracting a hydrogen atom from the polymer chain resulting in the formation of an alkyl radical (P•)^{30, 31}.

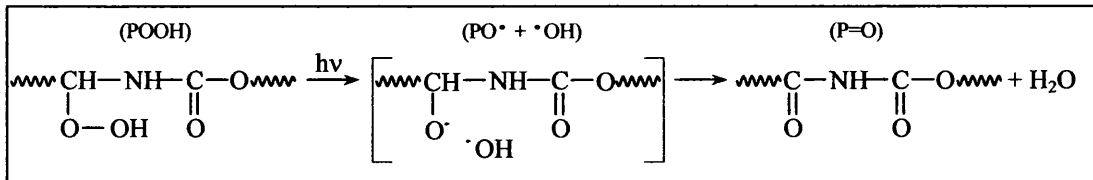


Figure 1.22 – The Cage Recombination Reaction

The recombination of alkoxy and hydroxy radical formed during initiation in aliphatic polyurethanes is illustrated in Figure 1.22. This reaction produces an acetylurethane species which reacts readily with water producing carboxylic acid and a primary amine³⁷. Recombination due to the cage effect, although common is not the only reaction route of radicals. Evolution of radicals may also occur via chain branching and scission mechanisms.

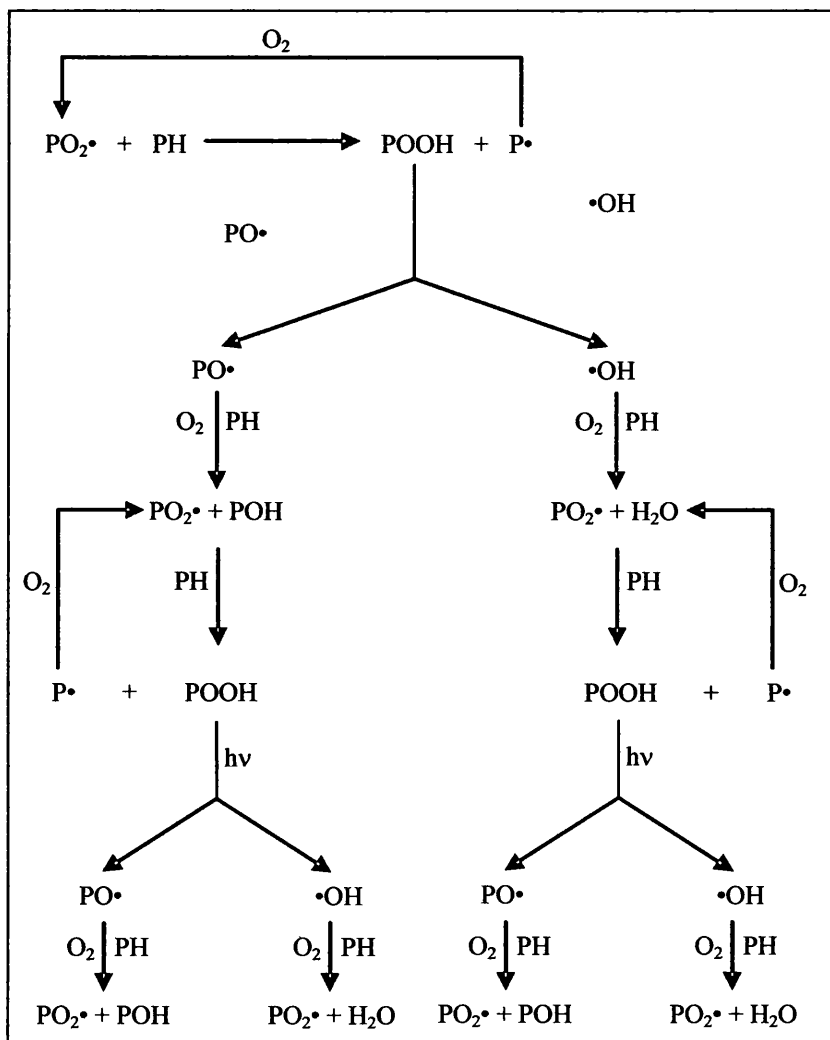


Figure 1.23 – The Chain Branching Process

Chain branching of the alkoxy and hydroxy radicals formed by hydroperoxide (POOH) photolysis causes degradation of the polymer via either alkoxy or hydroxy hydrogen abstraction. This process is represented in Figure 1.23 and is the main cause of the auto-accelerated kinetics often observed in polymer photo-oxidation.

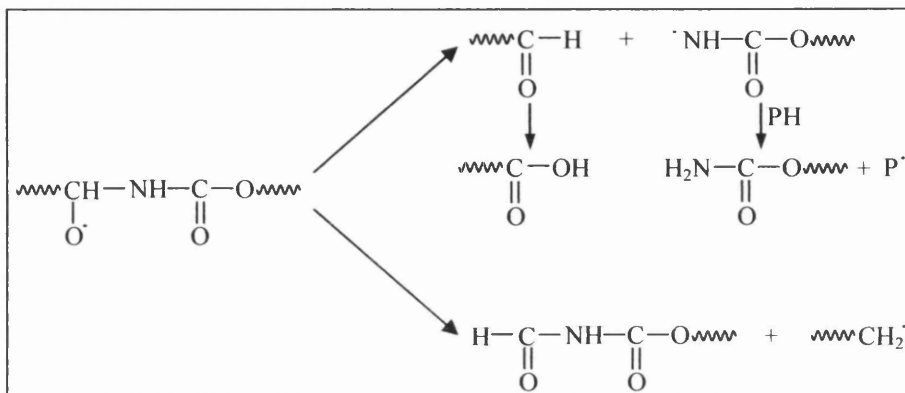


Figure 1.24 – Chain Scission of Alkoxy Radicals Formed During Polyurethane Oxidation

The alkoxy radicals produced during POOH photolysis can also undergo scission as shown in Figure 1.24. Scission of alkoxy radicals resulting from polyurethane photo-oxidation produce amines, alcohols peresters and aldehydes (which are readily oxidised to carboxylic acids)³⁷.

The reaction profile for the formation of hydro peroxide and carbonyl groups during photo-oxidation is shown in Figure 1.25. The initial increase in the levels of hydroperoxide is due to oxygen scavenging by alkyl radicals. These levels peak during initiation stages of oxidation then decrease rapidly as propagation dominates³⁰. During propagation chain branching and scission reactions produce macro radicals which can each consume several molecules of oxygen, resulting in an increase in the level of carbonyl products.

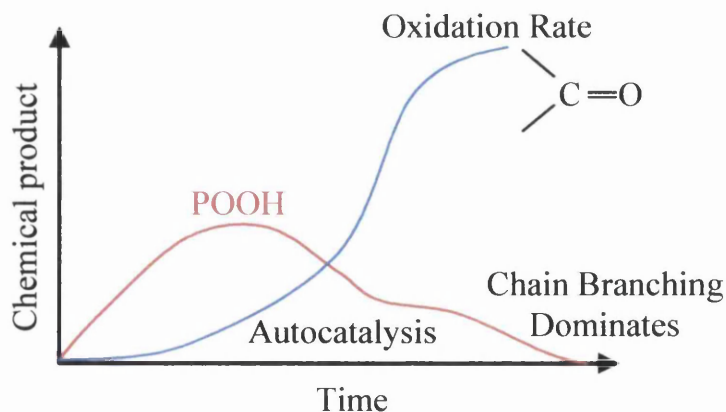


Figure 1.25 - Reaction Profile for the Oxidation of Polyethylene

1.4.2.3 Termination

Formation of free radicals during initiation is responsible for the polymer oxidation reactions that continue until the collision of two radicals results in termination. The most likely source of termination of these reactions is peroxy radicals which have relatively long lifetimes (several seconds) and a high affinity to combine with one another.

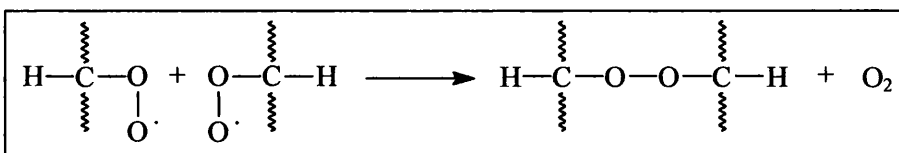


Figure 1.26 –Termination of Two Peroxy Radicals

Two PO_2^\cdot radicals combine to create an unstable tetra-oxide which via rapid oxygen loss forms a peroxide bridge between the two polymer molecules. This reaction is shown in Figure 1.26, resulting in cross-linking of the polymer and consequently an increase in stiffness which can lead to coating failure.

In systems where oxygenation is poor, alkyl radicals may become involved in the termination process, again leading to cross linking of the polymer. The chain length after oxidation varies significantly with polymer type, and is dependant upon factors such as chemical structure, light intensity, O_2 permeability and the reactivity of the peroxy and alkoxy radicals produced. A schematic flow diagram of the reactions occurring during photo-oxidation is shown in Figure 1.27.

Polyurethanes have a broad polymer range from which they are synthesised and as such have very complex chemical compositions as discussed in Section 1.2. Studies of polyurethanes are among the most challenging as photo-oxidation products are often equally complex and difficult to identify. During photo-oxidation polyurethanes undergo extensive cross linking of the polymer chain²⁵, resulting in physical changes that can cause failure. Studies of model polyurethanes based on aliphatic isocyanates³⁷ have identified carboxylic acids, amines, alcohols and peresters to be among the products of these degradation reactions.

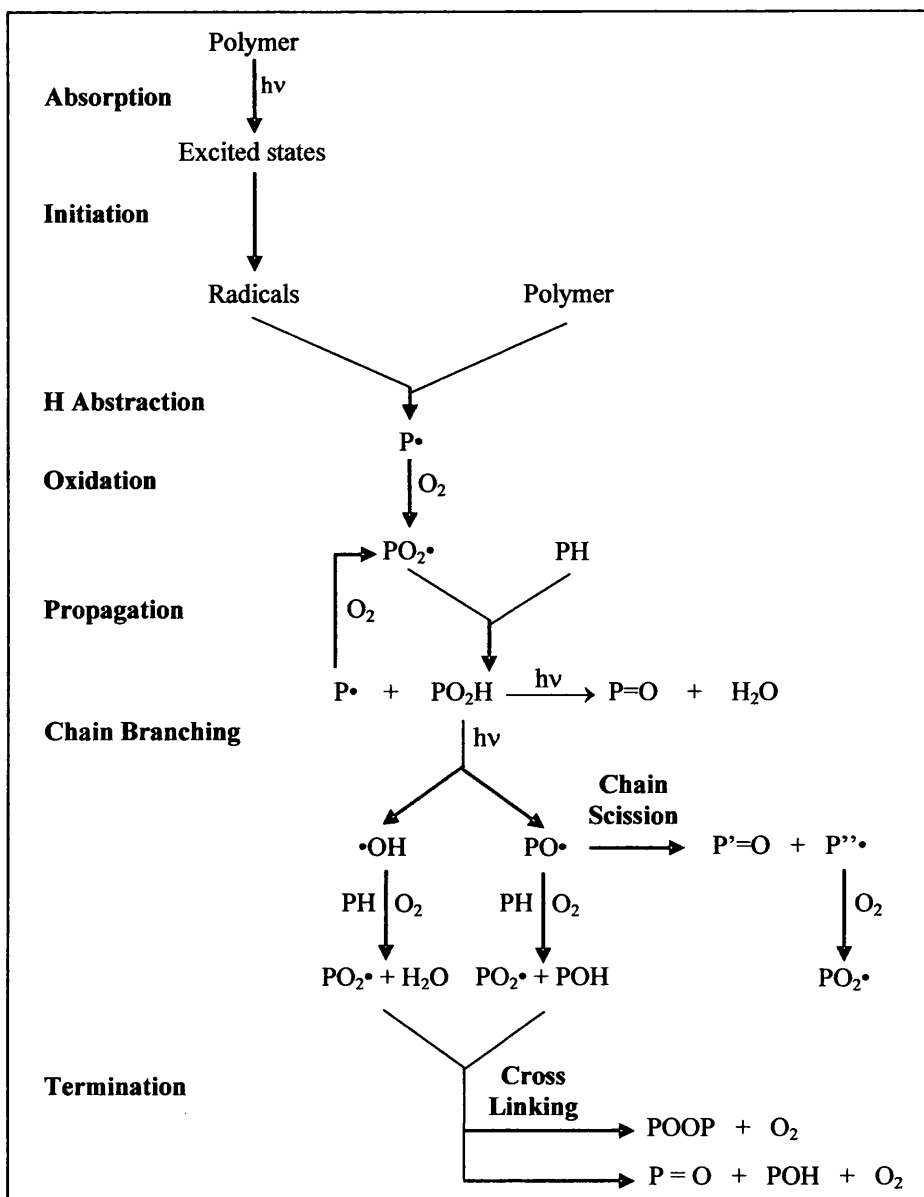


Figure 1.27 – Flow Diagram of Polymer Photo-Oxidation Reactions

1.5 Titanium Dioxide

Titanium dioxide (TiO_2) is the largest selling individual pigment within the inorganic pigment trade. The white pigment market is served almost exclusively by TiO_2 , which along with carbon black has a monopoly over the pigment industry because it has no effective competition from other pigments.

TiO_2 has dominated the pigment market, particularly that of white pigments for two reasons: Firstly, the properties of TiO_2 as a pigment are technically outstanding and un-matched by any other material⁴¹. Secondly, white pigments are commonly added to polymers as hiding agents and therefore play an important role in

the manufacturing of almost all commercial polymers. A white pigment is required in almost all but the darkest colours, while any other single pigment is only included in a small range of hues.

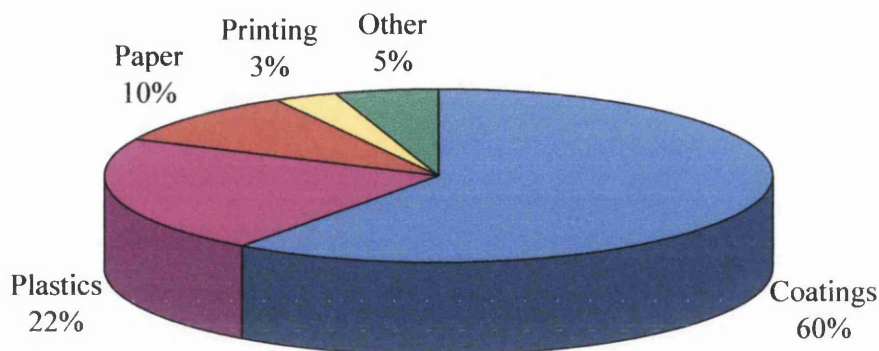


Figure 1.28 – Breakdown of End Use for TiO₂ Products in 2006

The breakdown of TiO₂ use in 2006 is illustrated in Figure 1.28⁴². It can be seen that pigmentary applications such as polymers, paints, paper and inks account for some 95% of TiO₂ usage. The remaining 5% was used in applications such as ceramics, welding rods and catalytic functions⁴¹.

1.5.1 Manufacturing Process of TiO₂

Pigmentary grade TiO₂ is commercially extracted from these ores by one of two processes: the sulphate process or the chloride process. A schematic diagram of the two processes is shown in Figure 1.29.

The sulphate process is low tech, labour intensive and prior to development of the chloride process was the primary route of TiO₂ manufacture. The more advanced chloride process uses automated anhydrous flame technology which lends itself to being a more continuous and environmentally friendly process. The popularity of the chloride process is enhanced by the fact that it produces a higher quality product which is easier to purify and has a narrower particle size distribution. Furthermore, the natural product of this process is rutile crystal TiO₂ which due to its higher stability and light scattering advantage has replaced anatase in almost all pigmentary applications.

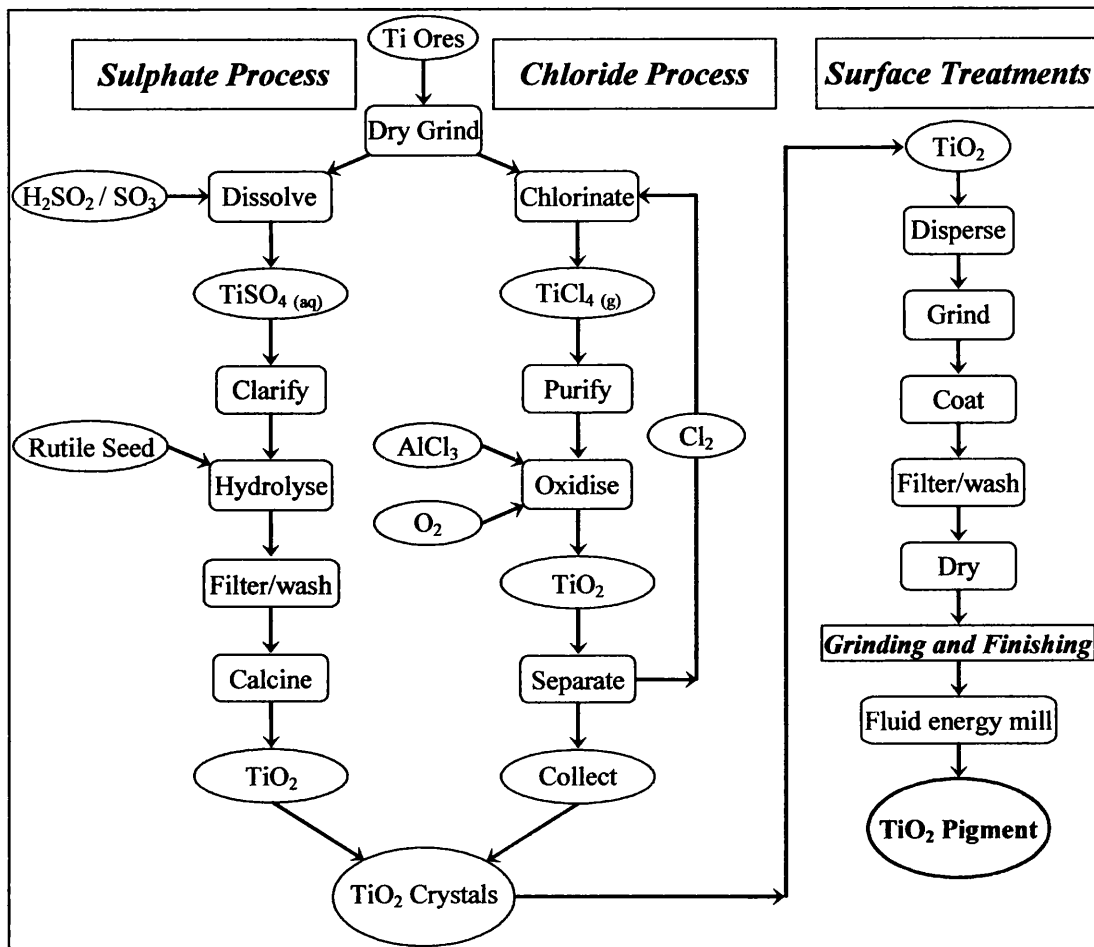


Figure 1.29 - Overview of the Basic Processes Involved TiO₂ Manufacturing

1.5.1.1 The Sulphate Process

The sulphate process is a labour intensive batch production process which used low-tech aqueous chemistry to extract TiO₂ from a titanium rich ore (FeTiO₃). The ore is dissolved in hot concentrated sulphuric acid to produce titanyl sulphate which is hydrolysed by boiling to produce a hydrated oxide. This titanium(IV)oxyhydroxide is then calcined at approximately 1000°C to yield anatase or rutile pigment grade TiO₂ particles.

1.5.1.2 The Chloride Process

The chloride process was commercialised in the 1950s by DuPont and since has become the primary route of TiO₂ production as it is a continuous process which produces less waste and yields a higher quality product. It does however require a far higher quality of ore, rutile and leucosene can be chlorinated directly however lower

grade ores such as ilmenite must be pre-treated by beneficiation to remove contaminants.

Ore and dry pulverised coke are fed into the chlorinator and fluidised with chlorine at 900-1700°C, this is an exothermic reaction and so the chlorination chamber requires constant cooling. Chlorination of the titanium-rich ore produces gaseous titanium tetrachloride (TiCl_4) and other metal chlorides which exit the chamber as a gas stream. This is then cleaned to remove the various contaminants and leave only TiCl_4 which is condensed and further purified via distillation to remove any remaining impurities.

The purified TiCl_4 is then vaporised and pre-heated before being flame oxidised using a specifically designed reactor which yields optimum pigment particle size. Co-oxidants such as AlCl_3 are injected into the TiCl_4 stream to promote formation of rutile crystals and minimise aggregation. TiO_2 crystals are grown to the correct size for optimum light scattering via chemical reactions or by ripening of sub-crystalline assemblies⁴¹. The bond strengths within the TiO_2 lattice are too high to be broken down by conventional grinding methods therefore crystal size is controlled during growth via additions of metal ions in minute concentrations.

The chlorine released during oxidation is separated from the TiO_2 and recycled back to the chlorinator. The TiO_2 is then further purified via aqueous hydrolysis to remove any remaining chlorine yielding purified pigment grade rutile TiO_2 . It is possible to produce anatase TiO_2 in the chloride process however given the advantages of rutile crystals compared to anatase the incentives to do so are low.

1.5.1.3 Surface Treatments

In order to improve or refine specific properties, pigment manufacturers apply inorganic and/or organic coatings to the TiO_2 . To increase photostability the TiO_2 particles are coated with precipitates of aluminium, silicon and zirconium oxides or oxy-hydrates. These inorganic coatings act as a barrier to ultraviolet (UV) light and prevent organic compound adsorption on the titania surface, thus reducing photoactivation of the TiO_2 and its catalytic effect on polymer degradation. The success of a coating in photostabilising TiO_2 is dependant on its effectiveness in reducing the surface area of exposed or 'active' TiO_2 on the pigment particle as illustrated in Figure 1.30.

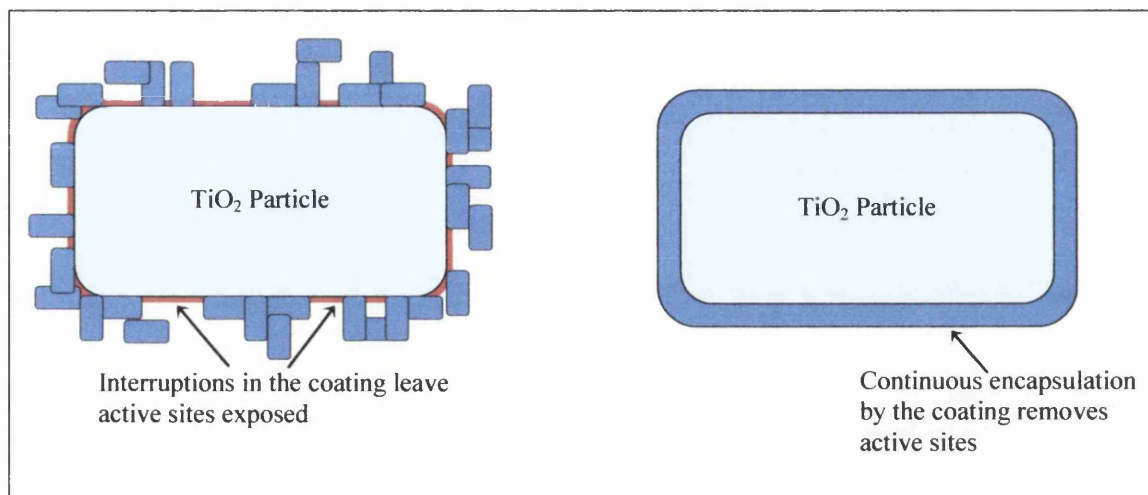


Figure 1.30 - Schematic Illustration of TiO₂ Coatings

Advances in processing methods have shifted the production of coated TiO₂ from large agitated vats to a more continuous processing route. The coatings are only a few atoms thick and are generally colloidal in nature so even minor alterations can significantly affect performance of the product. Within the TiO₂ industry photostabilising coatings are of immense value and details regarding both composition and application processes are closely guarded secrets. Manufacturers only supply very basic information about pigments and current techniques lack the sensitivity to analyse the coated pigments, as a result very little is known about the chemical or lattice structure of photostabilising coatings.

The dispersion characteristics of TiO₂ can be refined by application of organic surfactants. Polyalcohols and their derivatives⁴³ are used to promote wetting of the pigment particles in the polymeric coating medium. Kronos 2220 is coated with a polysiloxane to de-polarise the TiO₂ surface and improve wetting by the non-polar molecules in PVC⁴⁴. A schematic of the mechanism by which surfactants improve dispersion is shown in Figure 1.31. The hydrophilic polar heads of the surfactants attach themselves to the pigment surface via hydrogen bonding leaving the non-polar hydrocarbon ends free to link with the non-polar molecules of the polymer resin⁴³.

Pigments are designed for use with a specific polymer and are specified as such by manufacturers^{43, 45}. Optimum performance can only be guaranteed when a pigment is used with its specific polymer and variation from the specifications may have a detrimental effect on the aesthetics or durability of a coating.

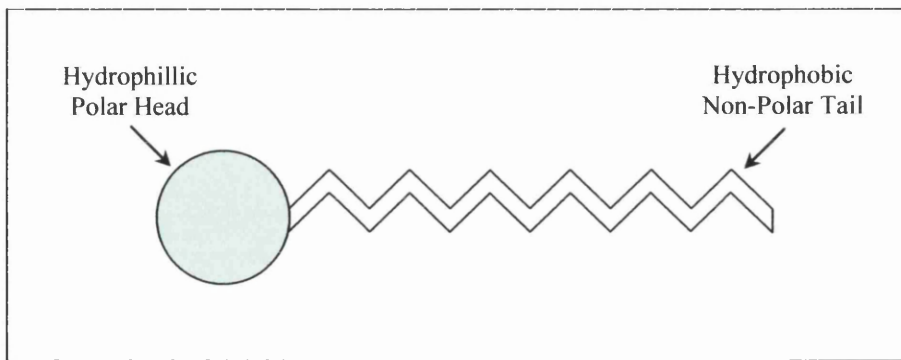


Figure 1.31 - Schematic Illustration of a Surfactant

The actual TiO_2 content of a coated pigment varies between grades and is typically in the region of 90-95%. It is essential that the amount of coating applied to pigments is kept as low as possible in order to maintain the optical properties of TiO_2 ⁴⁴. If the percentage of TiO_2 (relating to the total pigment) is too low then the ability of the pigment to 'shield' the polymer is reduced. This results in an increase in direct photolysis of the polymer due to higher UV penetration^{44, 46}.

1.5.1.4 Grinding and Finishing

In order to break down aggregates and agglomerates formed during the manufacturing processes the TiO_2 is ground using a fluid energy mill as shown in Figure 1.32. Pigment particles are injected into the disk-shaped mill which uses steam to accelerate the pigment particles to high speed. The high particle density and speed within the mill causes collisions between the particles which work to break down agglomerates.

During the grinding process the fluid mill also roughly grades the pigment particle size. The fluid is injected via an inlet at the edge of the mill and flows to the outlet at the centre creating centrifugal forces within the mill. Large agglomerates are thrown outwards towards the edges of the mill by the centrifugal forces where they continue to undergo collisions and are ground further. The finer particles are carried by the fluid to the centre of the mill where they are discharged along with the fluid and channelled to a cyclonic gas-solid separator to recover the pigment. The separated pigment is then transferred to bags or transport containers and allowed to cool, which due to the excellent thermal insulation properties of TiO_2 can take a while.

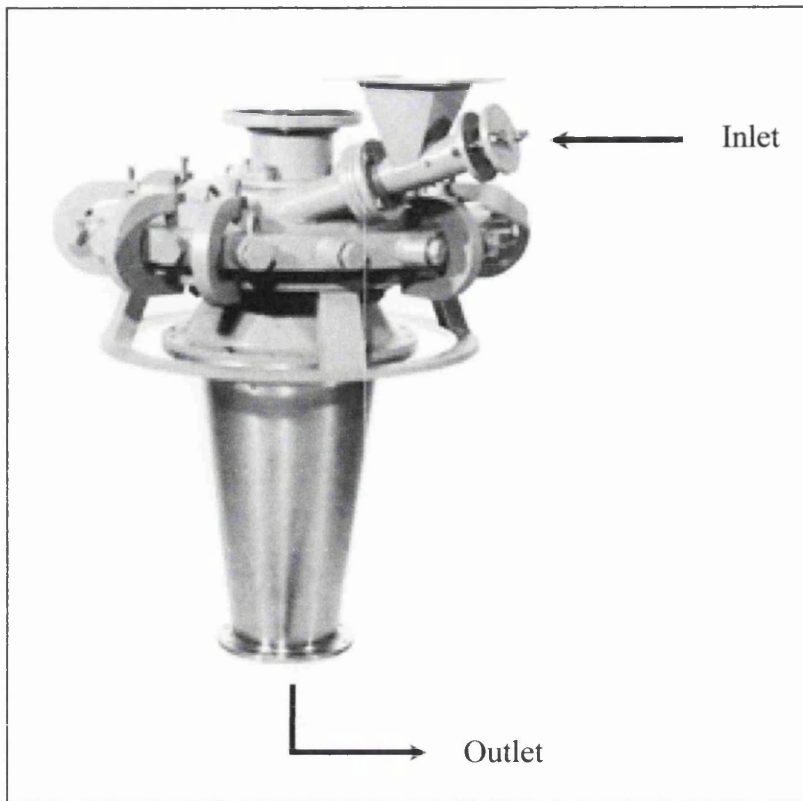


Figure 1.32 - Typical Fluid Energy Mill

1.5.2 Characteristics

The high abundance of TiO_2 coupled with the safe production, processing and disposal make it economical to produce. Titanium is highly abundant occurring naturally as a component of many minerals, four of which - ilmenite (FeTiO_3), rutile (TiO_2), anatase (TiO_2), and leucosene ($\text{TiO}_2 \cdot X\text{FeO} \cdot Y\text{H}_2\text{O}$)⁴¹ serve as ores.

Pigmentary TiO_2 is produced commercially in two crystal phases - anatase and rutile as shown in Figure 1.33 both phases are similarly priced and unlike some lead based white pigments are chemically inert and non-toxic. The anatase and rutile phases of TiO_2 differ in their lattice structure, refractive indices, densities and photoactivity properties.

The main advantage of TiO_2 over other pigments is its superb optical and refractive properties. The refractive index of TiO_2 is unmatched by any other pigmentary material⁴³ and so its ability to confer opacity to a coating is unsurpassed by any other white pigment. For a paint to hide a substrate it has to be able to prevent light from passing through the paint film, hitting the substrate and then reflecting back to the observer. This can be achieved either by complete absorption or reflectance of visible light. Black pigments achieve a hiding effect by absorbing all wavelengths of

incident light, thus appearing black to the eye. White pigments such as TiO_2 provide opacity by scattering and reflecting all wavelengths of incident light. Due to the differences between these hiding mechanisms there is no point in comparing the hiding power of black and white pigments.

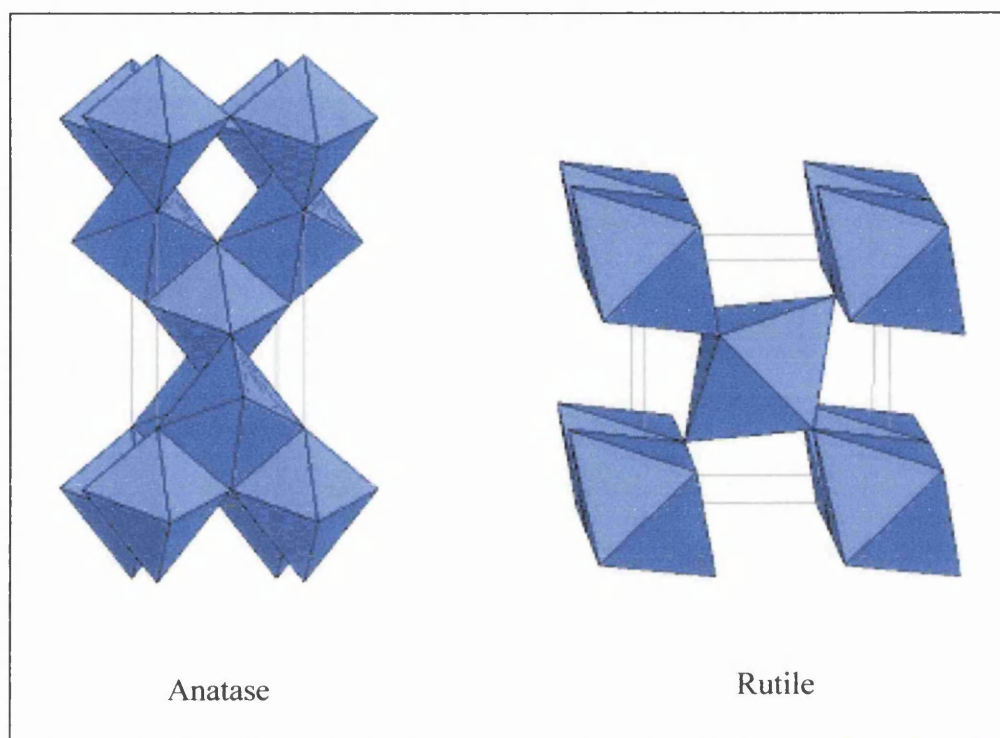
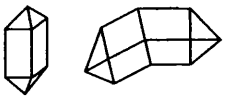
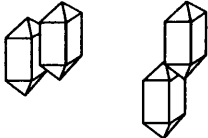
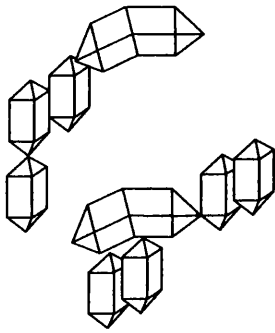


Figure 1.33 – Crystal Structure of Anatase and Rutile TiO_2

The hiding power of a white pigment can be maximised by identifying and producing the optimum pigment particle size for most efficient light scattering. Identification of TiO_2 particle size for optimum light scattering used to be found by trial and error until the introduction of the Mie theory⁴⁷. The Mie calculations are used to identify optimum particle size for scattering of white and green light. The relevance of green light scattering is because the human eye is more sensitive to the wavelengths corresponding to green light and so correlates with perception of brightness.

The Mie calculations assume that that all pigment particles are spherical in shape with a narrow size distribution. In reality, there are a number of crystallite shapes and assemblies present in pigmentary TiO_2 as illustrated in Table 1.3 and therefore calculated values do not correlate exactly with empirical measurements. However, considering the difficulty in measuring and describing the shape and size distribution of pigmentary TiO_2 the differences are acceptable.

Table 1.3 - Typical Types of Particle Coagulation

	<p>Primary Particles: These are single TiO₂ crystal or their crystallographic twins, (twins are two or more lattices inter-grown to some deducible law of symmetry). They range in diameter from 0.1 to 0.3 μm.</p>
	<p>Aggregates: These are primary particles that are connected via grain boundaries, they share crystal faces.</p>
	<p>Agglomerates: These are assemblies of crystallites and aggregates that are bonded together via weak forces. They adhere together at edges and faces.</p>
<p>Not Pictured</p>	<p>Flocs: these are associations of smaller particle assemblies that are bonded extremely weakly. They form spontaneously and disperse under modest shear. They are composed of crystallites, aggregates and agglomerates joined across corners or held together by short-range attractive forces.</p>

The anatase phase of TiO₂ was the first to be used commercially as a pigment however rutile has now surpassed it for two reasons: An equal amount of rutile actually contains fewer but more effective light scattering particles than anatase. The refractive index of rutile TiO₂ is higher than that of anatase²⁵ (2.7 compared to 2.55⁴³), this gives it a 20% light scattering advantage⁴¹ and thus superior capability as a hiding agent. Also the anatase form of TiO₂ is approximately 10 times more photochemically active than Rutile^{25, 47} and so Rutile TiO₂ is favoured in the coatings industry⁴⁸ – particularly for exterior and high UV applications. The purity of the TiO₂ crystal phase is of utmost importance when used as a pigment in high UV applications - typically an impurity level of no more than 1% anatase is acceptable.

Anatase TiO₂ is still commonly used in low UV applications such as paper and fibre production and such is its non-toxicity, as an optical whitener in many commercial products such as foods and toothpastes. More recently anatase TiO₂ has found favour in the photocatalyst industry where increased photoactivity is advantageous in applications such as water purification^{49, 50}, anti-bacterial⁵¹ and self-cleaning products^{52, 53}.

1.5.3 Photoactivity of TiO₂

Solid materials can be categorised into three different types: conductors, semi-conductors and insulators. In order for a material to exhibit conductive properties an electron must be promoted from the valence to the conduction band. Promotion of an electron from the valence to the conduction band is the lowest energy transition possible as there are no molecular orbitals between the bands. Excitation will therefore only occur if an electron is supplied with sufficient energy to allow it to cross the band gap. The categorisation of a material is dependant upon the energy gap (otherwise known as the band gap) between the conduction and valence bands as shown in Figure 1.34.

Insulating materials have a large band gap between the conduction and valence bands. In these materials the energy of visible light is too low to promote an electron across the band gap and so the valence band remains full and the conduction band empty. As a result there is very little room for electron movement and so the material exhibits very low electrical conductivity.

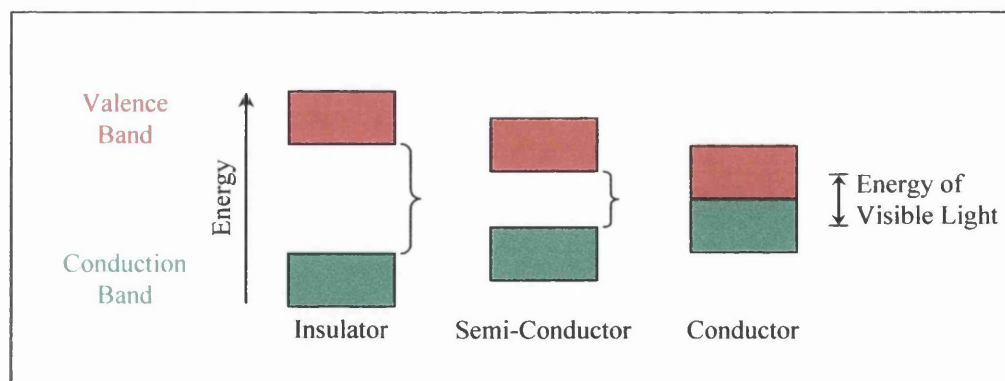


Figure 1.34 - Illustration of Band Gaps and Classification of Solid Materials

Conductors have a very small band gap between the valence and conduction bands. Small amounts of energy as visible light or ambient heat are able to excite an

electron sufficiently to cross the band gap from the valence band to the conduction band. This results in high electron mobility (as both the valence and conduction bands are only partly filled following excitation) and therefore high electrical conductivity. Semi-conducting materials have intermediate band gap energies that lie in between the two extremes of conductors and insulators. In conditions of low energy i.e. low temperature and low light levels they remain in their ground state and behave as insulators. However when supplied with sufficient energy either through light or heat, electrons can be promoted from the valence band to the conduction band resulting in conductive properties.

TiO₂ is a white semi-conducting material with band gap energy of 3.2eV for the Rutile crystal phase. Visible wavelength light is of slightly lower energy than that of the band gap and therefore does not cause excitation of the TiO₂. As a result TiO₂ remains an insulator and reflects all incident visible light, which gives it extreme optical whiteness. The band gap energy of TiO₂ actually corresponds to the wavelength energy of UV light (~380 nm). This correspondence is significant as incident UV irradiation is of sufficient energy to promote an electron across the band gap and thus induce conductive properties in the TiO₂. This excitation creates a highly mobile electron (e⁻) in the conduction band and equally mobile an electron hole (h⁺) in the valence band.

Both the excited electron and electron hole (which is effectively considered to hold a positive charge since it is in the absence of a negative charge) are highly reactive species. The electron has excess energy which it seeks to lose by migrating to the TiO₂ particle surface and transferring to another molecule (often oxygen) via reduction of that molecule. The electron hole does not have excess energy however it is a low energy site that is capable migrating to the surface and accepting an electron in its excited oxidative state. Excited electrons are able to lose their excess energy via this recombination process thus allowing conversion of light energy to chemical energy by the TiO₂.

TiO₂ is classified as a network solid - one 0.2 μm particle contains approximately three-quarters of a billion network bonded atoms in a single extended network or array. A TiO₂ crystal is made up of network bonded Ti⁴⁺ and O²⁻ ions, the valence band is made up of oxygen atomic orbitals and the conduction band from the titanium atomic orbitals. On promotion of an electron from the valence band to the

conduction band the Ti^{4+} ion becomes a Ti^{3+} ion and the O^{2-} ion becomes O^{\cdot} . Being a network solid, TiO_2 is theoretically an octahedral lattice consisting of an infinite array of titanium ions each surrounded by six oxygen ions as shown in Figure 1.35.

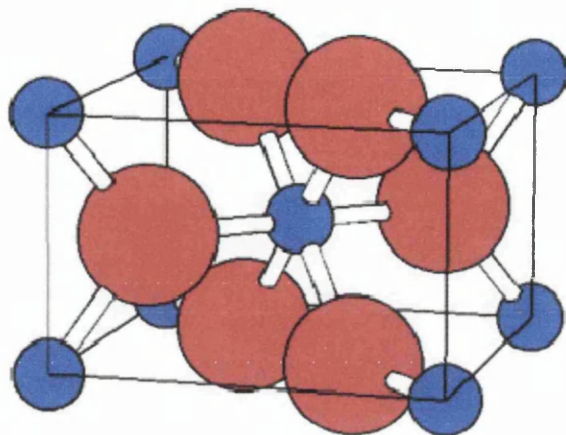


Figure 1.35 - Unit Cell of Rutile TiO_2

This is true of the bulk crystal lattice however at the surface hydroxyl (OH) and water groups can be adsorbed and cause surface interference with the idealistic crystal structure. At the TiO_2 crystal surface oxygen atoms tend to bond with a few titanium atoms and possibly some adsorbed hydrogen atoms, while the oxygen atoms bond to a few titanium atoms and possibly some hydrogen. This manifests itself in such a way that at the surface the Ti^{4+} are replaced with H^+ and the surface potential becomes far less positive than in the remaining bulk of the crystal. As a result, the negative electrons preferentially remain in the bulk crystal near the higher positive charge while the positive holes migrate away from the positive charge towards the crystal surface⁵⁴.

1.5.4 Photocatalysis by TiO_2

As described in above, the band gap energy of TiO_2 corresponds to the wavelength of UV light. Therefore incident UV irradiation (<390nm) is able to promote an electron from the valence band into the conduction band resulting in production of mobile and highly reactive e^- and h^+ species as shown in Equation 1.2.



Immediately following excitation it is common for the electron and hole to recombine to TiO_2 . If this however does not occur, it is possible for the excited electron to reduce a nearby oxygen atom and form a highly reactive oxygen radical as

shown in Equation 1.3. This leaves the positive hole free to oxidise any nearby hydroxyl anions to hydroxyl radicals as shown in Equation 1.4, reverting the TiO₂ back to its ground state.



The O₂• produced via oxygen reduction then undergoes further reactions in the presence of water to form per-hydroxyl radicals as shown in Equation 1.5.



The complete reaction process shown in Equation 1.6 does not feature TiO₂ since it is completely regenerated to its ground state upon oxidation of the electron hole in Equation 1.4. TiO₂ acts only as a catalyst to the reaction producing the highly reactive HO₂• and OH• radicals which are responsible for oxidation of the organic/polymeric component of a coating. Figure 1.36 shows a schematic illustration of TiO₂ photocatalysed polymer oxidation. There are likely to be a large number of unidentified intermediates produced during this reaction, which along with the reaction products are largely dependant on the polymer itself.

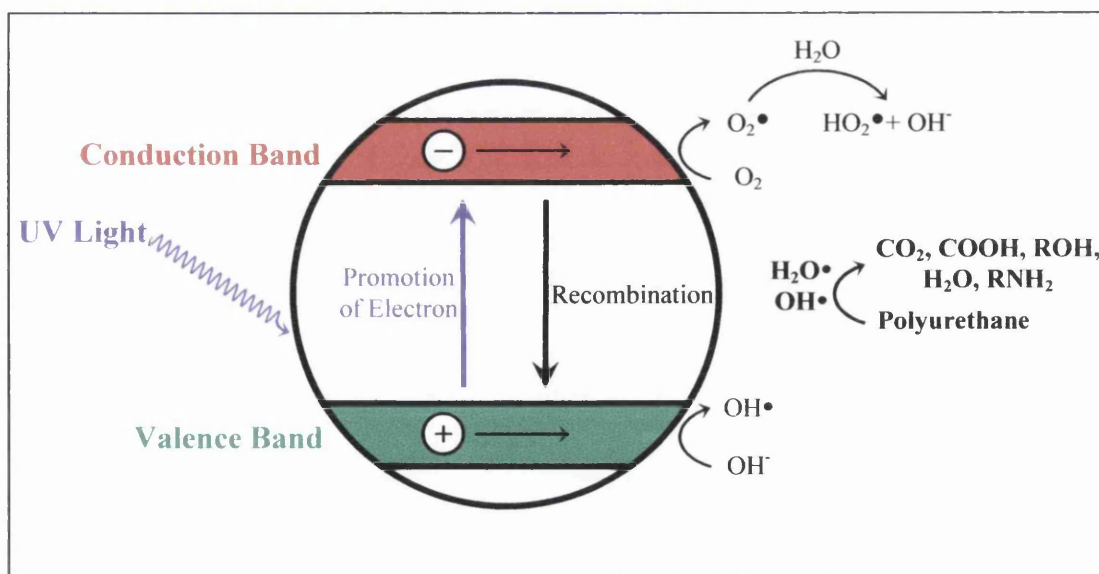


Figure 1.36 - Simplified Illustration of TiO₂ Photocatalysed Oxidation of Polyurethane

As previously discussed the reactions occurring during TiO₂ photocatalysed oxidation primarily manifest themselves as gloss loss and colour change. If allowed to

continue oxidation can lead to chalking and changes to the physical properties of the paint such as cracking and increased porosity.

1.5.4.1 Further Influences of TiO₂ on Coating Degradation

The photoactivity grade and dispersion of TiO₂ pigments can significantly affect the durability of a polymer coating. As previously described, TiO₂ is highly UV absorbent and can therefore act to shield polymer molecules from direct photolysis by UV. A highly photoactive grade however, upon absorbing UV irradiation becomes photoactive and photocatalyses oxidation of the surrounding polymer to such an extent that any positive effect of shielding is significantly overshadowed. One obvious solution to this problem would be to use a less photoactive pigment, however lower UV absorbency may lead to an increase in direct photolysis of the polymer by the UV light component.

The preferred method of protection is to apply surface treatments to a more photoactive grade of TiO₂. Inorganic oxides of silicon aluminium and zirconium are applied to the TiO₂ pigment to increase stability. These coatings protect the polymer from the effects of pigment photoactivity whilst not actually decreasing the ability of the TiO₂ particles to absorb and scatter UV. The literature^{35, 55, 56, 57, 58, 59, 60} has shown that incorporation of stabilised pigments significantly reduces polymer photo-oxidation compared to more photoactive TiO₂ grades.

Other factors such as paint film thickness and dispersion or flocculation of the pigment particles may influence the effectiveness of TiO₂ and therefore the characteristics of a coating. In a thin coating it is possible for UV to penetrate the coating and reflect back off the substrate and as a result not all the incident UV is absorbed. As a result less photo-oxidation will occur in comparison to a thicker coating which absorbs the entire UV component. Although this scenario may be preferable from a durability point of view, due to light reflection from the substrate the coating may not exhibit complete opacity.

Pigment dispersion also affects the photocatalytic activity of TiO₂, literature⁶¹ has shown that reducing agglomerates and consequently improving dispersion reduces photocatalytic oxidation of 2-propanol. This phenomenon can be applied to coatings and the decreased photo-oxidation is a combination of two effects:

Firstly, pigment agglomerates do not provide the same level of shielding to the polymer compared to well dispersed particles. As a result the film is more easily

penetrated by UV light in comparison to a coating with well dispersed pigment as illustrated in Figure 1.37. For a coating with a specific pigment loading the presence of TiO_2 agglomerates results in large areas of effectively un-pigmented polymer. The agglomerated pigment particles shield one another and not the polymer, leaving it more susceptible to direct photolysis. In contrast well dispersed pigment particles absorb more UV irradiation thus preventing it penetrating the coating and causing direct degradation of the polymer.

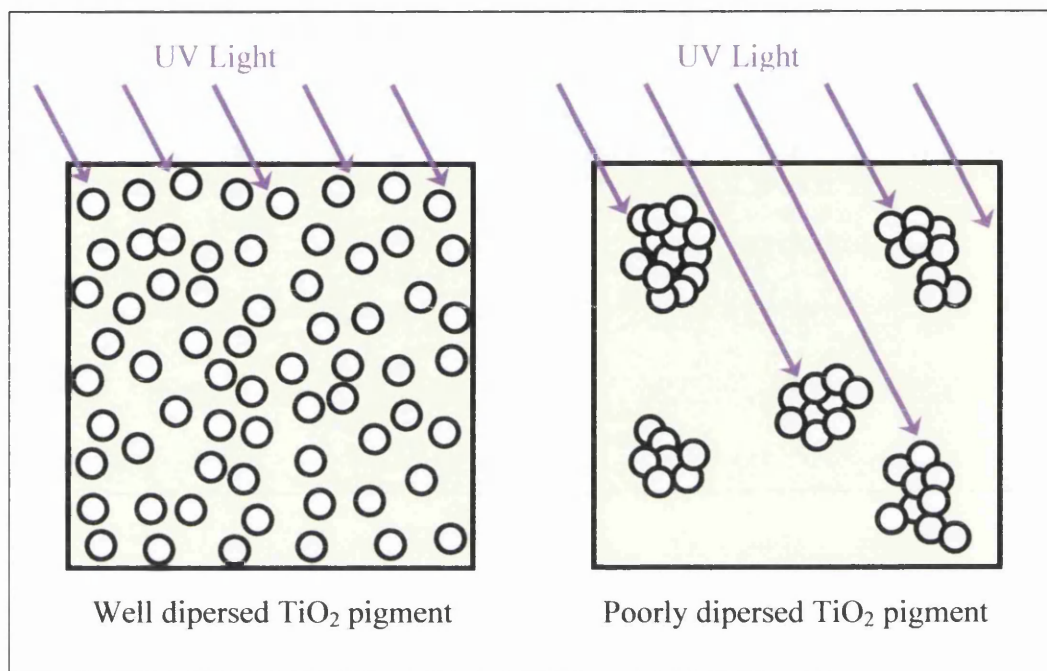


Figure 1.37 - Schematic Illustration of TiO_2 Dispersion Effects in a Polymeric Coating

Secondly, due to the close confines of particles within TiO_2 agglomerates the particles are able to facilitate charge transfer between one another as illustrated in Figure 1.38a. Increased likelihood of charge transfer reduces that of recombination between the electron and hole. This increases the likelihood of the free radical formation and subsequent oxidation reactions within the surrounding polymer. Well dispersed, discrete particles as illustrated in Figure 1.38b cannot transfer charge between one another facilitate charge transfer and the majority of the time recombination between the electron and hole occurs with no detrimental effect on the coating.

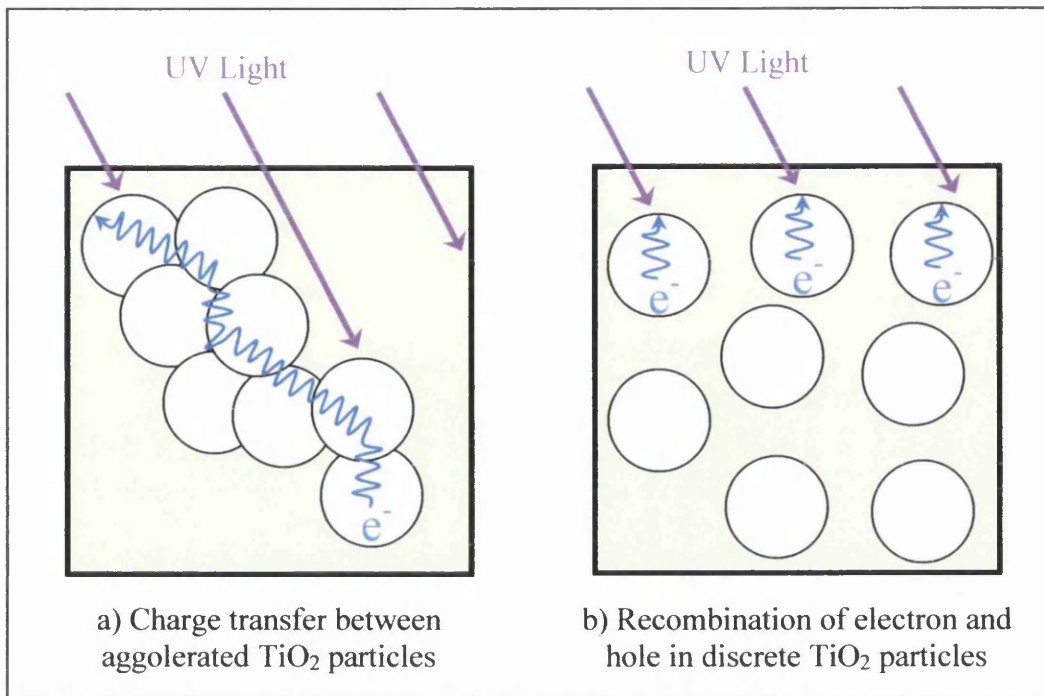


Figure 1.38 (a & b) - Schematic Illustration of Charge Transfer in Agglomerated and Discrete TiO_2 Pigment Particles

The effects of pigment dispersion in a coating system may at times contrast those which are anticipated. In the case of a stabilised TiO_2 grade good dispersion of the pigment provides good UV absorption, light scattering and protection of the binder. However if pigment is considered to be photoactive and likely to cause photocatalysis of oxidation then some agglomeration may be desirable as agglomerated particles shield one another from the UV. This results in less absorption of UV irradiation and photoactivation of TiO_2 thus reducing photocatalysed oxidation of the polymer.

1.6 Weathering and Accelerated Testing

Evaluation of coating durability is of utmost importance in the pre-finished steel industry. In order to continually improve and develop coatings manufacturers require a means of benchmarking the performance of new products against current systems to give an accurate prediction of durability.

Ideally coating durability should be assessed by exposure of a system to its expected service environment however, given current expectancies of the service life for most products this would take an inconceivably long time. With guarantees on

many products exceeding twenty years natural weathering would be unacceptably slow if the continual progress now expected from the industry is to be achieved. As a result manufacturers have become reliant upon accelerated durability testing to provide reliable performance data in a shorter time frame.

Accelerated durability testing artificially simulates ageing of a coating by exposure to more severe conditions than those expected of the service environment for example, UV irradiation that is either of higher intensity or longer duration than natural sunlight. During development of accelerated test methods it is important to ensure that while the conditions applied in the test are capable of accelerating weathering effects that they are not overly aggressive. If conditions are overly aggressive they can interfere with the natural mechanisms of degradation giving results that are inconsistent with natural weathering⁶². The continual search for tests that more closely simulate natural weathering has led to the development of enhanced means of testing which offer more genuine results than older testing systems.

The environment to which a coating system is exposed is highly significant as different combinations of environmental factors such as sunlight (UV exposure) temperature, oxygen, humidity, rainfall and pollutants can influence the nature and rate of degradation^{62, 63}. At present polymeric coating systems are tested using a combination of natural weathering at commercial sites and modern accelerated techniques to achieve the most accurate results in optimum time.

1.6.1 Natural Exposure

Natural exposure is a crucial factor in benchmarking coating durability. The weathering results gained from natural exposure are often viewed as the primary test and the standard to which laboratory tests must match⁶⁴. In order to generate natural exposure data in a short enough time-frame it has become standard to carry out weathering in commercial sites such as Florida, Arizona, and the Hook of Holland.

On identification of the expected service environment of a coating it is possible to identify a location which offers similar but more severe conditions to those expected during service. Samples are exposed in the chosen location for a period of no less than two years to allow acceptable time for natural weathering and degradation to occur. Although this is a lengthy process in comparison to laboratory based accelerated tests, external exposure is necessary to guarantee durability

specifications within the industry. External exposure in these locations of extreme climate provides reliable natural weathering data in a far shorter and more acceptable time-frame than exposure in expected service conditions.

The sub-tropical climate of Miami, Florida has become the standard for external weathering in the paint and automotive (OEM) industries⁶⁵. The high humidity, temperature, rainfall, UV intensity make Miami more severe than about 95% of the U.S⁶⁶. External exposure in Florida provides an accelerated yet reliable performance prediction of coatings intended for service in Europe. South facing exposure of samples angled at 45° are widely acknowledged to undergo the same degree of weathering in one year at Florida compared to four years in Europe^{62, 67}.

The Hook of Holland provides both a marine and highly industrialised environment. This location provides a more harsh combination of corrosive species than would normally be present and is primarily used to assess their effects on products intended for service in highly corrosive service environments.

The weathering site in the Arizona desert is used to benchmark products intended for service in hot, dry climates such as the Middle East and Australia. The average high temperature of 25°C, high UV intensity and low annual rainfall of 200mm have also made the Arizona desert popular as commercial site for EMMA/EMMAQUA testing which is discussed in more detail in Section 1.6.1.3.

When testing a coating system via natural exposure it is of great importance to record the environmental conditions for the entire test duration. Variables such as the intensity and length of UV exposure, temperature, humidity, rainfall, pH and other contaminants can significantly affect degradation and must therefore be considered during durability analysis. It is also important to consider the time of exposure as this can affect the amount and rate of degradation occurring for example, six months of exposure from July to December is very different to six months from October to March. External exposure equipment has been developed to enhance or concentrate the weathering variables present during natural exposure allowing acceleration of natural degradation mechanisms.

1.6.1.1 Adjusted Angle Open Back Rack

Test specimens are supported by two thin rails at either end of the panel with the back of the panels left open to allow radiation of heat and prevent overheating as shown in Figure 1.39. The irradiation angle of the south facing rack is decreased with

the seasonal angle of the sun to ensure maximum UV irradiation throughout the duration of external testing. Samples are positioned 45° from horizontal during the winter months and the irradiation angle adjusted in 10° increments throughout the seasons to 5° from horizontal in summer.

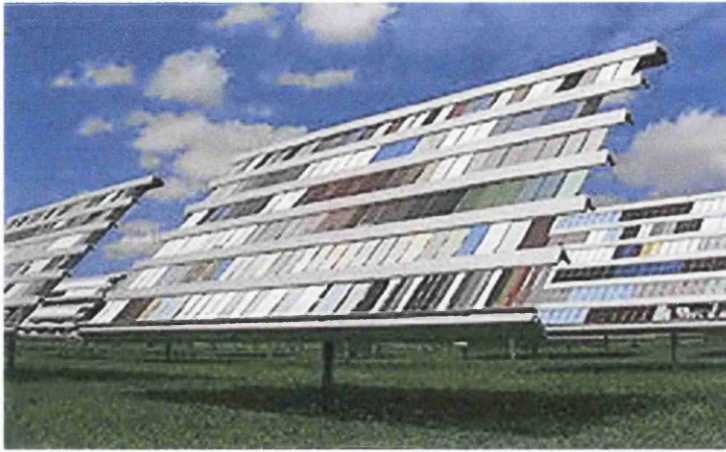


Figure 1.39 - Adjusted Angle Open Back Rack

1.6.1.2 Adjusted Angle Standard Black Boxes

These are used to simulate the UV exposure and temperatures experienced by horizontal surfaces during the summer. The samples are placed on the top of the box with no visible openings as shown in Figure 1.40. This inhibits air circulation and creates a dead air cavity inside the box - designed to simulate the inside of a car on a hot day. The irradiation angle can be altered according to the seasonal angle of sunlight, further increasing the effects of irradiation even when the sun is at its weakest.



Figure 1.40 - Adjusted Angle Standard Black Boxes

1.6.1.3 EMMA/EMMAQUA (Equatorial Mount with Mirrors for Acceleration)

Test samples are mounted on a rack with Fresnel mirrors positioned as shown in Figure 1.41. The mirrors focus sunlight onto a small area of test panel thus intensifying the natural solar irradiation by anything from 5-15 times while the rotatable rack tracks the angle of sunlight throughout the day to increase testing efficiency and. In addition to increased UV intensity, EMMAQUA also simulates precipitation or high humidity levels via use of programmable water jets that deliver distilled water at designated times. It is possible through use of EMMAQUA testing to generate external degradation results in a four to five month test period - theoretically equivalent to 24-30 months of external exposure in Florida or ten years in Europe⁶².

In order to prevent overheating and consequent thermal degradation a fan positioned at the rear of the rack maintains air circulation over the back of the specimen panels however, care must still be taken when interpreting the results. The increased intensity of irradiation in EMMA and EMMAQUA causes sample temperatures far higher than under normal exposure conditions and cause possible initiation of thermo-oxidation mechanisms which may be mistaken for UV induced oxidation.



Figure 1.41 - EMMA/EMMAQUA Test Rig

1.6.2 Artificial Exposure

Unlike external exposure tests, laboratory-based accelerated weathering tests have the advantage of fully controlled and easily reproducible exposure conditions. This is however, only truly useful if the degradation stages are of the same nature as experienced by a system within its service environment. It is widely accepted that the greater the acceleration, the lower the correlation with real-time external exposure. UV irradiation of too high an intensity can introduce new higher energy photochemistries that initiate degradation mechanisms not found under natural weathering conditions leading to poor correlation of results.

1.6.2.1 Xenon Arc

Xenon arc is considered to provide the best simulation of full spectrum natural sunlight providing radiation from wavelengths of ~330nm continuing through the visible light spectrum as shown in Figure 1.42. The system is able to monitor the spectrum and via the use of filters remove unwanted wavelengths for example, that of shorter wavelength than natural sunlight. The type of filter used is dependant on the coating system being tested and the conditions to which the end product will be exposed. Via filtering it is possible to simulate a range of conditions including daylight and window glass, allowing an accelerated simulation of the effects of service environment on the product.

Xenon arc is also able to simulate effects of moisture through water spray and/or humidity control systems. Control of humidity is recommended in the testing of many systems due to its effect on the rate and type of coating degradation. The Ci 65 CAM 180 xenon arc test runs a 180 minute cycle consisting of irradiation and water spray stages as follows:

Stage 1 – 40 minutes irradiation at 70°C with no precipitation

Stage 2 – 20 minutes irradiation at 70°C with rain (water spray) on the sample front

Stage 3 – 60 minutes irradiation at 70°C with no precipitation

Stage 4 – 60 minutes with no irradiation at 38°C and rain (water spray) on the front and back side of the sample

One disadvantage of xenon arc is the high degree of temperature fluctuation seen between the light and dark cycles, which can introduce mechanical changes to the coating and affect the rate of degradation.

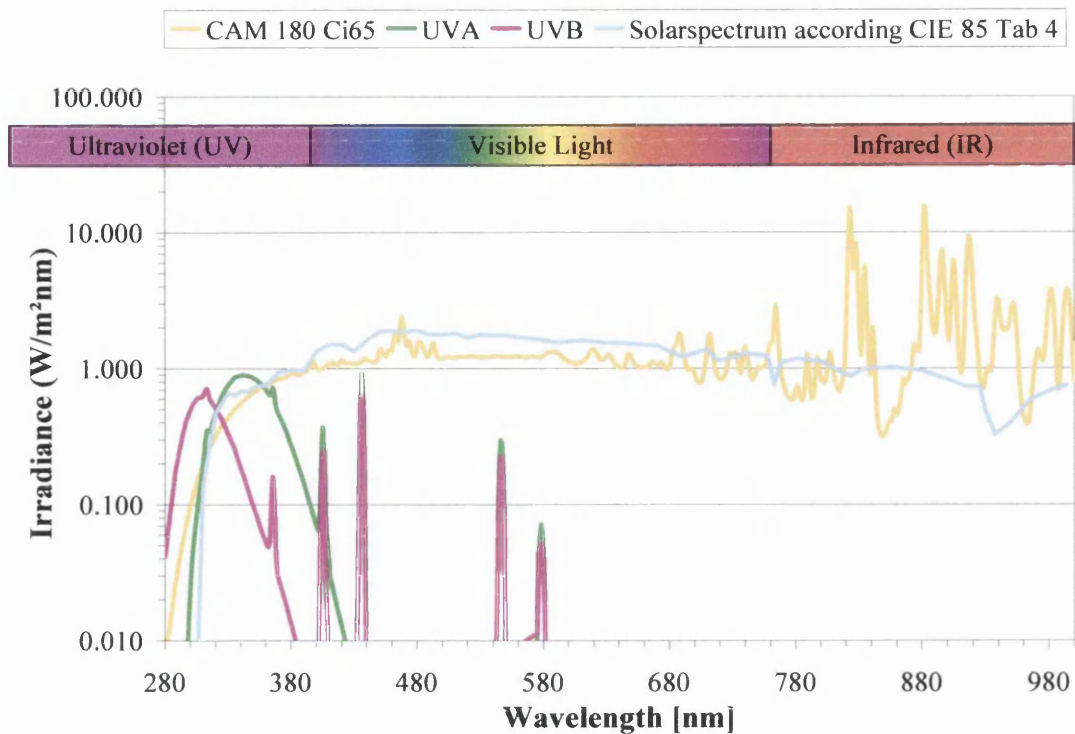


Figure 1.42 - Wavelength Spectra of Natural Sunlight, QUV and Xenon Arc

1.6.2.2 QUV A/QUV B

QUV enables simulation of both UV A and UV B irradiation dependant on the lamps used during testing. UV A lamps emit irradiation at about λ_{\max} 340nm, producing a spectrum that most closely matches the UV component of natural sunlight.

UV B lamps produce irradiation at about λ_{\max} 313nm, thus simulating the shorter wavelength irradiation that often causes the most degradation in coating systems. The drawback of QUV B is that the intensity of UV B irradiation is far higher than that found in natural sunlight – the UV B component of which is very small as shown in Figure 1.42. The increased intensity of aggressive UV B irradiation causes changes to the degradation mechanisms that are widely acknowledged within the coating industry to be inconsistent with that of natural weathering.

Samples are exposed in a weathering chamber to cycles of high intensity UV irradiation, elevated temperatures, and moisture - which includes both condensation humidity and water sprays. The controlled and flexible mix of these aggressive weathering variables intends to reproduce the damage caused by sunlight, rain and condensed surface moisture or dew. The samples are mounted in test racks, placed in the QUV chamber and subjected to set weathering cycles - dependant on the intended

application of the systems. The regular cycle for QUV A and B testing is 4 hours of dry irradiation at 60°C followed by 4 hours of condensation with no irradiation at 50°C. This cycle is repeated for extended periods of time - up to thousands of hours, simulating periods of time than would be expected for the service life of a system.

There is no precise correlation between the resistance of a system to QUV testing and external environment durability as sunlight, heat, and relative humidity vary from one place to another. One test is therefore unable to reproduce all weathering conditions, for example the behaviour of a given system in a desert or at a coast. Despite this QUV weathering is useful in the comparison of different paint systems as conditions are easily controlled and reproducible, unlike natural external exposures. Test results provide a benchmark for coating durability when compared to systems with QUV and external weathering performance data.

1.6.3 Physical Measures of Degradation

The durability of a coating is commonly assessed by measuring physical changes in the coating properties that are known to occur as a result of degradation. These changes occur at the coating surface and include weight loss, film thickness loss, gloss loss, chalking, colour change, crazing, cracking and delamination (loss of adhesion).

1.6.3.1 Loss of Coating Weight and Film Thickness

The degradation and loss of surface polymeric material can be quantitatively expressed as a measurement of dry film thickness (DFT) or weight loss. Oxidation of polymeric matrix produces - amongst other things, carbon dioxide and water which escape the film as gasses leading to a reduction in physical matter and consequently mass.

1.6.3.2 Gloss Loss and Chalking

Coating gloss is a measure of surface roughness and is commonly used as a major physical measurement of polymer degradation in the coatings industry⁶⁸. Loss of gloss occurs as a result of unequal degradation at the coating surface⁶⁹ causing the coating to become pitted and rough. A decrease in coating gloss is evidence of degradation occurring and thus gloss retention (compared to the initial gloss) is used to measure the resistance of a coating to degradation.

If this degradation is allowed to continue it becomes more serious and can result in chalking of the coating. In the presence of UV light TiO_2 can initiate free-radical reactions, which cause oxidation of the polymer component surrounding the pigment particle as shown in Figure 1.43. This results in exposure of the insoluble TiO_2 at the coating surface, which appears as a chalky white residue as illustrated in Figure 1.44.

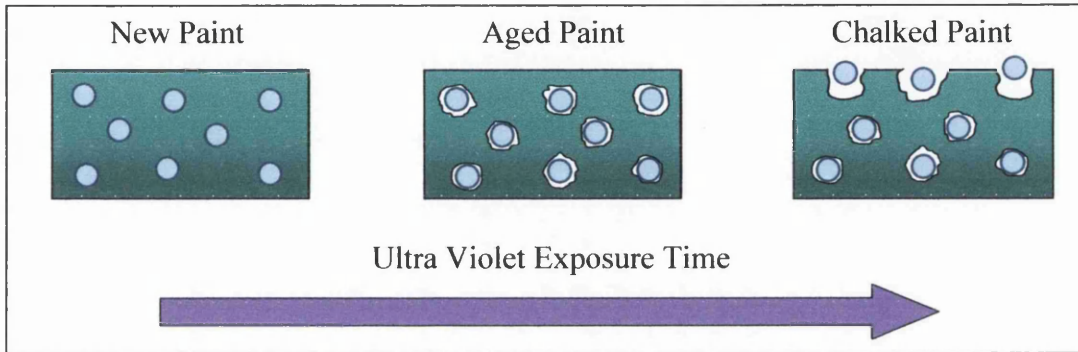


Figure 1.43 - Chalking of TiO_2 Pigmented Paint

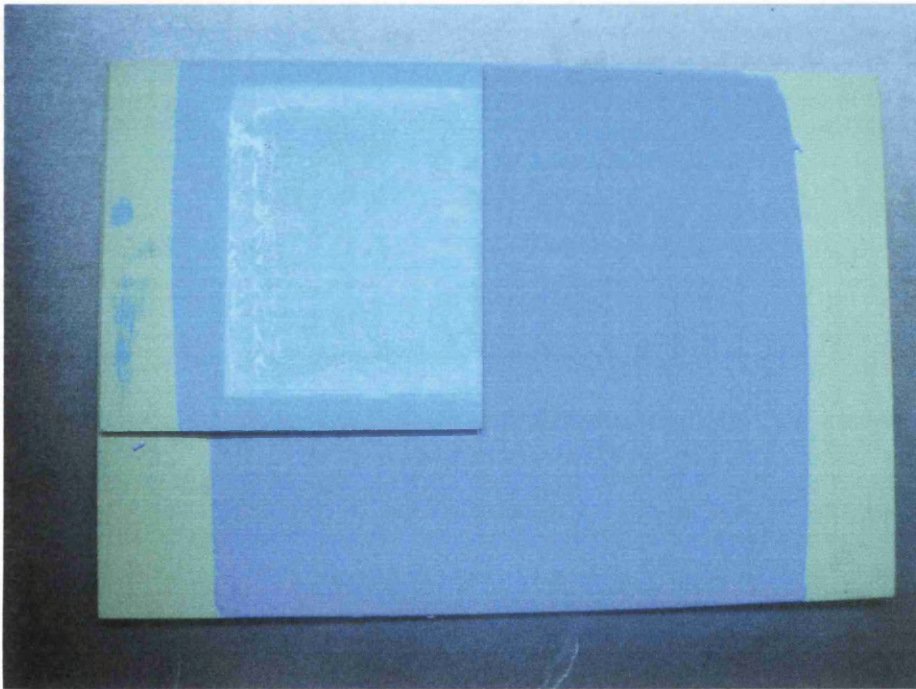


Figure 1.44 – Example of a Coating Exhibiting Severe Chalking Set Against the Control

Gloss loss is measured by monitoring light reflection of the coating surface, while chalking can more easily be assessed visually or by using an adhesive tape pull. Both of these methods can be used to measure the extent of degradation quickly and

easily however, they are physical measurements and therefore not as sensitive and accurate as chemical analysis techniques.

1.6.3.3 Colour Retention

The colour change of a coating is significant when assessing durability as even slight changes in the colour are indicative of the chemical and physical changes within the polymer that are associated with degradation mechanisms. During weathering the colour of a coating can change in numerous ways including, fading, darkening, whitening (in the case of chalking⁷⁰) or overall yellowing of the film^{25, 36, 71}. This is not only an indication of degradation, but is also (and equally important as colour primarily used to improve aesthetics) unsightly and undesirable to the consumer.

Colour can be quantitatively measured using a spectrophotometer and the most common method of data generation in the coatings industry uses the CIE Lab colour space. This measures colour as coordinates on the L, a and b axes and gives measurements for the lightness, position between magenta and green and position between yellow and blue respectively. This provides accurate data on the colour that can be used to identify the amount of colour change occurring during weathering.

1.6.3.4 Crazeing and Cracking

The exposure of a coating to weathering sources and subsequent degradation causes the occurrence of chemical reactions, resulting in scission of the long polymer chains that make up the coating, to short brittle chains. The scission of these chains and changes in the chemical and physical structure of the film leads to increased stress in these areas. This increase in stress coupled with a decrease in flexibility causes the coating to crack^{72, 73}, and in extreme cases flake off prior to gloss loss or chalking.

1.6.4 Chemical Tests used to Quantify Degradation

As previously discussed, it is understood that oxidation of a polymer manifests itself as physical changes^{59, 70, 74} in the coating. Within the coatings industry these changes are often used to assess degradation however, events such as gloss loss, chalking and colour change only occur after a significant period of time. In contrast,

the chemical processes that lead up to these physical changes occur from the outset of the weathering process and can be identified in a far shorter time period⁷⁵.

Measurement of these chemical changes allows identification and quantification of degradation far in advance of the occurrence of physical changes, which may take months or even years to become apparent. Increased understanding of the mechanisms involved in polymer photo-oxidation has led to an increase in the number of chemical techniques^{75, 76, 77, 78} available for measurement of degradation. With continued improvement in the understanding and quantification of degradation, the correlation between accelerated weathering and natural exposure continues to improve.

1.6.4.1 Infrared and Fourier Transform Infrared Spectroscopy

Infrared (IR) spectroscopy is one of the oldest techniques of analysing the chemical composition of substances and has become an indispensable technique in the study of polymer degradation. Infrared spectroscopy works on the principle that each substance has a unique combination of chemical bonds that absorb IR radiation at specific energies and wavelengths. By measuring the amount and wavelengths of IR energy absorbed by these bonds it is possible to identify the chemical composition of a substance, as no two dissimilar substances have the same combination of chemical components and bonds.

Organic molecules often contain many of the same functional groups and as a result the absorbance spectra for these substances often look very similar. In this case particular attention is paid to the lower wavenumbers (1400 to 400 cm^{-1}), which correspond directly to the backbone stretches and vibrations influenced by the functional groups present in a molecule. The fingerprint region is so-called as the absorbencies between 1400 to 400 cm^{-1} are unique to a specific molecule and can provide positive identification of its composition.

Historically IR spectroscopy was carried out using a double-beam infrared spectrometer that used a grating to split the signal into discrete wavelengths which were examined individually. A chopper was used to alternately examine the reference and sample beams and the difference in signal was then sent in a linear fashion. This procedure was carried out for the entire IR spectrum and was very time consuming and complex.

Modern infrared spectrometers use Fourier transform interferometry and are capable of scanning all wavelengths of interest in a single scan. The IR light is guided into the sample via an interferometer, and the resultant beam (or interferogram) translated to an absorbance spectrum by complex Fourier transform calculations^{79, 80}. Current instruments have the ability to digitally add and subtract spectra allowing far more accurate post run analysis and comparison. One such calculation - and probably the most relevant, is measurement and subtraction of the background spectrum from that of the sample to ensure that the spectrum is genuinely indicative of the sample. This ability for spectral modification alongside the extensive library of spectral analysis available has greatly improved the speed and precision of chemical identification and analysis.

The development and use of numerous techniques in IR analysis has led to a far better understanding of the degradation mechanisms occurring within different polymers. Selection is dependant on the nature of sample, areas of interest and the technical expertise/apparatus available. The most commonly used technique in studying polymer degradation are transmission^{36, 37}, attenuated total reflectance (ATR)⁸¹ and photoacoustic spectroscopy⁸².

Transmission

The IR beam is passed through a thin sample and the transmission radiation measured to give data on the amount and wavelengths of energy absorbed by the sample. This method provides high quality spectra⁷⁵ but practically sample thickness can pose a challenge as samples should be thin ($\sim 5\text{-}7\mu\text{m}$ max)⁷⁶ enough to transmit light. If the sample thickness is too high then attenuation can occur, causing distortion of the spectrum.

One drawback of transmission spectroscopy is that commercial coating samples are often too thick (the topcoat thickness of commercial samples can range from 25-200 μm) or are applied on non-IR transmitting substrates such as steel. This can be overcome by preparation of the sample by microtoming however this requires a significant amount of skill to ensure high quality samples. The spectra gained from transmission IR are representative of the bulk sample and thus this method is not suitable for analysing localised areas of interest as they may be lost in the full spectrum.

Attenuated Total Reflectance (ATR)

This method uses an IR transparent crystal (or internal refraction element IRE) to penetrate a small distance into the sample providing uniform surface contact and thus high spectrum quality^{75, 76}. Radiation is reflected at the interface between the crystal and sample and an evanescent wave is formed which can infiltrate a small distance into the sample^{76, 83}. During each reflection the sample surface selectively absorbs wavelengths of the IR light and thus the radiation loses energy at these wavelengths to give a spectrum of the surface and near-surface material. As measurements are gained by reflection ATR spectroscopy can be carried out on thick and low transmission samples with minimal or no preparation.

Recent developments have lead to the development of an ATR image mapping technique. This relatively new practice has the ability to map small areas of interest in a coating with a spatial resolution of 4µm. This technique is particularly useful in analysis of multilayer coatings as it is possible to identify and analyse individual layers within a cross section sample, giving far greater insight into the entire coating system.

Photoacoustic Spectroscopy (PAS)

This is a non-destructive technique that directly measures the absorbance spectrum of a polymer based coating without direct radiation, reflection or transmission⁷⁶. Modulated mid infrared radiation is used to establish alternated heating and cooling which impacts on the coupling gas in contact with the sample. This causes expansion and contraction of the gas which is detected by an acoustic detector and transducer into a photoacoustic signal. PAS provides a quick means of analysing coatings with little or no sample preparation.

Gaseous Product Detection

Recent work on chemical analysis of coating degradation has lead to the development of reactors which, when used in photoactivity tests in conjunction with the FTIR give quantitative data on the rate and degree of coating photodegradation^{73, 76}. These methods use transmission FTIR in conjunction with a gas cell fitted with metal-halide windows (usually calcium fluoride or potassium chloride) which do not exhibit IR spectra or react with ambient moisture.

There are two main ways of carrying out gaseous product detection, both of which measure the evolution of carbon dioxide (CO₂) as a product of polymer photo-

oxidation. The first^{39, 57, 61, 84, 85, 86} measures evolved CO₂ from a polymeric sample irradiated with UV light from within the gas cell at regular intervals. The second^{35, 55, 56, 60} and most relevant to this research, measures evolved CO₂ from a sample irradiated in an flat chamber connected by a closed loop system to the gas cell. This system measures CO₂ evolution at timed intervals providing a cumulative plot, which can be used to monitor the kinetics and calculate the rate of photo-oxidation.

1.6.4.2 Tube Photoactivity Test Reactor⁵⁵

The first irradiation apparatus of this description was the tube reactor which used a series of interconnecting tubes in a closed loop system series as shown in Figure 1.45. The irradiation chamber consists of two hinged half-cylinders each housing 6 x 8W Coast Wave Blacklight UV lamps ($\lambda_{\mu\alpha\xi}$ 365nm) set on a semi-circular aluminium reactor. Four internally coated tubes were connected to a diaphragm pump and the gas stream circulated into a gas cell containing calcium fluoride windows mounted in the FTIR spectrometer. The CO₂ levels in the system were measured by the FTIR as set intervals using timed scans providing a cumulative plot of evolution throughout the test duration.

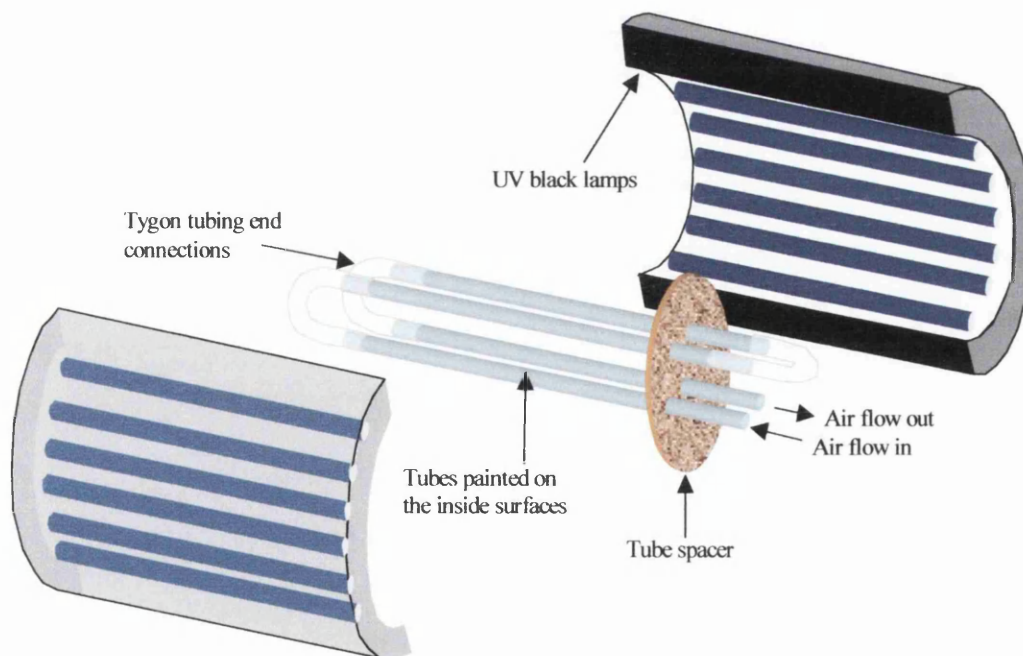


Figure 1.45 - Four Tube Arrangement and Lamp Set Up

1.6.4.3 The Flat Panel Reactor⁵⁶

Although successful the tube photoactivity reactor posed practical challenges in production of coated samples, most notable the difficulty in producing uniformly coated samples of a known thickness. As a result a flat panel reaction cell was developed, allowing irradiation of flat coated samples in a closed loop system similar to that of the tube reactor as shown in Figure 1.46.

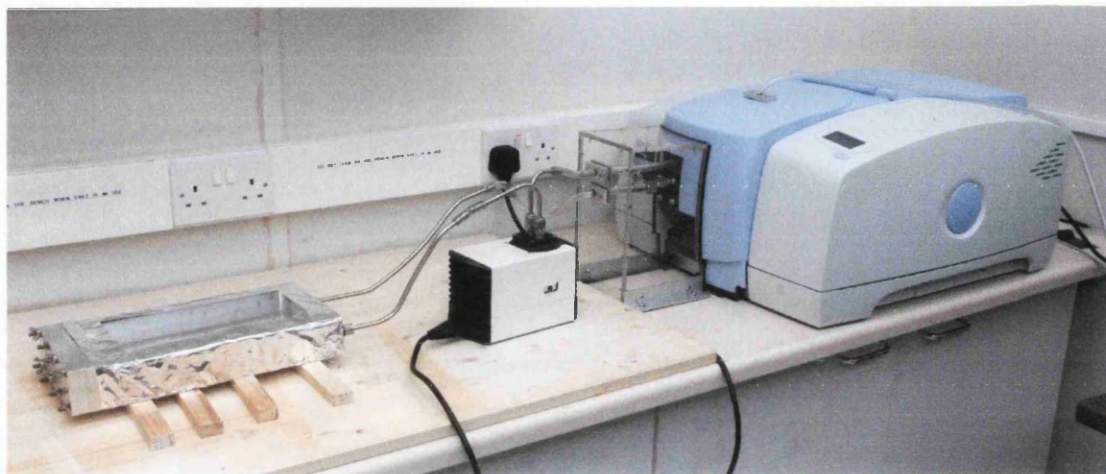


Figure 1.46 – The FTIR Flat Panel Irradiation Apparatus

The reaction cell is machined from a single block of aluminium with small bore holes drilled into the cell to provide air circulation over the sample. A negative air pressure is set up within the cell by means of 25 x 0.5mm inlet holes on one side and 25 x 1mm output holes on the other to ensure rapid mixing and maximum exhaustion of the gaseous products. The coated sample is introduced through a slit in the reactor, which is closed by a sealed metal block incorporating a metal tongue which fills the slot snugly to prevent dead air spaces and gas escape from the opening.

The window through which the panel is irradiated is bonded with epoxy and protected by an aluminium foil cover to prevent direct irradiation and subsequent degradation of the adhesive, minimising potential of gas leakage. The apparatus is connected in a closed loop system using stainless steel piping with a minimal number of joints to minimise air escape. The gas within the system is circulated using a diaphragm pump into the gas cell within the FTIR sampling compartment as shown in Figure 1.47, where the concentration of CO₂ is measured by the FTIR at timed intervals.



Figure 1.47 – Close-up of Gas Cell within the FTIR Sampling Compartment

The advantage of this apparatus in comparison with the initial reactor is the ability to calculate the exact surface area and film thickness of the flat panel of paint. This allows more accurate calculation of CO₂ evolved versus paint coverage and subsequent quantification of the photo-oxidation rate.

1.7 Conclusions and Aims

Polymer photo-oxidation still proves a challenge to the coatings industry, particularly with the increased focus on improving product aesthetics and durability over recent years.

The development of the FTIR flat panel irradiation apparatus⁵⁶ described in Section 1.6.4.3, has provided a rapid means of evaluating coating stability by measuring the CO₂ evolved as a product of photo-oxidation. Although successful, the use of this apparatus has until present been limited to model PVC and polyethylene

coatings^{35, 56, 60, 87, 88}. This thesis aims to use this test to evaluate the durability of different polymers, namely polyurethane and polyester-melamine coatings.

The first stage of this work investigates the effects of different TiO₂ pigments and polymer components on coating durability. The results from the flat panel irradiation apparatus are compared to results of QUV A and xenon arc weathering in order to make an accurate prediction of coating durability.

Commercially produced coatings commonly contain additives to improve the durability or aesthetic appearance of the product. The majority of pre-finished steel products are not white and therefore a range of coloured coatings are evaluated in Chapter Five.

Colorcoat Prisma[®] is a very successful polyurethane coated pre-finished steel product which has increased significantly in popularity over recent years. Polyamide beads are incorporated into Colorcoat Prisma[®] to produce a textured product with an excellent aesthetic appearance. Chapter Six investigates the effect of texturing agents on the durability of polyurethane coating systems.

1.8 References

1. Corus Colors Ltd, *Colorcoat HPS200[®] Ultra*. 2008: Flintshire, Wales.
2. Corus Colors Ltd, *The Colorcoat Building Manual*. 2005: Flintshire, Wales.
3. Graziano, F., *Metal Finishing*, 2000. **98**(6): p. 175-176.
4. Trethewey, K.R. and Chamberlain, J., *Corrosion for Science and Engineering*. 2 ed. 1995, Longman Scientific and Technical: Essex.
5. Elvins, J., Spittle, J.A., and Worsley, D.A., *Corrosion Engineering, Science and Technology*, 2003. **38**(3): p. 197-204.
6. Wilson, A.D., Nicholson, J.W., and Prosser, H.J., *Surface Coatings* Vol. 2. 1988, Elsevier Applied Science Publishers: London.
7. Williams, G., McMurray, H.N., and Worsley, D.A., *Journal of the Electrochemical Society*, 2002. **149**(4): p. B154-B162.
8. Williams, G. and McMurray, H.N., *Corrosion Science: a Retrospective and Current Status in Honor of Robert P Frankenthal*, 2002. **2002**(13): p. 453-463.
9. Williams, G. and McMurray, H.N., *Electrochemical and Solid State Letters*, 2003. **6**(3): p. B9-B11.
10. McMurray, H.N., Williams, D., Williams, G., and Worsley, D., *Corrosion Engineering Science and Technology*, 2003. **38**(2): p. 112-118.
11. Williams, G. and McMurray, H.N., *Electrochemical and Solid State Letters*, 2004. **7**(5): p. B13-B15.
12. Williams, G., Holness, R.J., Worsley, D.A., and McMurray, H.N., *Electrochemistry Communications*, 2004. **6**(6): p. 549-555.
13. McMurray, H.N. and Williams, G., *Corrosion*, 2004. **60**(3): p. 219-228.
14. Lambourne, R. and Strivens, T.O., *Paint and Surface Coatings* 2ed. 1999, Woodhead Publishing: Cambridge.

15. Corus Colors Ltd, *Colorcoat Prisma*[®] 2005: Flintshire, Wales.
16. Bock, M., *Polyurethanes for Coatings*. European Coatings Literature, ed. U. Zorll. 2001, Vincentz Network: Hanover.
17. Boxall, J. and Von Frauhhofer, J.A., *Concise Paint Technology*. 1977, Elek Science: London.
18. Wright, P. and Cumming, P.C., *Solid Polyurethane Elastomers*. 1969, Maclaren and Sons: London.
19. Wicks, D.A. and Wicks Jr., Z.W., *Progress in Organic Coatings*, 2001. **43**(1-3): p. 131-140.
20. Lomolder, R., Plogmann, F., and Speier, P., *Journal of Coatings Technology*, 1997. **69**(868): p. 51-57.
21. Wicks Jr., Z.W., N., J.F., and Pappas, S.P., *Organic Coatings Science and Technology* Vol. 1 - Film Formation, Components and Appearance. 1992, John Wiley and Sons: New York.
22. Van Der Weij, F.W., *Journal of Polymer Science Part a - Polymer Chemistry*, 1981. **19**(2): p. 381-388.
23. Degussa AG, *Vestosint*[®] *Polyamide 12 Coating Powder*: Marl, Germany.
24. The HMMM Coalition, *Final Submission for Hexamethoxymethylmelamine*. No. 201-15310A. 2004.
25. Mc Kellar, J.F. and Allen, N.S., *Photochemistry of Man-Made Polymers*. 1979, Applied Science Publishers: London.
26. Allen, N.S. and Mc Kellar, J.F., *The Role of Luminescent Species in the Photooxidation of Commercial Polymers*, in *Developments in Polymer Degradation*, N. Grassie, Editor. 1979, Applied Science Publishers: London. p. 129-158.
27. Pospisil, J., Pilar, J., Billingham, N.C., Marek, A., Horak, Z., and Nespurek, S., *Polymer Degradation and Stability*, 2006. **91**(3): p. 417-422.
28. Allen, N.S. and Edge, M., *Fundamentals of Polymer Degradation and Stabilisation*. 1992, Elsevier Applied Science Publishers: London.
29. Rabek, J.F., *Photodegradation of Polymers, Physical Characteristics and Applications*. 1996, Springer Verlag: Berlin
30. Gardette, J.L., Gaumet, S., and Philippart, J.L., *Journal of Applied Polymer Science*, 1993. **48**(11): p. 1885-1895.
31. Scott, G., ed. *Developments in Polymer Stabilisation* Vol. 1. 1979, Elsevier Applied Science Publishers: London.
32. Cheremisinoff, N.P., ed. *Handbook of Polymer Science and Technology*. Vol. 3. Applications and Processing Operation. 1989, Marcel Dekker Inc: New York.
33. Bacaloglu, R. and Fisch, M., *Polymer Degradation and Stability*, 1994. **45**(3): p. 315-324.
34. Gupta, T. and Adhikari, B., *Thermochimica Acta*, 2003. **402**(1-2): p. 169-181.
35. Robinson, A.J., *The Development of Organic Coatings for Strip Steels with Improved Resistance to Photodegradation*. 2005, Eng. D, University of Wales Swansea
36. Wilhelm, C., Rivaton, A., and Gardette, J.L., *Polymer*, 1998. **39**(5): p. 1223-1232.
37. Wilhelm, C. and Gardette, J.L., *Polymer*, 1997. **38**(16): p. 4019-4031.
38. Mielewski, D.F., Bauer, D.R., and Gerlock, J.L., *Polymer Degradation and Stability*, 1991. **33**(1): p. 93-104.
39. Wilhelm, C. and Gardette, J.L., *Polymer*, 1998. **39**(24): p. 5973-5980.

40. Cunliffe, A.V. and Davis, A., *Polymer Degradation and Stability*, 1982. **4**(1): p. 17-37.
41. Braun, J.H., *Journal of Coatings Technology*, 1997. **69**(868): p. 59-72.
42. Adams, R., *Focus on Pigments*, 2007. **2007**(1): p. 1-2.
43. Kronos International Inc, *Kronos Titanium Dioxide in Plastics*. 1993: Leverkusen, Germany.
44. Kronos International Inc, *More than 30 Years of Reliability in PVC Profile Protection - Kronos 2220 and Kronos 2222 TiO₂*. 2002: Leverkusen, Germany.
45. Kronos Worldwide Inc, *Application Fields for Kronos TiO₂ Grades (Plastics)*. (Cited 28th February 2008). Available from: <http://www.kronostio2.com/>.
46. Diebold, M.P. *Unconventional Effects of TiO₂ on Paint Durability*. in *5th Nürnberg Conference*. 1999. Nuremberg, Germany
47. Bohren, C.F. and Huffman, D.R., *Absorption and Scattering of Light by Small Particles* 1998, Wiley Interscience: New York.
48. Marrion, A.R., ed. *The Chemistry and Physics of Coatings*. 1994, The Royal Society of Chemistry: Cambridge

49. Ollis, D., Pelizzetti, E., and Serpone, N., *Photocatalysis: Fundamentals and Applications*. 1989, Wiley Interscience: New York.
50. Morris, S., *Photocatalysts for Water Purification* 1992, Ph.D, University College of Swansea.
51. Chung, C.J., Lin, H.I., and He, J.L., *Surface and Coatings Technology*, 2007. **202**(4-7): p. 1302-1307.
52. Cai, R., Van, G.M., Aw, P.K., and Itoh, K., *Comptes Rendus Chimie*, 2006. **9**(5-6): p. 829-835.
53. Guan, K., *Surface and Coatings Technology*, 2005. **191**(2-3): p. 155-160.
54. Marganski, R.E., *Abstracts of Papers of the American Chemical Society*, 1998. **216**: p. U608-U608.
55. Worsley, D.A. and Searle, J.R., *Materials Science and Technology*, 2002. **18**(6): p. 681-684.
56. Robinson, A.J., Searle, J.R., and Worsley, D.A., *Materials Science and Technology*, 2004. **20**(8): p. 1041-1048.
57. Christensen, P.A., Dilks, A., Egerton, T.A., and Temperley, J., *Journal of Materials Science*, 1999. **34**(23): p. 5689-5700.
58. Jin, C.Q., Christensen, P.A., Egerton, T.A., Lawson, E.J., and White, J.R., *Polymer Degradation and Stability*, 2006. **91**(5): p. 1086-1096.
59. Gesenhues, U., *Polymer Degradation and Stability*, 2000. **68**(2): p. 185-196.
60. Searle, J.R., *Titanium Dioxide Pigment Photocatalysed Degradation of PVC and Plasticised PVC Coatings*. 2002, Eng. D, University of Wales Swansea.
61. Egerton, T.A. and Tooley, I.R., *Journal of Physical Chemistry B*, 2004. **108**(16): p. 5066-5072.
62. Genevay, J.P., *Predicting Durability of Industrial Coatings*, article in *Corrosion Management*, 2005. **64**(March/April): p. 13-17.
63. Jarrold, J., *Polymer, Paint and coatings Journal*, 1997. **932**(3): p. 21.
64. Putman, W.J., Martin, J.L., and Pekara, D. *Overview of Outdoor Accelerated Paint Weathering Tests*. in *IBEC, Automotive Body Painting*. 1994.
65. Pickett, J.E. and Gardner, M.M., *Polymer Degradation and Stability*, 2005. **90**(3): p. 418-430.
66. Bauer, D.R., *Polymer Degradation and Stability*, 2000. **69**(3): p. 307-316.

67. Scott, J.L., *Journal of Vinyl Technology*, 1994. **16**(2): p. 116-123.
68. Morse, M.P., *Accelerated Outdoor Weathering Tests for Evaluating the Durability of Coatings*, in *Permanence of Organic Coatings*, G.G. Schurr, Editor. 1982, American Society for Testing and Materials: Philadelphia. p. 43-66.
69. Van Der Ven, L.G.J., Leuverink, R., Henderiks, H., and Van Overbeek, R., *Progress in Organic Coatings*, 2003. **48**(2-4): p. 214-218.
70. Birmingham, J.N., *Journal of Vinyl & Additive Technology*, 1995. **1**(2): p. 84-87.
71. Singh, R.P., Tomer, N.S., and Bhadraiah, S.V., *Polymer Degradation and Stability*, 2001. **73**(3): p. 443-446.
72. Oosterbroek, M., Lammers, R.J., Vanderven, L.G.J., and Perera, D.Y., *Journal of Coatings Technology*, 1991. **63**(797): p. 55-60.
73. Nichols, M.E., Gerlock, J.L., Smith, C.A., and Darr, C.A., *Progress in Organic Coatings*, 1999. **35**(1-4): p. 153-159.
74. Allen, N.S. and Katami, H., *Polymer Degradation and Stability*, 1996. **52**(3): p. 311-320.
75. Adamsons, K., *Chemical Depth Profiling of Automotive Coating Systems Using IR, UV-VIS and HPLC Methods*, in *Service Life Prediction - Methodologies and Metrologies*, J.W. Martin and Bauer, D.R., Editors. 2002, American Chemical Society: Washington, DC. p. 185-211.
76. Bauer, D.R. and Adamsons, K., *The Role of Fundamental Mechanistic Studies in Practical Service Life Predictions*, in *Service Life Prediction - Methodologies and Metrologies*, J.W. Martin and Bauer, D.R., Editors. 2002, American Chemical Society: Washington, DC. p. 162-184.
77. Gerlock, J.L., Smith, C.A., Cooper, S.A., Kaberline, T.J., Prater, T.J., Carter (III), R.O., Kucherov, A.V., Misovski, T., and Nichols, M.E., *A Brief Review of Paint Weathering Research at Ford*, in *Service Life Prediction - Methodologies and Metrologies*, J.W. Martin and Bauer, D.R., Editors. 2002, American Chemical Society: Washington, DC. p. 212-249.
78. Jean, Y.C., Cao, H., Zhang, R., Yuan, J.P., Chen, H.M., Mallon, P., Huang, Y., Sandreczki, T.C., Richardson, J.R., Calcara, J.J., and Peng, Q., *Characterization of Physical and Chemical Deterioration of Polymeric Bridge Coatings*, in *Service Life Prediction - Methodologies and Metrologies*, J.W. Martin and Bauer, D.R., Editors. 2002, American Chemical Society: Washington, DC. p. 299-315.
79. Press, W.H., Flannery, B.P., Teukolski, S.A., and Vetterling, W.T., *Numerical Recipes in C - The Art of Scientific Computing* 1ed. 1988, Cambridge University Press: New York.
80. Arfken, G., *Mathematical Methods for Physicists*. 3 ed. 1985, Academic Press: London.
81. Wernstahl, K.M., *Polymer Degradation and Stability*, 1996. **54**(1): p. 57-65.
82. Yang, X.F., Vang, C., Tallman, D.E., Bierwagen, G.P., Croll, S.G., and Rohlik, S., *Polymer Degradation and Stability*, 2001. **74**(2): p. 341-351.
83. Jin, C.Q., *FTIR Studies of TiO₂ Pigmented Polymer Photodegradation*. 2004.
84. Christensen, P.A., Dilks, A., Egerton, T.A., and Temperley, J., *Journal of Materials Science*, 2000. **35**(21): p. 5353-5358.
85. Christensen, P.A., Egerton, T.A., Martins-Franchetti, S.M., Jin, C., and White, J.R., *Polymer Degradation and Stability*, 2008. **93**(1): p. 305-309.

86. Fernando, S.S., Christensen, P.A., Egerton, T.A., and White, J.R., *Polymer Degradation and Stability*, 2007. **92**(12): p. 2163-2172.
87. Robinson, A.J., Wray, J., and Worsley, D.A., *Materials Science and Technology*, 2006. **22**(12): p. 1503-1508.
88. Martin, G.P., *The Stabilisation of PVC Plastisol using Hydrotalcite (HT)*. 2007, Eng. D, University of Wales Swansea.

Chapter 2

Experimental Techniques

2.1 Coated Sample Preparation

This research has focussed on durability testing of polyurethane, polyester-melamine and model Poly Vinyl Chloride (PVC) coatings. A range of coatings containing different commercially available titanium dioxide (TiO₂) grades, colour pigment additions and texturing agents were produced to test the effects of these components on coating durability.

The polyurethane and polyester-melamine paints were solvent-borne, one-component, oven curing coating systems. These coatings contained the basic constituents of any polymeric coating system - polymer resin, pigment and solvent. A small amount of additives were also present to increase the casting and curing capabilities of the coating.

The PVC coatings were simple model paint systems consisting of only three basic components, PVC resin, Tetrahydrofuran (THF) solvent and pigment. This section outlines the techniques used for formulating coatings.

2.1.1 Polyurethane and Polyester-Melamine Coating Formulation

The polyurethane and polyester-melamine coatings were all one component, oven cured formulations produced in conjunction with Bayer Material Science, Leverkusen. The polyurethane coatings tested throughout this research were all produced by reaction of a polyfunctional, hydroxyl bearing polyester with a blocked polyisocyanate. The polyester-melamine coatings were based on the same polyester resins used in the polyurethane coatings cross-linked with hexamethoxy-methylmelamine (HMMM).

2.1.1.1 White Pigmented Polyurethane Coatings

In all cases the coatings were produced in two stages. Firstly a formulation of polyester resin, TiO₂ pigment and solvents was prepared and ground in a bead mill. The formulation was then filtered and the polyisocyanate, catalysts and other components were added to produce a fully formulated coating.

Formulation

The polyester resin, TiO₂ pigment, and solvents were weighed into a 500ml bottle in the order specified by the production guidelines. The bottle was then topped up with 80-100g of glass grinding beads and ground in a bead mill for 15 minutes to ensure even mixing and deagglomeration of the pigment particles. Once mixing was

complete the pigment particle size was measured using a Hegman draw down gauge, to ensure formulation grind size of <math><5\mu\text{m}</math>.

Let-Down

The formulation was produced in excess to allow for loss during the grinding process, and following grinding was filtered to remove the glass beads. The formulation was then weighed into a 250ml bottle and let down with appropriate additions of polyester resin, polyisocyanate, solvent, catalyst and flow agents as specified by the guidelines. This was shaken for a further 15 minutes to ensure uniform mixing and allowed to stand for 5 minutes prior to casting.

The formulation guidelines for the first series coating containing the standard polyester and HDI isocyanate and the second series containing an adapted polyester and HDI isocyanate are shown in Table 2.1 and Table 2.2 respectively. The third series coatings based on the IPDI polyisocyanate and the HDI/IPDI were produced according to the guidelines in Table 2.3 and Table 2.4 respectively. The coating based on the IPDI polyisocyanate was formulated with flexible polyester, while the Coating based on the HDI/IPDI polyisocyanate contained the same adapted polyester polyol as the second series HDI coatings.

Table 2.1 - Formulation Guidelines for First Series White Pigmented Polyurethane Coatings Based on a Standard Polyester Polyol and HDI Polyisocyanate

Formulation	% by wt. addition
Desmophen T 1665, 65% by wt. (polyester)	9.50
TiO ₂ pigment	28.66
Solvesso 200 S (solvent)	8.10
Let-Down	
Desmophen T 1665, 65% by wt.	21.20
Desmodur BL 3175, 75% by wt. (isocyanate)	11.60
Celluloseaceto butyrate CAB 531-1, 10% by wt. (flow agent)	6.88
Acronal 4 F, 50% by wt. (flow agent)	1.38
Addocat 201 (DBTL), 10% by wt (catalyst)	0.86
Solvesso 200 S	11.82

**Table 2.2 - Formulation Guidelines for Second Series White Pigmented Polyurethane Coatings
Based on an Adapted Polyester Polyol and HDI Polyisocyanate**

Formulation	% by wt. addition
Desmophen T XP 2326, 60% by wt. (polyester)	8.73
TiO ₂ pigment	26.20
1-Methoxypropyl acetate-2 (flow agent)	2.30
Solvesso 200 S (solvent)	5.00
Let-Down	
Desmophen T XP 2326, 60% by wt.	28.38
Desmodur BL 3175, 75% by wt. (isocyanate)	5.24
Celluloseaceto butyrate CAB 531-1, 10% by wt. (flow agent)	6.55
Acronal 4 F, 50% by wt. (flow agent)	1.31
Catalyst 201N 10% by wt. (catalyst)	0.78
Solvesso 200 S	15.51

**Table 2.3 - Formulation Guidelines for Third Series White Pigmented Polyurethane Coatings
Based on a Flexible Polyester Polyol and IPDI Polyisocyanate**

Formulation	% by wt. addition
Desmophen T 1775, 70% by wt. (polyester)	9.74
TiO ₂ pigment	29.23
Solvesso 200 S (solvent)	7.80
Let-Down	
Desmophen T 1775, 70% by wt.	15.73
Desmodur BL 4265, 65% by wt. (isocyanate)	15.59
Celluloseaceto butyrate CAB 531-1, 10% by wt. (flow agent)	7.30
Acronal 4 F, 50% by wt. (flow agent)	1.46
Catalyst 201N, 10% by wt. (catalyst)	0.87
Solvesso 200 S (solvent)	12.28

**Table 2.4 - Formulation Guidelines for Third Series White Pigmented Polyurethane Coatings
Based on an Adapted Polyester Polyol and HDI/IPDI Polyisocyanate**

Formulation	% by wt. addition
Desmophen T XP 2326, 60% by wt. (polyester)	9.70
TiO ₂ pigment	29.11
1-Methoxypropyl acetate-2 (flow agent)	2.56
Solvesso 200 S (solvent)	5.56
Let-Down	
Desmophen T XP 2326, 60% by wt.	31.53
Desmodur VP LS 2352/1, 60% by wt. (isocyanate)	7.28
Celluloseaceto butyrate CAB 531-1, 10% by wt. (flow agent)	7.28
Acronal 4 F, 50% by wt. (flow agent)	1.46
Addocat 201 (DBTL), 10% by wt (catalyst)	0.87
Solvesso 200 S	4.65

In each case these formulations produced a one component coating with a binder/pigment ratio of 1:1. Dibutyltin dilaurate (DBTL) was added to the system as a catalyst to reduce the curing temperature of the coating to PMT ~232°C. If DBTL was not present in the coating formulation the curing temperature would be significantly increased thus impairing the coating quality¹. Other components such as CAB 531-1 and Acronal 4 F were added to the coating to ensure good air-release and flow properties during the casting and curing process.

2.1.1.2 White Pigmented Polyester-Melamine Coatings

Like the polyurethane coatings, the white pigmented polyester-melamine coatings were produced in two stages – the formulation and let-down. The formulation – produced in excess was weighed into a bottle and ground in a bead mill before filtering and adding the let-down in appropriate additions according to the formulation guidelines. The first series coating containing the standard polyester and HMMM cross-linker was produced according to the guidelines in Table 2.5 and the second series coating containing the adapted polyester and HMMM cross-linker (Cymel 303) according to Table 2.6.

Table 2.5 - Formulation Guidelines for First Series White Pigmented Polyester-Melamine Coatings Based on a Standard Polyester Polyol and HMMM Cross-Linker

Formulation	% by wt. addition
Desmophen T 1665, 65% by wt. (polyester)	9.70
TiO ₂ pigment	29.20
Solvesso 200 S (solvent)	7.80
Let-Down	
Desmophen T 1665, 65% by wt.	30.73
Cymel 303 (melamine)	2.98
Celluloseaceto butyrate CAB 531-1, 10% by wt. (flow agent)	7.30
Acronal 4 F, 50% by wt. (flow agent)	1.52
Catalyst 1786B, 50% by wt. (catalyst)	0.18
Butyl diglycol	4.00
Solvesso 200 S	6.59

Table 2.6 - Formulation Guidelines for Second Series White Pigmented Polyester-Melamine Coatings Based on an Adapted Polyester Polyol and HMMM Cross-Linker

Formulation	% by wt. addition
Desmophen T XP 2326, 60% by wt. (polyester)	8.91
TiO ₂ pigment	26.72
1-Methoxypropyl acetate-2 (flow agent)	2.24
Solvesso 200 S (solvent)	4.88
Let-Down	
Desmophen T XP 2326, 60% by wt.	28.95
Cymel 303 (melamine)	4.09
Celluloseaceto butyrate CAB 531-1, 10% by wt. (flow agent)	6.68
Acronal 4 F, 50% by wt. (flow agent)	1.34
Catalyst 1786B (catalyst)	0.13
Solvesso 200 S	17.68

2.1.1.3 Commercial Colour Pigmented Polyurethane Coatings

Recent work² has shown the addition of secondary coloured pigments to affect PVC photodegradation. Polyurethane coatings were produced in a range of five colours; white, red, green, blue and beige to assess the effects of coloured pigment additions on polyurethane photodegradation. These were matt coatings based on the coating formulation used to produce the first series white pigmented polyurethanes. These coatings were formulated in each of the five colours according to the formulation guidelines shown in Table 2.7. Each of the coatings was produced using Tronox R-KB-4 TiO₂ pigment with appropriate additions of the secondary coloured pigments were added in accordance with the formulation guidelines.

Table 2.7 - Formulation Guidelines for Polyurethane Coatings Based on Standard Polyester Polyol and HDI Polyisocyanate Pigmented with Commercial Colour Blends

Formulation	White	Red	Green	Blue	Beige
	% by wt. addition				
Desmophen T 1665, 65% by wt.	8.73	12.75	12.38	16.06	10.71
Tronox R-KB-4	26.27	0.34	6.57	1.58	15.63
Lanxess Bayferrox 130 M		8.13			0.14
Lanxess Bayferrox 303 T		2.75			0.60
Lanxess Bayferrox 3950		0.29	0.82		
Lanxess Chromeoxide Green GN-M			4.44	1.56	
Degussa Lamp Black 101			1.28	3.95	
Heubach Heucodur Blue 2R				12.25	
Heubach Heucodur Yellow 6R					2.98
Solvesso 200 S	7.44	2.28	3.23	5.08	5.08
Let Down					
Desmophen T 1665, 65% by wt.	19.47	15.43	28.45	18.54	23.91
Desmodur BL 3175, 75% by wt.	10.57	1.07	15.43	12.97	12.97
Addocat 201 N, 10% by wt.	0.74	1.87	1.07	0.90	0.90
Acronal 4 F, 50% by wt.	1.28	9.37	1.87	1.58	1.58
CAB 531-1, 10% by wt.	6.43	11.92	9.37	7.89	7.89
Solvesso 200 S	15.18	5.35	11.92	13.07	12.71
Deuteron MK	3.89	12.75	5.35	4.57	4.90

A white coating was produced as a control to assess the effects of matting agent addition of coating photo-oxidation. The coatings were produced in the same manner as the white pigmented polyurethane paints outlined in Section 2.1.1.1. The coating formulation was produced in excess to allow for loss during grinding and filtering. A polyester co-reactant resin was weighed into a bottle and appropriate amounts of pigment and solvent were added in amounts specified by the guidelines. The bottle was then topped up with 80-100g of glass grinding beads and ground in a bead mill for 1-3 hours depending on the particle size of the secondary pigments. The particle size was measured using a Hegman draw down gauge to ensure a formulation grind size of <math><5\mu\text{m}</math>. The formulation was then filtered and the let-down added. Appropriate additions of the components were weighed into the formulation in the order specified by the formulation guidelines.

2.1.1.4 Textured Polyurethane Coatings

Textured coatings were produced to investigate the effects of texturing agent on polyurethane resin stability. White HDI and HDI/IPDI polyurethane coatings pigmented with Tronox R-KB-4 TiO_2 were produced by the method described in Section 2.1.1.1 according to the formulation guidelines in Table 2.1 and Table 2.4 respectively. Following the addition of the let down and shaking, a 4% by weight addition of texturing agent was added to the coating. The coating was then shaken for a further 5 minutes to ensure even dispersion of the texturing agent prior to casting. The coatings produced and details of the texturing agent are shown in Table 2.8.

Figure 2.8 – Texturing Agent Additions to White Pigmented Polyurethane Coatings

Polyurethane Resin	Texturing Agent (4% by wt. addition)
Standard polyester and HDI polyisocyanate	56 μm polyamide beads
Standard polyester and HDI polyisocyanate	50 μm glass beads
Adapted polyester and HDI/IPDI polyisocyanate	56 μm polyamide beads

2.1.2 Production of Polyurethane/Polyester-Melamine Coated Samples

Samples were coated onto steel substrate by the draw-bar coating method using a #038 coiled coating bar to give a 20 μm \pm 1 μm dry film thickness. The formulated coating was mechanically shaken for 15 minutes to ensure any settled

pigment was evenly dispersed then left to stand for 5 minutes allowing air trapped in the paint to escape prior to casting. The systems were coated onto an iron phosphate pre-treated, un-primed, galvanised steel substrate and oven cured. The time and temperature required for the substrate to achieve a PMT of 232°C was determined prior to coating and was dependant on both the substrate and the curing oven.

Prior to casting the substrate and draw bar were cleaned with ethyl acetate and allowed to air dry. A thin line of paint was poured along the top of the substrate and the draw bar coated in the paint and drawn down the substrate in one swift movement as shown in Figure 2.1. Care was taken to ensure an even draw speed and pressure distribution over the sample in order to produce a coating of uniform thickness. The wet sample was oven cured at a high temperature for the appropriate length of time (52 seconds in an oven set at 340°C) then water quenched and dried. Coated samples were checked using a permascope to ensure an even dry film thickness of $20\mu\text{m} \pm 1\mu\text{m}$.

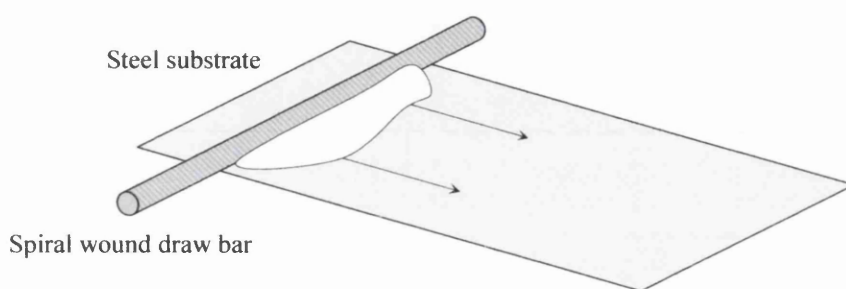


Figure 2.1 – Polyurethane and Polyester-Melamine Flat Panel Coating Process

2.1.3 Model PVC Coating Formulation

The model PVC coatings were simple, air curing paint systems consisting of PVC resin, THF solvent and pigment.

2.1.3.1 White Pigmented PVC Coatings

A range of model coatings were produced to test the photoactivity of different commercial TiO_2 pigments in PVC. The coatings were produced with a pigment loading of 30 per hundred resin (PHR) to facilitate comparison with an existing bank of photoactivity data.

3g of TiO_2 pigment was dispersed in 100ml of THF solvent and mixed for 5 minutes using the high sheer mixer (Heidolph Type RZR1 Variable Speed Mixer) to ensure homogenous particle dispersion. 10g of laboratory grade powdered PVC

(Aldrich MW ca 95000) was then quickly and evenly poured into the mixing dispersion. Adding the PVC relatively quickly produced an even dissolution of the PVC powder with no agglomeration of PVC particles. The coatings were stirred for a further 5 minutes at a constant rate of approximately 1000 rpm to ensure complete PVC dissolution. Paints were then transferred to a solvent bottle and stirred via a magnetic stirrer plate and bar for a further 24 hours prior to casting to ensure complete dissolution of the PVC.

2.1.3.2 Colour Pigmented PVC Coatings

Although the majority of organically coated products are not white, most coloured coatings are pigmented with significant amounts of TiO₂ to increase their covering power. Published work² has documented the effects of adding a single secondary coloured organic pigments to TiO₂ pigmented PVC coatings. The coloured polyurethane coatings outlined in Section 2.1.1.3 contain a blend of inorganic pigments to produce colours more closely associated with commercially produced coloured coatings.

Table 2.9 - Formulation Guidelines for Model PVC Coatings Pigmented with Commercial Colour Blends

Formulation	White	Red	Green	Blue	Beige
	% by wt. addition				
Tetrahydrofuran (THF) (ml)	100 ml	100 ml	100 ml	100 ml	100 ml
Tronox R-KB-4	3.00	0.09	1.65	0.67	2.42
Lanxess Bayferrox 130 M		2.12			0.02
Lanxess Bayferrox 303 T		0.72			0.09
Lanxess Bayferrox 3950		0.08	0.19		
Lanxess Chromeoxide Green GN-M			1.02	0.12	
Degussa Lamp Black 101			0.15	0.18	
Heubach Heucodur Blue 2R				1.90	
Heubach Heucodur Yellow 6R					0.46
Laboratory Grade PVC	10.00	10.00	10.00	10.00	10.00

Model PVC coatings were produced containing the pigment combinations used in the polyurethane coatings to assess the effects of pigment blends on PVC photocatalysed oxidation. Colour pigmented PVC coatings were produced according

to Table 2.9 to maintain a constant inorganic pigment loading of 30 PHR - in keeping with the white pigmented PVC coatings outlined in Section 2.1.3.1.

The appropriate pigment additions specified in Table 2.9 were dispersed in 100 ml THF solvent and mixed for 5 minutes using the high sheer mixer. 10g of powdered PVC was then added to the mixing dispersion and stirred for a further 5 minutes before transferring to a solvent bottle. The colour pigmented coatings were ultrasonicated for 5 minutes to remove any remaining pigment agglomerations and then stirred for a further 24 hours using a magnetic stirrer plate and bar prior to casting.

Coatings containing single secondary coloured pigment additions were also produced to investigate the effects of each colour on PVC photo-oxidation separately. Coatings were formulated using pigment additions of 30 PHR Degussa P25 and 1 PHR of a secondary inorganic coloured pigment to facilitate comparison with existing data for the single secondary pigment additions.

The coatings were produced by dispersing 3g of Degussa P25 and 0.1g of the secondary coloured pigment in THF before adding 10g of powdered PVC and stirring as with the coatings containing the commercial coloured pigment additions. The secondary pigments tested and their composition is shown in Table 2.10.

Table 2.10 – Inorganic Coloured Pigments Tested in Model PVC Coatings

Pigment Name	Composition
Lanxess Bayferrox 130 M	Iron oxide red
Lanxess Bayferrox 303 T	Manganese ferrite black
Lanxess Bayferrox 3950	Zinc ferrite yellow/orange
Lanxess Chromeoxide Green GN-M	Chromium oxide green
Degussa Lamp Black 101	Carbon black
Heubach Heucodur Blue 2R	Cobalt aluminate blue
Heubach Heucodur Yellow 6R	Chrome antimony titanate yellow

2.1.4 Production of PVC Coated Samples

Coated glass sample panels were produced by placing two layers of electrical insulation tape (140µm) down each side of a glass panel to give a consistent height

profile to the dried coating of approximately $20\mu\text{m} \pm 2\mu\text{m}$. Paint was poured onto a secondary panel at the top of the coating panel and drawn down using a glass bar in one swift continuous movement to avoid skinning of the paint. A schematic of the PVC flat panel sample production method can be seen in Figure 2.2. Panels were then allowed to dry in a cool dark environment for a minimum of seven days to ensure full evaporation of all THF and minimise any effect it may have on CO_2 evolution.

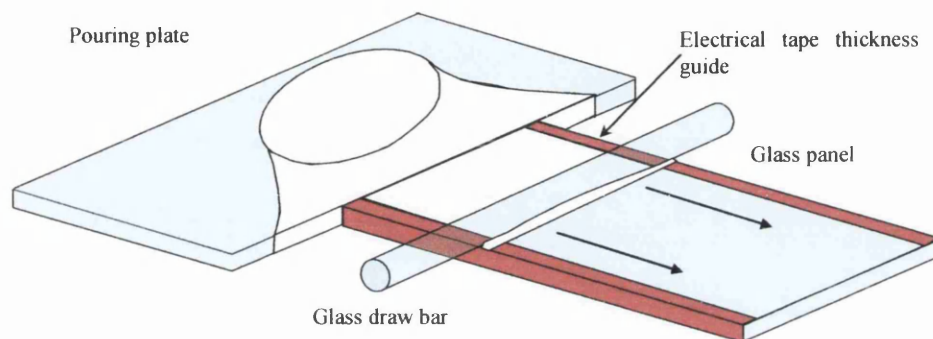


Figure 2.2 – PVC Flat Panel Coating Process

2.2 Accelerated Weathering Techniques

This work used a number of accelerated testing methods to classify coating degradation as a result of titanium dioxide (TiO_2) pigment photoactivity. The evolution of carbon dioxide (CO_2) gas as a product of TiO_2 photocatalysed polymer degradation is well documented^{3, 4, 5, 6, 7, 8}. Exploitation of this phenomenon has led to the development of an accelerated weathering test which allows measurement of CO_2 evolution using a Fourier Transform infrared (FTIR) spectrometer^{2, 9, 10, 11}. Measurement of CO_2 evolution allowed an assessment of coating durability and quantitative analysis of polymer degradation.

QUV A and xenon arc accelerated weathering tests were also used to evaluate coating durability. Use of QUV A and xenon arc weathering to classify coating durability allowed the accuracy of the CO_2 evolution test to be analysed in comparison with commercially accepted methods.

2.2.1 The Fourier Transform Infrared Spectrometer (FTIR) Spectrometer

The FTIR spectrum for CO_2 is comprised of a double peak between 2300 and 2400 cm^{-1} . Via use of a custom written program it was possible to integrate the peak area between 2210 and 2480 cm^{-1} and measure CO_2 concentration at timed intervals. The CO_2 concentration was measured using a Perkin Elmer Spectrum 100 FTIR

Spectrometer controlled by automatic data collection software. The automatic data collection program allowed full operator control over the instrument allowing scheduling of automated scans throughout the test duration. This allowed measurement of CO₂ gas accumulation at regular intervals, which facilitated identification of reaction kinetics.

Irradiation times range from 8 to 60 hours depending on pigment photoactivity and stability of the polymeric resin. Without software to facilitate automation of scans this work would be impractical as control over the time interval between scans would be decreased and the test accuracy impaired. Previous work⁹ using the FTIR spectrometer to measure CO₂ evolution as a product of polymer photo-oxidation developed a Visual Basic program that allowed control over the instrument and automation of scans at desired time intervals.

2.2.2 The Automatic Data Collection Program (Evolgas)

Due to the commission of a new FTIR spectrometer for this research it has been necessary to update the instrument automation software. The Evolgas software was developed with the full range of practical and data processing functions present in the first version software. This allowed fully automated data collection and definition of testing parameters prior to test initiation.

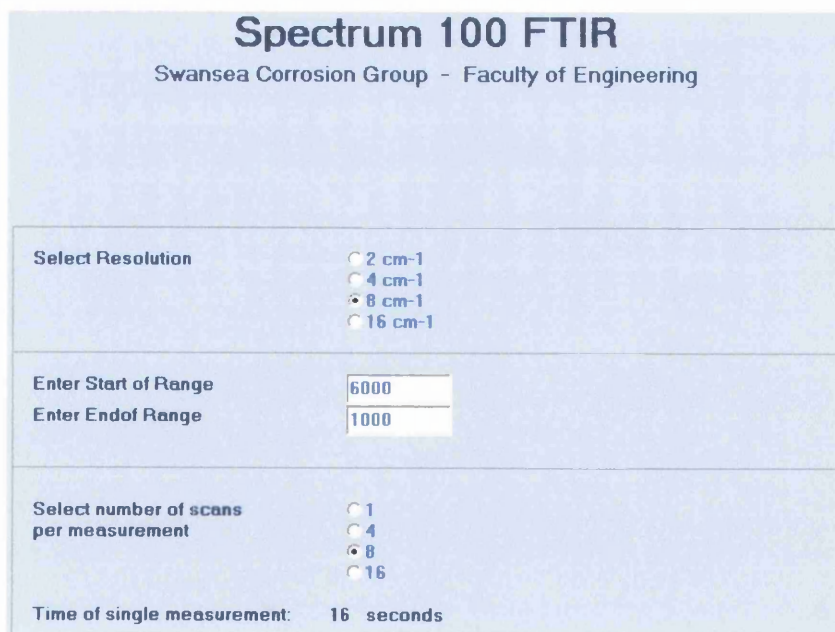


Figure 2.3 -The Evolgas Scan Control User Interface

Scan Settings

Figure 2.3 shows the Evolgas scan control interface that allows definition of the scan parameters prior to the start of the experiment. The scan resolution, wavenumber and the number of scans performed per measurement can be determined by the operator.

Timed Scan Control

The timer control interface shown in Figure 2.4 allows automation of scans throughout the test duration. It is possible to identify four testing stages, allowing more scans to be carried out at significant points which require a greater level of detail (for example the injection of CO₂ during the calibration process). The software calculates the time of each stage giving a clear view of each cycle time allowing automation to best fit the test requirements.

Spectrum 100 FTIR	
Swansea Corrosion Group - Faculty of Engineering	
First Stage Scan time: 16 seconds Select delay: 1 Time of 1 cycle: 1.00 Enter number of cycles: 11	Time now: 14:31 Wed, 14/06 Total time to end of first stage: 11.00 minutes
Second Stage Select delay: 10 Time of 1 cycle: 10.00 Enter number of cycles: 1	Second stage will start at approx: 14:42 Wed, 14/06 Total time to end of second stage: 21.00 minutes
Third Stage Select delay: 10 Time of 1 cycle: 10.00 Enter number of cycles: 1	Third stage will start at approx: 14:52 Wed, 14/06 Total time to end of third stage: 31.00 minutes
Fourth Stage Select delay: 10 Time of 1 cycle: 10.00	Fourth stage will start at approx: 15:02 Wed, 14/06 Fourth stage will continue until halted by user

Figure 2.4 - The Evolgas Timer Control User Interface

Processing Control

The processing options interface shown in Figure 2.5 allows multiple parameters to be defined and recorded thus allowing automatic processing of spectra as they are scanned. These pre-defined scan parameters allow the change in concentration for a defined scan area (for example that of CO₂) to be recorded in a log file throughout the test duration.

Spectrum 100 FTIR

Swansea Corrosion Group - Faculty of Engineering

Area Parameters

	Area Start	Area End	Base Start	Base End	Name
<input checked="" type="checkbox"/> Area 1	2480	2210	2480	2210	CO2
<input type="checkbox"/> Area 2					
<input type="checkbox"/> Area 3					
<input type="checkbox"/> Area 4					
<input type="checkbox"/> Area 5					
<input type="checkbox"/> Area 6					
<input type="checkbox"/> Area 7					
<input type="checkbox"/> Area 8					

Figure 2.5 - The Evolgas Spectra Processing Options User Interface

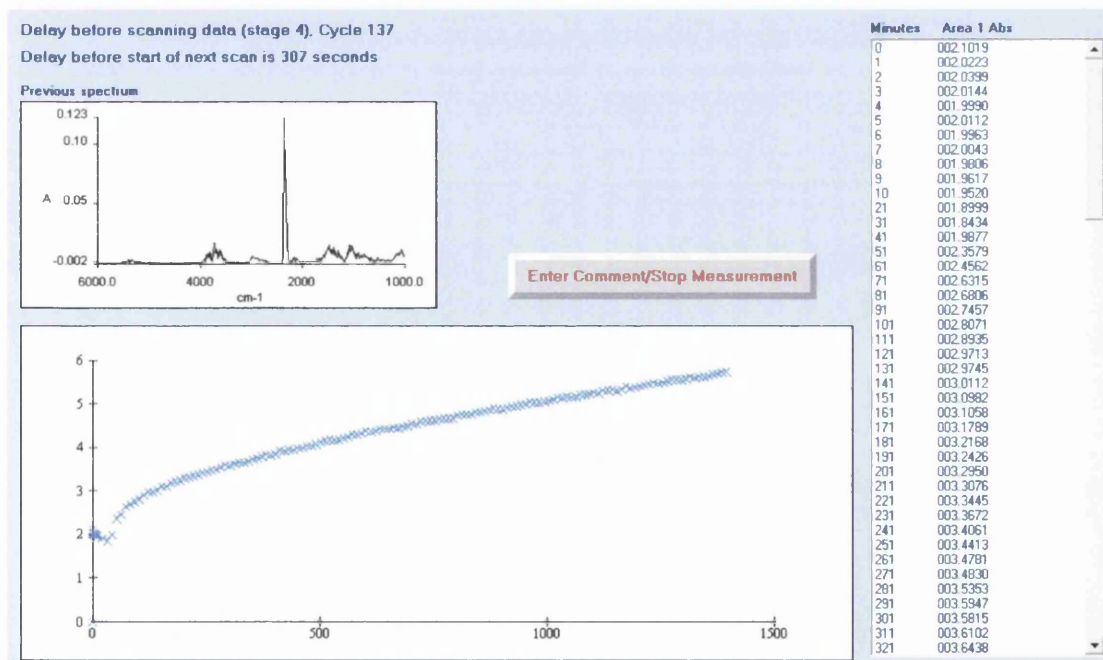


Figure 2.6 - Screen Showing Test Progress and Log File

The Log File

The interface shown in Figure 2.6 displays test progress as a list of readings and a plot of measured CO₂ concentration. The Evolgas software allows comments to be added to the log file allowing changes to the test to be recorded, for example injections of CO₂ during the calibration process or change of test sample. All events during the test duration whether automated or operator initiated are recorded and listed in a log file giving a complete record for the test.

2.2.3 The Irradiation Apparatus

Previous research^{9, 10, 12} has led to development of a closed loop system which incorporates an irradiation chamber into the FTIR spectrometer. This apparatus has allowed accumulation of evolved CO₂ gas in the system and measurement of concentration by FTIR spectroscopy.

The irradiation chamber was connected in a closed loop system to a KNF Neuberger LABOPORT pump (Model number N86KN.18) 6l/min neoprene diaphragm pump which circulated the headspace gas through the system. The total apparatus volume was less than 1litre therefore the flow rate of the pump was sufficient to ensure constant gas flow within the system, reducing the detection time of evolved CO₂ gas.

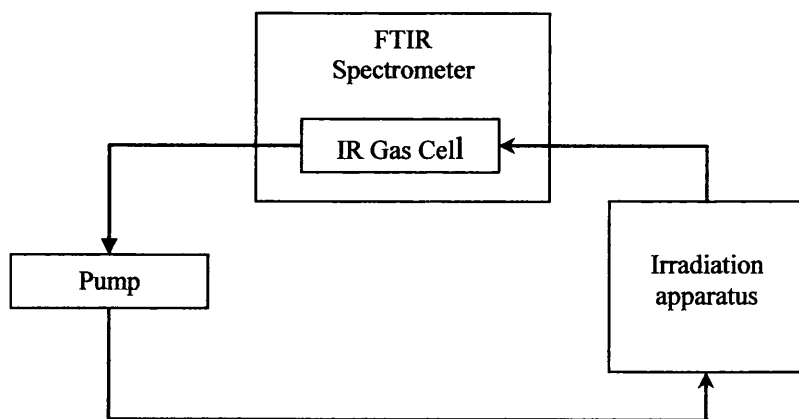


Figure 2.7 - Schematic Flow Diagram of Apparatus

The headspace gas was circulated into a gas cell mounted in the FTIR spectrometer sample chamber where the concentration of CO₂ in the system was measured. Automated scans were performed by the FTIR spectrometer at timed intervals giving a cumulative plot of CO₂ evolution over the test duration. A

schematic of the system flow showing the connection of the components which comprise the system is shown in Figure 2.7.

2.2.3.1 The IR Gas Cell

As seen in Figure 2.7 the headspace gas was circulated through the irradiation apparatus into the gas cell mounted in the FTIR spectrometer, where the concentration of CO₂ was measured. The gas cell path-length is variable according to that required by the operator and can range from 10cm to 400cm. This particular apparatus setup incorporated an Infrared Analysis inc. Ultra-Mini Long (240cm) Path Cell, Model 2.4 PA shown in Figure 2.8.

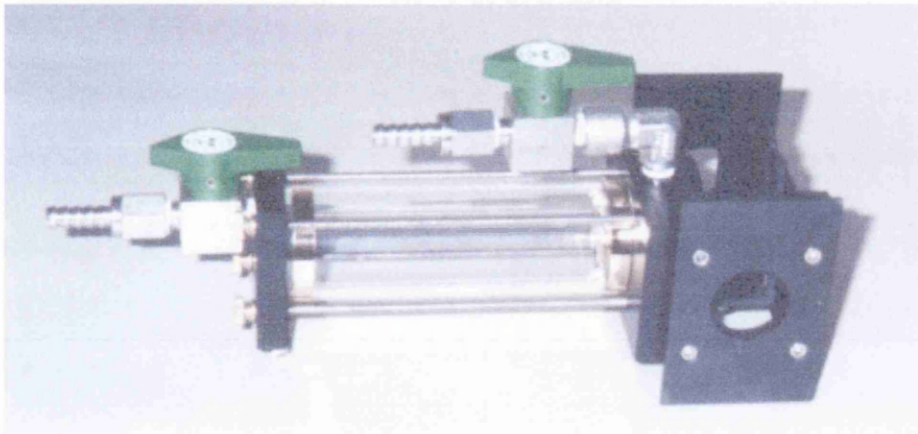


Figure 2.8 - The 2.4m Path-Length IR Gas Cell

The cell body was made of borosilicate glass and housed a system of three white cell mirrors coated with protective gold. These mirrors were permanently aligned in the cell body and by means of a multiple passing system provided a 2.4m optical path folded in a volume of 100cc. The optical beam travelled through a calcium fluoride (CaF₂) window where it was focussed via two moveable mirrors. The diverging beam was focussed by the entrance mirror onto the first objective mirror which focused the beam back to the field mirror. The field mirror then reflected the beam to back to the second objective mirror which in turn reflected it back to the field mirror. This multiple passing sequence continued for 24 passes to give a path-length of 2.4m. On the final pass the beam was focussed onto the exit mirror, out of the cell and into the optics of the FTIR spectrometer where the spectra were scanned and CO₂ concentration in the cell measured.

2.2.3.2 The Flat Panel Reactor Cell

Previous research has led to the development of testing apparatus which facilitated sample irradiation in a closed circuit loop. The first of these was the tube photoactivity test reactor^{9, 12} which was successfully used for photoactivity testing of model coating systems. Limitations of the apparatus due to difficulty of producing uniformly coated tubes lead to the conception of a flat panel irradiation apparatus^{9, 10} shown in Figure 2.9.

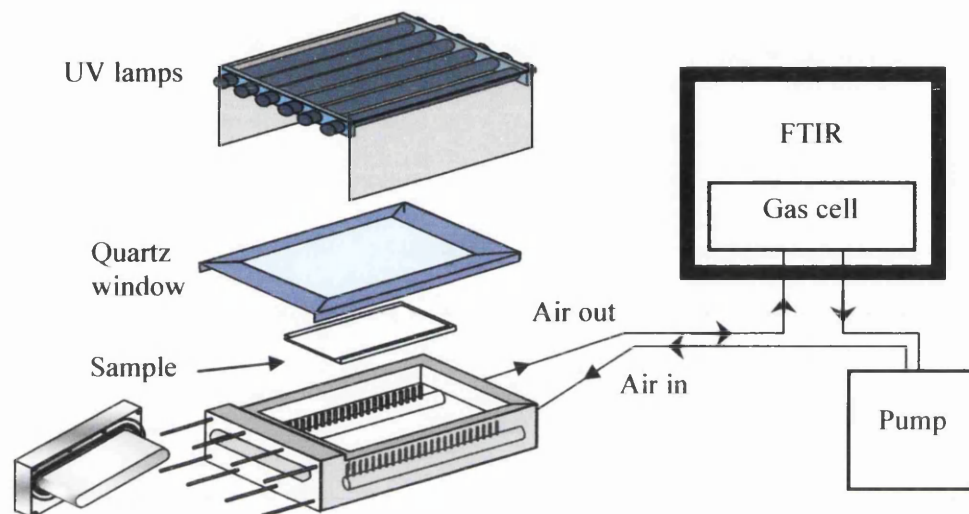


Figure 2.9 – The FTIR Flat Panel Irradiation Apparatus

Coated samples were placed in the aluminium reaction cell and irradiated through the quartz windows by means of a bank of 6 UV lamps. The evolved CO₂ was circulated through the closed loop system by a pump. Measurement of CO₂ concentration in the system was carried out at 10 minute intervals by means of a gas cell placed in the sampling compartment of the FTIR spectrometer.

The flat panel irradiation cell was designed to provide a large surface area in a small volume, thus providing a versatile and efficient means of sample irradiation. The irradiation cell was machined from a single block of aluminium to minimise joints and therefore potential for gas leakage. The aluminium block was milled to provide a flat sample stage capable of accommodating flat panel samples up to 220mm x 100mm in size. Coated samples were introduced into the reactor through a narrow slit opening at the end which was sealed using a fitted aluminium block which filled the slit snugly and prevented formation of dead air spaces in the cell. This block was tightened onto the cell using 8 wing-nuts and the seal enhanced using a renewable O-ring seal which further prevented gas escape from the cell opening.

Samples were irradiated through the quartz window by means of a bank of 6 x 8W Coast Wave Blacklight UV lamps (Coast Air: radiation λ_{max} 355-365nm). The lamps were set on polished aluminium which provided a maximum reflection of UV and ensured maximum sample irradiation. The maximum temperature achieved in the cell during irradiation was 40°C. The temperature was checked regularly to ensure that degradation was not thermally induced. The quartz window was bonded onto the aluminium cell with a two-component marine-strength epoxy adhesive seal which was protected by an aluminium foil cover to prevent direct irradiation and subsequent degradation.

Small bore holes were drilled into the material on either side of the sample stage. Air intake was provided by 24 x 1/2mm holes on one side and outlet by 24 x 1mm holes on the other. This provided a negative air pressure at the air outlet ensuring rapid gas mixing and maximum exhaustion of the gas products in the headspace of the cell. It was ensured that the total cross-sectional area of the outlet holes did not exceed the cross sectional area of the circulatory system connections to maintain rapid the mixing via pressurised airflow. Joints in the system connection were minimised to reduce potential for air escape, where necessary Swagelock 1/4 OD stainless steel gas fittings are used to provide an airtight renewable seal.

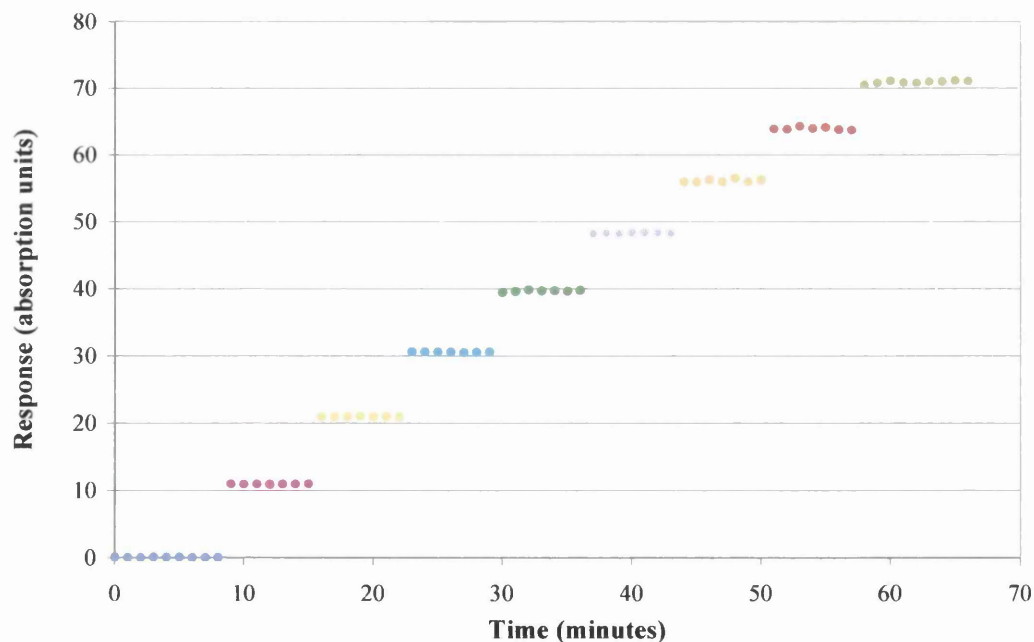


Figure 2.10 - Response of the FTIR Flat Panel Reactor Apparatus to Injections of 100µl CO₂

This apparatus was designed to facilitate rapid mixing of the headspace gas and thus a rapid response to changes in CO₂ concentration. Figure 2.10 shows the measured response to introductions of 100µl CO₂ into the system. The short time taken for measurements to stabilise following introductions of CO₂ was indicative of the efficiency of gas mixing within the apparatus.

2.2.3.3 Calibration of the FTIR Flat panel Reactor Apparatus

Evolved CO₂ as a product of photo-oxidation was measured by the FTIR spectrometer in units of absorption. This work aimed to quantify the reaction kinetics by reporting CO₂ evolution as a function of irradiated surface area, it was therefore necessary to calculate the calibration factor of the apparatus to facilitate conversion. By irradiating flat panel samples the exact surface area and film thickness of sample could be defined. By determining a calibration factor for the apparatus it was possible to convert the FTIR response in absorbance units to CO₂ evolution versus coating surface area. This provided a quantitative measurement of the rate and amount of CO₂ evolved as result of photo-oxidation.

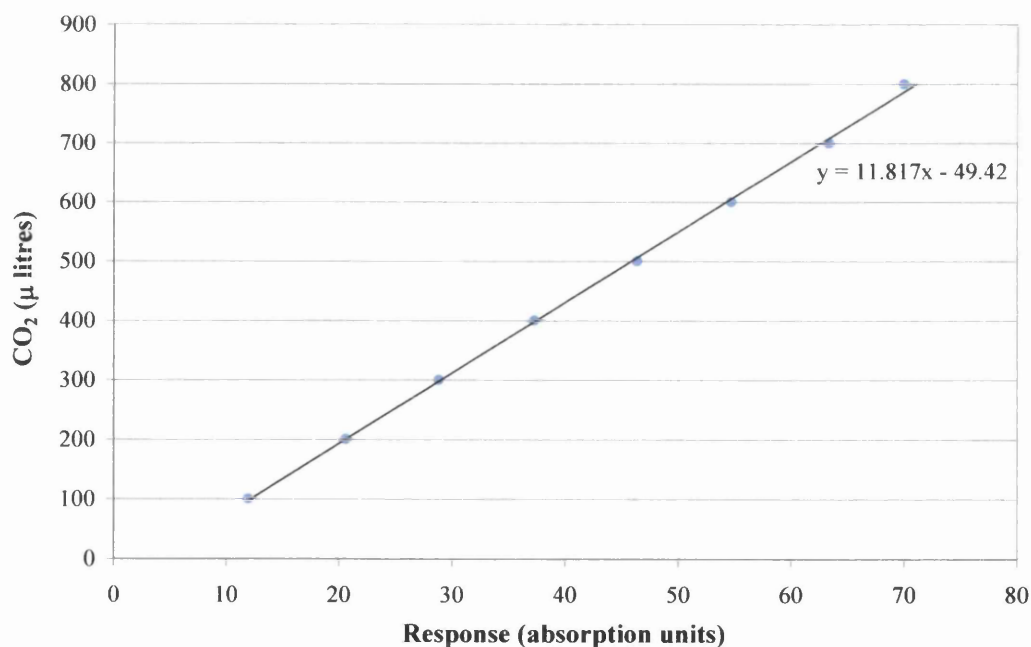


Figure 2.11 - The Instantaneous Response of the Apparatus to Injections of 100µl CO₂

The response of the FTIR spectrometer to introductions of known volumes of CO₂ gas in absorption units was measured and converted to volume measurements. The response to successive injections of 100µl CO₂ was monitored and recorded as

shown in Figure 2.10. The instantaneous response to each 100 μ l introduction in absorption units was calculated and plotted against the explicit volume of CO₂ as shown in Figure 2.11.

The gradient of this plot allowed calculation of the volume of CO₂ gas required to provide a system response of 1 absorption unit. This was then converted to mol of CO₂ by dividing the volume by that of 1mol of gas at room temperature and pressure (r.t.p.). Dividing the amount of CO₂ in mol by the irradiated surface area (in m²) gave a calibration factor which allowed CO₂ measurements to be reported as μ mol.m⁻². The calculation of apparatus calibration factor is shown in Figure 2.12

<p>Calculation of CO₂ required producing 1 abs unit response</p> <p>11.817 μl = 1 abs unit</p> <p>\therefore 1 abs unit = 1.1817 x 10⁻⁵ dm⁻³</p> <p>1mol gas at r.t.p. = 24 dm³</p> <p>1.1817 x 10⁻⁵ /24</p> <p>\therefore 1 abs unit = 4.92375 x 10⁻⁷ mol CO₂</p> <p>\therefore 1 abs unit = 0.492375 μmol CO₂</p> <p>Calculation of CO₂ evolution per area unit</p> <p>(For sample size of 160cm²)</p> <p>1m² = 10,000cm²</p> <p>10,000/160</p> <p>\therefore 62.5 panels in 1m²</p> <p>Calibration factor to convert abs units to μmol.m⁻² CO₂</p> <p>0.492375 x 62.5</p>
--

Figure 2.12 – The Calibration Calculation for the FTIR Flat Panel Irradiation Apparatus

2.2.4 Commercial Accelerated Weathering Methods

The primary focus of this work was to evaluate the durability of polyurethane and polyester-melamine coatings. Although it is widely accepted that no accelerated weathering method can provide a perfect evaluation of coating durability, it was important to assess the accuracy of the FTIR flat panel irradiation apparatus in

comparison with commercially accepted testing methods. All polyurethane and polyester-melamine coatings were tested using QUV A 340 and Xenon Arc (Ci 65) weathering.

2.2.4.1 QUV A

Polyurethane and polyester-melamine coated panels were irradiated in the QUV A (UV-340) chamber for 2000 hours. Samples were subjected to a continuous cycle of 4 hours UV A irradiation at 60°C followed by 4 hours of dew at 40°C with no irradiation for the test duration. The coatings were tested for gloss retention at 250 hour intervals for a total of 2000 hours.

2.2.4.2 Xenon Arc

The durability of polyurethane and polyester-melamine coatings was also tested using xenon arc (Ci 65) weathering. Coated samples were placed in the weathering chamber and subjected to a continuous cycle of 40 minutes irradiation at 70°C followed by 20 minutes irradiation and water spray at 70°C, and then 60 minutes of irradiation followed by 60 minutes of water spray at 38°C. The gloss retention of samples was tested at 250 hour intervals for 2000 hours.

2.2.4.3 Gloss Measurement

Coating gloss is a measure of the overall surface roughness and reflectivity. A smooth surface will reflect a large portion of the light that falls onto it giving the appearance of high shine (or gloss). As coating degradation manifests, pits and cracks form on the coating surface, this phenomenon is called micro-cracking. The formation of these cracks causes the coating surface to become rough, consequently decreasing the coating gloss. In addition degradation of the polymer surrounding TiO₂ particles causes migration of pigment particles to the surface, which can reduce gloss.

Coating gloss was measured using a gloss meter which was placed on the coating surface. A tungsten filament lamp (2.5 V 60 mA) emits a light flash which hits the surface of the coating at a pre-determined angle. The light is reflected by the coating at the same incident angle to a silicon photo-element where the reflected light is measured as shown by the schematic in Figure 2.13. The angle at which the gloss is measured can be selected manually; 20°, 60° or 85° to the normal of the surface of the coating. A five point average of 60° gloss retention was taken for each of the

polyurethane and polyester-melamine coatings at 250 hour intervals throughout the test duration.

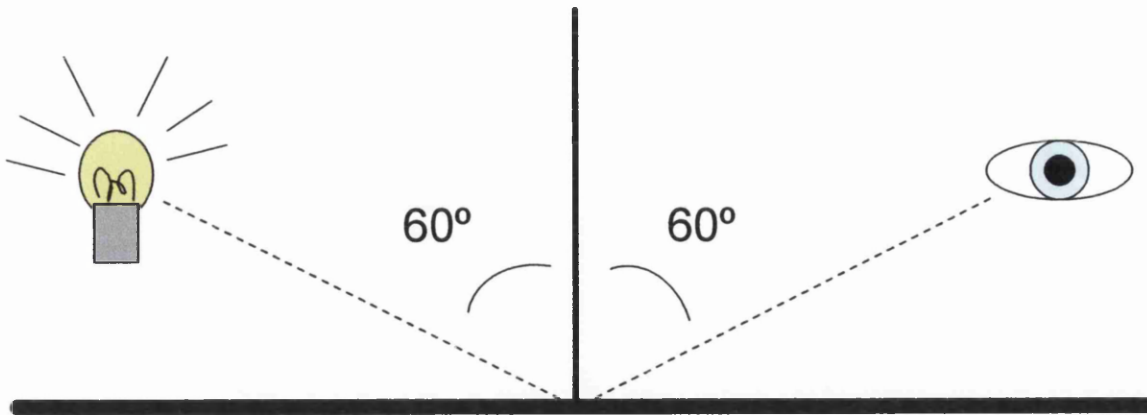


Figure 2.13 - A Schematic of 60° Coating Gloss Measurement

2.2.4.4 Colour Measurement

Degradation is known to cause a darkening effect or more specifically a change in the colour of a coating which is often visible to the human eye. This change not only affects the aesthetic appearance but is also indicative of the reactions occurring within the coating. Recent work¹³ has shown that the most effective and fundamental way of quantifying colour change is achieved by the measurement of reflectance spectrum.

Colour was measured using a Gretag Macbeth Spectrolino spectrophotometer set at 45°/0° geometry. The Gretag Macbeth Spectrolino uses a gas filled tungsten type A lamp (D50) light source which closely imitates natural daylight. A collimated beam of light illuminates the coating surface at a 45° angle with the surface normal (at a 90° angle to the surface of the coating) and the reflective response is captured by a standard observer set at a 2° angle with the surface normal. A five-point average value for the CIE-XYZ, CIE L*a*b measurements and the visible light reflectance spectrum between 380nm – 730nm was taken to give a colour reading. The measurements before and after weathering were compared to assess the effects of degradation on coating colour.

2.3 References

1. Bock, M., *Polyurethanes for Coatings*. European Coatings Literature, ed. U. Zorll. 2001, Vincentz Network: Hanover.
2. Robinson, A.J., Wray, J., and Worsley, D.A., *Materials Science and Technology*, 2006. **22**(12): p. 1503-1508.

3. Christensen, P.A., Dilks, A., Egerton, T.A., and Temperley, J., *Journal of Materials Science*, 1999. **34**(23): p. 5689-5700.
4. Marganski, R.E., *Abstracts of Papers of the American Chemical Society*, 1998. **216**: p. U608-U608.
5. Christensen, P.A., Dilks, A., Egerton, T.A., and Temperley, J., *Journal of Materials Science*, 2000. **35**(21): p. 5353-5358.
6. Jin, C.Q., Christensen, P.A., Egerton, T.A., Lawson, E.J., and White, J.R., *Polymer Degradation and Stability*, 2006. **91**(5): p. 1086-1096.
7. Fernando, S.S., Christensen, P.A., Egerton, T.A., and White, J.R., *Polymer Degradation and Stability*, 2007. **92**(12): p. 2163-2172.
8. Christensen, P.A., Egerton, T.A., Martins-Franchetti, S.M., Jin, C., and White, J.R., *Polymer Degradation and Stability*, 2008. **93**(1): p. 305-309.
9. Searle, J.R., *Titanium Dioxide Pigment Photocatalysed Degradation of PVC and Plasticised PVC Coatings*. 2002, Eng. D, University of Wales Swansea.
10. Robinson, A.J., Searle, J.R., and Worsley, D.A., *Materials Science and Technology*, 2004. **20**(8): p. 1041-1048.
11. Robinson, A.J., *The Development of Organic Coatings for Strip Steels with Improved Resistance to Photodegradation*. 2005, Eng. D, University of Wales Swansea
12. Worsley, D.A. and Searle, J.R., *Materials Science and Technology*, 2002. **18**(6): p. 681-684.
13. Wijdekop, M., *Investigation into the Weathering of Organic Coated Steel and Application of Mathematical Modelling to the Data*. 2004, Eng. D, University of Wales Swansea.

Chapter 3

The Effect of Titanium Dioxide Photoactivity Grade on Polyurethane and Polyester-Melamine Photo-Oxidation

3.1 Introduction

As a pigment, titanium dioxide (TiO_2) offers a unique combination of properties^{1, 2} that makes it the most widely used pigment in the market. The optical properties of TiO_2 are technically superior in comparison to other pigments providing superb optical whiteness and opacity. In Section 1.52 it was seen that TiO_2 has a high refractive index which facilitates effective light scattering and thus affords excellent opacity to a coating. The opacity of TiO_2 as a pigment has led to its use in almost all but the darkest coatings regardless of colour as a means of 'hiding' the substrate.

The semi-conducting nature of TiO_2 can pose a challenge to coating manufacturers particularly when developing coatings for exterior applications. In Section 1.53 it was shown that TiO_2 can become photoactivated by incident UV irradiation^{1, 3} and initiate degradation reactions within the surrounding polymer^{4, 5, 6}. These reactions cause chemical¹ and physical^{7, 8, 9} changes and can result in chalking¹, discolouration^{2, 10} and failure of the polymeric coating.

Literature has shown that TiO_2 pigment photoactivity significantly affects the rate of coating degradation^{11, 12, 13, 14, 15}. The photoactivity of TiO_2 is dependant on the number of active sites present on the pigment particle. To increase photostability pigment manufacturers coat the TiO_2 with silica, alumina and zirconia to act as a barrier to UV and reduce the number of active sites. The success of these coatings in reducing the number of active sites and thus increasing pigment photostability is communicated via an A to C grading system. The most photostable pigments are classified as grade A and are suited to high UV and exterior applications. Grade B pigments are less photostable and grade C pigments are highly photoactive and are suitable only for applications where little or no UV is expected.

The development of a coating for exterior applications requires extensive durability testing using a combination of accelerated and natural weathering tests. Previous research^{11, 12, 13, 14, 15, 16} has described methods of quantifying polymer photo-degradation by measurement of carbon dioxide (CO_2) evolution. This method has provided a means of screening pigment photoactivity and the effect on coating durability in a significantly shorter time than commercially recognised methods such as QUV and xenon arc.

3.1.1 Aims

A flat panel irradiation system incorporated into a Fourier Transform infrared (FTIR) spectrometer as described in Section 2.2.3 has facilitated CO₂ measurement as a means of quantifying polymer photo-oxidation. Previous work^{17, 18} has used this method to evaluate the effects of TiO₂ photoactivity on coating durability, which although successful has until present been limited to model PVC and polyethylene (PE) coatings.

This chapter will investigate use of this test in quantifying degradation as a result of TiO₂ pigment photoactivity in different polymers, namely polyurethane and polyester-melamine coatings. The results obtained will be compared with those gained from QUV A and xenon arc weathering to give a durability ranking for each of the coatings.

3.2 Experimental Techniques

3.2.1 Titanium Dioxide Pigments

The coatings were pigmented using a variety of TiO₂ pigments with differing photoactivities as defined in Table 3.1.

Table 3.1 - Characteristics of Commercial TiO₂ Pigments Tested

Pigment	TiO ₂ Content	Stabilisers	Photoactivity Grade	Uses
Kronos 1001	99	-	C	Interior coatings, inks and paper
Kronos 2300	94.5	Al	B	Interior coatings
Kronos 2220	92.5	Al,Si	A	Exterior coatings
Tronox R-KB-4	94	Al,Si,Zr	A	Exterior, industrial and automotive coatings

3.2.2 The First Series Polyurethane and Polyester-Melamine Coatings

The first series polyurethane and polyester-melamine coatings were one component coatings based on un-stabilised commercial formulations. The polyurethane coatings as comprised a UV stable HDI based polyisocyanate and standard durability hydroxyl-bearing polyester. The polyester-melamine coating contained the same polyester with a melamine-formaldehyde (HMMM) cross-linker. Despite the absence of commercial stabilisers these polymers were inherently more stable than model PVC coatings and consequently less susceptible to photo-degradation.

3.2.2.1 Polyurethane and Polyester-Melamine Coating Preparation

The polyurethane and polyester-melamine coatings were prepared as described in Section 2.1.1.1 and Section 2.1.1.2 respectively. According to the formulation guidelines TiO₂ pigment was dispersed in polyester resin and hydrocarbon solvent and ground in a bead mill for 15 minutes to ensure even mixing and deagglomeration of pigment particles. The formulation was filtered into a bottle and appropriate measures of polyester resin, cross-linker, catalyst, flow agent and solvent added. The coatings were shaken for a further 15 minutes to ensure uniform mixing and allowed to rest for 5 minutes prior to casting.

3.2.2.2 Production of Polyurethane/Polyester-Melamine Coated Samples

Coated sample panels were produced by the draw-bar coating method explained in Section 2.1.2. A thin line of paint was poured along the top of the substrate and drawn down the substrate in one movement. The coated panels were oven cured at a PMT of 232°C and water quenched. Each sample was then checked to ensure full curing and a dry film thickness of 20µm.

3.2.3 Assessing Pigment Photoactivity in the Fourier Transform Infrared (FTIR) Flat Panel Irradiation Apparatus

The FTIR flat panel irradiation apparatus used to assess pigment photoactivity is described in Section 2.2.3. Coated polyurethane and polyester-melamine sample panels were placed into the reactor and irradiated in the closed loop system for 2500 minutes. The concentration of CO₂ gas in the system was measured via a gas cell incorporated into the FTIR spectrometer at timed intervals to give a cumulative

measurement of CO₂ evolution. The rate of CO₂ evolution was taken between 500 and 2500 minutes giving a quantitative analysis of degradation rates.

As a control each sample set tested in the FTIR flat panel irradiation apparatus included an un-pigmented coating. This allowed the effects of different TiO₂ pigments to be directly identified and the photoactivity of pigmented coatings to be ranked.

3.2.4 Assessing Coating Durability in Commercial Weathering Tests

Polyurethane and polyester melamine coatings were subjected to QUV A and xenon arc weathering as described in Section 2.2.4.1 and Section 2.2.4.2 respectively. Coatings were tested in continuous cycles of QUV A (UV 340) and xenon arc (Ci 65/CAM 180) for 2000 hours and the gloss retention measured at 250 hour intervals. The initial gloss values for the first series pigmented polyurethane and polyester-melamine coatings are shown in Table 3.2 and Table 3.3 respectively.

Table 3.2 - Initial 60° Gloss Values for the First Series Polyurethane Coatings

Pigment	Initial 60° Gloss
Kronos 1001	89
Kronos 2300	78
Kronos 2220	73
Tronox R-KB-4	82

Table 3.3 - Initial 60° Gloss Values for the First Series Polyester-Melamine Coatings

Pigment	Initial 60° Gloss
Kronos 1001	79
Kronos 2300	72
Kronos 2220	68
Tronox R-KB-4	82

3.3 Results and Discussion

3.3.1 Evolution of Carbon Dioxide

The FTIR flat panel irradiation apparatus was used to measure the concentration CO₂ gas in the apparatus headspace at timed intervals throughout the test duration. Figure 3.1 shows FTIR spectra illustrating the increasing concentration of evolved CO₂ throughout irradiation of a polyurethane coating containing Kronos 1001 TiO₂ pigment.

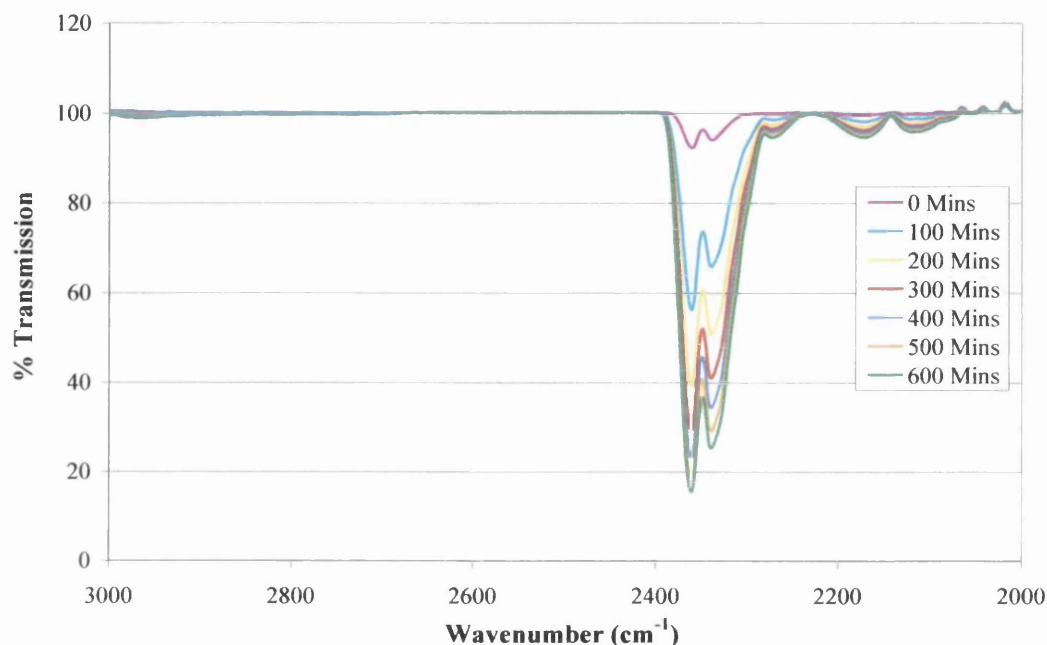


Figure 3.1 - Spectra Showing Increase in Headspace CO₂ Concentration with Time

The only volatile detected at significant levels during degradation was CO₂ with trace amounts of carbon monoxide (CO) at 2220-2230cm⁻¹. Any degradation intermediates produced during photo-degradation are either present at extremely low levels or remain bound in the polymer.

Figure 3.2 shows CO₂ concentration versus irradiation time for a TiO₂ pigmented polyurethane coating. Although CO₂ evolution levels were very low when testing the polyurethane and polyester-melamine coatings the apparatus was of high enough resolution to define concentration with little interference. The gradient of the plot between 500 and 2500 minutes was used to calculate the rate of CO₂ evolution and give a quantitative measure of coating oxidation.

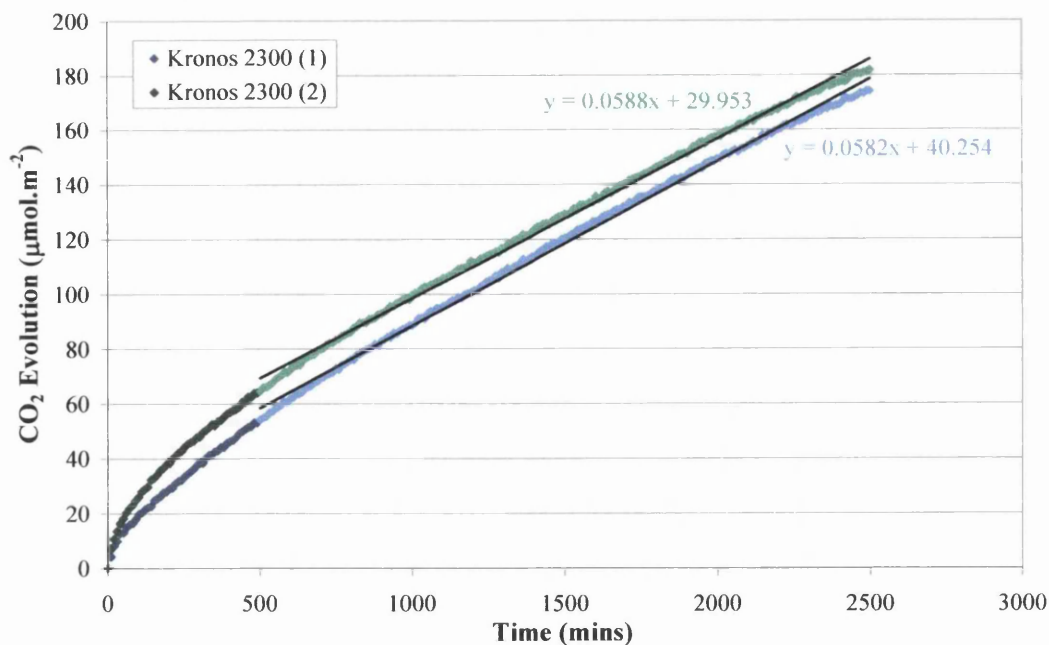


Figure 3.2 – CO₂ Evolution during Irradiation of a TiO₂ Pigmented Polyurethane

The effects of TiO₂ photocatalysis on coating degradation were assessed using the rate of CO₂ evolution between 500 and 2500 minutes averaged from multiple sample irradiations. Un-pigmented films produce CO₂ by direct photolysis and subsequent oxidation of the polymer and thus comparisons between un-pigmented and pigmented samples allowed direct quantification of TiO₂ photocatalysis.

3.3.2 Weathering Results for the HDI based Polyurethane Coatings Formulated with the Standard Polyester Resin

3.3.2.1 CO₂ Evolution Rates

The CO₂ evolution rates for the standard durability HDI based polyurethane coatings are illustrated in Figure 3.3. It can be seen that pigmentation with the grade C TiO₂ Kronos 1001 photocatalysed the degradation. The average CO₂ evolution rate on irradiation of these coatings was three times greater than that of un-pigmented polyurethane.

Addition of stabilised grade A or B TiO₂ pigments reduced coating photo-oxidation and thus CO₂ evolution rates to below that of un-pigmented polyurethane. The low rates of CO₂ evolved by these coatings are a result of the high refractive index of TiO₂ which reduces light penetration into the polymer film and the efficiency of the pigment coating in reducing photocatalysis.

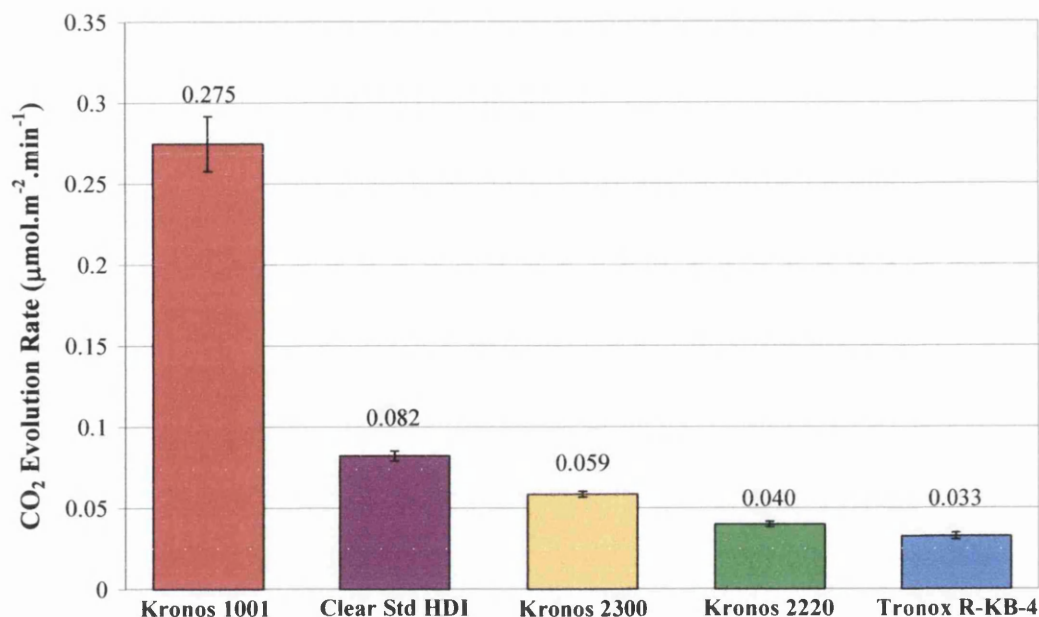


Figure 3.3 –CO₂ Evolution Rates of Standard Durability Polyurethane Coatings

In the case of Tronox R-KB-4 and Kronos 2220 the reduction in light penetration and the efficiency of the inorganic coating was so great that photo-oxidation was reduced to levels significantly lower than that of un-pigmented polyurethane. This does not indicate the absence of photocatalysis as even stable pigments have some photocatalytic effect over polymer oxidation. The low rate of photo-oxidation is a result of low light penetration and high TiO₂ stability the effects of which overshadow any photocatalytic effects of the pigment.

It is appropriate to consider the addition of any TiO₂ pigment as affording a level of shielding to the polymer. All TiO₂ pigments reduce light penetration into polymer however in the case of photoactive TiO₂ grades such as Kronos 1001 any shielding is overshadowed by increased oxidation as a result of TiO₂ photocatalysis.

The difference in photoactivity between grade B (Kronos 2300) and grade A (Kronos 2220 and Tronox R-KB-4) TiO₂ pigments is shown in Figure 3.3. As anticipated the coatings pigmented with grade B TiO₂ Kronos 2300 showed higher rates of CO₂ evolution than those containing more photostable grade A pigments. The polyurethanes pigmented with grade A Tronox R-KB-4 and Kronos 2220 TiO₂ showed the highest durability and thus lowest CO₂ evolution rates. It can be seen from Figure 3.3 that the lowest CO₂ evolution rates were obtained from the coating pigmented with Tronox R-KB-4 indicating it to be the most stable pigment for use with the standard durability HDI based polyurethanes.

3.3.2.2 QUV A Gloss Retention

The QUV A gloss retention results for the TiO₂ pigmented polyurethane coatings are shown in Figure 3.4. The coating pigmented with Kronos 1001 TiO₂ was the least durable and exhibited significant loss of gloss compared to the other coatings.

The photoactive Kronos 1001 pigment has photocatalysed degradation of the coating resulting in chalking of the coating and consequently the rapid decrease in gloss retention exhibited in Figure 3.4. In comparison, the coatings pigmented with the more photostable grade B Kronos 2300 and grade A Kronos 2220 and Tronox R-KB-4 TiO₂ showed significantly improved durability and gloss retention.

The gloss retention results for the coatings pigmented with Kronos 2220 and Kronos 2300 showed an increase in coating gloss over the test duration. From these results it appears that the coating containing Kronos 2300 is more stable in QUV than that containing Kronos 2220 pigment. The Kronos 2300 coating showed a smaller gloss increase and appeared more stable in the final hours of testing compared to the Kronos 2220 pigmented coating which exhibited the beginnings of gloss loss by 2000 hours of QUV.

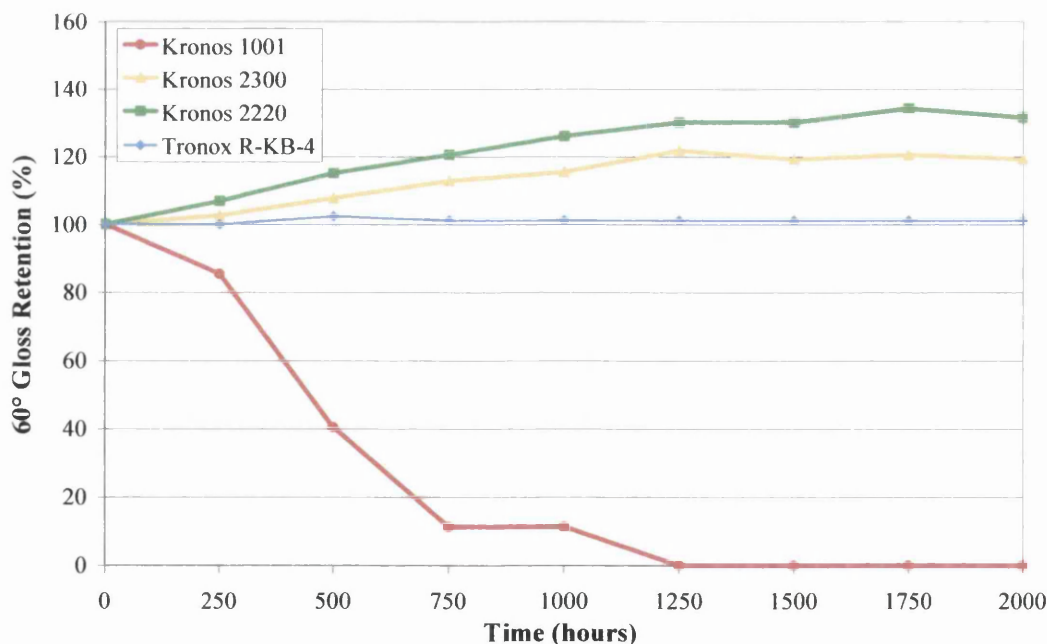


Figure 3.4 – QUV A Gloss Retention of Standard Durability Polyurethane Coatings

Similar gloss increases have been shown in the literature¹⁹, however the mechanism by which this phenomenon occurs and its significance on coating

durability is not yet fully understood. Investigations into the gloss increase have proved inconclusive in identifying the mechanism of gloss increase however, we have considered three theories:

Relaxation of the Cured Polymer

The coil coating process requires a high PMT (>200°C) to be reached in less than 60 seconds to ensure complete curing of the coating at reasonable line speeds. The high speed of curing can lead to the polymer curing in a thermodynamically unfavourable geometry. During QUV and xenon arc testing thermal and humidity cycling can cause the system temperature to fluctuate around its glass transition temperature (T_g).

These fluctuations can cause a step by step relaxation of the polymer from its original metastable state to one more energetically favourable. This relaxation is dependant on the surface tension of the cured coating. Coil coated polymers always cure with a degree of corrugation which is unfavourable and so relaxation to a less corrugated geometry is likely.

Investigations into this phenomenon were carried out by placing coated samples in an oven and alternating the temperature between 60°C and 40°C at four hour intervals. There was however no change in gloss after 500 hours.

Polishing

In pigmented systems directly after fabrication some pigment particles may be loosely bound at the coating surface⁷. During the condensation or water spray cycles of QUV or xenon arc these particles may be washed away causing the coating surface to become smoother and thus increase in gloss.

Refractive index of TiO₂ Pigment during Initial Stages of Oxidation

During the initial stages of weathering the onset of polymer degradation can lead to enrichment of TiO₂ at the coating surface, however at these early stages the pigment particles remain enveloped by the binder. Since refractive index of rutile TiO₂ is 2.7²⁰ and that of the polymer is 1.5-1.6 enrichment of TiO₂ at the coating surface could lead to an increase in the amount of light reflected by the coating, thus increasing the gloss reading. Investigations into partially weathered coatings were carried out using scanning electron microscopy in order to determine whether enrichment of TiO₂ was occurring, however no conclusions to either confirm or refute this theory were reached.

The gloss retention results for the coating pigmented with Tronox R-KB-4 remained stable throughout the test duration. This coating did not exhibit a significant change in gloss retention and therefore showed the highest stability of all the standard HDI polyurethanes under QUV A testing.

3.3.2.3 Xenon Arc Gloss Retention

The xenon arc gloss retention results for the HDI polyurethane coatings are shown in Figure 3.5. QUV testing was carried out under standard conditions with UV intensity of $0.68 \text{ W.m}^{-2}.\text{nm}^{-1}$ @ 340 nm, over the 2000 hour test duration this subjected the samples to a UV dose of 131 MJ.m^{-2} . Xenon arc weathering was carried out under standard conditions with UV intensity of $0.55 \text{ W.m}^{-2}.\text{nm}^{-1}$ @ 340 nm, subjecting the samples to a UV dose of 346 MJ.m^{-2} over the 2000 hour test duration.

Xenon arc weathering subjected the samples to 2.6 times as much UV radiation as QUV. Comparison between Figure 3.4 and Figure 3.5 however, showed xenon arc weathering to have accelerated coating degradation by up to 4 times that of QUV. This further increase could be due to the xenon arc spectrum containing lower wavelength, higher energy irradiation compared to that of QUV. The xenon arc spectrum also contains irradiation at wavelengths greater than 400nm which could also contribute to degradation. This coupled with the greater temperature fluctuation makes xenon arc weathering more severe than QUV A, resulting in faster failure of the test samples.

Pigmentation with Kronos 1001 photocatalysed coating degradation causing heavy chalking and consequently a value of zero gloss within 500 hours of weathering. The coatings pigmented with Kronos 2220 and Kronos 2300 exhibited a similar initial gloss increase to those shown in QUV A weathering. At 250 hours of xenon arc weathering the coatings pigmented with Kronos 2220 and Kronos 2300 showed gloss increases similar to those seen at 1000 hours of QUV A testing as illustrated in Figure 3.4.

The occurrence of this increase at the beginning of xenon arc and throughout QUV A testing showed that the gloss increase is likely to be an initial exposure phenomenon. Due to the more severe nature of xenon arc the period of gloss increase in the coatings appears arrested compared to those in QUV A. In xenon arc weathering the coatings began to show loss decrease at around 500 hours while those in QUV A continue to show increased gloss for the test duration.



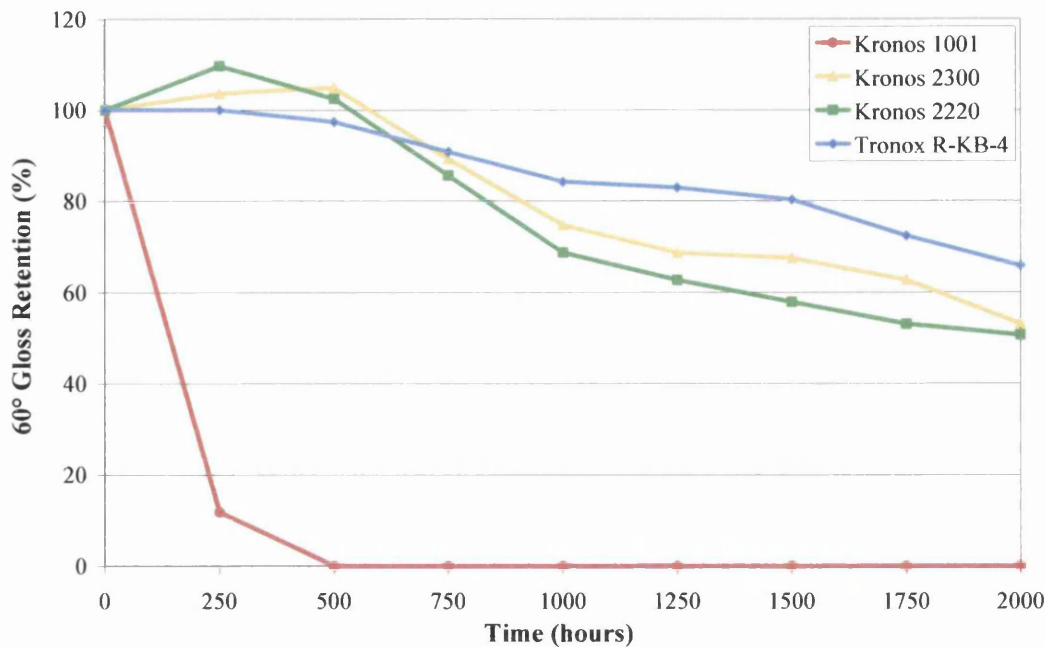


Figure 3.5 –Xenon Arc Gloss Retention of Standard Durability Polyurethane Coatings

At 250 hours of xenon arc weathering the gloss retention values for each of the coatings were similar to those seen at 1000 hours of QUV A weathering. Both coatings pigmented with Kronos 2220 and Kronos 2300 showed an increase in gloss while the coating pigmented with Tronox R-KB-4 did not exhibit notable gloss change in either test indicating it to be the most stable. Due to these similarities it is predicted that the coatings weathered in QUV A would have undergone similar levels of chalking if the test durations had been extended.

The coating containing Tronox R-KB-4 TiO₂ pigment exhibited the most stable gloss values throughout testing and at 2000 hours of xenon arc had the highest gloss retention value of all the pigmented coatings. The polyurethanes pigmented with Kronos 2300 and Kronos 2220 showed lower gloss retentions indicating lower coating durability.

3.3.2.4 Standard Durability HDI Based Polyurethane Rankings

The pigmented coatings were assigned a performance ranking in each weathering test as shown in Figure 3.6. Coatings were ranked according to durability in QUV A and xenon arc as a percentage change in coating gloss at 2000 hours as shown in Figure 3.4 and Figure 3.5 respectively. Durability performance in the CO₂ evolution apparatus was ranked according to secondary (500-2500 minutes) CO₂ evolution rate shown in Figure 3.3. The IPDI polyurethane pigmented with Kronos

1001 exhibited the highest CO₂ evolution rate (0.594 μmol.m⁻².min⁻¹) and is discussed in detail in Chapter 5. The CO₂ ranking was expressed as a percentage of this - the highest CO₂ evolution rate.

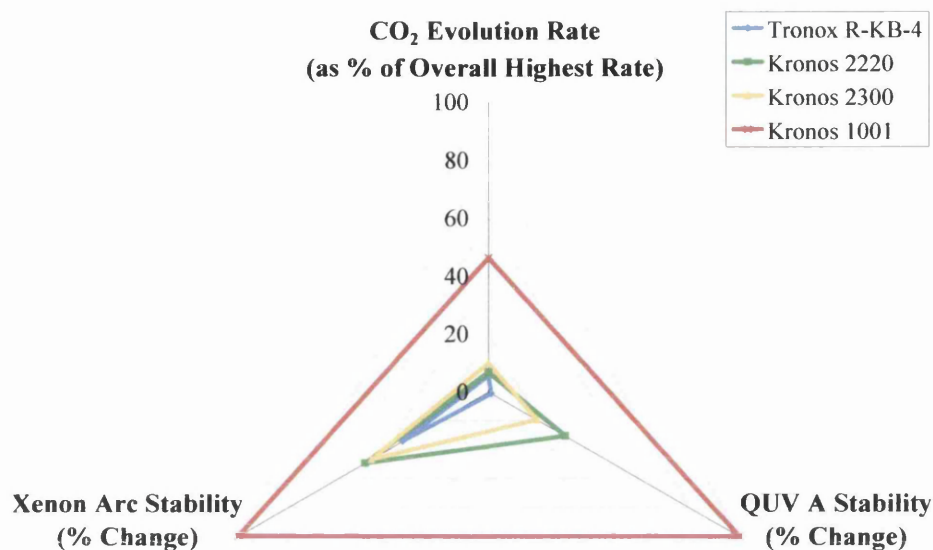


Figure 3.6 – Ranking of Standard Durability Polyurethane Coatings According to Durability in CO₂ Measurement Apparatus, QUV A and Xenon Arc Weathering

This method of ranking allowed a direct comparison between each of the pigmented coatings where the coating represented by the smallest area showed the highest overall durability. The areas representing each coating were measured and a photoactivity ranking index derived from these as illustrated in Figure 3.7.

The coating ranking in Figure 3.6 showed that the coating pigmented with Tronox R-KB-4 was represented by the smallest area and as such was the most durable. The other TiO₂ pigmented coatings were represented by larger areas and were therefore of lower durability, which is more clearly illustrated in Figure 3.7.

The coating pigmented with Tronox R-KB-4 was the most stable of the standard durability polyurethanes and thus the reactivity index was set at 1, such that all the other photoactivity index values in the thesis could be directly compared. All photoactivity indices throughout this work are expressed as a ratio of this - the photoactivity index assigned to the Tronox R-KB-4 pigmented standard durability HDI coating. An index value of less than 1 indicates the coating to be more durable than the standard polyurethane pigmented with Tronox R-KB-4, and a value greater than 1 indicates it to be less durable.

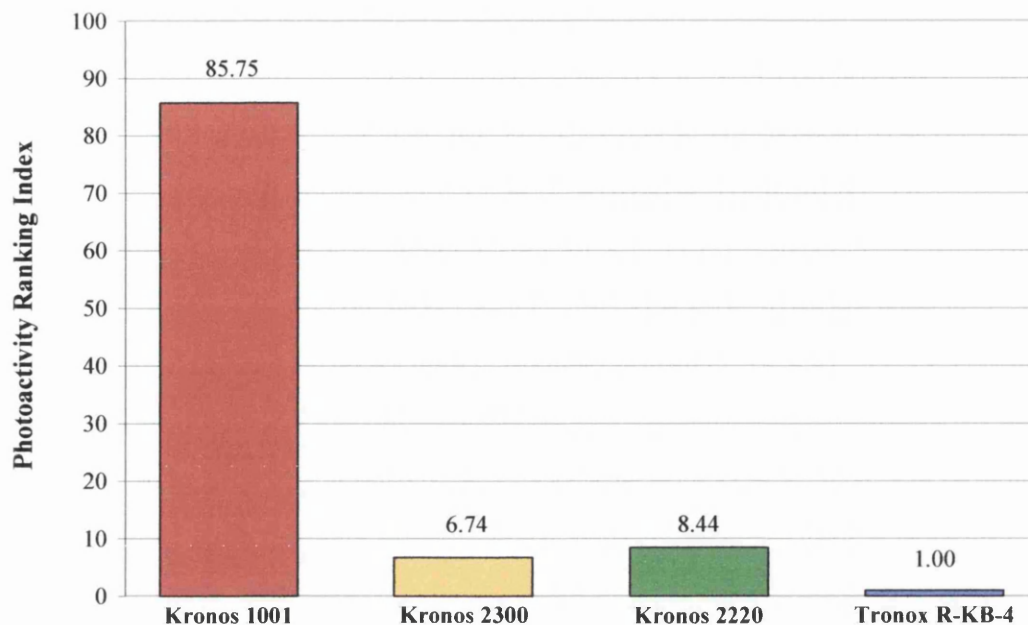


Figure 3.7 – Photoactivity Ranking Indices of Standard Durability Polyurethane Coatings

The photoactivity ranking index showed that pigmentation with the photoactive Kronos 1001 caused significant photocatalysis of coating degradation, giving a ranking index of over 85 times that of the Tronox R-KB-4 coating. The coatings pigmented with the more photostable Kronos 2220 and 2300 showed ranking indices more comparable to that of the Tronox R-KB-4 pigmented coating. These pigments did not photocatalyse degradation however the coatings did not perform as well as the coating pigmented with Tronox R-KB-4 in any of the weathering tests and as such showed higher ranking indices. The coating pigmented with Kronos 2300 exhibited a lower photoactivity index therefore higher durability than that pigmented with Kronos 2220.

Ranking the coatings according to performance in each test illustrated the differences between testing methods and allowed a straightforward assessment of durability when comparing the performance of a coating in each weathering test. This ranking is however, implicit and not indicative of actual coating lifetime.

3.3.3 Weathering Results for the Polyester-Melamine Coatings Formulated with the Standard Polyester Resin

3.3.3.1 CO₂ Evolution Rates

The CO₂ evolution rate results for standard durability pigmented polyester-melamine coatings are shown in Figure 3.8. The results gained from irradiation of the

Kronos 1001 pigmented polyester-melamine coatings were comparable to those of the polyurethane coatings illustrated in Figure 3.3. This coating exhibited a significantly higher rate of CO₂ evolution than the un-pigmented polyester-melamine, clearly illustrating the degree to which this photoactive TiO₂ grade photocatalysed oxidation of the polymer matrix.

The coatings pigmented with the more photostable Tronox R-KB-4, Kronos 2220 and Kronos 2300 TiO₂ grades exhibited lower CO₂ evolution rates than that of the un-pigmented polymer. This reduction in CO₂ evolution rate was indicative of increased durability against complete oxidation as a result of pigment stability and polymer shielding.

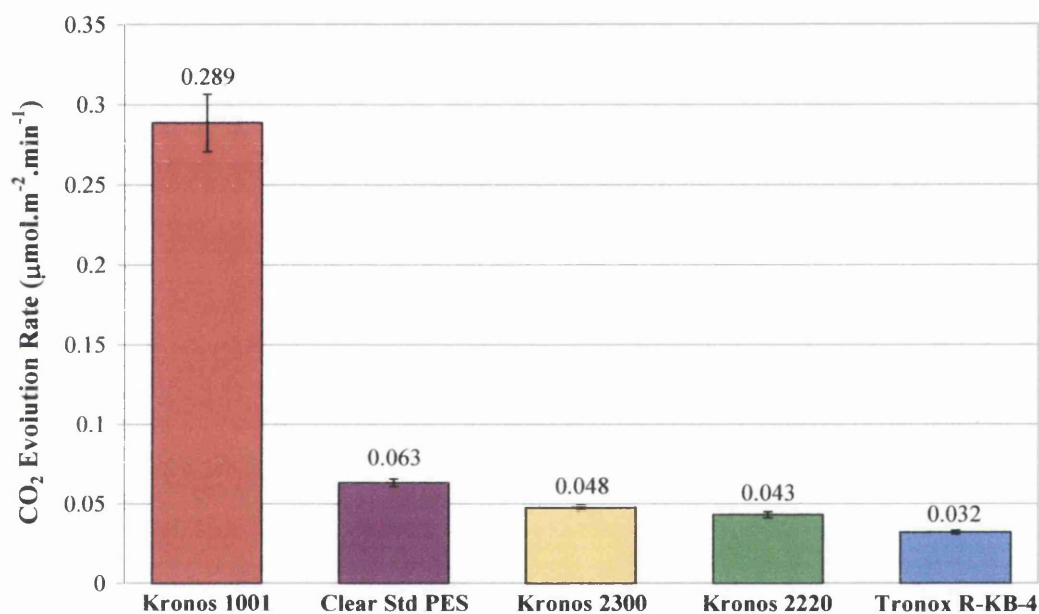


Figure 3.8 – CO₂ Evolution Rates of Standard Durability Polyester-Melamine Coatings

Each of the coatings pigmented with the photostable TiO₂ grades showed good durability however the CO₂ evolution rate results highlighted differences in pigments stability. As anticipated the coating pigmented with the grade B Kronos 2300 showed the highest CO₂ evolution rate of the grade A and B pigments. The coating pigmented with Tronox R-KB-4 exhibited the lowest CO₂ evolution rate of all polyester-melamine coatings which was inline with results for the standard durability polyurethane coatings.

3.3.3.2 QUV A Gloss Retention

The QUV A gloss retention results for the pigmented polyester-melamine coatings are shown in Figure 3.9. The coating pigmented with the photoactive Kronos 1001 showed poor gloss retention throughout indicating the occurrence of TiO₂ photocatalysed oxidation. The coating pigmented with the more photostable pigment grades exhibited significantly higher durability and gloss retention than the Kronos 1001 coating.

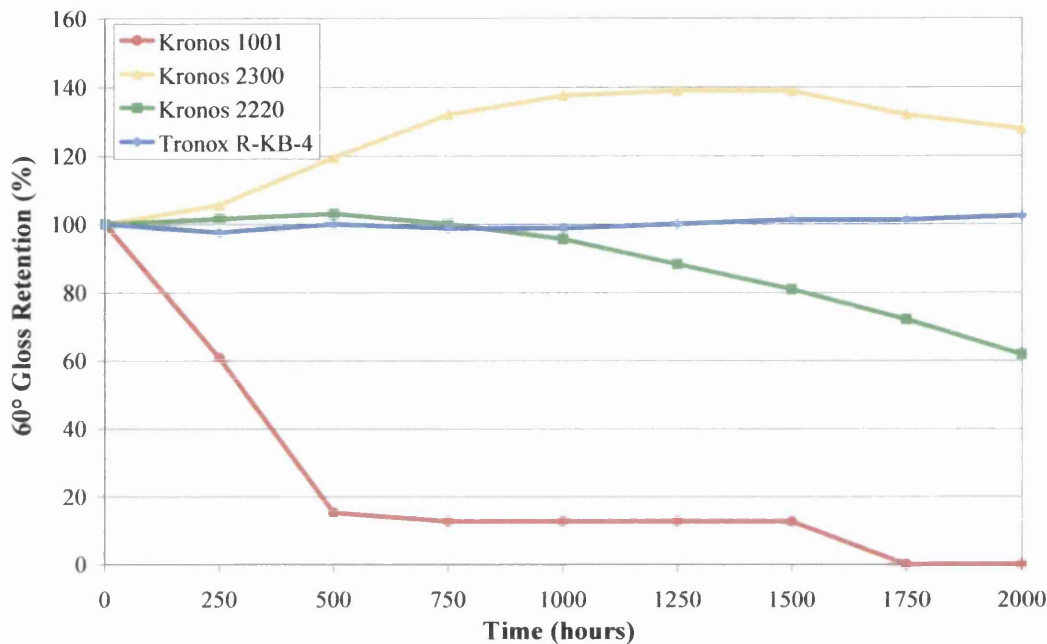


Figure 3.9 – QUV A Gloss Retention of Standard Durability Polyester-Melamine Coatings

The gloss retention results for the coating pigmented with Tronox R-KB-4 remained stable throughout the test duration showing the highest durability of all the pigmented polyester-melamine coatings. The coating containing Kronos 2300 exhibited a similar gloss increase as the polyurethane coatings and showed higher durability than the coating pigmented with Kronos 2220 which showed a significant decrease in gloss after 1000 hours of QUV A. The poor performance of this coating could be due to interactions between the polymer resin and the TiO₂ coating.

3.3.3.3 Xenon Arc Gloss Retention

Xenon arc weathering subjects samples to a more harsh weathering cycle than QUV A causing degradation to occur in a much shorter time. Each of the pigmented coatings tested can be seen in Figure 3.10 to have undergone a level of degradation indicated by the reduction in coating gloss.

The coating pigmented with Kronos 1001 showed very poor durability and failed after just 500 hours of xenon arc weathering. The coatings pigmented with the more photostable pigments showed increased durability however those containing Kronos 2220 and Kronos 2300 showed a significant reduction in gloss retention. In this instance pigmentation with the grade A Kronos 2220 provided higher durability than the grade B Kronos 2300 producing a coating with final gloss retention 10% higher than the grade B pigment.

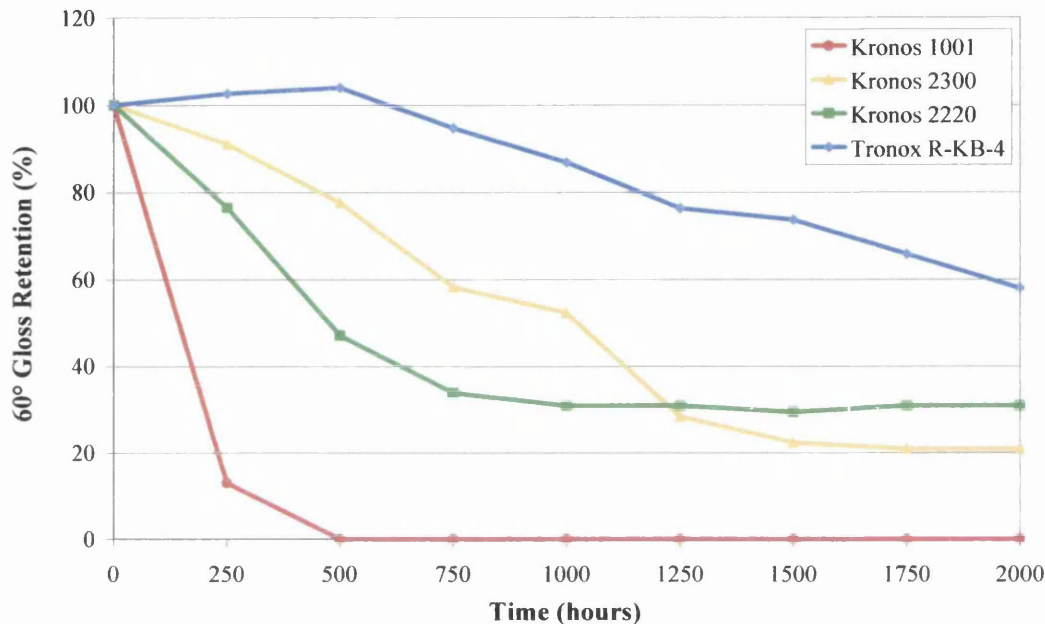


Figure 3.10 – Xenon Arc Gloss Retention of Standard Durability Polyester-Melamine Coatings

The polyester-melamine pigmented with Tronox R-KB-4 showed the highest durability in xenon arc weathering. This coating performed significantly better than the other coatings and exhibited final gloss retention double that of the polyester-melamine pigmented with the grade A Kronos 2220. It should however be noted that the rate of gloss change in the coating pigmented with Kronos 2300 was higher than that of the Kronos 2220 coating in the final hours of testing.

3.3.3.4 Standard Durability Polyester-Melamine Rankings

The durability ranking for each of the pigmented polyester-melamine coatings according to performance in CO₂ measurement, QUV A and xenon arc are shown in Figure 3.11 and allowed a direct comparison between the pigment grades.

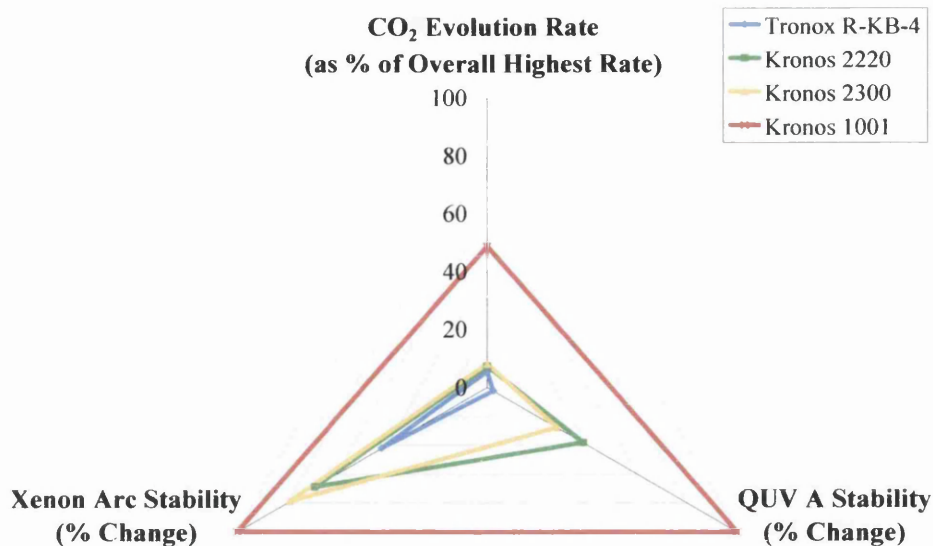


Figure 3.11 – Ranking of Standard Polyester-Melamine Coatings According to Durability in CO₂ Measurement Apparatus, QUV A and Xenon Arc Weathering

The areas representing each pigmented coating were calculated and expressed as photoactivity ranking indices relative to the standard durability HDI based polyurethane pigmented with Tronox R-KB-4 as shown in Figure 3.12.

The photoactivity ranking index illustrated in Figure 3.12 showed pigmentation with Kronos 1001 to have produced a coating of significantly lower durability than the more photostable grade A and B TiO₂ pigments. The performance of the polyester-melamine pigmented with Kronos 1001 was comparable to that of the polyurethane coating pigmented with Kronos 1001. The poor performance in each of the tests indicated photocatalysed coating degradation as a result of high pigment photoactivity.

The coating pigmented with grade A Tronox R-KB-4 showed the highest durability of all the pigmented standard durability polyester-melamine coatings. This coating exhibited the best performance in each of the weathering tests and as a result the lowest photoactivity ranking index. However, testing showed the polyester-melamine coatings to be around 1.7 times more unstable than the corresponding pigmented polyurethane coatings.

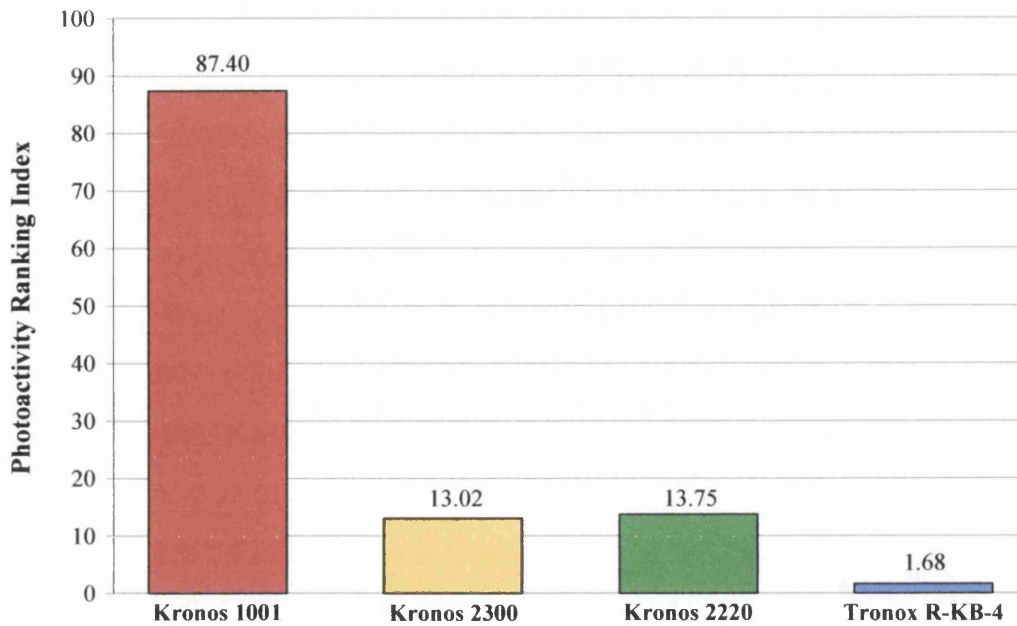


Figure 3.12 – Photoactivity Ranking Indices of Standard Durability Polyester-Melamine Coatings

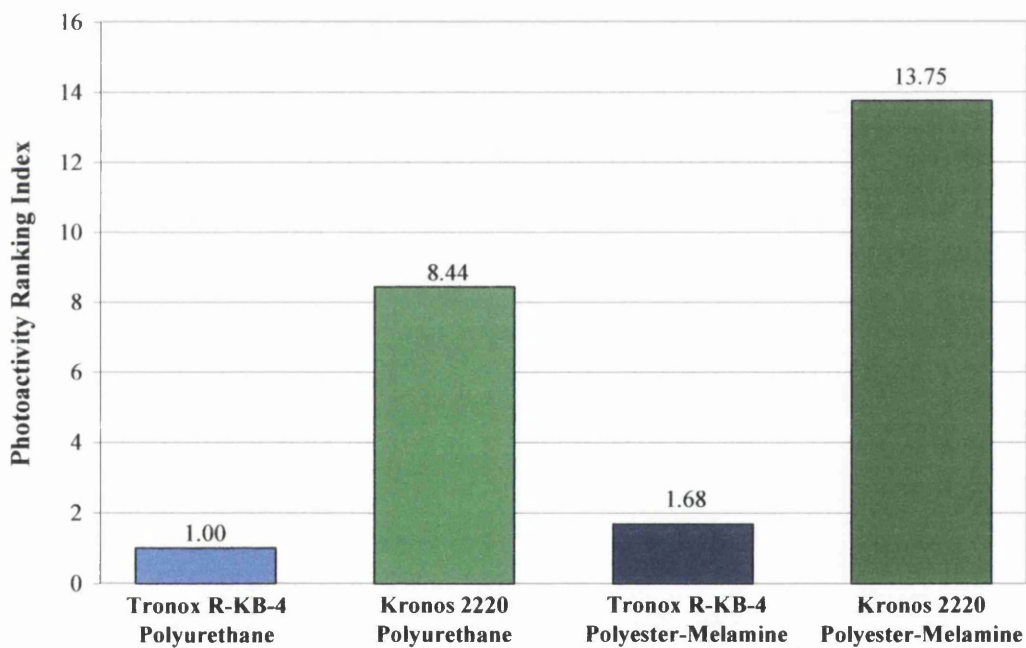


Figure 3.13 – Comparison between Photoactivity Ranking Indices of Stable Pigmented Standard Durability Polyurethane and Standard Durability Polyester-Melamine Coatings

Pigmentation with Kronos 2220 and Kronos 2300 TiO₂ grades showed lower durability than the Tronox R-KB-4 pigmented coating. The reactivity indices for both coatings were significantly higher the most durable polyester-melamine indicating their inferior performance in each of the tests compared to the coating pigmented with

the Tronox R-KB-4 TiO₂. From the overall comparison of coating durability using the photoactivity ranking indices it was seen that the coating pigmented with Kronos 2220 showed marginally higher photoactivity than the other grade A and B pigmented coatings. It was expected that these differences were in part due to the TiO₂ pigment coating its compatibility with the polymer resin.

The photoactivity ranking indices for both the polyurethane and polyester-melamine coatings pigmented with the stabilised Kronos 2220 and Tronox R-KB-4 TiO₂ grades are illustrated in Figure 3.13. Comparison between the coatings types showed the standard HDI polyurethane was significantly more durable than the polyester-melamine when pigmented with grade A stabilised TiO₂.

3.4 Conclusions

This work has shown that measurement of CO₂ evolution using the FTIR flat panel irradiation apparatus on polyurethane and polyester-melamine coatings is practical and useful. Via measurement of CO₂ evolution it has been possible to rapidly evaluate TiO₂ pigment photoactivity and the effects on polymer degradation, allowing prediction of coating durability in significantly shorter times than QUV A or xenon arc. Slight discrepancies in the photoactivity rankings between the testing methods were observed and are a result of differences in the nature of irradiation and analysis. The CO₂ evolution apparatus measured chemical changes in the bulk polymer and thus complete photo-mineralisation while gloss retention analysis measured the physical surface effects of degradation.

Xenon arc weathering subjects samples to harsher conditions than QUV A and as such the rate of coating degradation was increased. Differences in irradiation wavelength and temperature fluctuation caused discrepancies between the two commercially accepted test methods. The gloss increase shown in QUV A weathering was less apparent in xenon arc. This was most likely due to the harsher conditions of xenon arc compared to QUV A and indicated the gloss increase to be an initial exposure phenomenon. The gloss increase is therefore most likely caused by relaxation of the polymer due to temperature fluctuation around its glass transition temperature (T_g).

Ranking the coatings according to performance in each test illustrated the differences between testing methods and allowed a straightforward assessment of

durability. Via calculation of a photoactivity ranking using standard percentage units it was possible to directly compare the durability of each coating while accounting for performance in each of the weathering methods. The choice of photoactivity index measurement at 2000 hours accelerated testing is arbitrary however it does allow for systems to be compared according to a standard calculation.

Addition of photoactive TiO₂ pigments causes significant photocatalysis of coating degradation. In both polyurethane and polyester-melamine resins pigmentation with Kronos 1001 produced a coating with poor durability. These coatings exhibited high CO₂ evolution rates and poor gloss retention in both QUV A and xenon arc weathering.

The high refractive index of TiO₂ affords a level of shielding to the polymer and thus reduces penetration of UV light. Pigmentation with photostable TiO₂ grades caused a reduction in CO₂ evolution rate compared to the un-pigmented coatings due to the shielding effect. The reduction in UV light absorption coupled with pigment stability reduced the occurrence of photoactivation and therefore oxidation.

Each of the grade A and B TiO₂ pigments showed good photostability and reduced coating degradation, however in both polyurethane and polyester-melamine coatings pigmentation with Kronos 2300 produced a more durable coating than Kronos 2220. This goes against the observed total coating stability measurement gained by CO₂ evolution and suggests that there may be a dispersion issue with Kronos 2220 pigment in polyurethane and polyester-melamine coatings. Unstable dispersion of the pigment near the coating surface could lead to greater changes in the surface properties of the coating such as gloss.

The work highlights the importance of using a wide variety of tests to assess coating durability. For example using gloss retention results from QUV A and xenon arc weathering alone could lead to choices of titania which may still be 'active' for total degradation (CO₂ evolution). Similarly, choices made solely on assessment of CO₂ evolution will lead to problems in the coating surface stability (gloss). In this instance, the closer correlation between the CO₂ testing and xenon arc weathering compared to QUV A suggests that the former two test methods provide the most reliable ranking of performance. It is clear that the exposure time of 2000 hours QUV A was insufficient to fully assess the durability of these polyurethane and polyester-melamine coating systems.

Both the polyurethane and polyester-melamine coatings pigmented with Tronox R-KB-4 performed best in each of the weathering tests. As all pigments are rutile TiO₂ this increase in stability is most likely due to the surface coating on the pigment and its effectiveness in reducing the number of active sites on the TiO₂ particles.

Comparison between the photoactivity ranking indices showed that the pigmented polyester-melamine coatings were of lower durability than the polyurethane coatings showing photodegradation rates around 1.7 times faster than the polyurethane systems.

3.5 References

1. Mc Kellar, J.F. and Allen, N.S., *Photochemistry of Man-Made Polymers*. 1979, Applied Science Publishers: London.
2. Boxall, J. and Von Fraunhofer, J.A., *Concise Paint Technology*. 1977, Elek Science: London.
3. Ollis, D., Pelizzetti, E., and Serpone, N., *Photocatalysis: Fundamentals and Applications*. 1989, Wiley Interscience: New York.
4. Egerton, T.A. and King, C.J., *Journal of the Oil & Colour Chemists Association*, 1979. **62**(10): p. 386-391.
5. Hollande, S. and Laurent, J.L., *Polymer Degradation and Stability*, 1997. **55**(2): p. 141-145.
6. Diebold, M.P., *Jocca-Surface Coatings International*, 1995. **78**(6): p. 250-256.
7. Gesenhues, U., *Polymer Degradation and Stability*, 2000. **68**(2): p. 185-196.
8. Arnaud, R. and Lemaire, J., *Photocatalytic Oxidation of Polyolefins*, in *Developments in Polymer Degradation*, N. Grassie, Editor. 1979, Applied Science Publishers: London. p. 159-186.
9. Allen, N.S. and Katami, H., *Polymer Degradation and Stability*, 1996. **52**(3): p. 311-320.
10. Wilhelm, C., Rivaton, A., and Gardette, J.L., *Polymer*, 1998. **39**(5): p. 1223-1232.
11. Worsley, D.A. and Searle, J.R., *Materials Science and Technology*, 2002. **18**(6): p. 681-684.
12. Robinson, A.J., Searle, J.R., and Worsley, D.A., *Materials Science and Technology*, 2004. **20**(8): p. 1041-1048.
13. Christensen, P.A., Dilks, A., Egerton, T.A., and Temperley, J., *Journal of Materials Science*, 1999. **34**(23): p. 5689-5700.
14. Christensen, P.A., Dilks, A., Egerton, T.A., and Temperley, J., *Journal of Materials Science*, 2000. **35**(21): p. 5353-5358.
15. Jin, C.Q., Christensen, P.A., Egerton, T.A., Lawson, E.J., and White, J.R., *Polymer Degradation and Stability*, 2006. **91**(5): p. 1086-1096.
16. Christensen, P.A., Egerton, T.A., Martins-Franchetti, S.M., Jin, C., and White, J.R., *Polymer Degradation and Stability*, 2008. **93**(1): p. 305-309.
17. Searle, J.R., *Titanium Dioxide Pigment Photocatalysed Degradation of PVC and Plasticised PVC Coatings*. 2002, Eng. D, University of Wales Swansea.

18. Robinson, A.J., *The Development of Organic Coatings for Strip Steels with Improved Resistance to Photodegradation*. 2005, Eng. D, University of Wales Swansea
19. Pickett, J.E., Gardner, M.M., Gibson, D.A., and Rice, S.T., *Polymer Degradation and Stability*, 2005. **90**(3): p. 405-417.
20. Kronos International Inc, *Kronos Titanium Dioxide in Plastics*. 1993: Leverkusen, Germany.

Chapter 4

The Effect of Changes to the Polymer Resin on Coating Durability

4.1 Introduction

Chapter Three discussed the effects of titanium dioxide (TiO₂) photostability on coating durability and illustrated the importance of using UV stabilised pigments. Although pigment photostability grade has been shown to affect the rate of coating degradation the chemical compatibility between a coated TiO₂ pigment and a polymer resin should also be carefully considered when optimising coating durability.

It is common when discussing polymers to assume a single raw material structure. In the case of most polymers such as PVC (~ CHCl – CH₂ – CHCl – CH₂ ~) and polyethylene (~ CH₂ – CH₂ – CH₂ – CH₂ ~) this is true, however the generic name polyurethane covers a range of polymers. Historically polyurethanes were so called because the predominant chemical group was urethane (RHCOOR) and any polymer comprised of organic units linked with a urethane group is classified as such. Recently, although the urethane group is still present modification of the polymer chain with other structurally important groups has lead to the availability of a huge range of polymers which fall into the polyurethane category^{1, 2}. Polyurethanes have numerous possible precursors and therefore a correspondingly large number of possible final structures and properties. Descriptive names which more accurately describe the polymer structure such as polyesterurethane, polyetherurethane and polyurea-urethane although technically correct are complicated and thus often forsaken for the general term polyurethane².

This work has focussed on polyesterurethane coatings produced by reaction of a hydroxyl-bearing polyester co-reactant with a blocked polyisocyanate^{1, 3}. Developments in polyurethane technology have lead to the availability of a large range of both polyisocyanate and polyester precursors and therefore a large number of polyesterurethane resins.

4.1.1 Aims

This chapter will investigate the UV durability of different polyurethane and polyester coating resins. Carbon dioxide (CO₂) evolution measurement, QUV A and xenon arc weathering will be used to assess the effects of changing components of the polyurethane resin on coating durability.

Literature⁴ has suggested that the polyester component of a polyurethane has negligible effect on coating photo-oxidation as it is the urethane function that is most susceptible to oxidation. This will be investigated by comparison of the standard

durability coatings discussed in Chapter Three with polyurethane and polyester-melamine coatings containing an adapted polyester polyol anticipated to improve durability. These coatings are based on the same HDI based polyisocyanate and melamine-formaldehyde (HMMM) cross-linkers and will allow evaluation of the effects of the polyester component on coating durability.

This section will also investigate the stability of polyurethane coatings containing different polyisocyanate cross-linkers. Coatings based on a HDI/IPDI polyisocyanate and an IPDI polyisocyanate will also be evaluated to identify the optimum formulation for high durability coatings.

4.2 Experimental Techniques

4.2.1 Titanium Dioxide Pigments

Each of the second and third series coatings were pigmented with the same TiO₂ pigments used to pigment the first series polyurethane and polyester-melamine coatings: Kronos 1001 (Grade C), Kronos 2300 (Grade B), Kronos 2220 (Grade A) and Tronox R-KB-4 (Grade A). The pigment loading varied between the different coating resins as illustrated in Table 4.1.

Table 4.1 – Polyurethane Coating TiO₂ Pigment Loadings in

Coating	TiO₂ Loading (PHR)
First Series Standard HDI Polyurethane	28.66
Second Series ‘Improved’ HDI Polyurethane	26.20
Third Series IPDI Polyurethane	29.23
Third Series HDI/IPDI Polyurethane	29.11
First Series Standard Polyester-Melamine	29.20
Second Series ‘Improved’ Polyester-Melamine	26.72

4.2.2 The Second and Third Series Polyurethane and Polyester-Melamine Coatings

The second and third series polyurethane and polyester-melamine coatings were un-stabilised one-component oven curing coatings based on commercial formulations. These coatings were formulated with different polyol and cross-linker

components as defined in Table 4.2 to investigate the effects of changing the resin on coating durability.

Table 4.2 – Polyurethane and Polyester-Melamine Coating Formulations Tested

Coating	Cross-Linker	Polyester Polyol
First Series HDI Based Polyurethane (Tested in Chapter 3)	Standard Durability HDI	Standard Durability
First Series HMMM Based Polyester-Melamine (Tested in Chapter 3)	Standard Durability HMMM	Standard Durability
Second Series HDI Based Polyurethane	Standard Durability HDI	‘Improved’ Durability
Second Series HMMM Based Polyester-Melamine	Standard Durability HMMM	‘Improved’ Durability
Third Series IPDI Based Polyurethane	Standard Durability IPDI	Standard Durability Increased Flexibility
Third Series HDI/IPDI Based Polyurethane	Excellent Durability HDI/IPDI	‘Improved’ Durability

The second series polyurethanes comprised the same HDI based polyisocyanate as used in the first series polyurethanes and the adapted hydroxyl bearing polyester based on adipic acid, isophthalic acid, phthalic anhydride, 1-6-hexanediol, neopentyl glycol and trimethyl propane. The polyester-melamine coatings were formulated using the adapted polyester co-reactant and the standard durability melamine-formaldehyde (HMMM) cross-linker as used in the first series coatings.

The third series coatings were both polyurethane resins based on different polyisocyanate cross-linkers. The first was based on a cycloaliphatic IPDI polyisocyanate, which although is less flexible than the HDI polyisocyanate has a particularly high chemical resistance. The IPDI polyisocyanate was combined with a highly flexible branched hydroxyl bearing polyester based on adipic acid, maleic anhydride, neopentyl glycol and trimethyl propane. This increased the coating flexibility to a more acceptable level and produced a coating with standard UV durability and very high chemical resistance. The second was based on a HDI/IPDI combination polyisocyanate and the same polyester co-reactant as used in the second

series coatings. Both the polyester and polyisocyanate components of these coatings were anticipated to be of improved durability and to produce a coating with excellent UV stability. It was anticipated that changes to the coating resin would effect a continual improvement in durability compared to the first series coatings discussed in Chapter Three.

4.2.2.1 Polyurethane/Polyester-Melamine Coating Preparation

The second and third series polyurethane coatings were prepared as described in Section 2.1.1.1 and the second series polyester-melamine coatings as described in Section 2.1.1.2. According to the formulation guidelines TiO₂ pigment was dispersed in a polyester resin and hydrocarbon solvent (Solvesso 200 S) and ground in a bead mill for 15 minutes to ensure even mixing and a pigment particle size of <5 μ m. The formulation was filtered into a bottle and reduced by appropriate addition of polyester resin, cross-linker, catalyst, flow agents and solvent. The coating was then shaken for a further 15 minutes and allowed to rest for 5 minutes prior to casting.

4.2.2.2 Production of Polyurethane/Polyester-Melamine Coated Samples

Coated steel samples were produced by the draw-bar coating method detailed in Section 2.1.2. A thin line of paint was poured along the top of the substrate and drawn down the substrate in one swift, even movement using a #038 coiled bar to give a 20 μ m dry film thickness. The sample was cured in the oven to a peak metal temperature (PMT) of 232°C and then water quenched and dried.

4.2.3 Assessing Coating Durability in the Fourier Transform Infrared (FTIR) Flat Panel Irradiation Apparatus

The CO₂ evolution of coated samples was measured using the flat panel irradiation apparatus as described in Section 2.2.3. Coated samples were irradiated in the reactor and the headspace gas was measured at timed intervals by FTIR spectroscopy. This gave a cumulative plot of CO₂ evolution from which the secondary rate of CO₂ evolution between 500 and 2500 minutes was used to rank coating durability. As a control a clear un-pigmented sample of each polymer resin was tested to allow evaluation of polymer durability of each polymer and the effects of pigmentation with different commercial TiO₂ grades.

4.2.4 Assessing Coating Durability in Commercial Weathering Tests

Polyurethane and polyester melamine coatings were subjected to commercial QUV A and xenon arc as described in Section 2.2.4.1 and Section 2.2.4.2 respectively. The coatings were tested in continuous cycles of QUV A (UV 340) (ISO 4892 T.3) and xenon arc (VDA 621-429/430 Ci 65/CAM 180) for 2000 hours and the gloss retention measured at 250 hour intervals to allow assessment of coating durability. The initial gloss values for the second series pigmented polyurethane and polyester-melamine coatings containing the adapted polyester are shown in Table 4.3 and Table 4.4 respectively.

Table 4.3 - Initial 60° Gloss Values for the Second Series Adapted Polyurethane Coatings

Pigment	Initial 60° Gloss
Kronos 1001	96
Kronos 2300	85
Kronos 2220	78
Tronox R-KB-4	94

Table 4.4 - Initial 60° Gloss Values for the Second Series Adapted Polyester-Melamine Coatings

Pigment	Initial 60° Gloss
Kronos 1001	91
Kronos 2300	78
Kronos 2220	79
Tronox R-KB-4	82

The initial gloss values for the third series polyurethane coatings based on the IPDI polyisocyanate are shown in Table 4.5 and those of the polyurethane coatings based on the HDI/IPDI polyisocyanate in Table 4.6

Table 4.5 - Initial 60° Gloss Values for the Third Series Polyurethane Coatings Based on an IPDI Polyisocyanate

Pigment	Initial 60° Gloss
Kronos 1001	96
Kronos 2300	86
Kronos 2220	89
Tronox R-KB-4	92

Table 4.6 - Initial 60° Gloss Values for the Third Series Polyurethane Coatings Based on a HDI/IPDI Polyisocyanate

Pigment	Initial 60° Gloss
Kronos 1001	84
Kronos 2300	76
Kronos 2220	72
Tronox R-KB-4	80

4.3 Results and Discussion

4.3.1 Weathering Results for the HDI Based Polyurethane Coatings Formulated with the Adapted Polyester Resin

4.3.1.1 CO₂ Evolution Rates

The CO₂ evolution rate results for the polyurethane coatings containing the adapted polyester are shown in Figure 4.1. As with the first series polyurethane coatings discussed in Chapter 3, pigmentation with the grade C Kronos 1001 photocatalysed degradation increasing CO₂ evolution rates to over five times that of the un-pigmented coating.

Pigmentation with stabilised TiO₂ grades reduced photo-oxidation and therefore the rate of CO₂ evolution to below that of the un-pigmented coating. This reduction is a result of polymer shielding by the TiO₂ which reduces light penetration into the coating and subsequently reduces the levels of direct oxidation of the

polymer. Although all TiO₂ pigments can be considered to exhibit both photocatalysis and shielding the overall effects are dependant on the pigment stability. In the case of stabilised grades the efficiency of the coating in reducing photocatalysis combined with the low light penetration is such that an overall reduction in photo-oxidation is observed.

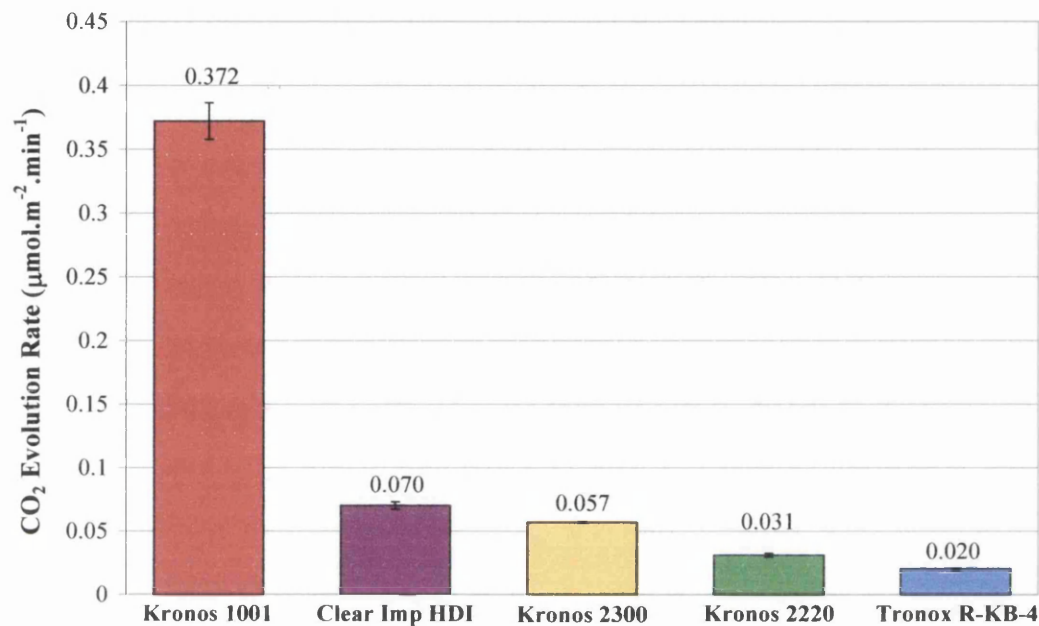


Figure 4.1 – CO₂ Evolution Rates of ‘Improved’ Polyurethane Coatings

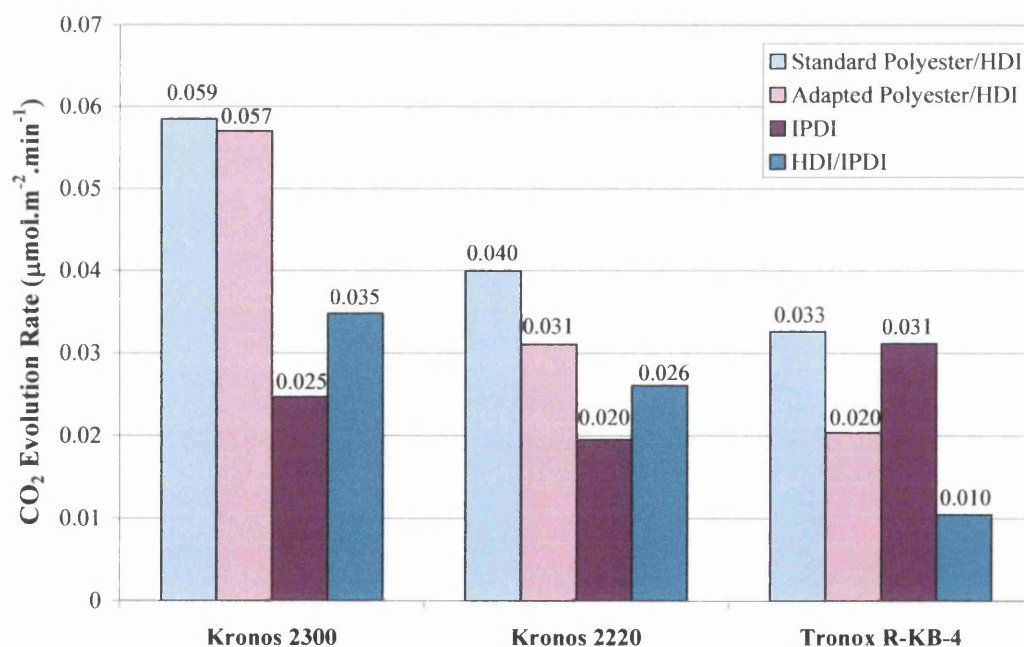


Figure 4.2 – Comparison of CO₂ Evolution Rates of all Polyurethane Resins Pigmented with Stabilised TiO₂

The grade B Kronos 2300 pigment showed a higher rate of CO₂ evolution than the more stable grade A Kronos 2220 and Tronox R-KB-4 pigments in all coatings except the polyurethane based on the IPDI polyisocyanate. This is because the stabilising coating on the Kronos 2300 pigment is less efficient in reducing photocatalysis than those used in the grade A pigments. Again the coating pigmented with Tronox R-KB-4 showed the lowest CO₂ evolution rate, giving the same pigment ranking according to CO₂ evolution as the standard durability polyurethanes. This is illustrated in Figure 4.2 which shows a comparison of CO₂ evolution rate for all of the stable pigmented polyurethane coatings.

The un-pigmented coating exhibited a lower CO₂ evolution rate than the standard durability un-pigmented polyurethane. This is significant as it indicates overall resin durability in the absence of pigment, which can alter coating chemistry and therefore durability. The formulation with the adapted polyester showed a reduced CO₂ evolution rate for both un-pigmented and stable TiO₂ pigmented polyurethane coatings in comparison to those containing the original standard durability polyester.

4.3.1.2 QUV A Gloss Retention

The QUV A gloss retention results for the HDI based polyurethane coatings formulated with the adapted polyester resin are illustrated in Figure 4.3. The coating pigmented with Kronos 1001 showed significant loss of gloss by 250 hours and complete failure by 750 hours. This was indicative of the high photocatalytic activity of this TiO₂ pigment and was in line with the rapid rate of CO₂ evolution shown above. The coating pigmented with the stabilised grade A and B pigments showed increased durability and gloss retention.

The coatings pigmented with Kronos 2220 and Kronos 2300 TiO₂ pigments showed a similar gloss increase to the first standard durability coating pigmented with these TiO₂ grades discussed in Chapter Three. Although the mechanism of gloss increase is unknown it is thought to be a result of either relaxation or polishing of the polymer surface or an artefact of the high refractive index of the TiO₂ pigment in comparison to that of the polymer. Any change in gloss is indicative of changes in the coating surface and therefore any gloss change can be viewed as instability of the coating resin.

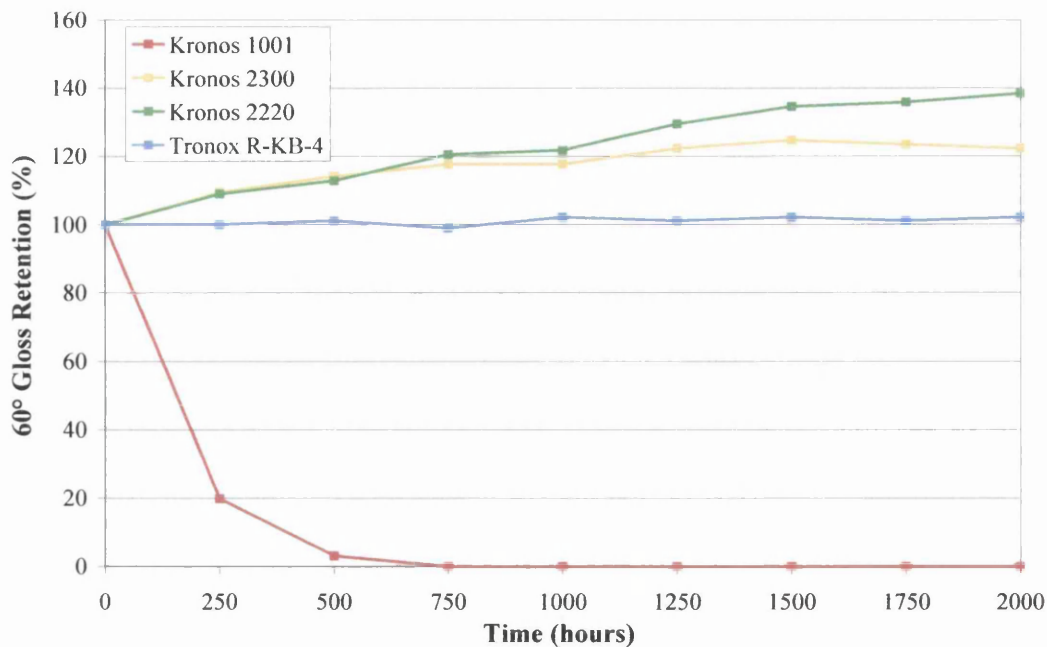


Figure 4.3 – QUV A Gloss Retention of ‘Improved’ Durability Polyurethane Coatings

Comparison between the coatings pigmented with Kronos 2220 and Kronos 2300 showed the former to have exhibited a larger increase and thus overall change in gloss, indicating it to be of lower stability in QUV A. Once again the coating pigmented with the Tronox R-KB-4 pigment did not show a significant change in gloss retention throughout the test duration, indicating it to be the most stable of the coatings tested.

4.3.1.3 Xenon Arc Gloss Retention

The xenon arc gloss retention results shown in Figure 4.4 confirm the photocatalysis of coating oxidation by Kronos 1001 seen in CO₂ evolution and QUV A testing. The coating pigmented with this photoactive TiO₂ grade showed complete failure (a gloss decrease of 97%) by 250 hours. Again, as discussed in Chapter Three the QUV A and xenon arc gloss retentions were corresponding at 500 hours of xenon arc and 1250 hours QUV A. This illustrates the severity of xenon arc weathering compared to QUV A, indicating it to be a better means of analysing coating durability within the 2000 hour test duration.

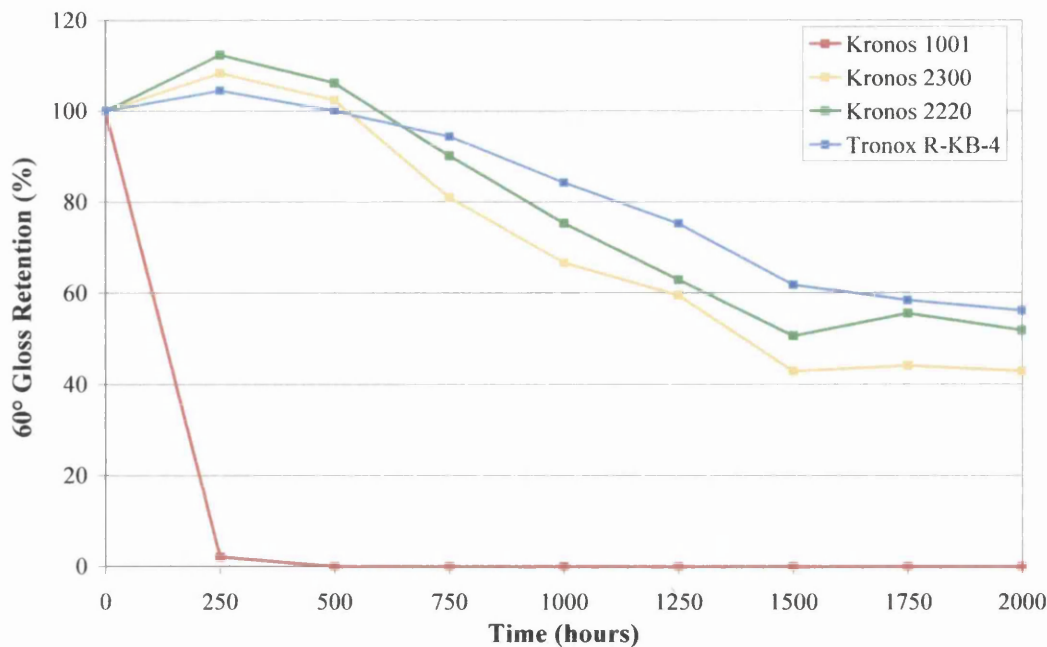


Figure 4.4 — Xenon Arc Gloss Retention of ‘Improved’ Durability Polyurethane Coatings

The coatings pigmented with the more stable TiO₂ grades showed significantly higher durability than the coating pigmented with Kronos 1001, each retaining at least 40% of the original coating gloss. The coating pigmented with the grade B Kronos 2300 showed the lowest gloss retention at 2000 hours, indicating it to be the least stable. The coatings pigmented with the grade A pigments showed similar gloss retention results – higher than that of the Kronos 2300 coating, however the coating pigmented with Tronox R-KB-4 performed better than that pigmented with Kronos 2220. The xenon arc gloss retention results gave the same performance ranking as the CO₂ evolution measurement, the ranking in order of highest to lowest durability was Tronox R-KB-4 > Kronos 2220 > Kronos 2300 > Kronos 1001.

It can be seen by the comparison of gloss retentions in Figure 4.5 that despite the reduction in CO₂ evolution shown by the adapted coatings, the gloss retention in xenon arc was only improved for the coating containing Kronos 2220 pigment. The coatings pigmented with Tronox R-KB-4 and Kronos 2300 TiO₂ grades showed lower gloss retention levels than the standard formulation coatings. This illustrated that the coatings may be of higher durability throughout the bulk of the polymer (CO₂) but the durability at the coating surface (gloss) was lower.

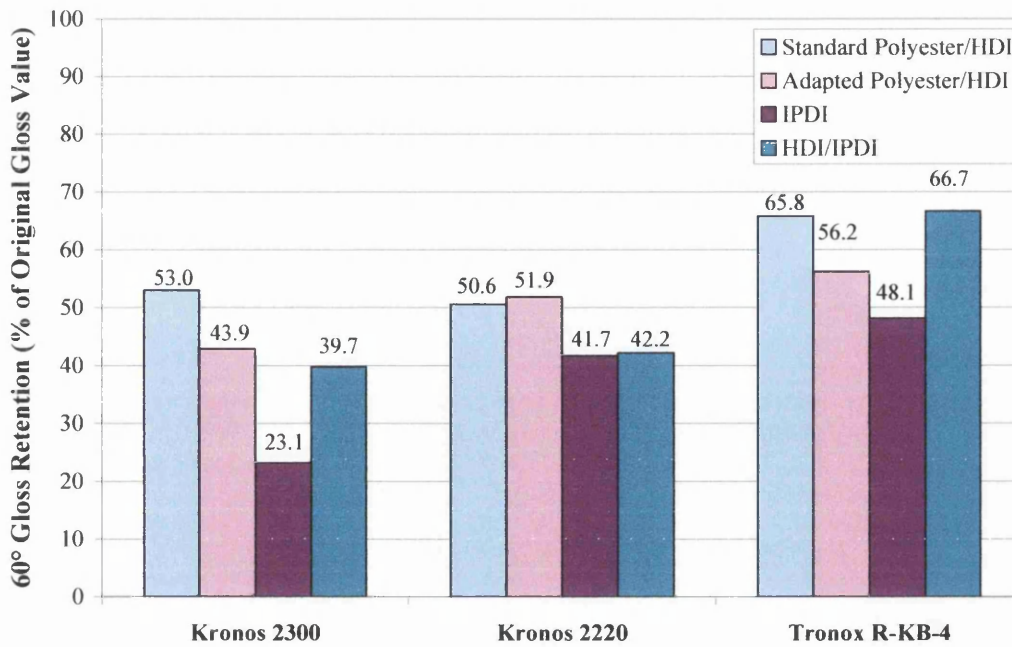


Figure 4.5 – Comparison of 60° Gloss Retention of all Polyurethane Resins Pigmented with Stabilised TiO₂ Following 2000 Hours of Xenon Arc

One possible reason for this discrepancy could be a result of different oxygen permeability into the coating which has been shown in the literature⁵ to affect CO₂ evolution. A review of the oxygen permeability of polymeric coatings⁶ has discussed the effect of increased cross-linking in reducing oxygen permeability through a polymeric film. It is likely that adaptation of the polyester component has increased the cross-linking density which reduces oxygen permeation through the film and consequently oxidation of the polymer. Oxidation and therefore evolution of CO₂ as a product requires is dependant on the presence of oxygen, in its absence oxidation cannot occur and thus CO₂ is not produced. A schematic of the effect of increased cross-linking density on polymer oxidation is shown in Figure 4.6. This illustrates the reduction in CO₂ evolution from the bulk as a result increased cross-linking reducing oxygen permeation and also UV penetration through the coating. Different TiO₂ grades undergo different reactions with the polymer which change the dispersion characteristics of the coating. This is significant as the optical properties of the pigment and therefore reflectance of UV by the particles is dependant on dispersion and so oxidation at the surface could be increased by reflection of light by the TiO₂.

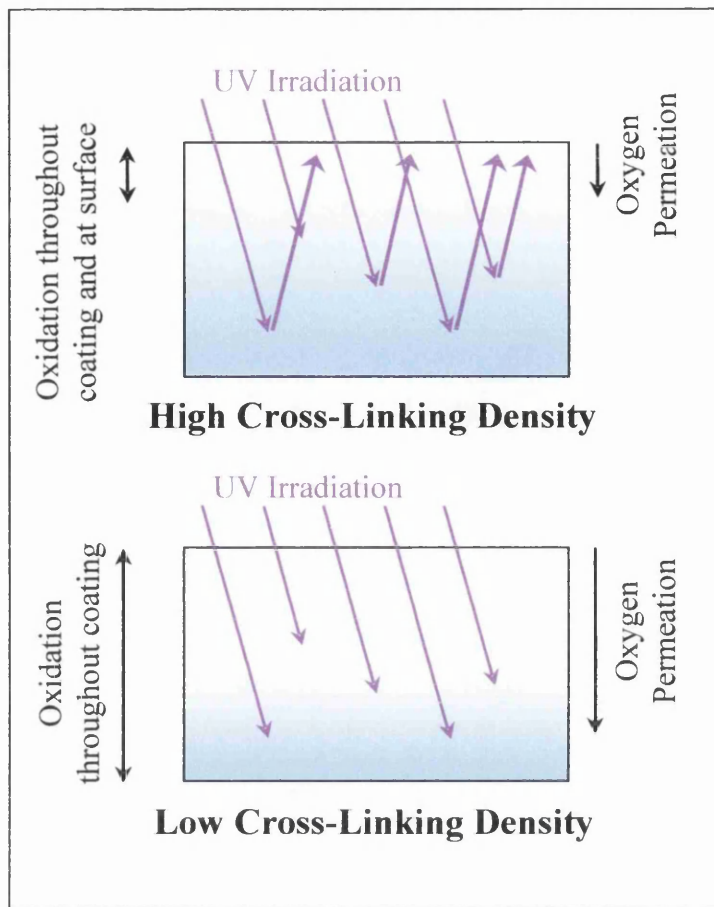


Figure 4.6 – Schematic Illustration of the Effects of Cross-Linking Density on Oxygen Permeation and UV Penetration through a Coating

Increased cross-linking density leads to lower oxygen permeation and UV penetration through the coating causing a reduction in oxidation and thus CO_2 evolution below the surface. It is shown here that the decreased UV penetration can also lead to reflection of photons at the surface which can lead to an increase in surface degradation as photons exiting the film come across regions of higher O_2 concentration. This is likely to be the reason for the discrepancy between the CO_2 evolution and xenon arc gloss retention results as the cross-linking density has confined CO_2 evolution to the surface thus reducing the level but at the same time increasing surface degradation. The low gloss retention therefore does not necessarily mean that the coating is of a lower overall durability but that there is increased degradation at the surface which could lead to aesthetic problems.

4.3.1.4 'Improved' Polyurethane Ranking

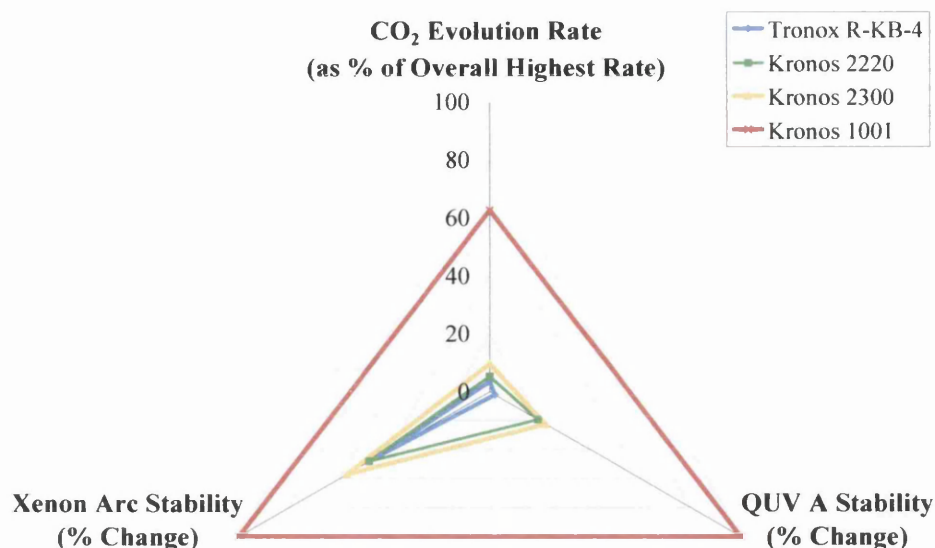


Figure 4.7 – Ranking of 'Improved' Durability Polyurethane Coatings According to Durability in CO₂ Measurement Apparatus, QUV A and Xenon Arc Weathering

Each of the pigmented polyurethane coatings formulated with the adapted polyester resin was ranked according to performance in each of the three tests as shown in Figure 4.7. Coatings were ranked according to durability in QUV A and xenon arc as a percentage change in gloss retention. They were also ranked according to CO₂ evolution results as a percentage of the highest CO₂ evolution rate gained from each of the coatings - the highest CO₂ evolution rate was gained from the third series IPDI polyurethane pigmented with Kronos 1001.

This allowed a direct comparison between each of the pigmented coatings and via measurement of the area covered by each of the coatings allowed the photoactivity ranking to be calculated. The photoactivity ranking was calculated as a ratio of the most durable standard performance HDI based polyurethane – that pigmented with Tronox R-KB-4 and allowed comparison between each of the pigmented coatings and between the different coating types as shown in Figure 4.8.

The photoactivity ranking shows that pigmentation with the photoactive Kronos 1001 pigment photocatalysed degradation of both coating resins. For both the first and second series polyurethanes the ranking indices were over 85 times that of the respective Tronox R-KB-4 pigmented coatings. As anticipated the Kronos 2300 gave a higher photoactivity ranking than the grade A pigments, with the coating pigmented with Tronox R-KB-4 again exhibiting the lowest photoactivity. This

indicates that for HDI based polyurethane coatings pigmentation with the grade A Tronox R-KB-4 produces the most stable coating across the range of tests.

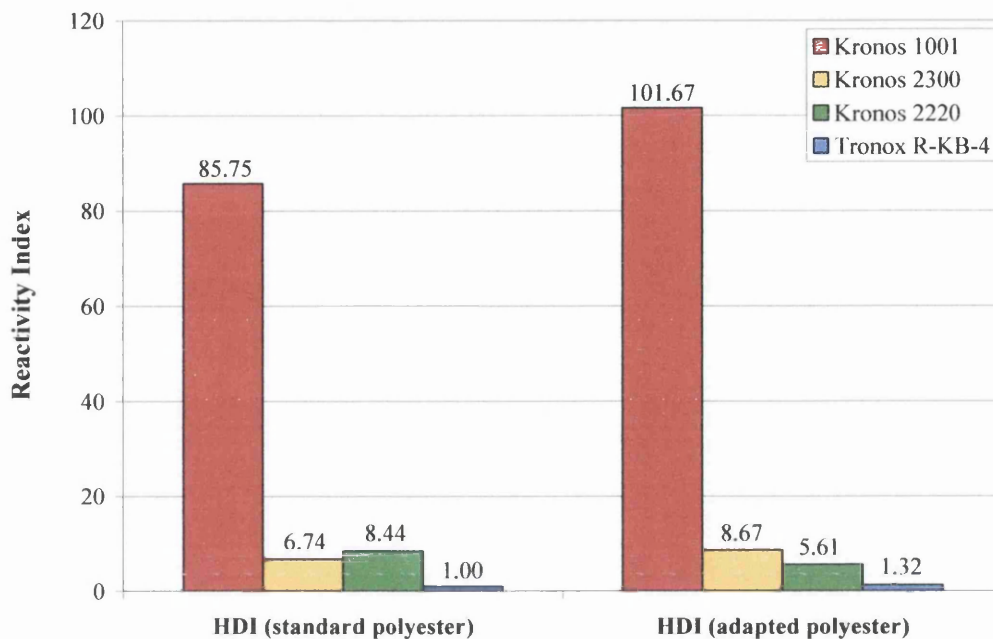


Figure 4.8 – Photoactivity Ranking Indices of Standard Durability Polyurethane Coatings

Comparison between the photoactivity indices for the first and second series coatings showed that in the majority of cases adaptation of the polyester resin was detrimental to the overall stability of the pigmented coatings. The only coating to have exhibited an increase in durability across all testing methods was the one pigmented with Kronos 2220. Despite the apparent increase in durability it is not advisable to use Kronos 2220 pigment in polyurethanes for commercial use. Kronos 2220 was designed specifically as a pigment for use in PVC coatings and showed elevated degradation rates compared to the Tronox R-KB-4. It was seen in Chapter Four that Kronos 2220 showed lower pigment/resin compatibility than the other pigments producing a coating with the lowest initial gloss of all the pigmented polyurethane coating.

Despite the increased resin stability shown by the CO₂ evolution rate results, the photoactivity indices for the Tronox R-KB-4, Kronos 2300 and Kronos 1001 pigmented coatings contradict this. As discussed previously, this could be a result of increased cross-linking reducing oxidation in the bulk of the film concentrating degradation at the surface. The decrease in durability does not necessarily mean that the coating is of decreased durability but that it is more susceptible to surface

oxidation which can be a problem when aesthetics are important. These discrepancies further confirm the necessity to test full coating formulations as both surface and total coating stability are critical in the commercial production of coated products.

4.3.2 Weathering Results for the Polyester-Melamine Coatings Formulated with the Adapted Polyester Resin

4.3.2.1 CO₂ Evolution Rates

The CO₂ evolution rate results for the polyester-melamine coatings containing the adapted polyester polyol are shown in Figure 4.9. Like the polyurethanes, the polyester-melamine coatings formulated with the adapted polyester showed a reduced rate of CO₂ evolution compared to the standard durability polyester-melamine coatings shown in Figure 4.10.

As with all the coatings tested pigmentation with Kronos 1001 photocatalysed degradation giving a CO₂ evolution rate higher than that of the un-pigmented coating. Similarly, the coatings pigmented with more photostable pigments showed a reduction in CO₂ evolution compared to the un-pigmented polyester-melamine resin. The coatings pigmented with the Kronos 1001 and Kronos 2300 pigments show a small decrease in the photoactivity compared to the first series polyesters-melamine coatings.

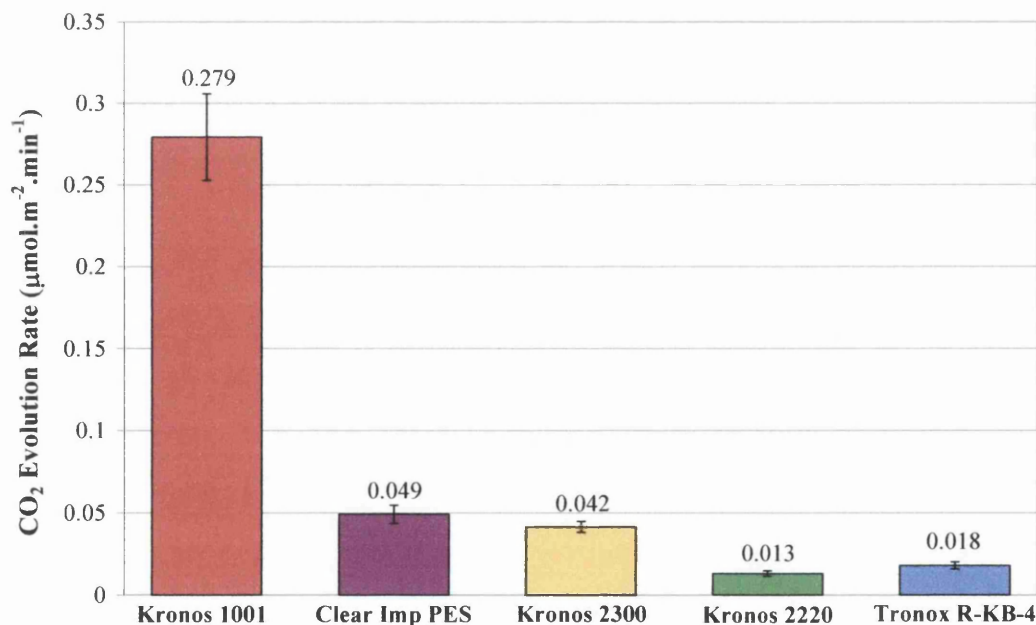


Figure 4.9 – CO₂ Evolution Rates of ‘Improved’ Durability Polyester-Melamine Coatings

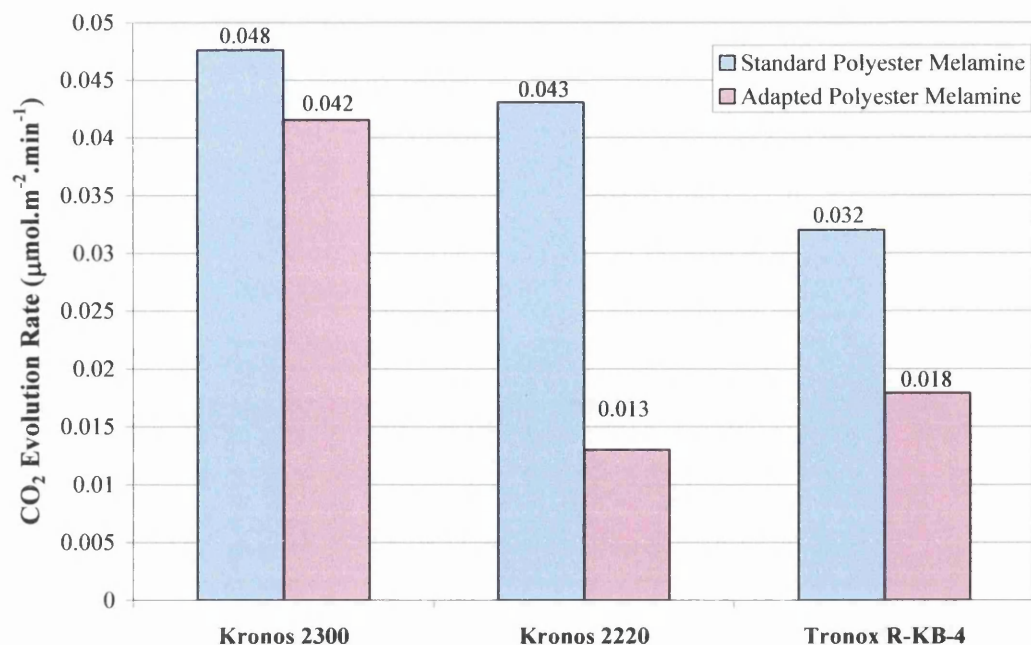


Figure 4.10 – Comparison of CO₂ Evolution Rates of all Polyester-Melamine Resins Pigmented with Stabilised TiO₂

The coatings containing the most photostable Kronos 2220 and Tronox R-KB-4 pigments showed a greater decrease in photoactivity both coatings exhibited a very low rate of CO₂ evolution. Unlike the first series polyester-melamine coating which showed Tronox R-KB-4 to have the highest stability of all the pigments tested the second series coatings showed Kronos 2220 to be the most stable in this test.

4.3.2.2 QUV A Gloss Retention

The QUV A gloss retention results for the second series polyester-melamine coatings shown in Figure 4.11 showed a decrease in durability in all pigmented coatings compared to the standard durability resin.

The coatings pigmented with the Kronos 2220 and Kronos 2300 TiO₂ grades showed similar trends in gloss change to the standard durability coatings. The coating pigmented with Kronos 2220 showed a gloss decrease similar that of the first series coating however the total reduction was lower, indicating lower durability. Similarly the Kronos 2300 showed a gloss increase comparable to the first series polyester however the gloss increase and thus the total gloss change was higher, representative of lower durability.

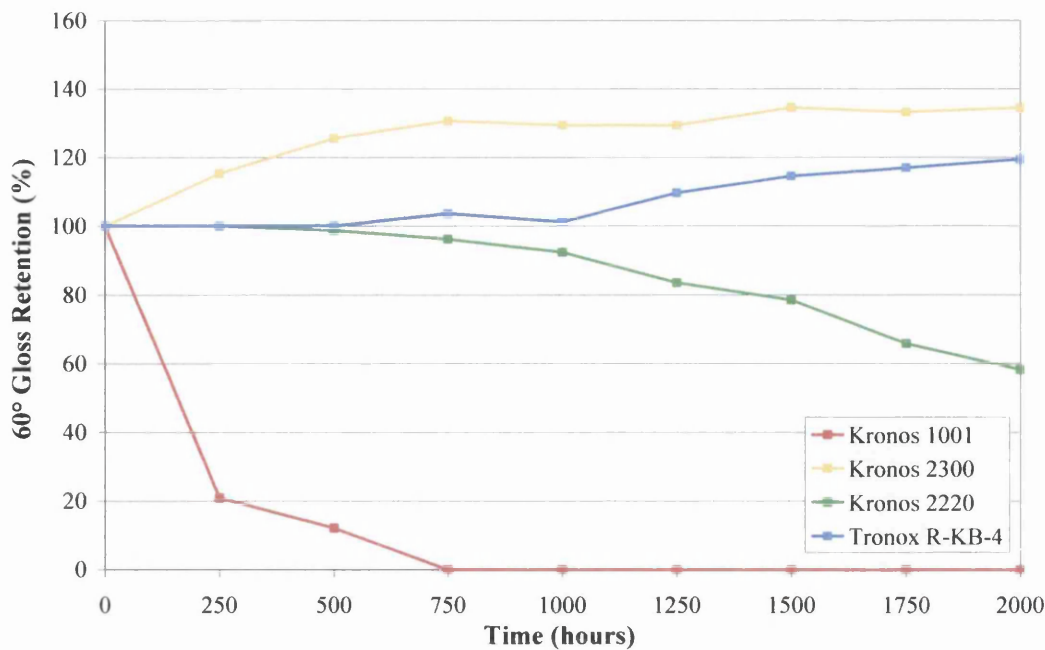


Figure 4.11 – QUV A Gloss Retention of ‘Improved’ Durability Polyester-Melamine Coatings

The coating pigmented with Tronox R-KB-4, although of higher stability than the other pigmented coatings containing the adapted polyester also showed a greater gloss change and therefore decreased durability compared to the coatings containing the standard polyester. The performance ranking of the pigmented coatings in QUV A in order of best to worst was Tronox R-KB-4 > Kronos 2300 > Kronos 2220 > Kronos 1001.

4.3.2.3 Xenon Arc Gloss Retention

The gloss retention results for the coatings are shown in Figure 4.12 and give the same performance ranking for the coatings as QUV A testing. The xenon arc gloss retention results show each of the coatings to have undergone gloss decrease over the test duration. All of the polyester-melamine coatings containing the adapted polyester showed lower durability than those containing the standard polyester as illustrated in Figure 4.13.

As anticipated, the coating pigmented with Tronox R-KB-4 showed better durability than those containing the Kronos 2220 and Kronos 2300 TiO₂ grades. As shown in Figure 4.10 all of the stable pigmented coatings showed improved durability according to CO₂ evolution rate. Figure 4.12 however showed the coatings pigmented with Tronox R-KB-4 and Kronos 2220 to have exhibited higher levels of surface

degradation, possibly due to the effects of increased cross-linking in the coatings formulated with the adapted polyester.

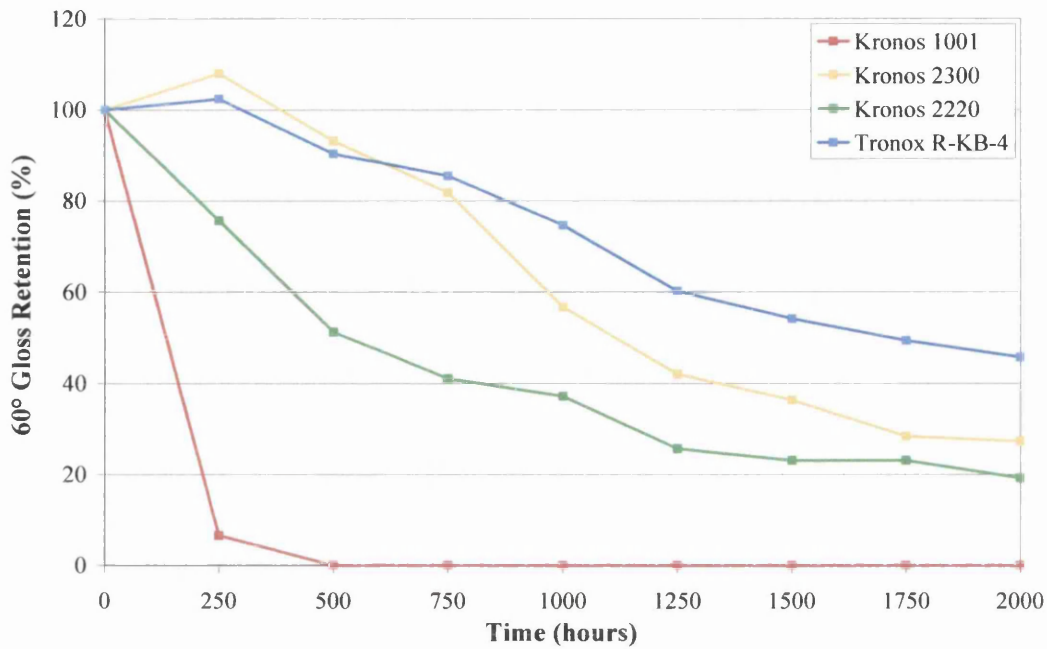


Figure 4.12 – Xenon Arc Gloss Retention of 'Improved' Durability Polyester-Melamine Coatings

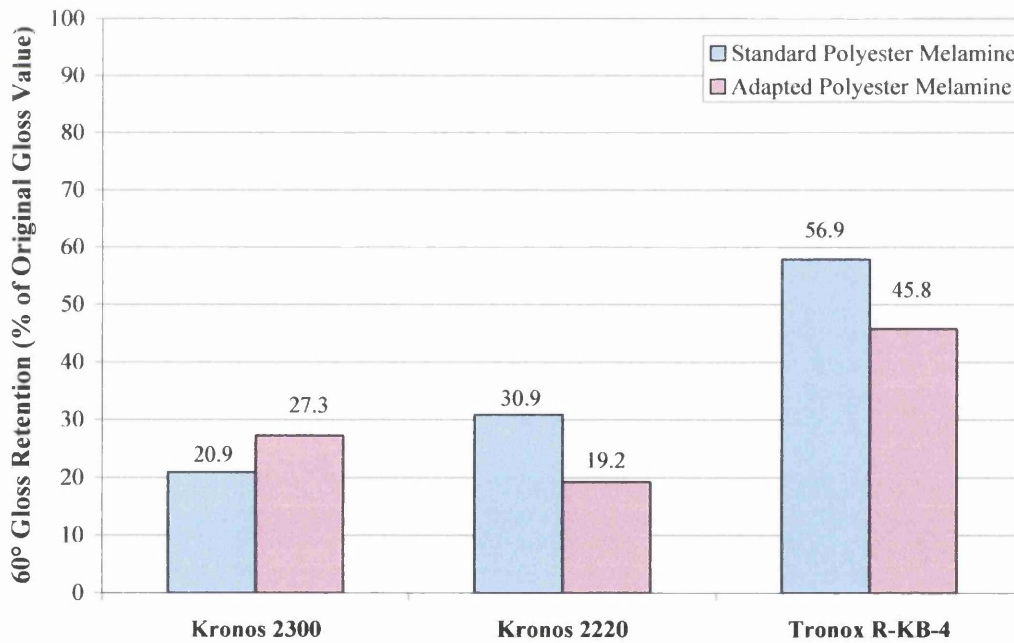


Figure 4.13 – Comparison of 60° Gloss Retention of all Polyester-Melamine Resins Pigmented with Stabilised TiO₂ Following 2000 Hours of Xenon Arc

4.3.2.4 'Improved' Polyester-Melamine Ranking

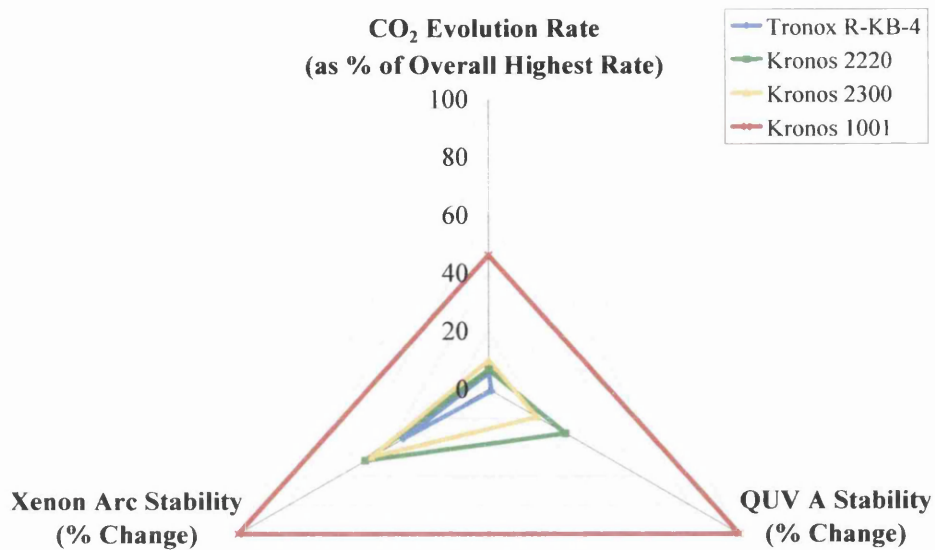


Figure 4.14 – Ranking of 'Improved' Durability Polyester-Melamine Coatings According to Durability in CO₂ Measurement Apparatus, QUV A and Xenon Arc Weathering

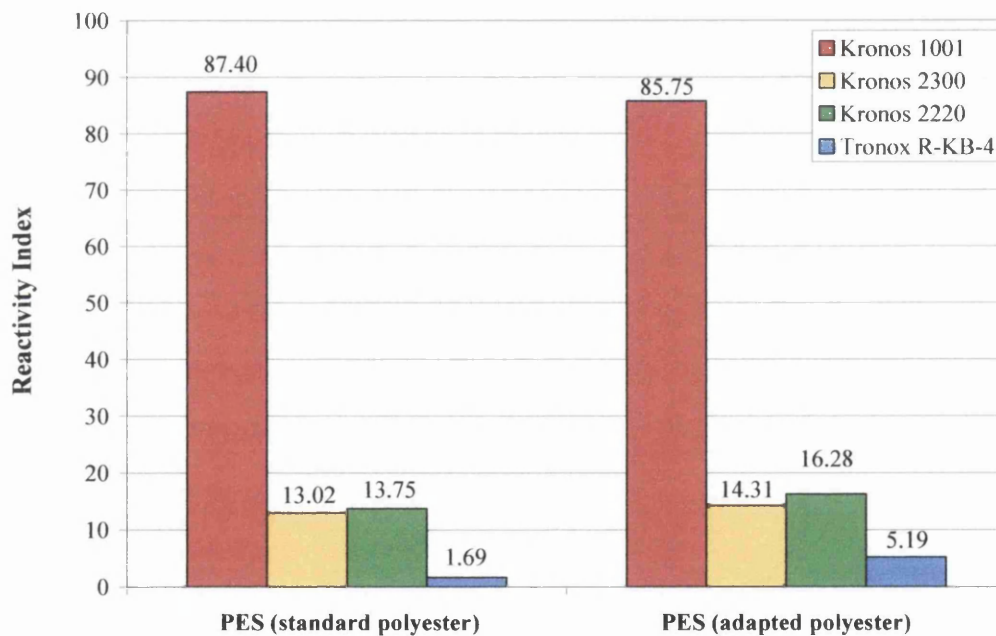


Figure 4.15 – Photoactivity Ranking Indices of Standard Durability Polyester-Melamine Coatings

The performance rankings for each of the pigmented polyester-melamine coatings formulated with the adapted polyol are shown in Figure 4.14. The photoactivity indices gained from these rankings are shown in Figure 4.15. Comparison between the first and second series polyester-melamine coatings shows

that changing the polyester had a negative effect on durability in all but the coating pigmented with Kronos 1001.

From Figure 4.15 it can be seen that all of the stable pigmented coatings formulated with the adapted polyester actually show a significant decrease in durability compared to the standard coatings discussed in Chapter Three. The pigment ranking in this coating was however the same as that given by testing of the standard polyester-melamine coatings. Once again it was shown that across the range of tests Tronox R-KB-4 produced the most stable coating, followed by Kronos 2300 and then Kronos 2220. Kronos 1001 was again shown to photocatalysed degradation and produce a low durability coating which is unsuitable for commercial use.

4.3.3 Weathering Results for the IPDI Based Polyurethane Coatings

4.3.3.1 CO₂ Evolution Rates

The CO₂ evolution rate results for the IPDI based polyurethane coatings are illustrated in Figure 4.16. The un-pigmented IPDI polyurethane showed the highest CO₂ evolution rate of all the polyurethane coatings, indicating it to be the least stable of all the polymers. This however was anticipated as the primary property of the IPDI cross-linker is chemical resistance unlike the other resins which were formulated for good weather stability.

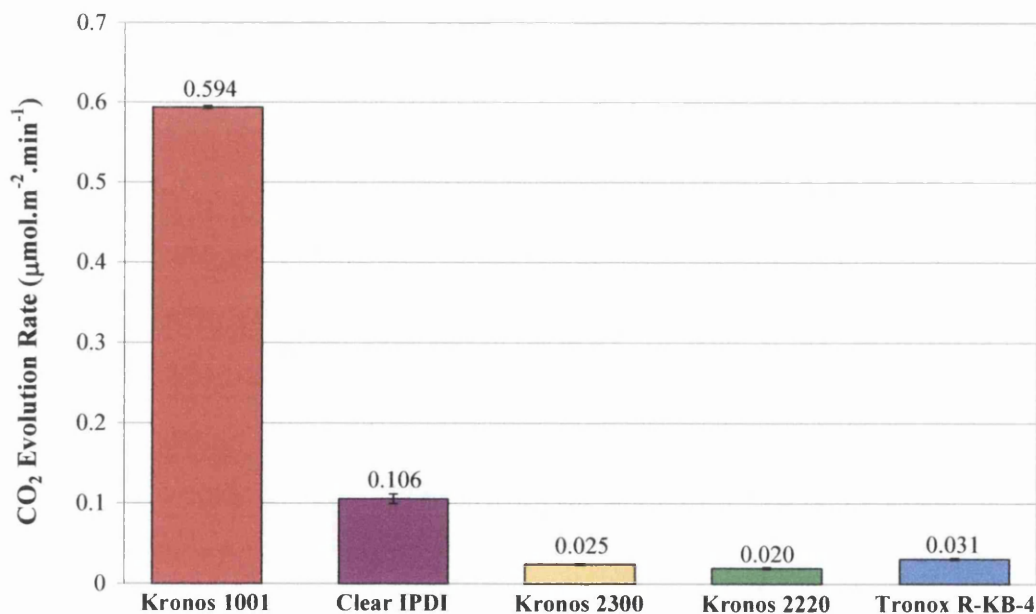


Figure 4.16 – CO₂ Evolution Rates of IPDI Based Polyurethane Coatings

The coating pigmented with Tronox R-KB-4 showed a lower rate of CO₂ evolution than the first series coating. However this rate was higher than the other coatings pigmented with the stable TiO₂ grades. Addition of Kronos 2300 and Kronos 2220 pigments reduced the CO₂ evolution rate to below that of all other coatings pigmented with these pigments. The coating pigmented with Kronos 2220 gave the lowest rate of all the coatings, indicating it to be the most stable pigment for use with the IPDI based resin in terms of total mineralisation (CO₂ evolution) rate.

Pigmentation with Kronos 1001 significantly increased the CO₂ evolution rate to a level higher than any of the other Kronos 1001 coatings. Addition of this Kronos 1001 pigment had a photocatalytic effect, increasing photo-oxidation of the polymer and consequently the rate of CO₂ evolution to levels significantly higher than that of the un-pigmented polymer. Once again the stabilised TiO₂ grades afforded a level of shielding to the polymer, reducing CO₂ evolution rates to levels lower than that of the clear resin.

4.3.3.2 QUV A Gloss Retention

The QUV A gloss retention results for the third series IPDI polyurethane in Figure 4.17 also showed that addition of Kronos 1001 pigment photocatalysed coating degradation. This coating failed after just 500 hours of testing, while the coatings pigmented with the stabilised TiO₂ grades all remained stable or increased in gloss over the test duration.

The coating pigmented with Tronox R-KB-4 appears to be the most stable of the IPDI coatings as gloss retention remained stable throughout the weathering duration. The coatings pigmented with Kronos 2220 and Kronos 2300 showed a similar gloss increase to that seen in the first and second series polyurethanes in QUV A weathering. This increase is indicative of changes occurring within the polymer and showed them to be of lower durability than the coating containing the Tronox R-KB-4 pigment.

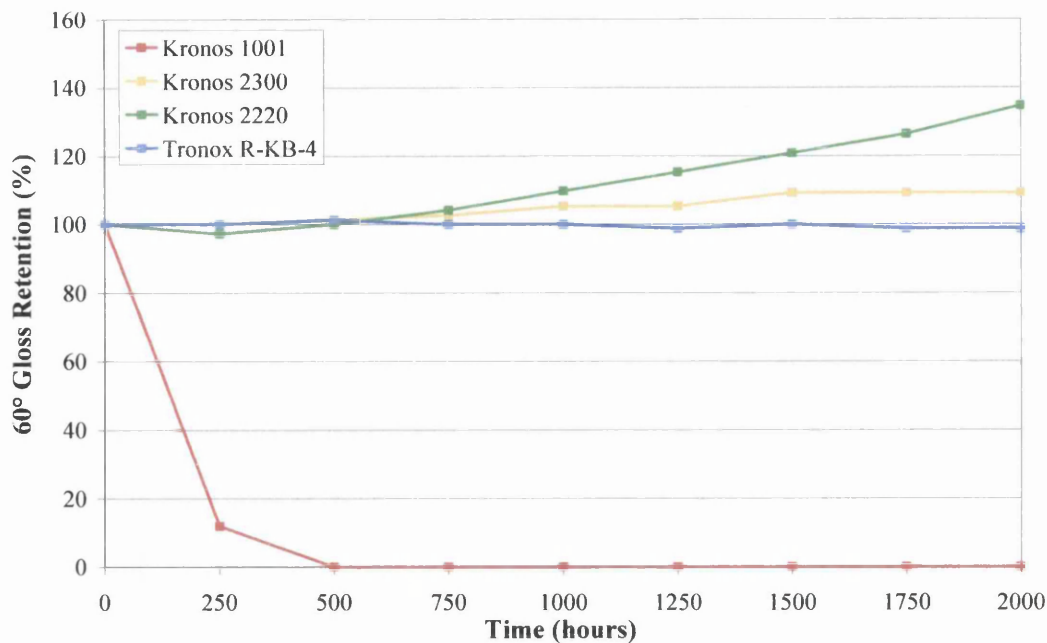


Figure 4.17 – QUV A Gloss Retention of IPDI Based Polyurethane Coatings

4.3.3.3 Xenon Arc Gloss Retention

Figure 4.18 shows the gloss retention results for the pigmented IPDI based polyurethanes following xenon arc weathering. These results showed the coating pigmented with Kronos 1001 to fail more quickly than the first series coatings and thus matched with the CO₂ evolution results shown in Figure 4.16.

The ranking given by xenon arc weathering showed Tronox R-KB-4 to be the most stable pigment followed by Kronos 2220 and then Kronos 2300. Both the gloss retention results and the CO₂ evolution rates for the coating pigmented with Kronos 2220 and Kronos 2300 were similar but indicated the Kronos 2220 TiO₂ grade to be slightly more stable. The coating pigmented with Tronox R-KB-4 had the highest gloss retention value of all the IPDI coatings, showing significantly higher durability than the other coatings. This result contradicts that given by the CO₂ evolution measurement and differences were most likely due to fundamental differences between the measurements. Despite the low CO₂ evolution rates for the IPDI coatings containing Kronos 2220 and Kronos 2300 the gloss retention results define the coatings as being of low stability. This suggests that the coatings are more stable in bulk but that the surface is more prone to damage.

Xenon arc gloss retention results predicted all of the third series IPDI coatings to be less stable than the first series HDI, second series HDI and the third series

HDI/IPDI coatings pigmented with the same TiO₂ grades. Likewise the CO₂ evolution showed the IPDI un-pigmented coating to be the least stable of all the resins tested.

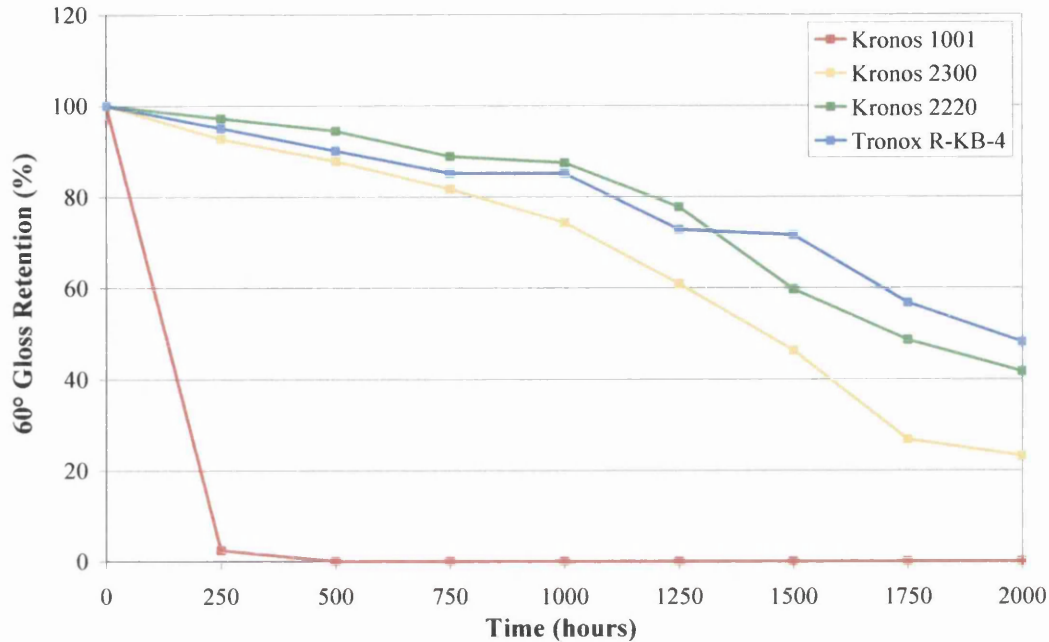


Figure 4.18 – Xenon Arc Gloss Retention of IPDI Based Polyurethane Coatings

4.3.3.4 IPDI Based Polyurethane Ranking

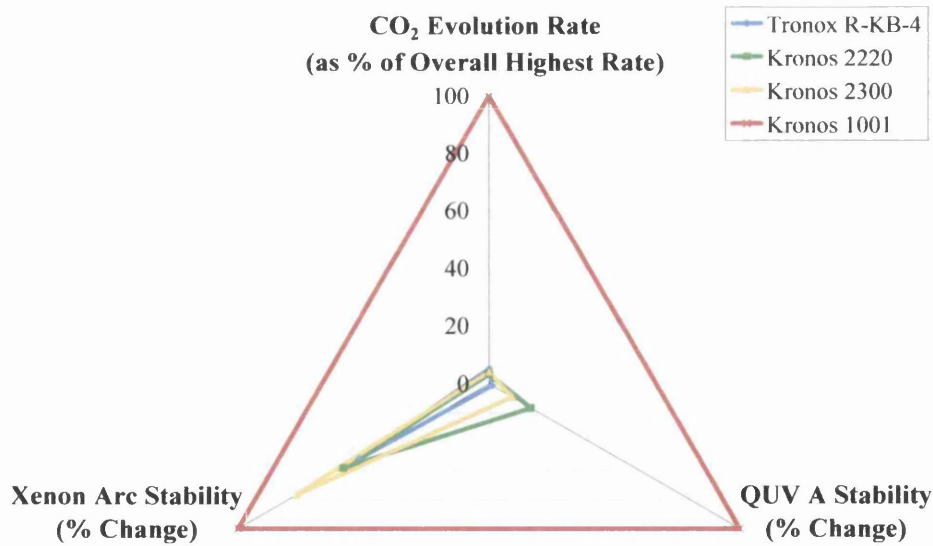


Figure 4.19 – Ranking of IPDI Based Polyurethane Coatings According to Durability in CO₂ Measurement Apparatus, QUV A and Xenon Arc Weathering

The performance ranking for pigmented IPDI polyurethanes shown in Figure 4.19 was used to calculate the photoactivity indices for each coating. Comparison

between the photoactivity indices for the IPDI polyurethanes shown in Figure 4.20 and those gained from the first and second series polyurethane coatings it can be seen that the resin showed significant decrease in durability when pigmented with the most stable Tronox R-KB-4 pigment.

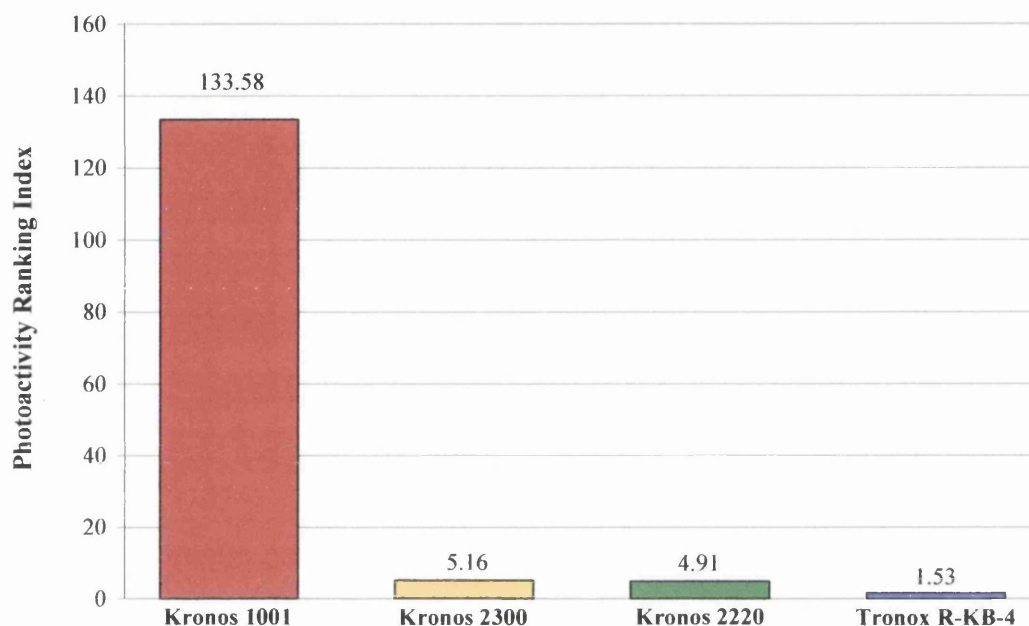


Figure 4.20 – Photoactivity Ranking Indices of IPDI Based Polyurethane Coatings

The coatings containing the Kronos 2220 and Kronos 2300 pigments showed better durability across the range of tests compared to the other polyurethane coatings pigmented with these TiO₂ grades. Despite this the photoactivity indices given by these coatings were over three times higher than any of the other coatings pigmented with Tronox R-KB-4. Once again it was shown that across the range of tests Tronox R-KB-4 produced the most stable coating and the increased photoactivity was due to the low resin stability as opposed to pigment photoactivity.

4.3.4 Weathering Results for the HDI/IPDI Based Polyurethane Coatings

4.3.4.1 CO₂ Evolution Rates

The CO₂ evolution rates for the third Series HDI/IPDI Polyurethane coatings can be seen in Figure 4.21. Irradiation of un-pigmented coatings gave a much lower CO₂ evolution rate than the other un-pigmented polyurethanes tested. This indicated the HDI/IPDI combination resin and adapted polyester co-reactant to be the most stable combination.

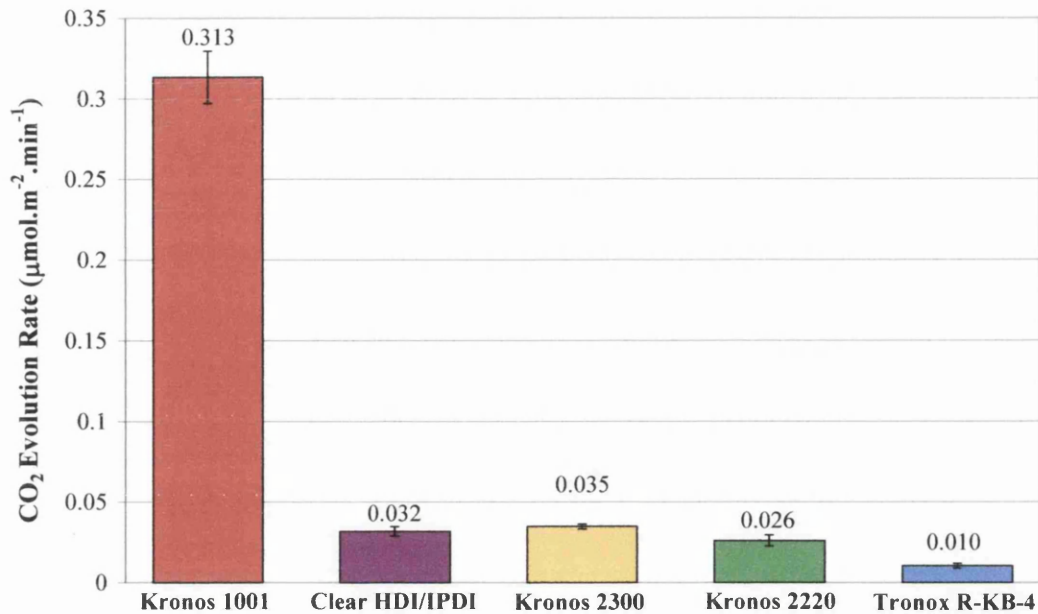


Figure 4.21 – CO₂ Evolution Rates of HDI/IPDI Based Polyurethane Coatings

Addition of the photostable Kronos 2220 and Tronox R-KB-4 effected a reduction in CO₂ evolution rate, indicating shielding of the polymer matrix by these pigments. Addition of Kronos 2300 pigment marginally increased the rate of CO₂ evolution to above that of the un-pigmented coating, this reflects the excellent stability of the clear HDI/IPDI resin. Kronos 2300 has a higher photoactivity potential than the other pigments. A decrease in rate in other polymers could be due to a higher compatibility with the resin than other pigment which effectively reduces the photoactivity below that of a pigment which is incompatible with the resin. Although this pigment appeared to be more stable in some cases Kronos 2300 is a grade B pigment with moderate to high photoactivity potential and therefore should not be used in exterior coatings. Addition of Kronos 1001 pigment significantly photocatalysed coating degradation increasing the rate of CO₂ evolution by over 10 times that of the un-pigmented coating.

The coatings containing Kronos 2220 and Tronox R-KB-4 both exhibited decreased rates of CO₂ evolution compared to the clear coating. The coating pigmented with Kronos 2220 showed better stability than the first and second series coatings. The rate of CO₂ evolution was higher than that of the IPDI polyurethane containing Kronos 2220 which showed good stability according to the CO₂ evolution. The HDI/IPDI combination polyurethane pigmented with Tronox R-KB-4 showed excellent stability in the CO₂ evolution measurement and gave the lowest rate of all

the coatings tested. It was apparent from this testing that the third series HDI/IPDI polyurethane is the most stable coating.

4.3.4.2 QUV A Gloss Retention

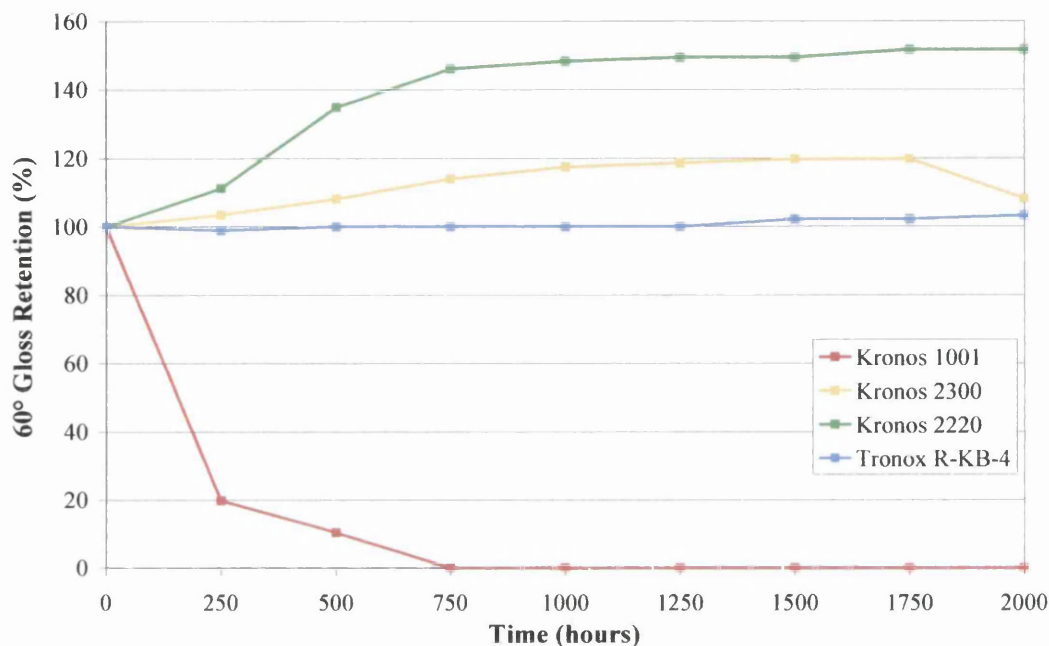


Figure 4.22 – QUV A Gloss Retention of HDI/IPDI Based Polyurethane Coatings

The QUV A gloss retention results for the third series HDI/IPDI polyurethane coatings shown in Figure 4.22. A significant increase in gloss was exhibited by the coatings pigmented with Kronos 2220 and Kronos 2300 indicating the occurrence of changes in the coating matrix. The coating pigmented with Tronox R-KB-4 again remained at a stable gloss value throughout the test duration, supporting the durability shown by xenon arc testing and CO₂ evolution measurement.

4.3.4.3 Xenon Arc Gloss Retention

The gloss retention results for the pigmented polyurethane coatings based on the HDI/IPDI cross-linker are illustrated in Figure 4.23. The photoactivity prediction of these coatings corresponded with that given by measurement of CO₂ evolution shown in Figure 4.21.

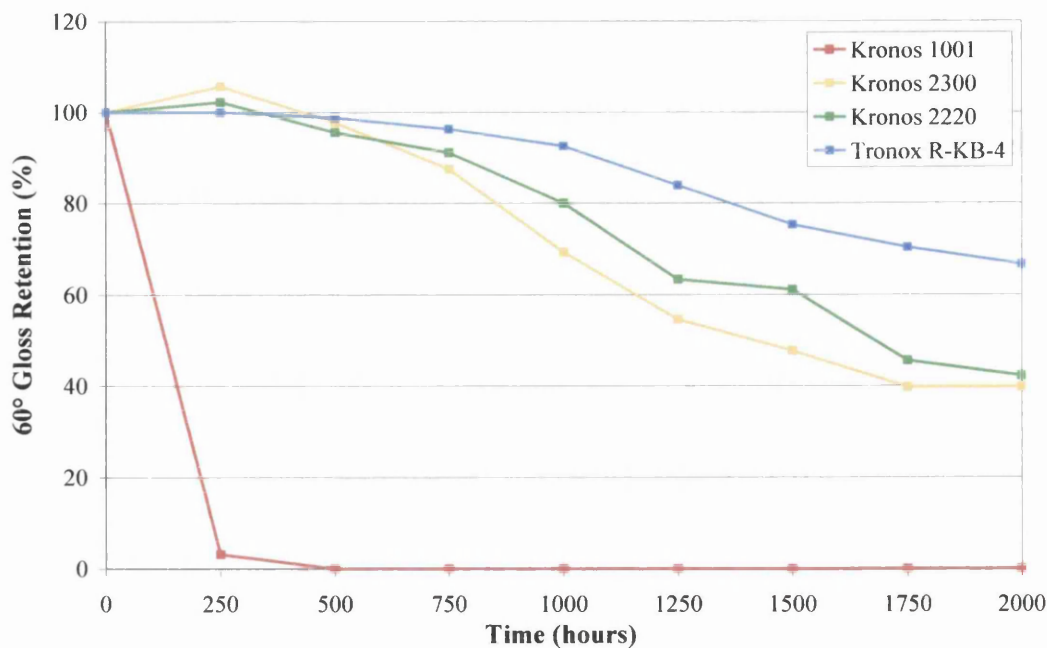


Figure 4.23 – Xenon Arc Gloss Retention of HDI/IPDI Based Polyurethane Coatings

The durability ranking from highest to lowest according to both xenon arc and CO₂ evolution was Tronox R-KB-4 >Kronos 2220> Kronos 2300 > Kronos 1001. The HDI/IPDI coating pigmented with Kronos 1001 showed lower durability than the standard durability polyurethane coatings in xenon arc, QUV A and CO₂ evolution measurement. Although this coating appears less stable when pigmented with Kronos 1001 the more photostable pigmented coatings all showed an increase in durability. The high photoactivity of Kronos 1001 is such that even the most stable coatings containing this pigment resins exhibit high levels of photocatalysed degradation.

The coating pigmented with Kronos 2300 showed a lower durability than the first and second series polyurethanes. This was anticipated as the CO₂ evolution measurements showed photocatalysis to be occurring in this pigmented coating. Tronox R-KB-4 showed the best stability of all pigments in the HDI/IPDI coating, QUV A gloss retention results showed no change in gloss which indicated the coating to be stable throughout the testing period. The final gloss retention of the HDI/IPDI coating pigmented with Tronox R-KB-4 following xenon arc weathering although similar to the first series HDI coating was slightly higher, these results predicted the coating to be the most durable coating tested in xenon arc.

The HDI/IPDI polyurethane coating gave the highest final gloss reading and lowest CO₂ evolution rate measurement of all coatings tested. This coating showed an excellent resin stability and particularly good durability when pigmented with Tronox

R-KB-4 which afforded the highest level of shielding against UV light. Each of the coatings tested in this work exhibited the highest durability when pigmented with Tronox R-KB-4 compared to the other pigmented coatings.

4.3.4.4 HDI/IPDI Based Polyurethane Ranking

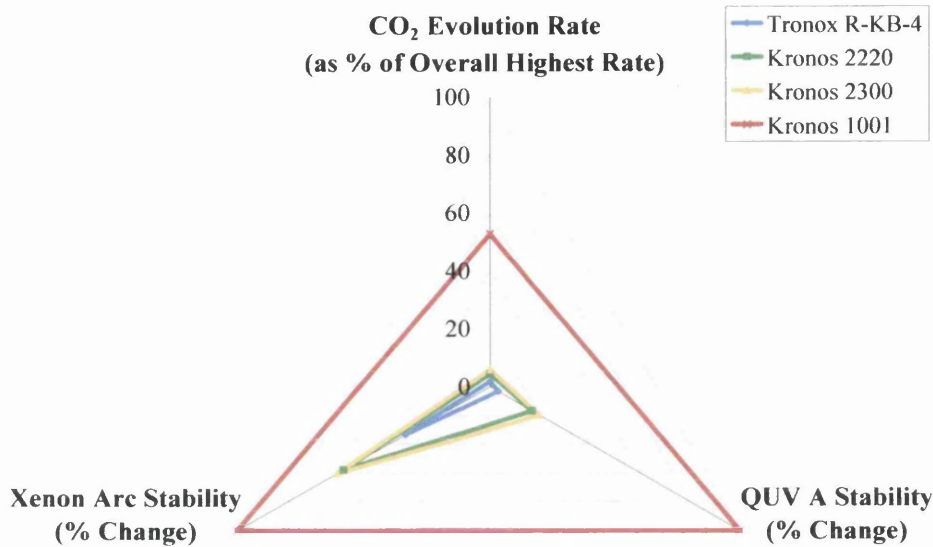


Figure 4.24 – Ranking of HDI/IPDI Based Polyurethane Coatings According to Durability in CO₂ Measurement Apparatus, QUV A and Xenon Arc Weathering

The performance ranking for pigmented HDI/IPDI polyurethanes is shown in Figure 4.24. This was used to calculate the photoactivity indices for each coating as a ratio of the area covered by standard HDI polyurethane pigmented with Tronox R-KB-4 as shown in Figure 4.25.

From Figure 5.25 it can be seen that Kronos 1001 TiO₂ photocatalysed degradation of all polyurethane coatings, giving photoactivity indices significantly higher than the other coating. The photoactivity indices for the coatings pigmented with stabilised TiO₂ grades is shown in Figure 4.26. The HDI/IPDI resin pigmented with Tronox R-KB-4 had the lowest photoactivity ranking index of all the coatings tested and therefore was the most durable coating. Across the range of weathering tests this coating consistently exhibited the best performance of all the polyurethanes and can therefore be said to be the most stable coating formulation and the one most recommended for commercial use.

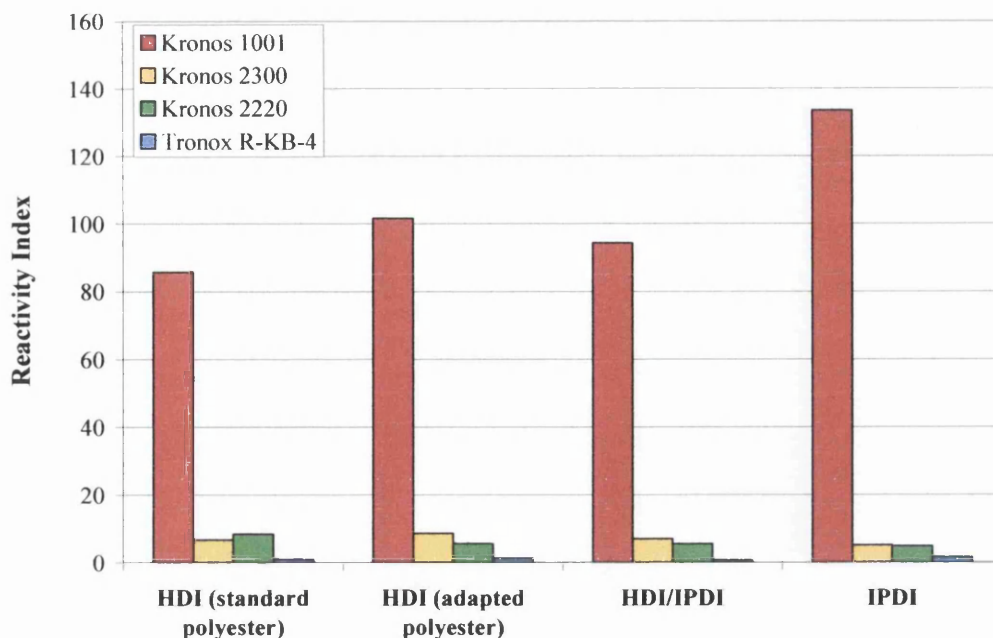


Figure 4.25 – Photoactivity Ranking Indices of HDI/IPDI Based Polyurethane Coatings

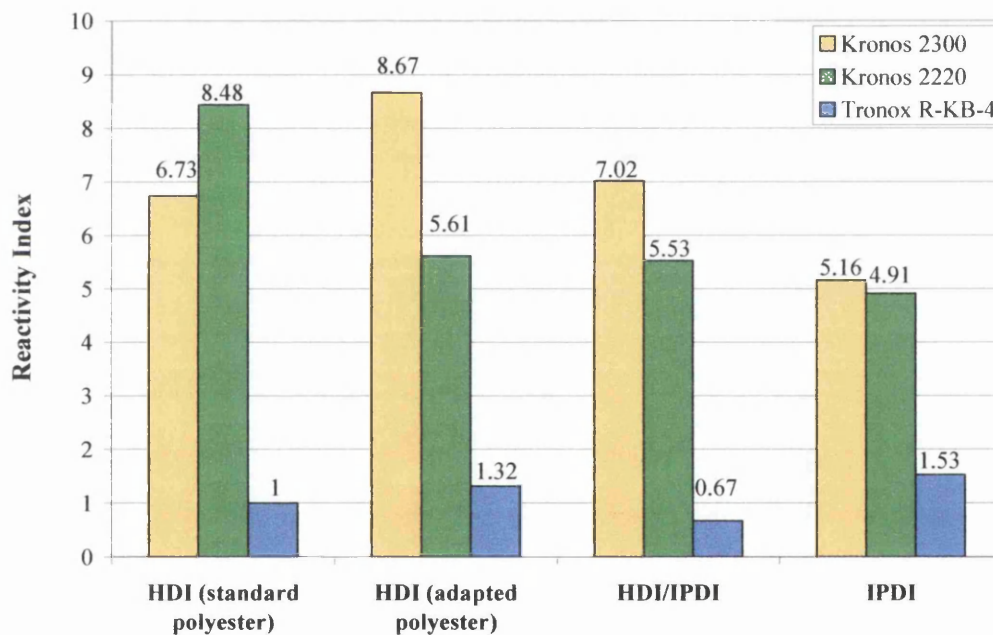


Figure 4.26 – Photoactivity Ranking Indices of HDI/IPDI Based Polyurethane Coatings Pigmented With Stabilised TiO₂ Grades

4.4 Conclusions

This work has shown that in all coatings addition of photoactive TiO₂ pigment caused significant photocatalysis of polymer oxidation. In all resins the coatings pigmented with Kronos 1001 exhibited a rate of CO₂ evolution over 10 times that of the un-pigmented coatings and rapid failure in both QUV A and xenon arc.

It was also shown that addition of stabilised pigment grades afforded a level of UV shielding to the polymer. In all cases pigmentation with Tronox R-KB-4 and Kronos 2220 decreased the rate of CO₂ evolution to below that of the un-pigmented coatings. This was also the general trend with Kronos 2300 pigment however the third series HDI/IPDI polyurethane pigmented with Kronos 2300 showed a higher rate of CO₂ evolution than the un-pigmented coating. This correlates with the classification of Kronos 2300 as a grade B pigment, which is confirmed by these coatings generally having a higher photoactivity ranking than the grade A TiO₂ pigments.

Commercial weathering showed all coatings pigmented with Tronox R-KB-4 to have a higher stability across the range of tests than those pigmented with Kronos 2220, Kronos 2300 and Kronos 1001.

The CO₂ evolution results for the un-pigmented coatings showed the third series IPDI based polyurethane to be the least stable coating resin. This result was not unexpected as the IPDI cross-linker is primarily used for applications requiring high chemical resistance and thus weather stability was not a priority during development of this resin.

Changes to the polymer resin in an attempt to improve coating durability did not provide the consistent improvements anticipated. In both polyurethane and polyester-melamine coatings changing the polyester polyol caused a general decrease in surface durability resulting in a higher photoactivity ranking compared to the coatings containing the standard polyester.

One possible reason for this could be a result of different oxygen permeability as a result of increased cross-linking of the polymers. Increased cross-linking has been shown to cause lower oxygen permeation through the coating, causing a reduction in oxidation and thus CO₂ evolution below the surface. In these cases incident UV is reflected back to the surface and degradation is focussed in this region leading to low gloss retention. This does not necessarily prove that the coating is unstable as increased cross-linking improves stability within the bulk polymer, however from an aesthetic point of view poor gloss retention is undesirable.

The HDI/IPDI based polyurethane was shown to be the most durable coating resin across the range of tests. The un-pigmented HDI/IPDI had a lower rate of CO₂ evolution than the other un-pigmented polyurethanes indicating it to be the most stable polymer resin. Pigmentation of this resin with Tronox R-KB-4 produced the most stable coating of all tested. This coating retained the highest percentage of initial

gloss following xenon arc weathering and also had the lowest CO₂ evolution rate of all coatings tested in the flat panel irradiation apparatus.

It is recommended from this work that polyurethane coatings developed for external high durability applications should be based on the HDI/IPDI based polyurethane pigmented with Tronox R-KB-4. It should however also be noted that this testing regime did not investigate the effects of further additions such as UV stabilisers and future developments should be undergo further testing to ensure continual improvement. It would also be beneficial in future studies to analyse photodegradation as a function of depth into the coating using the FTIR microscope to see if the lower CO₂ evolution rates corresponded to decreasing total degradation.

4.5 References

1. Boxall, J. and Von Fraunhofer, J.A., *Concise Paint Technology*. 1977, Elek Science: London.
2. Wright, P. and Cumming, P.C., *Solid Polyurethane Elastomers*. 1969, Maclaren and Sons: London.
3. Bock, M., *Polyurethanes for Coatings*. European Coatings Literature, ed. U. Zorll. 2001, Vincentz Network: Hanover.
4. Wilhelm, C. and Gardette, J.L., *Polymer*, 1997. **38**(16): p. 4019-4031.
5. Fernando, S.S., Christensen, P.A., Egerton, T.A., Eveson, R., Franchetti, S.M.M., Voisin, D., and White, J.R., *Materials Science and Technology*, Pending Publication 2008.
6. Sangaj, N.S. and Malshe, V.C., *Progress in Organic Coatings*, 2004. **50**: p. 28-39.

Chapter 5

The Effect of Coloured Pigmentation on Coating Photo-Oxidation

5.1 Introduction

The primary focus of this work has been on the durability of polyurethane coatings against the effects of ultraviolet (UV) light. Chapter Three and Chapter Four discussed the effects of titanium dioxide (TiO₂) grade and the polyurethane resin components on coating durability. These investigations were significant as the majority of coatings, even those that are not white, are pigmented with TiO₂ provide opacity^{1, 2}. The increasing popularity of pre-coated steels in the construction industry has resulted in the development of a huge variety of different coloured coatings. Previous work³ found that addition of single secondary coloured pigments affects the rate of coating photo-oxidation.

5.1.1 Aims

Previous work³ on coloured pigment additions focussed on additions of single secondary organic pigments to a PVC coating containing a photoactive (Degussa P25) grade of TiO₂. Commercial coatings for pre-finished steel products commonly contain more than one secondary coloured pigment, this work aims to assess the effects of inorganic coloured pigment blends on coating photo-oxidation. A range of coloured polyurethane coatings will be tested in QUV A, xenon arc and the carbon dioxide (CO₂) evolution apparatus^{4, 5} to assess the durability of coatings containing different pigment blends.

PVC coatings containing single secondary additions of the inorganic pigments will also be tested in the CO₂ evolution apparatus. This will allow comparison between the effects of organic and inorganic pigment additions on coating photo-oxidation.

5.2 Experimental Techniques

5.2.1 Colour Pigmented Coatings

Model PVC coatings containing single and mixed coloured pigment additions were tested in order to investigate the effect of colour on coating photo-oxidation. The coatings containing the single secondary pigment additions were produced with a photoactive (Degussa P25) TiO₂ grade. In order to investigate whether the effects of secondary coloured pigmentation differed with the chemical nature a range of organic and inorganic pigments were tested.

Model PVC coatings containing a photostable (Tronox R-KB-4) TiO₂ grade were pigmented with blends of inorganic coloured pigments to produce red, green blue and beige coatings more closely resembling those produced commercially. The coloured polyurethanes were based on the same weather stable HDI based polyisocyanate and standard durability hydroxyl-bearing polyester as those discussed in Chapter Three. These coatings were pigmented with the same inorganic pigment blends as the PVC coatings in order to investigate whether the pigments had a different effect in different polymers.

5.2.1.1 Model Colour Pigmented PVC Coating Preparation

PVC coatings containing the single secondary coloured pigment additions were produced via the same method detailed in Section 2.1.3.1. 3g of Degussa P25 TiO₂ and 0.1g of a secondary coloured pigment were dispersed in 100ml of THF solvent and mixed for 5 minutes using the high sheer mixer. 10g of powdered PVC was then added to the mixing dispersion and stirred for a further 5 minutes before transferring to a solvent bottle. The colour pigmented coatings were ultrasonicated for 5 minutes to remove any remaining pigment agglomerations and then stirred for a further 24 hours using a magnetic stirrer plate and bar prior to casting.

The secondary organic and inorganic coloured pigments tested are shown in Table 5.1 and Table 5.2 respectively.

Table 5.1 – Secondary Organic Pigments Tested

Pigment	Composition	Colour
Degussa P25	Titanium Dioxide (Inorganic)	White
Irgazin Red	Diketo-pyrrolo-pyrrole	Red O
Irgalite Green	Phthalocyanine	Green O
Irgalite Blue	Phthalocyanine	Blue O

Table 5.2 – Secondary Inorganic Pigments Tested

Pigment	Composition	Colour
Degussa P25	Titanium Dioxide (Inorganic)	White
Bayferrox 303 T	Manganese ferrite	Black I(1)
Lamp Black 101	Carbon black	Black I(2)
Printex Black	Carbon black	Black I(3)
Bayferrox 130 M	Iron oxide	Red I
Chromoxide Green GN-M	Chromium oxide	Green I
Heucodur Blue 2R	Cobalt aluminate	Blue I
Heucodur Yellow 6R	Chrome antimony titanate	Yellow I(1)
Sicotan Yellow	Titanium-oxide-chromate	Yellow I(2)
Bayferrox 3950	Zinc ferrite	Yellow I(3)

PVC coatings containing the commercial blends of coloured pigments were produced in the same manner as described above. In order to keep a constant inorganic pigment loading of 30 PHR the pigment additions were added according to the formulation detailed in Section 2.1.3.2. The appropriate pigment additions as specified in Table 2.9 were dispersed in 100 ml THF solvent and mixed for 5 minutes. 10g of powdered PVC was then added to the mixing dispersion and stirred for a further 5 minutes before transferring to a solvent bottle. The coatings were ultrasonicated for 5 minutes and then stirred for a further 24 hours using a magnetic stirrer plate and bar prior to casting.

5.2.1.2 Production of PVC Coated Samples

Coated glass sample panels were produced using the glass bar coating method as detailed in Section 2.1.4. Two layers of electrical insulation tape (~140µm) were placed down each side of a glass panel to give a consistent dry film thickness of approximately 20µm ± 2 µm. The coating was poured onto a secondary panel at the top of the coating panel and drawn down using a glass bar in one swift continuous movement. Coated panels were then allowed to dry in a cool, dark environment for a minimum of seven days to ensure full evaporation of all THF solvent.

5.2.1.3 Colour Pigmented Polyurethane Coating Preparation

The coloured polyurethane coatings were prepared as described in Section 2.1.1.3. According to the formulation guidelines in Table 2.7 the TiO₂ and blend of inorganic pigments were dispersed in polyester resin and hydrocarbon solvent and ground in a bead mill for 20-60 minutes (dependant on the pigment additions) to ensure even mixing and deagglomeration of pigment particles. The coating was checked with a Hegman draw down gauge to ensure a grind size of <5µm before filtering into a bottle and adding appropriate measures of polyester resin, cross-linker, catalyst, flow agent, solvent and matting agent. The coatings were then shaken for a further 15 minutes to ensure uniform mixing and allowed to rest for 5 minutes prior to casting.

5.2.1.4 Production of Polyurethane Coated Samples

Coated sample panels were produced by the draw-bar coating method as explained in Section 2.1.2. A thin line of paint was poured along the top of the substrate and drawn down the substrate in one movement. The coated panels were oven cured at a PMT of 232°C and water quenched. Each sample was then checked to ensure full curing and a dry film thickness of 20µm.

5.2.2 Assessing Coating Durability in the Fourier Transform Infrared (FTIR) Flat Panel Irradiation Apparatus

The FTIR flat panel irradiation apparatus used to assess pigment photoactivity is described in Section 2.2.3. The concentration of CO₂ gas in the system was measured using a gas cell incorporated into the FTIR spectrometer. The coated polyurethane sample panels were placed into the reactor and irradiated in the closed loop system for 2500 minutes. The rate of CO₂ evolution was taken between 500 and 2500 minutes using the long path length gas cell for maximum sensitivity. Due to the increased reactivity of the model PVC samples the panels were irradiated for 1000 minutes and the rate of CO₂ evolution taken between 800 and 1000 minutes. A shorter path-length (10cm) cell was used in the FTIR spectrometer due to the large amounts of CO₂ evolved from these coatings.

5.2.3 Assessing Coating Durability in Commercial Weathering Tests

The polyurethane coatings were subjected to QUV A and xenon arc weathering as described in Section 2.2.4.1 and Section 2.2.4.2 respectively. Coatings were tested in continuous cycles of QUV A (UV 340) and xenon arc (Ci 65/CAM 180) for 2000 hours and the gloss retention measured at 250 hour intervals. The colour pigmented polyurethane coatings were formulated with matting agent additions to produce coatings with an initial 60° gloss of 37.

5.3 Results and Discussion

5.3.1 CO₂ Evolution Rate Results for the Colour Pigmented Coatings

The CO₂ evolved from each of the colour pigmented coatings was measured using the FTIR flat panel irradiation apparatus in order to quantify the total photo-oxidation occurring in each of the coatings. This allowed a comparison between the effects of single pigment additions and the commercial colour blends in PVC and polyurethane coatings.

5.3.1.1 Model PVC Coatings Pigmented with Single Secondary Organic Colour Additions

The CO₂ evolution rate results for the model PVC coatings containing secondary organic pigment additions are shown in Figure 5.1. In order to compare the effects of coloured pigment additions to the standard white coating the secondary rates of CO₂ evolution (between 800 and 1000 minutes) for each colour were ratioed to the rate for the white coating. A rate ratio ($R^{\text{Colour}}/R^{\text{White}}$) of 1 is equal to the secondary rate of CO₂ evolution from the white PVC coating containing no secondary coloured pigment addition (31.272 μmol.m⁻².min⁻¹). A rate ratio value of greater than 1 implies an increase in photo-oxidation upon adding the colour and a number less than 1 signifies stabilisation of the coating through colour additions.

It can be seen that in all cases the addition of coloured organic pigments reduced the rate ratio of the coatings to below that of the white (30 PHR TiO₂ alone) coating. This indicates that the organic coloured pigment addition stabilised the coating and thus reduced photo-oxidation to below that of the white (non-coloured) coating. The blue and green organic pigment additions provided good protection, dramatically reducing the CO₂ evolution rates compared to the white coating. The

similarity in CO₂ evolution rate between the coatings was not unexpected since both pigments are as both pigments are phthalocyanines and therefore would be expected to absorb photons in a similar fashion and thus prevent TiO₂ photoactivation.

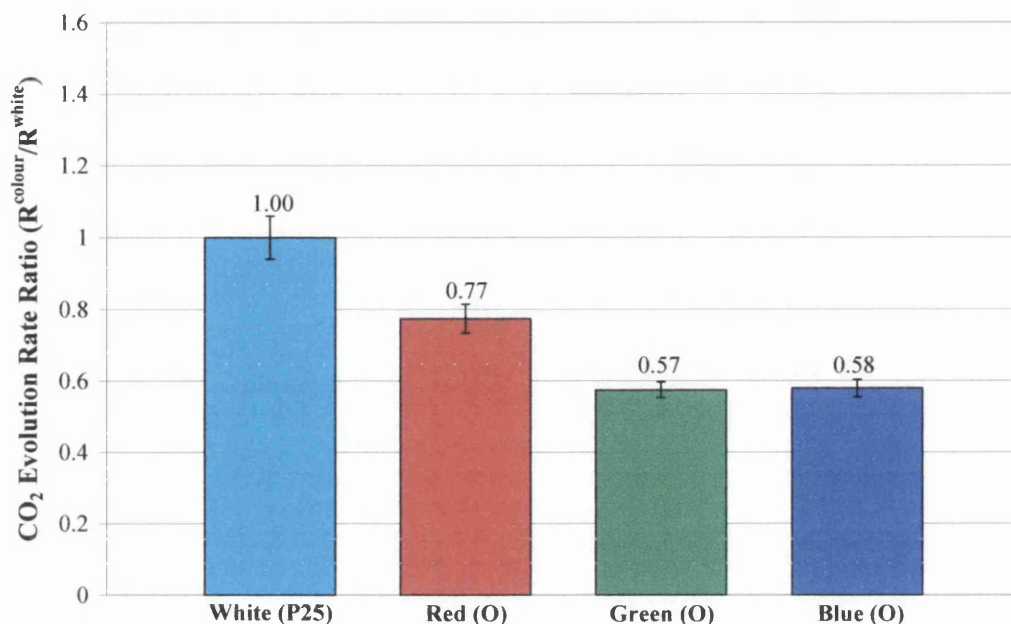


Figure 5.1 –CO₂ Evolution Rate Ratios of Model PVC Coatings Pigmented with Single Secondary Additions of Organic Coloured Pigments (Where 1 = 31.27 μmol.m⁻².min⁻¹)

Pigmentation with red diketo-pyrrolo-pyrrole reduced the rate of CO₂ evolution to below that of the white coating, however the degree of stabilisation was however less than that provided by the blue and green pigments. It is likely that this was due to light absorption characteristics of red pigments, which at first reflection is counter intuitive as it more effectively absorbs blue wavelength light photons that can activate the TiO₂. Since the red pigment absorbs blue light wavelengths it could potentially caused sensitisation of TiO₂ resulting in an increase in photo-oxidation and therefore CO₂ evolution rate. The blue and green pigments primarily absorb in the red part of the UV-Vis spectrum and therefore do not cause sensitisation of the TiO₂. This may also be related to direct attack on the organic pigment by the activated TiO₂ as discussed below.

Previous work⁶ on model PVC films pigmented with a photoactive (Degussa P25) grade of TiO₂ observed a significant increase in the rate of CO₂ evolution rate after approximately 5 hours of irradiation. The irradiated films showed an initial burst of CO₂ evolution between 0-50 minutes and then a transition to a much faster secondary rate. This ‘dual rate’ phenomenon was found to be a result of acid catalysis,

one of the photo-oxidation products of PVC is HCl gas which reacts with moisture to produce hydrochloric acid. It was found that this hydrochloric acid autocatalyses oxidation of PVC resulting in a significantly faster rate of CO₂ evolution in the latter stages of irradiation.

In order to investigate whether the coloured pigment additions affected the evolution of HCl gas and therefore autocatalysis of oxidation by hydrochloric acid the secondary rate of CO₂ evolution was ratioed to the initial rate. This gave an acid catalysis ratio ($R^{\text{Secondary}}/R^{\text{Initial}}$) where a value greater than 1 indicates a transition to a higher secondary rate of CO₂ evolution caused by HCl catalysis. The acid catalysis ratios in Figure 5.2 indicate a reduction in the degree of acid catalysis occurring upon pigmentation with secondary organic pigments compared to the standard white coating. The green pigment addition provided the greatest reduction in acid catalysis, while the red provided the least of all the organic pigments. It can be seen that despite a decrease in the degree of acid catalysis upon addition of coloured pigmentation, acid catalysis occurred in all coatings.

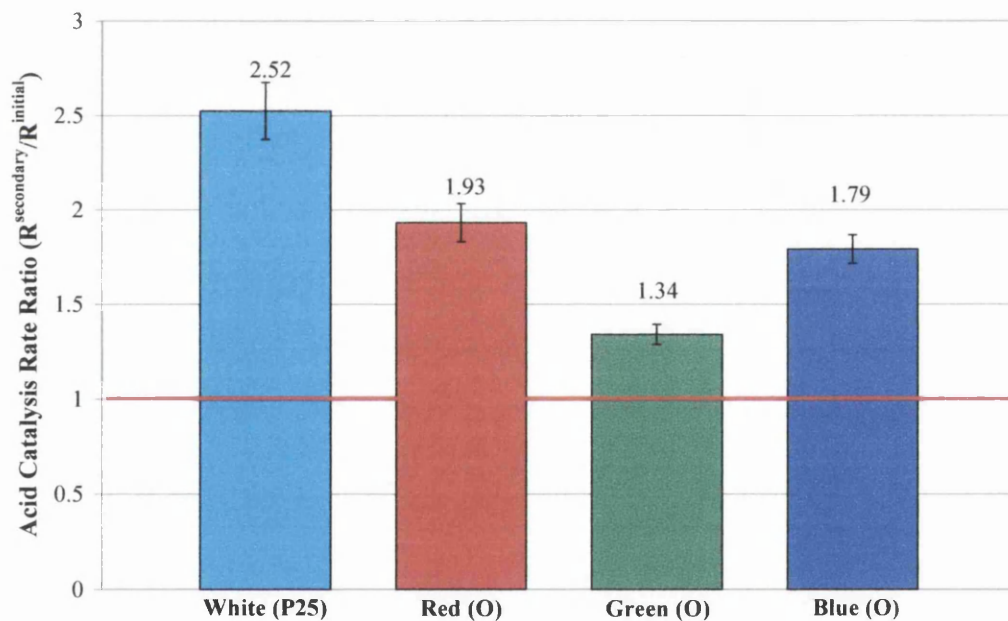


Figure 5.2 – Acid Catalysis Rate Ratios of Model PVC Coatings Pigmented with Single Secondary Additions of Organic Coloured Pigments

The reduction in acid catalysis upon addition of coloured pigmentation is most likely due to one of two things. Firstly, the HCl produced from PVC degradation could be attacking the dye molecules and therefore not catalysing the TiO₂, resulting in a reduction of oxidation. Secondly the oxidative effect of the photoactivated TiO₂

could be focussed on the coloured pigment molecules, reducing PVC oxidation and therefore production of the HCl that leads to the faster secondary rate. The colour stability of red coatings pigmented with active TiO₂ has been shown in recent work⁷ to be worse than that coatings containing green or blue pigments. As such it seems that direct oxidation of the pigment molecules is the most likely effect.

5.3.1.2 Model PVC Coatings Pigmented with Single Secondary Inorganic Colour Additions

The CO₂ evolution rate results for the model PVC coatings containing secondary inorganic pigment additions are shown in Figure 5.3. It can be seen in the majority of cases that the addition of inorganic secondary pigments results in a rate ratio of greater than 1, indicating an increase in photo-oxidation compared to the standard white coating. In contrast to the organic pigments the only exceptions to this were the titanium-oxide-chromate yellow I2 and zinc ferrite yellow I3 pigments, which showed a decrease in the CO₂ evolution rate compared to the white coating.

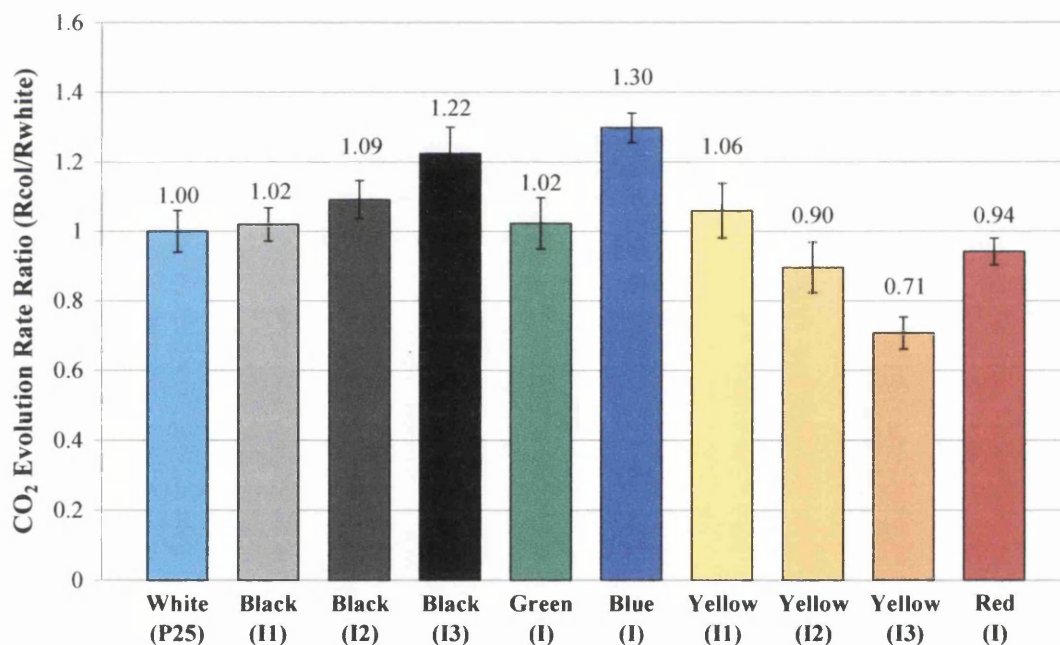


Figure 5.3 –CO₂ Evolution Rate Ratios of Model PVC Coatings Pigmented with Single Secondary Additions of Inorganic Coloured Pigments (Where 1 = 31.27 μmol.m⁻².min⁻¹)

The addition of black pigments, which absorb all wavelengths of photons rather surprisingly, increased the rate of photo-oxidation compared to the white coating. The I2 and I3 carbon black pigments (Degussa Lamp Black 101 and Degussa Printex respectively) showed a greater increase than the I1 black manganese ferrite

pigment. This is most likely due to facilitation of charge percolation by the carbon particles increasing photo-oxidation. It has been shown in a previous study³ that due to the conductive nature of carbon it is possible for the pigment particles to interact with the activated TiO₂ and transfer charge. The absorption of all light wavelengths by the black pigments could also contribute to the increase in coating degradation. Further work should be carried out on black coatings containing no TiO₂ pigment in order to investigate the effects of black pigments on sample temperature and therefore degradation.

Addition of the chrome-oxide green gave a similar rate of CO₂ evolution to the white coating. It is likely that the green pigment absorbs some of the harmful (blue) light wavelengths thus preventing the activating photons being reflected into the coating and causing oxidation. The blue pigmented coating however exhibited the highest CO₂ evolution rate of all the coatings. The clear increase in photo-oxidation upon addition of the blue pigment was most likely due to its poor absorbance of UV wavelength light, which resulted in more photoactivation. Since the blue pigment particles reflect the activating photons particles they increase photon 'lifetime' in the coating, allowing more chance of TiO₂ activation.

The organic blue and green pigments provided a degree of stabilisation to the coating which the inorganic blue and green pigments did not. It was discussed above that the most likely reason for coating stabilisation by the organic blue and green was due to attack being focussed on the organic pigment rather than the PVC coating. Due to their inorganic nature these inorganic pigments cannot be broken down in the same way as the organic blue and green pigments and therefore the reactions were focussed in the PVC resulting in more photo-oxidation.

The red iron oxide pigment absorbed blue light and therefore reduced activation of the TiO₂. As a result, this pigment reduced the rate of CO₂ evolution compared to the white coating. These results are significant as inorganic pigments are commonly perceived to be more stable than organic pigments most probably due to the increased colour stability of inorganic pigments compared to organic. This work has shown that inorganic pigments do not always provide the same level of stability against coating photo-oxidation of the polymeric matrix as organic pigments and that the benefit of a particular pigment is dependant on colour.

The coatings pigmented with the yellow titanate I1 and I2 pigments showed a similar CO₂ evolution rate as the standard white coating. This was not surprising

since these pigments are titania based and therefore would be expected to behave in a similar way to the white coatings. The zinc ferrite I3 pigment showed a lower rate of CO₂ evolution than the other yellows due to the absence of titania in the pigment which can itself become activated upon absorption of light. As the zinc ferrite pigment could not become photo-activated it provided better stability than the titania based yellow pigments.

The acid catalysis ratios for the coatings pigmented with the inorganic coloured pigments are shown in Figure 5.4. It can be seen that the manganese ferrite black I1 pigment addition reduced the occurrence of acid catalysis compared to the white coating. The coatings pigmented with the carbon black I2 and I3 pigments however showed a marked increase in acid catalysis in comparison. This was most likely due to charge transfer between the TiO₂ particles resulting in an increase in PVC photo-oxidation, which in turn produced more HCl gas. Pigmentation with the chromium oxide green caused an increase in the amount of acid catalysis. Due to its inorganic nature, degradative attack of the pigment did not occur as with the organic pigment and therefore it was focussed on the PVC.

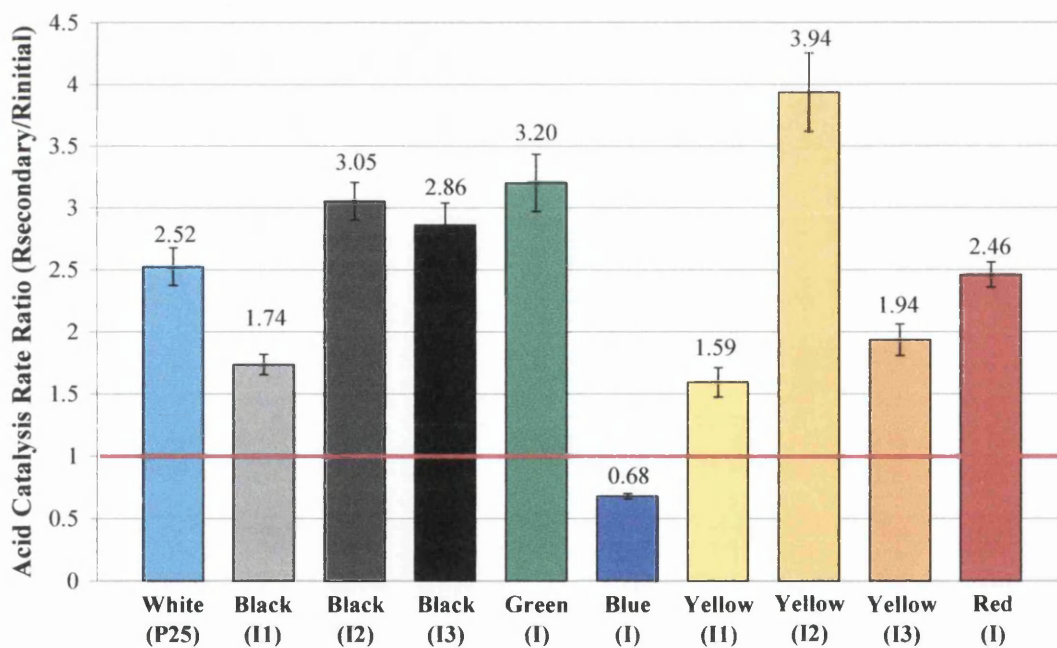


Figure 5.4 – Acid Catalysis Rate Ratios of Model PVC Coatings Pigmented with Single Secondary Additions of Inorganic Coloured Pigments

The blue pigmented coating showed a considerable decrease in acid catalysis rate ratio in comparison with the white coating. The value of less than 1 indicates that the secondary rate (800-1000 minutes) of CO₂ evolution was significantly lower than

the initial rate measured between 0 and 50 minutes. Although this coating did not show the 'dual rate' phenomenon exhibited by the other coatings it does not mean that acid catalysis did not occur. During the initial stages of testing the rate of CO₂ evolved by the blue pigmented coating indicated that acid catalysis of the PVC began to occur almost immediately following the start of irradiation. The high rate of CO₂ evolved by the blue pigmented coating was sustained for 700 minutes before trailing off. This trail off in CO₂ evolution was possibly due to the fact that much of the PVC in close proximity to the TiO₂ particles had been consumed during the earlier stages of degradation as a result of the immediate effects of HCl autocatalysis.

The chrome antimony titanate I1 yellow reduced acid catalysis compared to the white. The addition of antimony to the pigment provided good stability against the effects of HCl providing a significant reduction in acid catalysis compared to the other chrome titanate I2 pigment with no antimony addition. Antimony oxide compounds have been used for many years as PVC stabilisers as they interfere with the HCl production mechanisms which lead to autocatalytic failure. It is possible that the antimony addition to the pigment stabilised the coating against the catalytic effects of HCl resulting in a significantly lower acid catalysis ratio than the chrome titanate (yellow I2) pigment with no antimony.

The red iron oxide and orange zinc ferrite pigments provided a similar decrease in acid catalysis compared to the standard white coatings as the manganese ferrite I1 black pigment. It is possible that the iron present in these pigments underwent a reaction with the hydrochloric acid thus reducing its catalytic effect on coating oxidation.

5.3.1.3 Model PVC Coatings Pigmented with Multiple Inorganic Coloured Pigment Blends

The coatings containing the pigment blends were formulated with a photostable TiO₂ grade (Tronox R-KB-4). It can be seen from the logged CO₂ evolution rates in Figure 5.4 that this pigment was over 600 times more photostable than the TiO₂ used in the coating containing the single pigment additions (Degussa P25). This difference in TiO₂ photoactivity could have an additional effect on the pigment blends and further work should be carried out to compare the effects of pigment blends with photoactive TiO₂ and single coloured additions with photostable grades of titania.

The CO₂ evolution rate ratios for the PVC coatings pigmented with a photostable (Tronox R-KB-4) TiO₂ grade and the inorganic coloured pigment blends are shown in Figure 5.5. In all cases the coloured pigment additions significantly decreased coating stability compared to the standard white coating. It was shown in Figure 5.3 that some coloured pigment additions provided a degree of stabilisation to the coating compared to the standard white coating pigmented with the photoactive (Degussa P25) TiO₂.

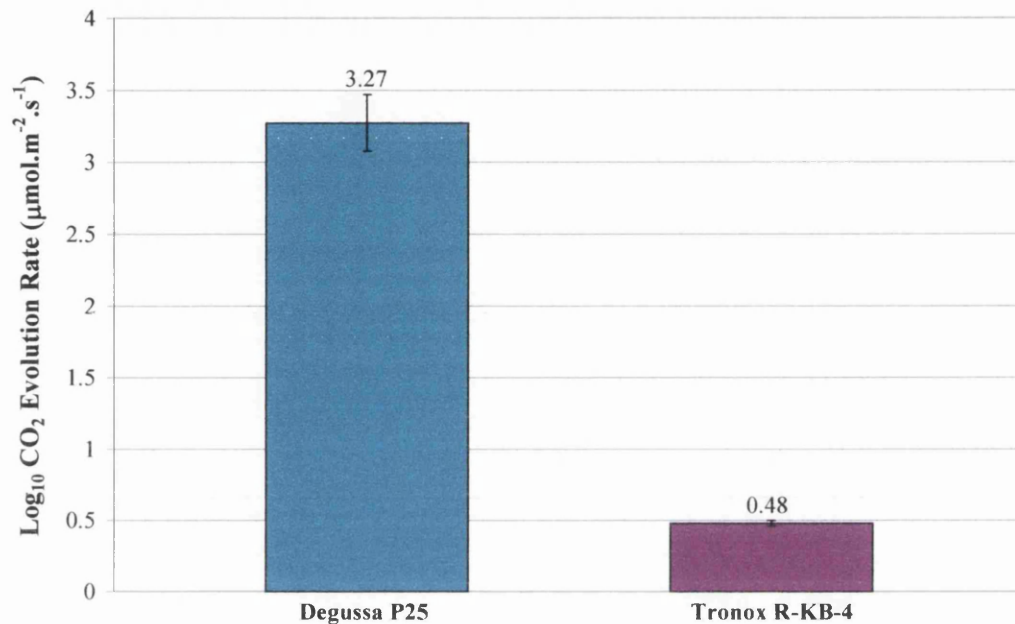


Figure 5.4 –Log₁₀ CO₂ Evolution Rates Model PVC Coatings Pigmented Photoactive (Degussa P25) and Photostable (Tronox R-KB-4) TiO₂ Grades

It is possible that the decrease in durability upon addition of coloured pigmentation shown in Figure 5.5 could be due to the photostability of the Tronox R-KB-4 TiO₂ pigment in comparison with Degussa P25. The high photostability of Tronox R-KB-4 is such that the pigment effectively reflects photons out of the coating and thus degradation is low. As all colours absorb and reflect photons they provide a level of screening to the TiO₂. In the case of a pigment with low photostability such as Degussa P25 this is advantageous since it reduces photon absorbance and therefore photoactivation of the TiO₂. In the case of Tronox R-KB-4 however, the addition of coloured pigment has the opposite effect. The increased absorbance as a result of coloured pigmentation means that more photons essentially become entrapped within the coating and can therefore cause more degradation of the PVC.

The blue coating showed the lowest stability of all the coatings. This was not unexpected as the blue pigment does not absorb blue light and therefore reflected the blue and UV component of the light spectrum into the coating. This resulted in more photoactivation of the TiO₂ and therefore photo-oxidation of the coating. The lower stability of both the blue and green coatings compared to the single pigment coatings shown in the previous section was probably in part due to the additions of carbon black in the coating. As described previously, carbon black pigment additions facilitate charge transfer between the TiO₂ particles resulting in an increase in photo-oxidation of the polymeric matrix.

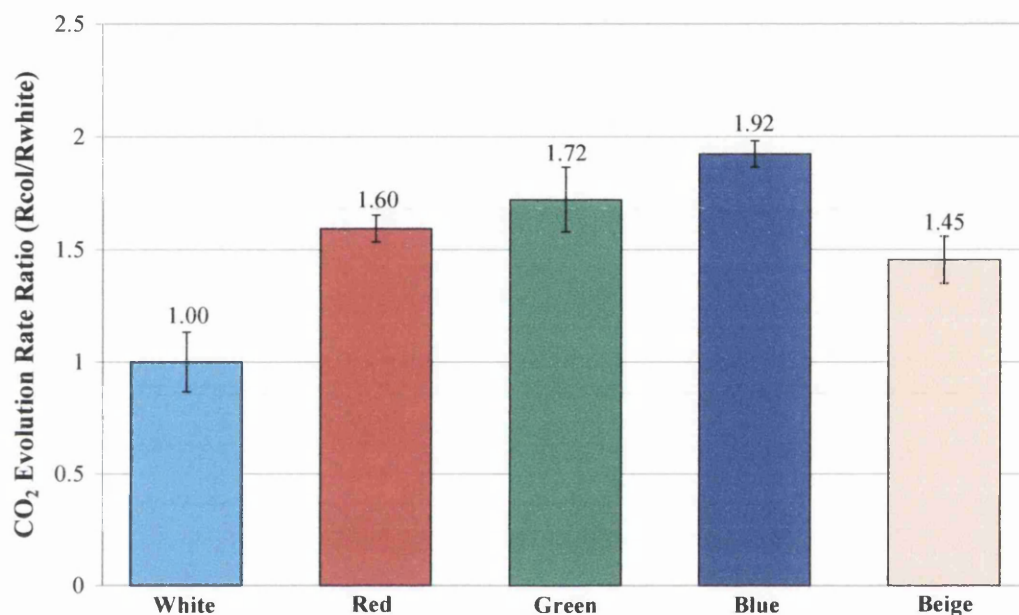


Figure 5.5 –CO₂ Evolution Rate Ratios of Model PVC Coatings Pigmented with Inorganic Coloured Pigment Blends (Where 1 = 0.169 μmol.m⁻².min⁻¹)

The red and beige coatings although of lower stability than the standard white, showed lower rates of CO₂ evolution than the blue and green coatings. This was most probably due to the fact that the black pigment in these coatings was the manganese ferrite. This pigment was shown in Figure 5.3 to give better stability to the coating than the carbon black pigments as it does not facilitate charge transfer between the TiO₂ particles. The iron oxide red pigment present in the red coating was also shown to provide good stability to the coating since it absorbs the most blue and UV light and therefore shields the TiO₂ from these wavelengths. The good stability of the beige coating was most likely due to the fact that the main component of the pigment blend was photostable TiO₂. The second largest pigment addition was the chrome antimony

titanate which provided good stability to the coating. Of all the coloured coatings, the absorbance characteristics of the pigment blend used in the beige coating were most like that of TiO₂ and therefore had the least accelerative effect on PVC degradation of all the colours. Despite the similarity between the absorbance characteristic of the white and beige coatings, the coloured pigment addition prevents the effective scattering and reflection of light by the TiO₂ and leads to greater degradation than for the pure white coating.

5.3.1.4 Polyurethane Coatings Pigmented with Inorganic Coloured Pigment Blends

The CO₂ evolution rate results for the colour pigmented polyurethane coatings are shown in Figure 5.6. Matting agent additions were added to each of the coating formulations to set the gloss values at a standard value of 38. It can be seen from the results that the addition of matting agent caused an increase in the rate of CO₂ evolved from the coatings. In Chapter Three the same coating formulation without the matting agent exhibited a CO₂ evolution rate of 0.033 μmol.m⁻².min⁻¹, compared to 0.060 μmol.m⁻².min⁻¹. It is clear from this that addition of matting agent caused a decrease in overall coating stability. Comparing the data with the matting agent additions did not however reveal a simple trend of adding more matting agent leading to greater photodegradation.

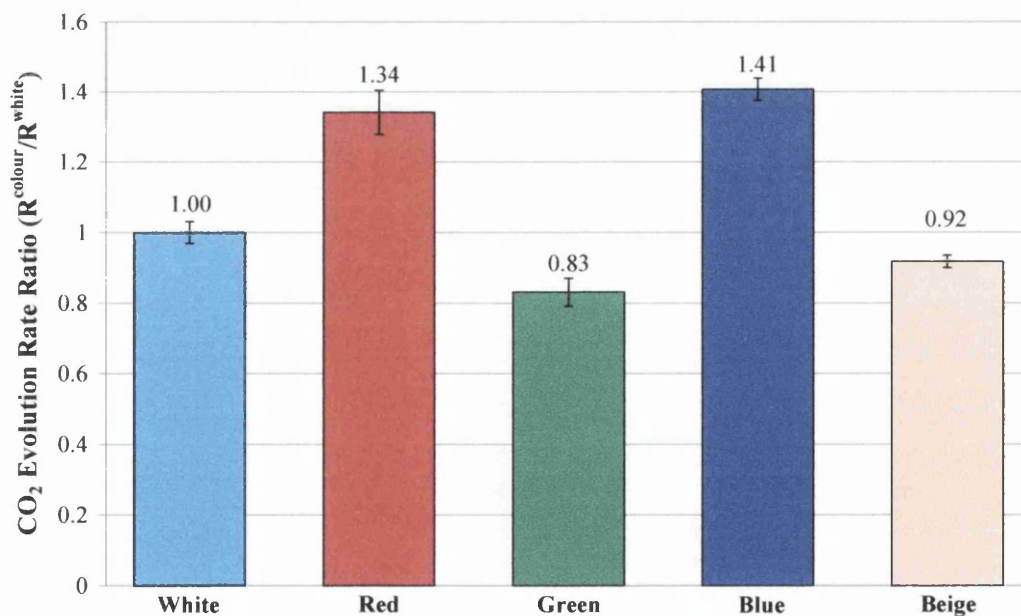


Figure 5.6 –CO₂ Evolution Rate Ratios of Polyurethane Coatings Pigmented with Inorganic Coloured Pigment Blends (Where 1 = 0.060 μmol.m⁻².min⁻¹)

Once again, the blue coating showed the lowest stability of all the coatings due to the reflection of blue and UV light into the coating, which resulted in more photo-oxidation. Although the rate ratios of the coatings were lower than those seen in the PVC coatings containing the inorganic pigment blends, the blue red and beige showed a similar ranking compared to the white coating. The greater stability of the red and beige coatings was most likely due to the absence of carbon black together with the UV absorbance of the pigments used.

The green pigmented coating showed far better stability than anticipated. The green pigment was shown above to reduce the stability of a PVC coating compared to the standard white. In this case however this particular pigment blend has provided additional stability to the coating, reducing the rate of CO₂ to below that of the standard white (Tronox R-KB-4) pigmented coating. It is possible that although the matting agent additions have reduced the stability of the white coating, the additions could assist in stabilising the coating when used in conjunction with particular pigment blends.

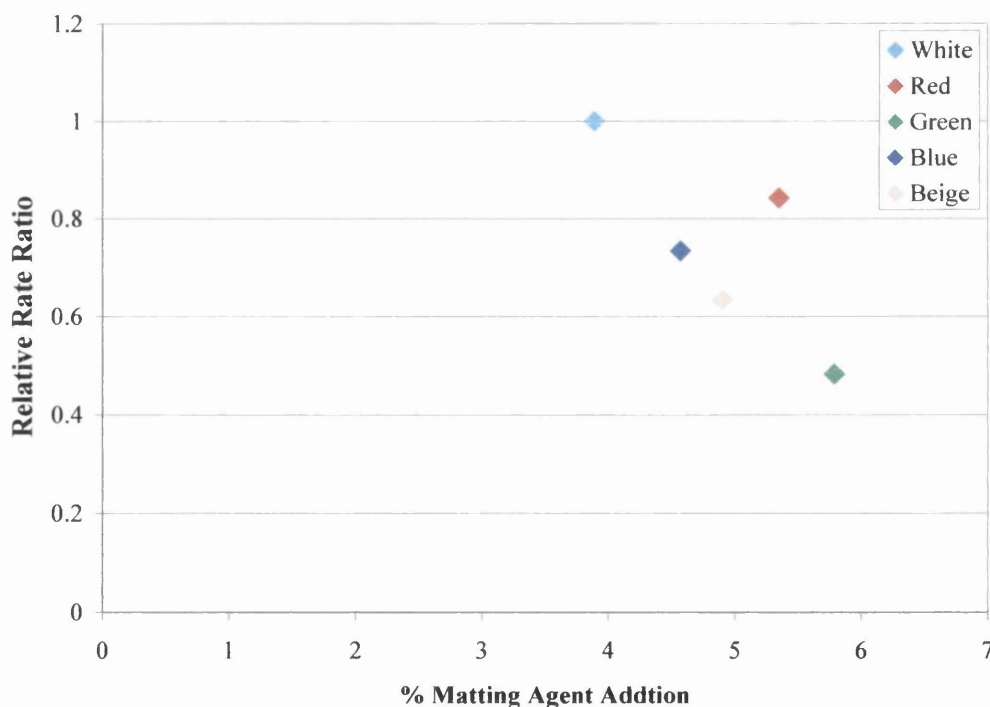


Figure 5.7 –Relative Rate Ratios of CO₂ Evolution Rates Gained from Coatings Pigmented with Inorganic Colour Blends against Percentage Matting Agent Addition

In order to try and see how matting agents were affecting overall performance the CO₂ evolution rates for the coloured coatings containing matting agent were

ratioed to that given by the corresponding colour PVC coating with no matting agent to give a relative rate ratio. These relative rate ratios were plotted against the percentage matting agent addition as shown in Figure 5.7. This illustrated that for most of the colours the addition of matting agent reduces the accelerative degradation that the inorganic colour pigmentation blends caused in PVC.

5.3.2 Commercial Weathering of Polyurethane Coatings Pigmented with Inorganic Coloured Pigment Blends

5.3.2.1 QUV A Gloss Retention

The QUV A gloss retention results for the colour pigmented polyurethane coatings are illustrated in Figure 5.8. Once again it can be seen that the addition of matting agent significantly reduced the stability of the white coating. The white coating with matting agent exhibited a significant gloss increase over the test duration while the gloss retention results for the coating with no matting agent remained stable throughout.

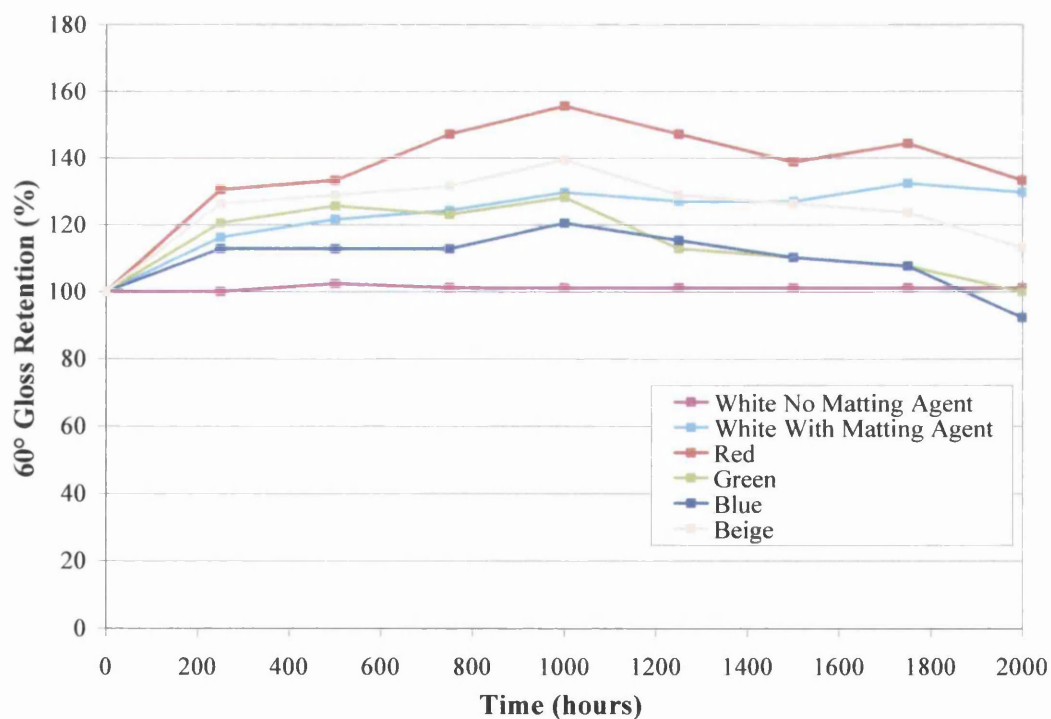


Figure 5.8 – QUV A Gloss Retention of Colour Pigmented Polyurethane Coatings

The white coating with no matting agent did not exhibit a significant change in gloss retention and therefore showed the highest stability of all the coatings. This was

not unexpected as the matting agent was organic and so could itself undergo photo-oxidation. This would not only increase the rate of CO₂ evolution as shown in the previous section but also its removal from the surface as a result of degradation could cause the increased coating gloss in the matted coatings as shown in Figure 5.8.

The red pigmented coating showed the greatest change in gloss over the test duration and was therefore the least stable of the coatings. The blue and beige coatings showed an increase in gloss during the initial stages of the test however at 2000 hours the gloss retention of the blue coating appeared to change more rapidly, indicating it to be less stable. Of all the coloured coatings the green coating showed the least change in gloss retention at the end of the test and therefore was the most stable.

5.3.2.2 Xenon Arc Gloss Retention

Figure 5.9 shows the gloss retention results for the colour pigmented polyurethane coatings following xenon arc weathering. These results once again illustrate the de-stabilising effect that the matting agent addition had on the white coating. The white coating with matting agent showed a significant gloss increase in the initial stages of testing before undergoing a rapid gloss decrease between 800 and 1200 hours.

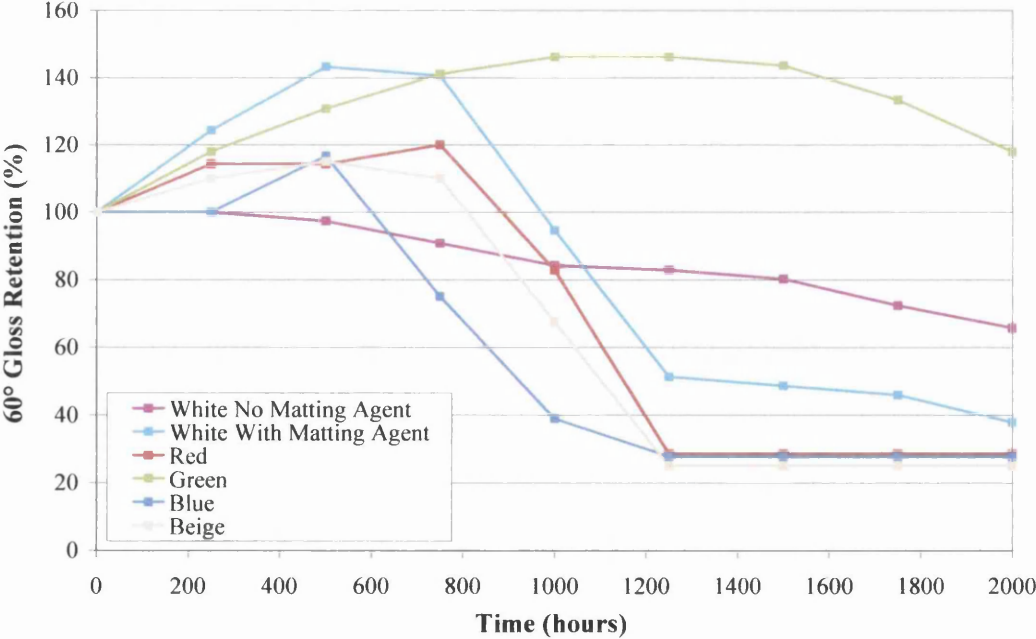


Figure 5.9 – Xenon Arc Gloss Retention of Colour Pigmented Polyurethane Coatings

The coating containing no matting agent did not exhibit an initial gloss increase and changes in gloss occurred much more slowly. At 2000 hours the coating with no matting agent retained 65% of its original gloss compared to the 37% retained by the coating with matting agent. This indicated that the coating containing no matting agent was significantly more stable than the coating with matting agent.

The blue coating showed the lowest stability of the coloured coatings as it exhibited the fastest gloss decrease over the test duration. The red and beige coatings gave similar performance showing similar changes in gloss retention over the test duration. The green coating exhibited outstanding gloss retention over the test duration. Like many of the other coatings the green pigmented polyurethane exhibited a gloss increase in the initial stages of testing, however in the green coating the gloss increase was much longer lived. The green coating only began to show a reduction in gloss at 1600 hours and following 2000 hours of testing continued to exhibit a significantly higher gloss than the other coatings, indicating it to be the most stable coating. It is clear that matting agent additions have reduced the durability performance of the coatings, particularly for the white material. The reduction in activity for the green coating was broadly in-line with the CO₂ evolution result and the apparent stabilising effect that the combination of matting agent and inorganic green pigment blends showed.

5.3.2.3 Colour Pigmented Polyurethane Rankings

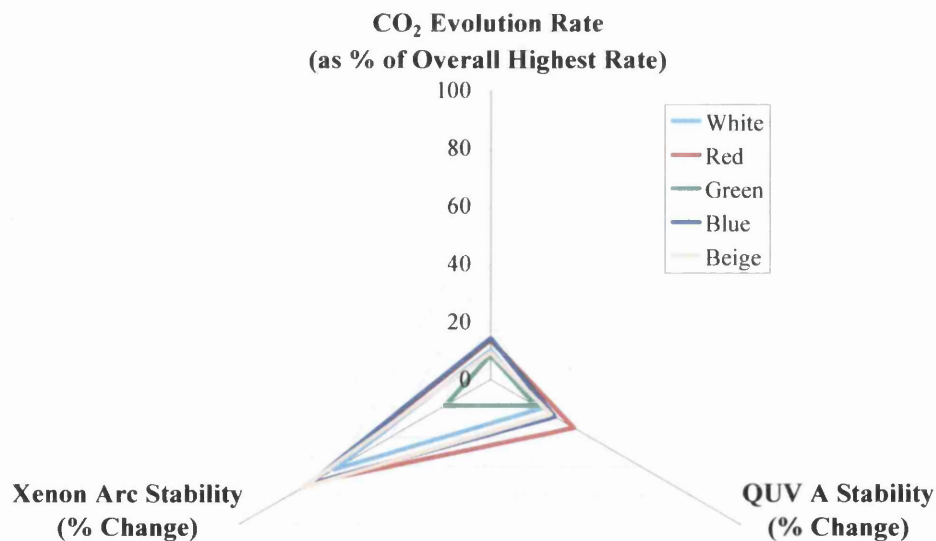


Figure 5.10 – Ranking of Colour Pigmented Polyurethane Coatings According to Durability in CO₂ Measurement Apparatus, QUV A and Xenon Arc Weathering

In order to provide a direct comparison with the other coatings tested throughout this work the colour pigmented coatings were assigned a performance ranking in each test method as shown in Figure 5.10. Coating durability was ranked according to percentage change in gloss at 2000 hours in QUV A and xenon arc. The secondary rate (500-2500 minutes) of CO₂ evolution was expressed as a percentage of 0.594 μmol.m⁻².min⁻¹. This value was gained from the IPDI polyurethane pigmented with Kronos 1001 and was the highest rate of CO₂ evolution given by any of the polyurethane coatings tested in this work.

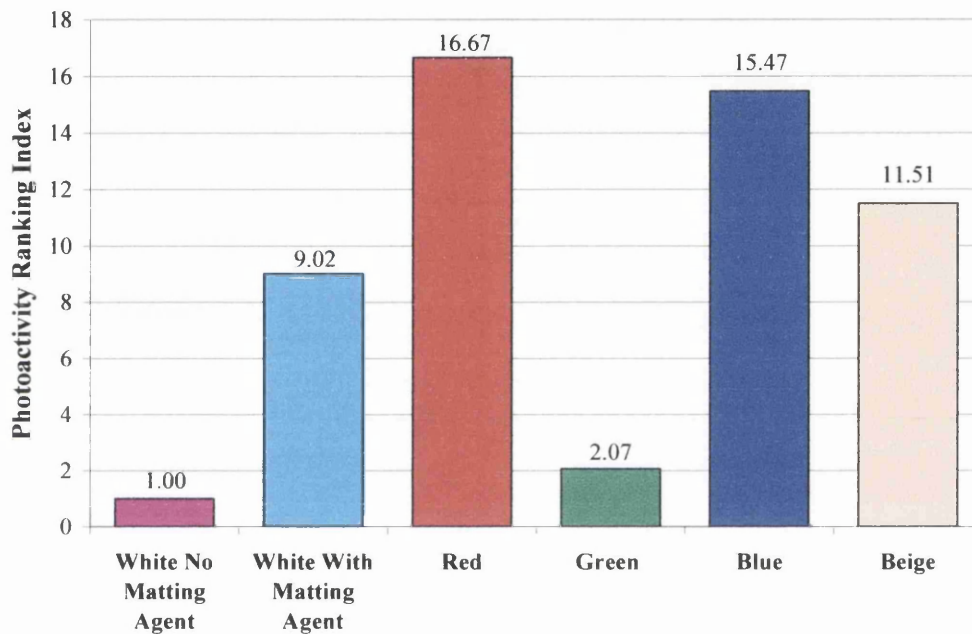


Figure 5.11 – Photoactivity Ranking Indices of Colour Pigmented Polyurethane Coatings

This method of ranking allowed a direct comparison between each of the coatings where the coating represented by the smallest area showed the highest overall durability. The areas representing each coating were measured and a photoactivity ranking index derived from these. All photoactivity indices were expressed as a ratio of the photoactivity index assigned the white (Tronox R-KB-4) pigmented standard durability HDI polyurethane with no matting agent. An index value of less than 1 indicates the coating to be more durable than the standard white polyurethane, and a value greater than 1 indicates it to be less durable.

The photoactivity ranking indices in Figure 5.11 show that addition of matting agent to the white coating increased its reactivity by 9.02 times. With the exception of the green coating the addition of coloured pigment blends reduced the stability of the

coating. The exceptional performance of the green coating in xenon arc has significantly improved its photoactivity index. From this it can be seen that the green coating was the most durable, followed by beige, blue and finally red.

5.4 Conclusions

In all cases the addition of single secondary coloured organic pigments stabilised the PVC coating matrix against oxidation and thus reduced the CO₂ evolution rate ratios of the coatings to below that of the standard white coating. The blue and green phthalocyanine pigments provided particularly good protection. Pigmentation with red diketo-pyrrolo-pyrrole reduced the rate of CO₂ evolution to below that of the white coating. The degree of stabilisation was however less than that provided by the blue and green pigments due to its absorption of blue wavelength light and subsequent sensitisation of the coating.

Each of the organic coloured pigments reduced the effect of acid catalysis on coating degradation in comparison with the standard white coating. This was most likely due to the pigment itself being attacked by the photoactivated TiO₂ and thus reducing degradation of the PVC coating. This indicates that colour stability could be compromised in organic pigmented systems but that the beneficial effect would be longer resin lifetime prior to chalking and porosity development.

The CO₂ evolution rate results for the model PVC coatings showed that in the majority of cases that the addition of inorganic secondary pigments resulted in an increase in photo-oxidation. These pigments also caused a general increase in the acid catalysis ratio. The only exception to this was the coating pigmented with the inorganic blue, which appeared to show acid catalysis in the initial stages of irradiation. Further work into the acid catalysis by these coatings should be carried out by the same means as in previous work^{6,7} to investigate this hypothesis. For example, by addition of an acid scavenger such as hydrotalcite it could be quickly seen if the blue pigment did indeed have immediate acid catalysis or if there is some other accelerative effect in operation such as the pigment changing moisture uptake by the film.

The inorganic pigments did not reduce total degradation of the organic resin in the same way as the organic pigment. Unlike the organic pigment, the inorganic pigments are such that rather than being attacked by the UV they allow UV attack of

the polymer. Further work should be carried out into this using colour measurement. It is anticipated that hydrochloric attack on the pigment would cause a greater change in colour of the polymeric matrix. This would also be advantageous to investigate whether the increased colour stability of inorganic pigment compared to organics is detrimental to the protection it provides to the polymer.

It was clear that ternary and quaternary pigment additions accelerated photo-oxidation. This could be due to charge percolation by the carbon black and should be investigated further by alteration of the black pigment additions. The addition of matting agent also appeared to have an accelerative effect of coating photo-oxidation however it is clear that this affected different colours in different ways and should be investigated further.

The work highlights the importance of using a wide variety of tests to assess coating durability as there were discrepancies between the results from different tests. The discrepancies between the results are also indicative of the level of caution needed when formulating paints with numerous components. It is clear that actions such as changing the polymer, adding matting agent or changing the pigment blend each had an effect on coating degradation. It should therefore be noted that no component of the coating can be changed without appropriate attention to the effects on coating stability.

5.5 References

1. Lambourne, R. and Strivens, T.A., *Paint and Surface Coatings Theory and Practice*. 1987, Ellis Horwood: Chichester UK.
2. Christie, R.M., *Colour Chemistry*. 2001, The Royal Society of Chemistry: Cambridge.
3. Robinson, A.J., Wray, J., and Worsley, D.A., *Materials Science and Technology*, 2006. **22**(12): p. 1503-1508.
4. Searle, J.R., *Titanium Dioxide Pigment Photocatalysed Degradation of PVC and Plasticised PVC Coatings*. 2002, Eng. D, University of Wales Swansea.
5. Robinson, A.J., Searle, J.R., and Worsley, D.A., *Materials Science and Technology*, 2004. **20**(8): p. 1041-1048.
6. Robinson, A.J., *The Development of Organic Coatings for Strip Steels with Improved Resistance to Photodegradation*. 2005, Eng. D, University of Wales Swansea
7. Martin, G.P., *The Stabilisation of PVC Plastisol using Hydrotalcite (HT)*. 2007, Eng. D, University of Wales Swansea.

Chapter 6

The Effect of Texturing Agent Additions on the Durability of Polyurethane Coatings

6.1 Introduction

The present study has focussed on polyurethane coatings for pre-finished steel products. Colorcoat Prisma[®] is a market leading textured polyurethane coated steel product that has seen a significant increase in popularity over recent years. The increase in product sales and the introduction of a new generation PVC plastisol product with a 40 year in-service guarantee¹ has increased the necessity to improve the durability of Colorcoat Prisma[®]

Texturing agents are incorporated into coatings primarily for aesthetic reasons, the different refractive indices of the polymer resin and polyamide additions result in non-uniform light scattering which can disguise small flaws in the coating. The incorporation of polyamide beads into the polyurethane topcoat not only improves product aesthetics but also provides additional reinforcement and abrasion resistance to the coating. Due to the high reactivity of polyisocyanates upon curing the functional carbonamide [- CO – NH -] group of the polyamide forms hydrogen bonds with the polymeric matrix².

Due to the high functionality of the polyisocyanates used in these coatings the polyamide becomes highly cross-linked within the final polyurethane structure. Incorporation of polyamide beads into polyurethane produces a reinforced coating with good resistance to abrasion and soiling, something that is particularly important for pre-finished steel products intended for external applications.

6.1.1 Aims

At present Colorcoat Prisma[®] has an in service guarantee of up to 25 years³, the aim of this research has been to identify more stable polyurethane resins in order to bring the guarantees more in line with the 40 years offered on HPS200[®] Ultra. The polyurethane formulation of Colorcoat Prisma[®] is currently based on a HDI polyisocyanate and standard durability polyester similar to the first series polyurethane discussed in Chapter Three.

In Chapter Four it was seen that coatings based on a HDI/IPDI polyisocyanate showed better durability than the standard HDI polyurethane. This chapter will investigate and compare the durability of HDI and HDI/IPDI polyurethane coatings containing similar additions of polyamide texturing agent as those used in Colorcoat Prisma[®] products.

Carbon dioxide (CO₂) evolution measurement will be used as a means of quantifying the effect of texturing agent on the durability of white (Tronox R-KB-4) pigmented HDI and HDI/IPDI based polyurethane coatings. Due to the increased roughness of the coatings upon addition of texturing agent, gloss retention measurement was less appropriate than in the previous chapters and therefore was not used.

6.2 Experimental Techniques

6.2.1 Textured Polyurethane Coatings

The coatings tested were un-stabilised, one-component, oven curing coatings pigmented with Tronox R-KB-4 titanium dioxide (TiO₂). The results for the HDI and HDI/IPDI polyurethane coatings pigmented with Tronox R-KB-4 showed this pigment to produce the most durable coating formulation.

A commercial polyamide texturing agent was added to the HDI and HDI/IPDI based polyurethanes to assess its effect on coating durability. The polyurethane coating based on the HDI polyisocyanate was also textured with an addition of 50µm glass beads to investigate the effects of a non-commercial texturing agent. The basic constituents of the coatings are shown in Table 6.1.

Table 6.1 – Texturing Agent Additions to White Pigmented Polyurethane Coatings

Polyurethane Resin	TiO₂ Pigment	Texturing Addition
First Series HDI Based Polyurethane	Tronox R-KB-4	None
First Series HDI Based Polyurethane	Tronox R-KB-4	4% by wt. 56µm polyamide beads
First Series HDI Based Polyurethane	Tronox R-KB-4	4% by wt. 50µm glass beads
Third Series HDI/IPDI Based Polyurethane	Tronox R-KB-4	None
Third Series HDI/IPDI Based Polyurethane	Tronox R-KB-4	4% by wt. 56µm polyamide beads

6.2.1.1 Textured Polyurethane Coating Preparation

The textured polyurethane coatings were produced as second and third series polyurethane coatings were prepared as described in Section 2.1.1.4. The basic HDI and HDI/IPDI polyurethane formulations were prepared as described in Section 2.1.1.1. According to the formulation guidelines TiO₂ pigment was dispersed in a polyester resin and hydrocarbon solvent (Solvesso 200 S) and ground in a bead mill for 15 minutes to ensure even mixing and a pigment particle size of <5µm. The formulation was filtered into a bottle and appropriate addition of polyester resin, cross-linker, catalyst, flow agents and solvent added. The coating was then shaken for a further 15 minutes before adding 4% by weight addition of the appropriate texturing agent. The coating was then shaken for a further 5 minutes to ensure even dispersion of the texturing agent prior to casting.

6.2.1.2 Production of Textured Polyurethane Coated Samples

Coated steel samples were produced by the draw-bar coating method detailed in Section 2.1.2. A thin line of paint was poured along the top of the substrate and drawn down the substrate in one swift, even movement using a #038 coiled bar to give a 20µm dry film thickness. The sample was cured in the oven to a peak metal temperature (PMT) of 232°C and then water quenched and dried.

6.2.2 Assessing Coating Durability in the Fourier Transform Infrared (FTIR) Flat Panel Irradiation Apparatus

The durability of the textured polyurethane coatings was measured using the flat panel irradiation apparatus as described in Section 2.2.3. The coated samples were placed in the flat panel reactor and irradiated with UV A light for 2500 minutes and the concentration of CO₂ gas in the reactor headspace measured at timed intervals using FTIR spectroscopy. This provided a cumulative plot of CO₂ evolution for the test duration from which the secondary rate of CO₂ evolution between 500 and 2500 minutes could be taken to give a quantitative assessment of coating durability.

6.3 Results and Discussion

6.3.1 CO₂ Evolution Rate Results from Textured Polyurethane Coatings

The CO₂ evolution rate results for the textured polyurethane coatings are shown in Figure 6.1. The results clearly show that the addition of texturing agents to the coating decreases durability compared to the un-textured coatings. A 4% by weight addition of 50µm glass beads to the HDI based polyurethane coating caused the rate of CO₂ evolution to increase to over twice that of the un-textured HDI polyurethane coating. The 4% by weight addition of the 56µm polyamide beads also caused the rate of CO₂ evolution to increase, however the rates of CO₂ evolution for both the polyamide textured coatings were lower than that containing the glass.

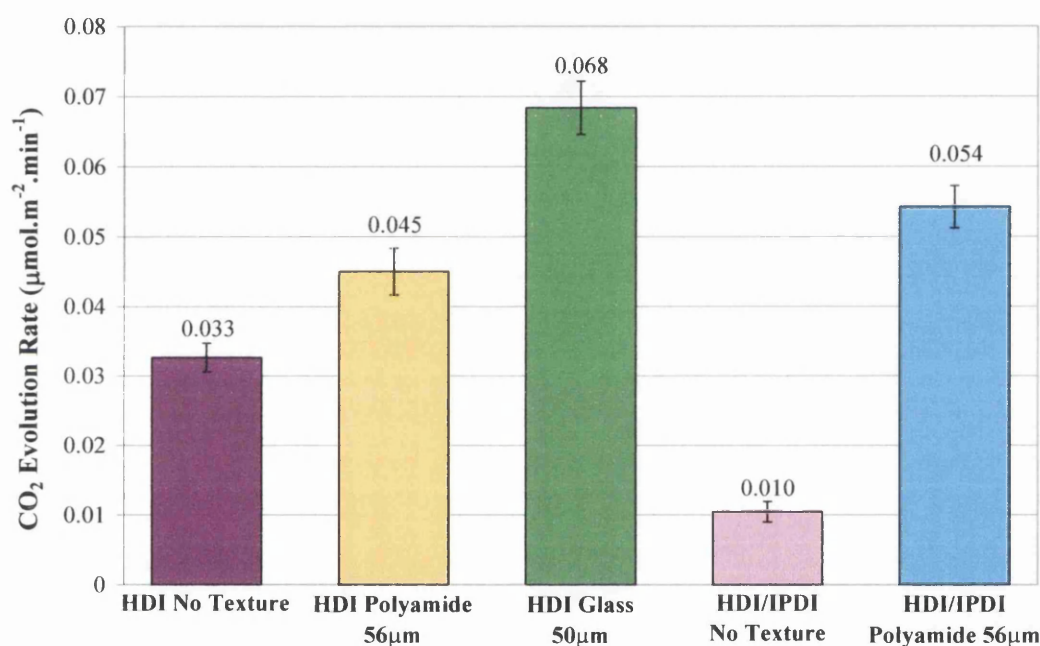


Figure 6.1 –CO₂ Evolution Rates of Textured Polyurethane Coatings

It is likely that the significant increase in CO₂ evolution upon adding the glass beads was due to a combination of two factors. Firstly, addition of texturing agent to the coating increases the effective surface area susceptible to oxidation, which would inevitably increase the amount of oxidation occurring. Secondly, it is probable that incident UV was refracted by the glass beads. The refractive properties of glass are such that upon penetration by UV the light could be drawn deeper into the bulk polymer, causing oxidation deeper in the polymer than would otherwise occur. The refraction of UV deeper into the polymer and increase in surface area resulted in a

significant increase in the rate of CO₂ evolved by the coating textured with glass beads in comparison to the un-textured polyurethane.

Incorporation of polyamide beads also resulted in an increase in the rate of CO₂ evolution compared to the un-textured coatings. It can be seen that the addition of polyamide caused the rate of CO₂ evolution to rise to 1.4 times that of the HDI based polyurethane coating containing no polyamide. Incorporation of the polyamide into the HDI/IPDI polyurethane resulted in a significantly higher increase in the rate of CO₂ evolution. It can be seen in the results that the CO₂ evolution rate gained from the textured HDI/IPDI coating was 5.4 times that evolved by the HDI/IPDI polyurethane containing no polyamide.

It is likely that the increase in CO₂ evolution was due to a combination of factors. Firstly the addition of texturing agent caused an increase in the surface area susceptible to degradation. It is also likely that incomplete bonding at the interface between the polyamide beads and the coating lead to increased oxygen permeation through the coating, which as discussed in Chapter Four can increase oxidation. Irradiations carried out on samples of the polyamide bead showed the beads themselves to undergo degradation. This degradation could contribute to the total CO₂ evolution, however since it was not possible to measure the surface area of the polyamide beads the actual contribution from the polyamide beads could not be calculated.

The HDI/IPDI coating containing the polyamide texturing agent showed a higher rate of CO₂ evolution than the HDI coating containing the polyamide. Since the polyamide beads undergo reaction with the coating resin on curing it is possible that this reaction sensitised the coating to degradation. The increased reactivity of the HDI/IPDI isocyanate compared to the HDI based isocyanate could account for the higher rate of CO₂ evolution in this coating.

6.4 Conclusions

The addition of glass beads significantly increased the rate of photo-oxidation due to the increase in surface area and refraction of UV into the polymer. It is likely that an increase in surface area upon addition of polyamide also caused an increase in photo-oxidation.

This work has shown that despite the increased durability of the HDI/IPDI polyurethane compared to the standard HDI based coating, addition of polyamide beads resulted in a significant decrease in coating durability. In both polyurethanes addition of the polyamide beads caused the system to undergo more photo-oxidation.

The most probable cause for the increased rate of CO₂ evolved by the textured coatings was increased oxygen permeation at the interface between the coating and the beads. However, in order to significantly improve the durability of textured coatings further work should be carried out to determine which mechanisms provide the greatest contribution to coating degradation.

6.5 References

1. Corus Colors Ltd, *Colorcoat HPS200[®] Ultra*. 2008: Flintshire, Wales.
2. Degussa AG, *Vestosint[®] Polyamide 12 Coating Powder*: Marl, Germany.
3. Corus Colors Ltd, *Colorcoat Prisma[®]* 2005: Flintshire, Wales.

Chapter 7

The Effect of Titanium Dioxide Pigment Dispersion on Polymer Photo-Oxidation

7.1 Introduction

Different titanium dioxide (TiO_2) pigments exhibit different dispersion characteristics in different coating resins. It is likely that this is due to the chemical compatibility between the inorganic stabilising coating on the TiO_2 pigment particles and the coating resin. Coated TiO_2 pigments are developed for use with particular polymer resins and are specified as such by the manufacturers^{1, 2}. It is therefore apparent that certain pigments would be particularly suited for use in a specific polymer resin while others are not. For example, Kronos 2220 TiO_2 is specifically produced for pigmentation of PVC³ and therefore may not necessarily exhibit optimum performance in other polymer types as has already been shown in Chapter Three.

The compatibility between a polymeric resin and coated TiO_2 must be carefully considered during coating formulation, particularly when durability and aesthetic appearance are of paramount importance. Previous research⁴ has shown a correlation between poor surface chemistry/resin compatibility and increased agglomeration of TiO_2 particles within the bulk coating. This aggregation can lead to reduced pigment efficiency⁵ from the point of view of refraction and can increase roughness of the surface leading to reduced gloss. Furthermore, it has been shown⁶ that agglomeration of particles causes significant changes to the optical properties of the dispersion which causes an increase in TiO_2 photoactivity.

7.1.1 Aims

This chapter aims to benchmark the stability of different commercial TiO_2 grades and the effects of dispersion of these pigments on the kinetics of polymer photo-oxidation. It is anticipated that coatings containing poorly dispersed TiO_2 will show higher rates of photo-oxidation than those containing the same loading of pigment at an optimum dispersion.

Model PVC coatings containing different dispersions of Kronos 2220 and Tronox R-KB-4 pigments at a 30 PHR loading were tested in the carbon dioxide (CO_2) evolution flat panel irradiation apparatus. The changes in CO_2 evolution rate between the coatings were used to quantify the effects of different dispersions on pigment photoactivity and subsequent TiO_2 photocatalysed oxidation of the PVC coating.

7.2 Experimental Techniques

7.2.1 TiO₂ Pigmented Model PVC Coatings

The model coatings PVC coatings tested in this section contained a 30 PHR loading of TiO₂ pigments which have been classified by the manufactures as being photostable grade A pigments. This allowed the variation in photostability between the different TiO₂ types to be illustrated. Coatings containing different dispersions of the grade A Kronos 2220 or Tronox R-KB-4 pigments were produced to allow assessment of the effects of TiO₂ agglomeration on photoactivity.

7.2.1.1 TiO₂ Pigmented PVC Coating Preparation

The coatings containing poorly dispersed pigment were produced via a different method to the well dispersed pigmented coatings in order to keep stirring time to a minimum. 10g of laboratory grade powdered PVC (Aldrich MW ca 95000) was added to 100ml of THF solvent while continually mixing with the high sheer mixer to prevent agglomeration of the PVC. The clear PVC resin was then transferred to a solvent bottle and stirred via a magnetic plate and bar for a further 24 hours prior to casting to ensure complete PVC dissolution. Following the 24 hours stirring 3g of TiO₂ was then added to the coating and stirred for 3 minutes to slightly disperse the pigment prior to casting.

The normal and ultradispersed pigmented coatings were produced using the traditional method of model coating formulation as described in Section 2.1.3.1. 3g of TiO₂ was dispersed in 100ml of THF solvent and mixed for 2 minutes using the high sheer mixer. 10g of laboratory grade was then quickly and evenly poured into the mixing dispersion and allowed to mix for a further 5 minutes before being transferred to a solvent bottle. The coating was stirred for a further 24 hours prior to casting to ensure complete PVC dissolution and homogenous particle dispersion. In order to produce a better pigment dispersion the coating was ultrasonicated for 5 minutes prior to casting using the Branson Sonifer 350 with a 1cm titanium probe in an attempt to completely break up all pigment agglomerations.

7.2.1.2 Production of PVC Coated Samples

Coated glass sample panels were produced using the glass bar coating method as detailed in Section 2.1.4. Two layers of electrical insulation tape (~140µm) were

placed down each side of a glass panel to give a consistent dry film thickness of approximately $20\mu\text{m} \pm 2\mu\text{m}$. The coating was poured onto a secondary panel at the top of the coating panel and drawn down using a glass bar in one swift continuous movement. Coated panels were then allowed to dry in a cool, dark environment for a minimum of seven days to ensure full evaporation of all THF solvent.

7.2.2 Assessing Pigment Photoactivity in the Fourier Transform Infrared (FTIR) Flat Panel Irradiation Apparatus

The FTIR flat panel irradiation apparatus was used to measure the evolution of CO_2 from the coatings as described in Section 2.2.3. Coated samples were irradiated in the reactor cell for 1000 minutes and the concentration of CO_2 gas in the system measured by the FTIR spectrometer at timed intervals. Due to the increased reactivity of the model PVC coatings compared to the polyurethanes, the time of irradiation was reduced from 2500 minutes to 1000 minutes. The rate of CO_2 evolution between 800 and 1000 minutes was used to give a quantitative analysis of coating photo-oxidation rate.

7.2.3 UV/Vis Spectroscopy

The UV absorbance of the PVC coatings was measured using the Perkin Elmer Lambda 2 UV/Vis spectrometer. The absorbance spectrum of each coating was measured between 240 and 800nm at 4nm intervals. Three spectra were collected for each coating and used to calculate the average absorbance spectrum.

7.3 Results and Discussion

7.3.1 CO_2 Evolution from Model PVC Coatings Pigmented with Different Commercial TiO_2 Grades

Five commercial grade A TiO_2 pigments under normal dispersion conditions were tested using the FTIR flat panel irradiation apparatus to assess durability in PVC coatings. The CO_2 evolution rate results in Figure 7.1 showed a wide variation in photostability between the different TiO_2 types which are all classified by the manufactures as being UV stable grade A pigments.

The coating pigmented with Kronos 2220 pigment showed the highest CO_2 evolution rate of all the coatings, this is significant as Kronos 2220 is used as a white

pigment in some commercial PVC plastisols. Given the increased stability shown by the Tronox R-KB-4 and the DuPont R105 pigments this indicates that although it is specifically developed for high durability in PVC use of a different pigment may help to increase product durability.

The coatings formulated with the DuPont R960 and TS6200 pigments also showed relatively high CO₂ evolution rates, particularly compared to the coating containing the DuPont R105 TiO₂. This pigment showed the highest stability in PVC and gave a CO₂ evolution rate 1.6 times lower than the Tronox R-KB-4, which until now has proved to be the most stable pigment. The Tronox R-KB-4 pigment did however show better stability than the Kronos 2220 and other DuPont pigments and has proved to provide excellent durability in polyurethane coatings.

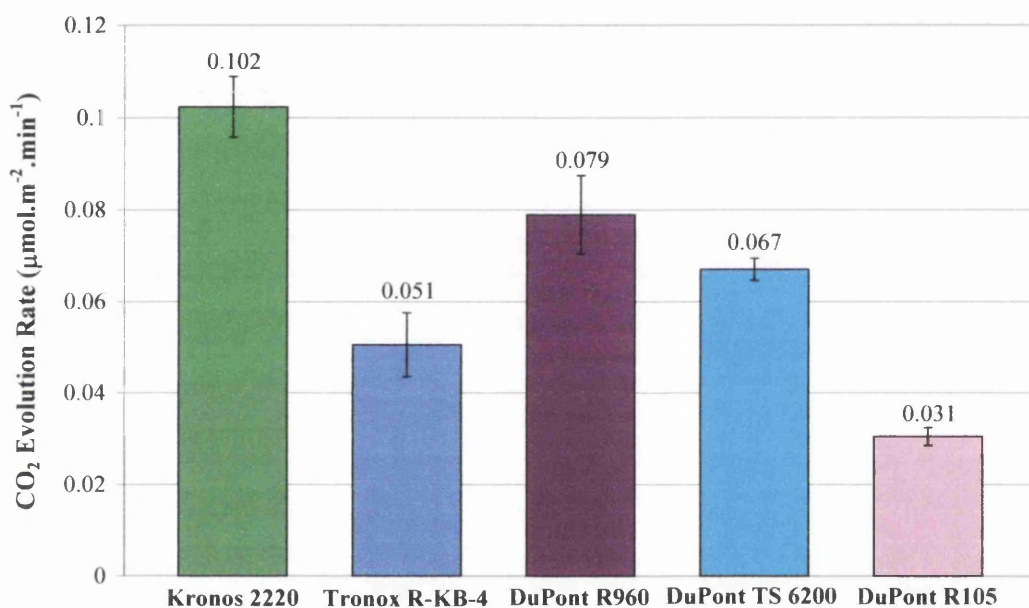


Figure 7.1 - CO₂ Evolution Rates of PVC Coatings Pigmented with Different Commercial TiO₂ Grades

For the purpose of continuity dispersion work was carried out on the two grade A pigments that have been extensively tested throughout this research - Kronos 2220 and Tronox R-KB-4. Due to their intended use in different polymers these pigments have very different dispersion characteristics in the same resin and therefore allowed an in depth investigation into the effects of dispersion on these pigments.

7.3.2 CO₂ Evolution from Model PVC Coatings Pigmented with Various Dispersions of Kronos 2220 and Tronox R-KB-4

The CO₂ evolution rate results for the range of dispersions of Kronos 2220 TiO₂ pigment in PVC are shown in Figure 7.2. The difference in CO₂ evolution rate observed between the normal and poorly dispersed pigmented coatings illustrated that dispersion does indeed affect pigment photoactivity and therefore coating oxidation.

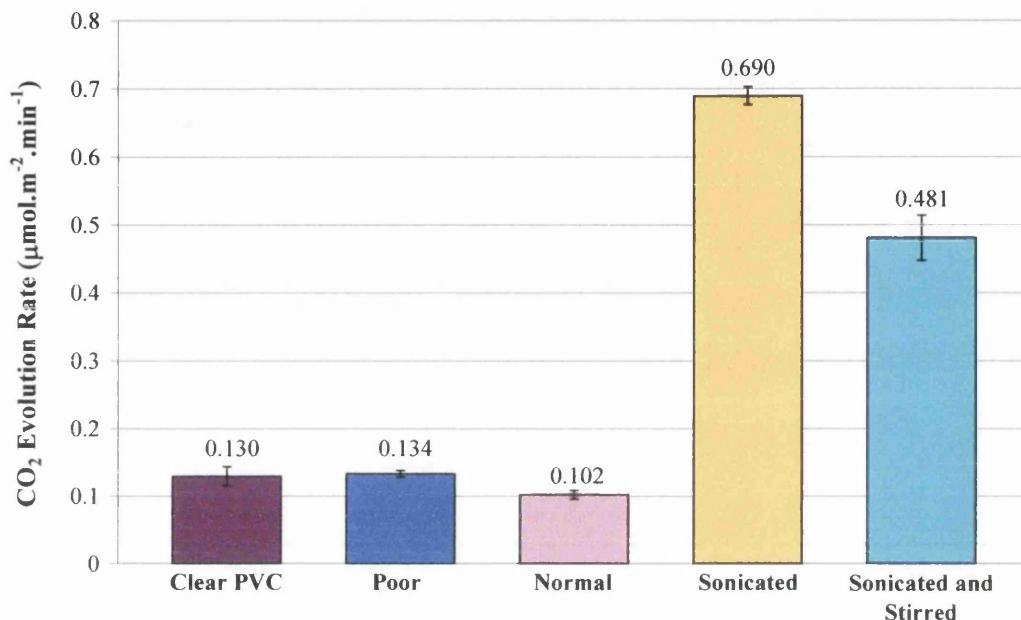


Figure 7.2 - CO₂ Evolution Rates of PVC Coatings Pigmented with Different Dispersions of Kronos 2220 TiO₂

The normal dispersion of Kronos 2220 showed a lower rate of CO₂ evolution than the un-pigmented PVC coating, indicating that the TiO₂ provided a level of shielding to the polymer. It has been discussed previously that the high refractive index of TiO₂ reduces UV penetration into the polymer and thus reduces the occurrence of direct photolysis of the polymer. All TiO₂ grades can be considered to provide a level of UV shielding however the effect on polymer degradation is dependent on pigment photoactivity. For example, although Kronos 1001 provided shielding to the polymer its photoactivity was such that the effect was negated by the increase in degradation as a result of photocatalysis. In the case of the Kronos 2220 the efficiency of the inorganic coating in reducing photoactivity was such that photo-oxidation was reduced to levels below that of the un-pigmented PVC.

The coating containing the poor dispersion of Kronos 2220 TiO₂ exhibited a slightly increased CO₂ evolution rate compared to that of the coating containing the

normal pigment dispersion. This showed that for the same pigment loading agglomeration of the TiO₂ particles causes an increase in coating photo-oxidation. Compared to discrete individual particles at the same pigment loading, large agglomerations of pigment provide a decreased level of shielding to the polymer leaving the coating more susceptible to penetration by ultraviolet (UV) light.

The poor dispersion of Kronos 2220 showed a slight increase in CO₂ evolution compared to the un-pigmented PVC which is likely a result of a combination of factors. Firstly the addition of pigment increases the porosity of a polymer and thus increases the effective surface area susceptible to oxidation, which coupled with the reduction in shielding caused by agglomeration of the TiO₂ particles could increase degradation.

Furthermore, the dispersion of TiO₂ can affect its photoactivity, it has been shown⁶ that large aggregates of TiO₂ show higher photoactivity than small discrete particles of the same pigment. This increase in photoactivity is a result of differences in the distribution of photon absorptions by discrete individual particles and agglomerates. A decrease in the total number of particles (as in agglomeration) causes these particles to absorb more UV and undergo less electron recombination, thus increasing the photoactivity of agglomerated TiO₂ particles.

The reason for reduced incidence of electron and hole combination within a pigment agglomerate compared to discrete particles lies with the semi-conducting nature of TiO₂. It is possible that once excited a TiO₂ particle can transfer its excited electron to an adjacent particle, which would result in the electron and hole being in different particles and thus unable to recombine. If the electron and hole are unable to recombine then it is possible for them to produce highly reactive free radicals which undergo reactions with the polymer resulting in oxidation.

Kronos 2220 is a grade of TiO₂ stabilised against UV with oxides of silicon and aluminium. These inorganic stabilising coatings act as a barrier to ultraviolet (UV) light and also prevent organics directly adsorbing on the TiO₂ active sites reducing the occurrence of photoactivation of the TiO₂ and its catalytic effect on polymer degradation. The effect of stabilisation was illustrated by the low CO₂ evolution rate for the normally dispersed coating as the shielding effect coupled with the efficiency of the coating in reducing photoactivation reduced degradation.

The poorly dispersed Kronos 2220 did not significantly reduce oxidation as the UV stability of the pigment was unable to compensate for the effects of

agglomeration. The effects of increased surface area and decreased shielding of the coating coupled with the increased photoactivity of agglomerated TiO₂ particles were greater than the effects of the pigment in decreasing oxidation and therefore CO₂ evolution rate was higher.

It was anticipated that further improving the pigment dispersion by ultrasonication would further decrease the rate of CO₂ evolution compared to the coating containing the normal dispersion of Kronos 2220 pigment. It can be seen in Figure 7.2 that this was not the case as ultrasonication caused the coating to exhibit a CO₂ evolution rate 6.7 times higher than the normally dispersed pigment. The significant increase in CO₂ evolution indicated that ultrasonication damaged the stabilising coating on the TiO₂ thus increasing its photoactivity.

In order to investigate whether the increase in photoactivity of the pigment was due to permanent coating damage the ultrasonicated coating was stirred for 48 hours before re-casting to allow the pigment to return to a more natural dispersion. The results showed a decrease in CO₂ evolution however the rate was still 4.7 times higher than that of the normally dispersed pigment in PVC. This indicated that although dispersion did have an effect on the rate the increase in photoactivity was predominantly a result of irreversible damage to the stabilising coating.

Ultrasonication generates sound waves in liquids which leads to the formation of small air bubbles in the liquid at the solid/liquid interface⁷ for example, at the TiO₂ particle surface. Under continued high intensity ultrasound these bubbles grow in size and then collapse, a phenomenon known as cavitation. This causes high speed impinging liquid jets, strong hydrodynamic shear-forces and massive localised heating (up to several thousand Kelvin)^{7, 8, 9}, which can result in surface damage and erosion. It is likely cavitation damage to the stabilising coating on the TiO₂ surface has left areas of titania effectively un-stabilised thus increasing pigment photoactivity and its catalytic effect on polymer degradation.

Figure 7.3 shows the CO₂ evolution rates for PVC coatings pigmented with different dispersions of Tronox R-KB-4 pigment. Once again it can be seen that the dispersion of TiO₂ pigment particles had a significant effect on coating photo-oxidation. The coating containing the normal dispersion of pigment showed a CO₂ evolution rate less than half that of the coating containing the poorly dispersed pigment.

A comparison between Figure 7.2 and Figure 7.3 showed Tronox R-KB-4 TiO₂ to be more stable than the Kronos 2220. At normal dispersions the coating pigmented with Tronox R-KB-4 exhibited a CO₂ evolution rate half that of the coating containing Kronos 2220. This indicates that the stabilising coating on the Tronox R-KB-4 was more effective at reducing photoactivation of the titania than that on the Kronos 2220 pigment.

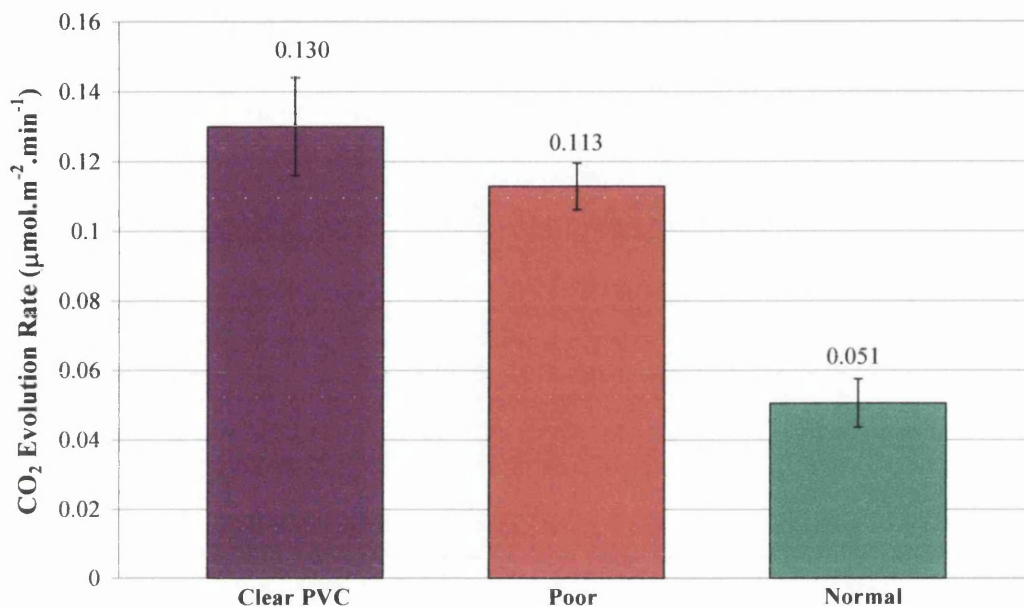


Figure 7.3 - CO₂ Evolution Rates of PVC Coatings Pigmented with Different Dispersions of Tronox R-KB-4 TiO₂

The coatings pigmented with poor dispersions of both Kronos 2220 and Tronox R-KB-4 had fewer discrete TiO₂ particles than the corresponding normal dispersions. This is illustrated in Table 7.1 and Table 7.2 which are shown and will be discussed in more detail in the next section. Despite this it is clear from the reduction in CO₂ evolution rate compared to the un-pigmented PVC that a level of shielding was still supplied by the pigment, reducing the level of direct oxidation of the polymer. The overall reduction in CO₂ evolution rate was more indicative of the efficiency of the stabilising coating than the effects of shielding. Despite the increase in CO₂ evolution rate compared to the un-pigmented PVC the coating containing the poorly dispersed Kronos 2220 was still afforded a level of shielding by the pigment however the effects of its photoactivity were dominant.

The increased efficiency of the coating in reducing photoactivity was further illustrated by the reduction in CO₂ evolution rate for the coating containing poorly

dispersed Tronox R-KB-4 pigment compared to the un-pigmented PVC. Unlike the poor dispersion of Kronos 2220 pigment the coating containing the poor dispersion of Tronox R-KB-4 exhibited a lower rate of CO₂ evolution than the un-pigmented PVC.

The increased intensity of incident UV on the TiO₂ as a result of there being fewer discrete particles compared to a normal dispersion did not cause the same level of photoactivation seen in the Kronos 2220. The resultant increase in photoactivation combined with increased surface area and reduced shielding by the poorly dispersed Kronos 2220 was such that it caused a slight increase in oxidation compared to un-pigmented PVC. This was not the case for the Tronox R-KB-4 as even at poor dispersion it reduced oxidation indicating that the stabilising coating on the Tronox R-KB-4 was more successful in reducing TiO₂ photoactivation than that on the Kronos 2220 TiO₂.

7.3.3 Dispersion Analysis of Coated Samples (SEM)

SEM analysis of the coatings showed there to be a significant difference in the number of discrete TiO₂ particles between the different pigment dispersions. Typical SEM images for the PVC coating pigmented with poor and normal dispersions of Kronos 2220 are shown in Figure 7.4 and Figure 7.5 respectively.

Analysis of the SEM images summarised in Table 7.1 confirmed that there were significantly fewer discrete TiO₂ particles in the coating containing the poor pigment dispersion than in the normal coating. It was seen in Figure 7.4 that although there was the same loading (30 PHR) of TiO₂ much of the pigment had agglomerated into one large aggregate and thus there were far fewer particles visible at the coating surface. This was consistent with the CO₂ evolution results as the decrease in the number of discrete particles increases UV absorbance and thus pigment photoactivation and reduces shielding, resulting in increased photo-oxidation of the PVC.

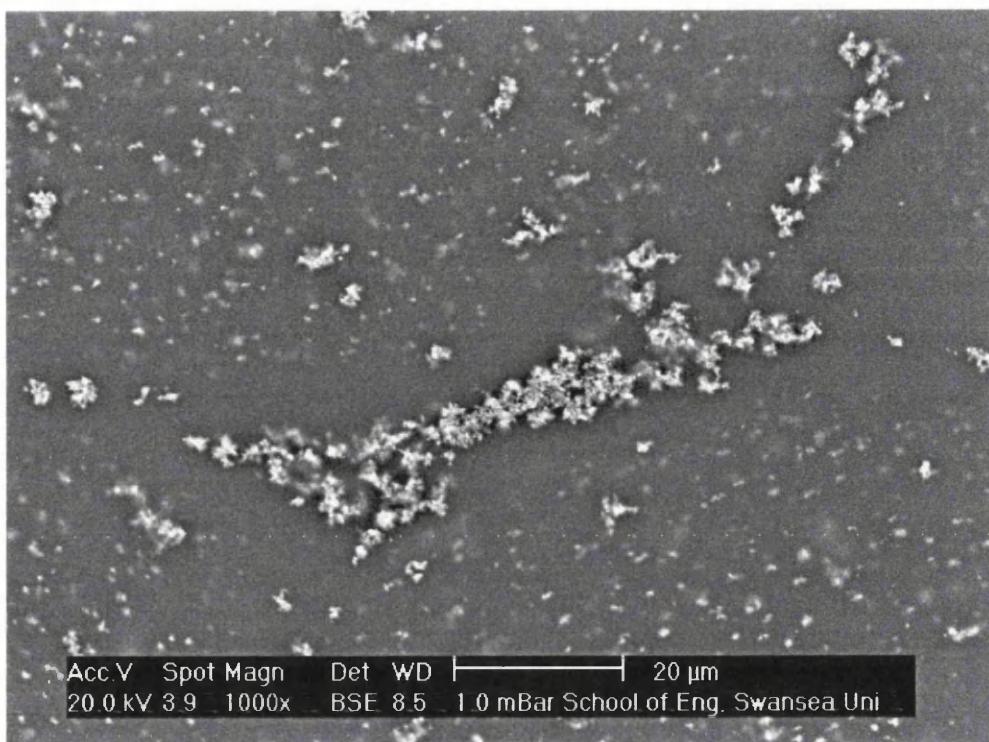


Figure 7.4 - SEM Image of Poor Pigment Dispersion of Kronos 2220 in PVC (1000x)

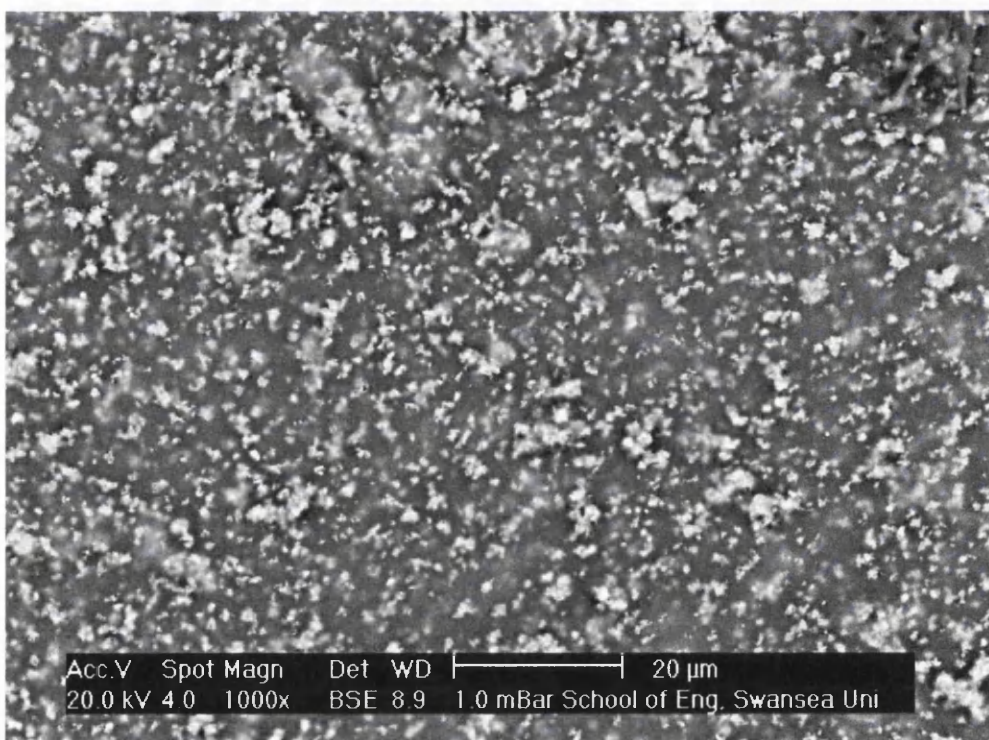


Figure 7.5 - SEM Image of Normal Pigment Dispersion of Kronos 2220 in PVC (1000x)

In order to confirm that ultrasonication did improve the dispersion of pigment and that the significant increase in CO₂ evolution rate was due to stabilising coating

damage SEM analysis was also carried out on these coatings. A typical SEM image for the ultrasonicated coating is shown in Figure 7.6, from this it can be seen that ultrasonication did not impair dispersion. Analysis of the images in Table 7.1 confirmed that ultrasonication did increase the number of particles per mm^2 and the surface area coverage by the TiO_2 .

Figure 7.7 shows the pigment dispersion of the ultrasonicated coating following stirring. It can be seen that stirring following sonication allowed the pigment to return to a more natural dispersion with some aggregation of the TiO_2 particles however was clear from the CO_2 evolution rates in Figure 7.2 that damage to the stabilising coating was permanent. It is likely that the increased CO_2 evolution rate for the ultrasonicated coating compared to the ultrasonicated/stirred coatings was due to instability in the pigment dispersion which could have increased coating porosity and therefore surface area susceptible to oxidation.

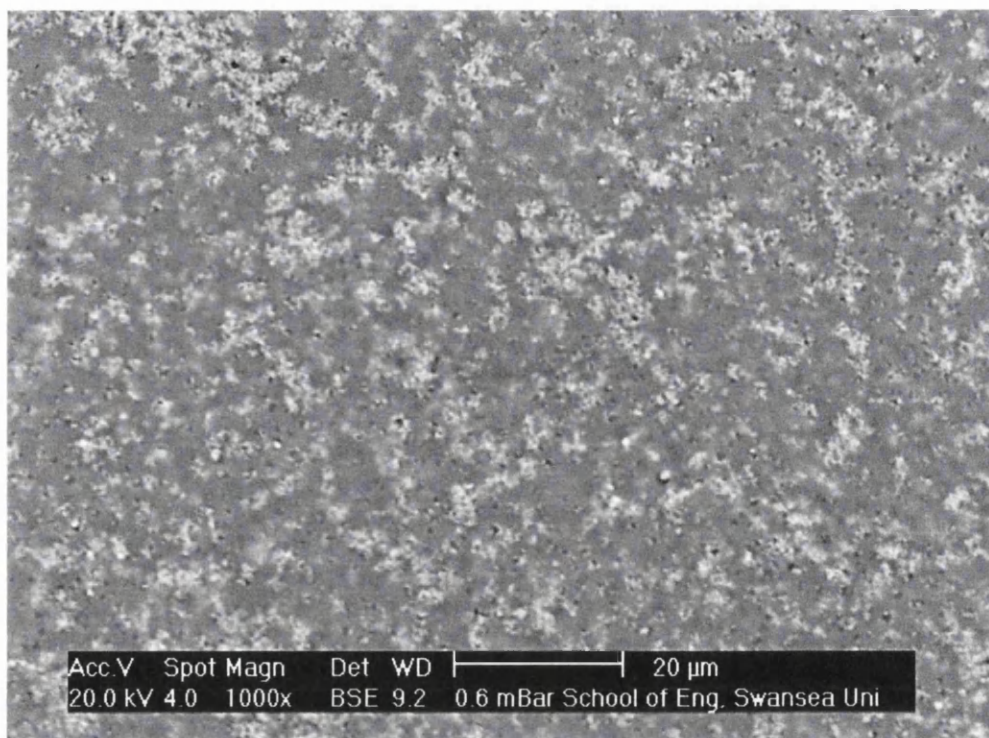


Figure 7.6 - SEM Image of Ultrasonicated PVC Coating Pigmented with Kronos 2220 (1000x)

Even at the maximum magnification of our SEM it is impossible to resolve the coating applied to the TiO_2 . Since the dispersion was not radically affected by ultrasonication it is clear that the increase in photo-oxidation exhibited by this coating was a result of damage to the TiO_2 pigment during ultrasonication. Cavitation damage

to the stabilising coating on the pigment particles during ultrasonication increased the photoactivity of the pigment which resulted in it having a considerable photocatalytic effect on coating oxidation.

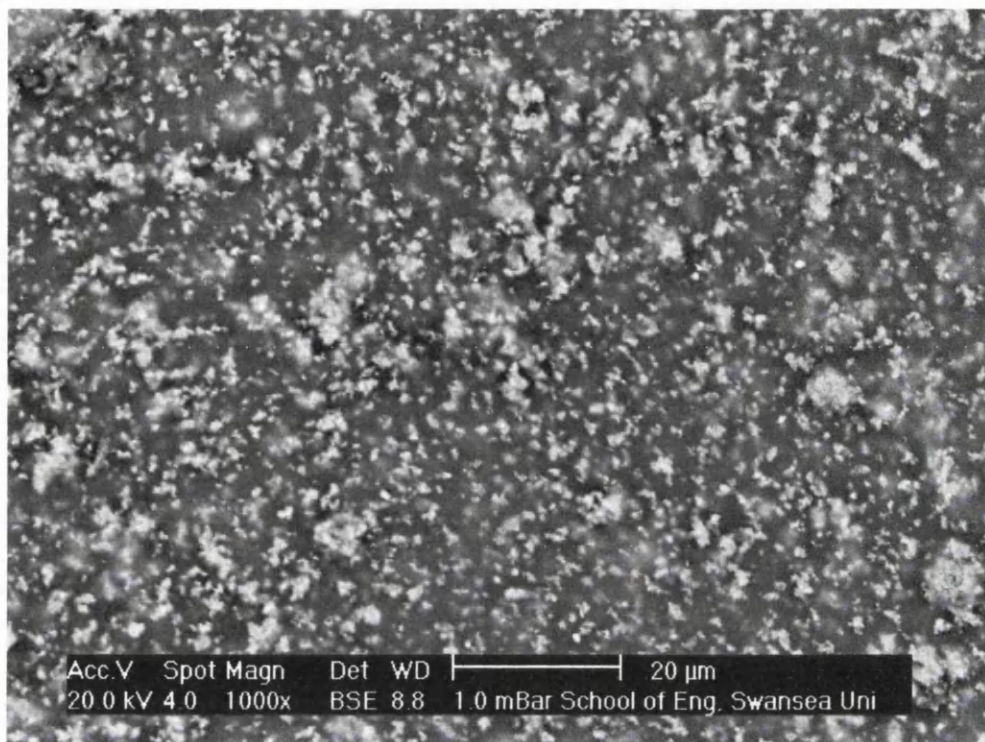


Figure 7.7 - SEM Image of Ultrasonicated PVC Coating Pigmented with Kronos 2220 Following Stirring (1000x)

Table 7.1 also shows significant differences between the surface area covered by the normal and poor dispersions of TiO_2 . The surface area covered by the normally dispersed TiO_2 was 5.3 times higher than that of the poor dispersion of pigment. This indicates that as well as increasing TiO_2 photoactivity pigment agglomerations also provided less shielding to the polymer resin than discrete particles, resulting in an overall increase in photo-oxidation of the coating.

Table 7.1 – Number of Counted Particles and Surface Area Coverage of PVC Coatings Pigmented with Different Dispersions of Kronos 2220 TiO₂

Dispersion	Number of TiO₂ Particles (per mm²)	Surface Area Coverage by TiO₂ (%)	Average Particle Size (μm)
Poor	66098	6.48	4.8
Normal	123738	34.84	2.4
Ultrasonicated	150357	36.73	1.9
Ultrasonicated and Stirred	106094	35.32	2.6

The effects of dispersion on the number and surface area coverage of Tronox R-KB-4 can be seen in Table 7.2. Again there was a significant decrease in the number of particles and coverage by TiO₂ at a poor dispersion, which can be further seen in Figure 7.8 and Figure 7.9 which illustrate dispersion in the poor and normal coatings respectively.

Table 7.2 – Number of Counted Particles and Surface Area Coverage of PVC Coatings Pigmented with Different Dispersions of Tronox R-KB-4 TiO₂

Dispersion	Number of TiO₂ Particles (per mm²)	Surface Area Coverage by TiO₂ (%)	Average Particle Size (μm)
Poor	98516	3.00	3.2
Normal	118781	29.41	1.5

Once again it can be seen that the poorly dispersed pigment formed relatively large agglomerations while the normally dispersed TiO₂ provide a more even coverage to the coating surface. Analysis of the surface coverage showed that the coverage by the normally dispersed pigment was 9.8 times higher than that of the poor dispersion of Tronox R-KB-4. This confirms that the poor dispersion of TiO₂ provided a significantly lower level of shielding to the PVC than the normal dispersion which resulted in an increase in CO₂ evolution rate in comparison.

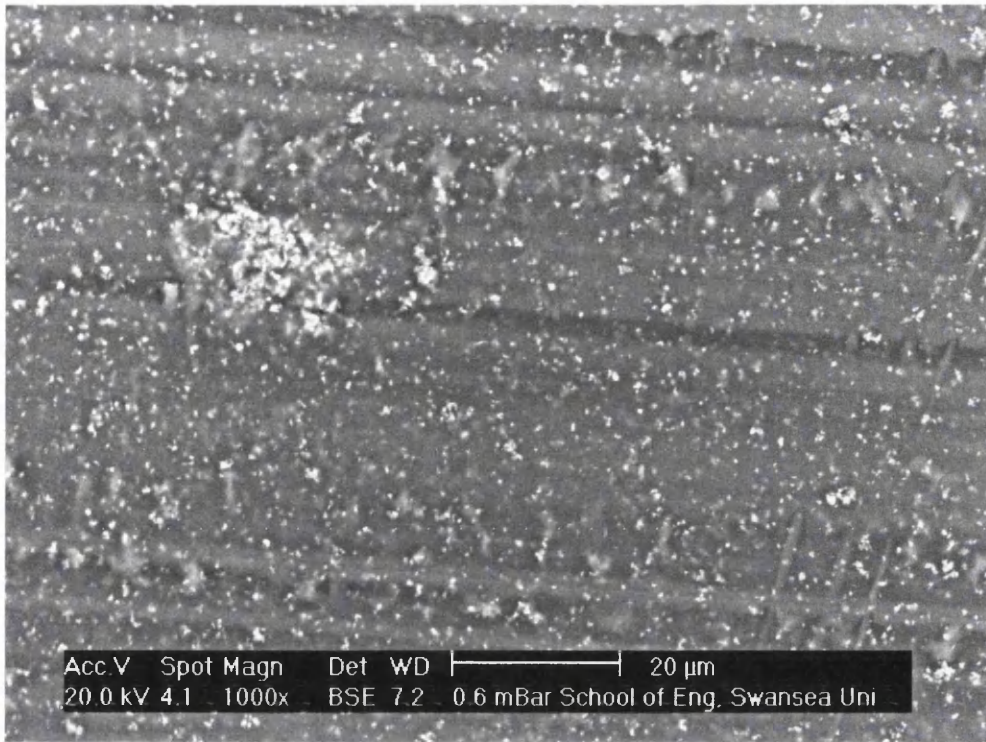


Figure 7.8 - SEM Image of Poor Pigment Dispersion of Tronox R-KB-4 in PVC (1000x)

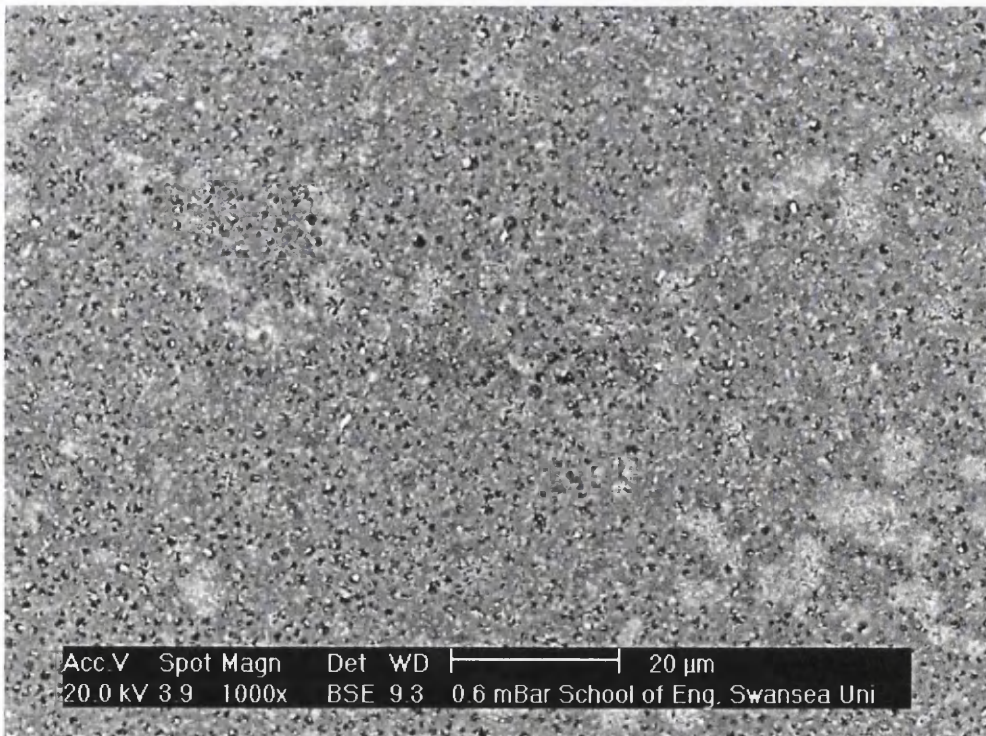


Figure 7.9 - SEM Image of Normal Pigment Dispersion of Tronox R-KB-4 in PVC (1000x)

The coating pigmented with a poor dispersion of Tronox R-KB-4 showed a greater reduction and lower overall surface area coverage than the Kronos 2220 TiO₂. This indicates that the increase in CO₂ evolution shown by the Kronos 2220 pigmented coating compared to the un-pigmented PVC was not a result of reduced shielding but of the increased photoactivity of this pigment within an agglomeration.

The absorbance spectrum for each of the pigmented PVC films is shown in Figure 7.10. It can be seen that the poor dispersions of both Kronos 2220 and Tronox R-KB-4 showed significantly lower absorbance than the respective coatings containing the normal dispersion of TiO₂ pigment. This confirms that agglomeration of pigment particles causes a reduction in polymer shielding by the TiO₂.

The absorbance spectra for both the poor and normal dispersions of Tronox R-KB-4 were significantly higher than the respective Kronos 2220 pigmented coatings, particularly in the UVA region between 315 and 400nm. In Table 7.1 and Table 7.2 it was seen that both the poor and normal dispersions of Tronox R-KB-4 provided less surface area coverage than corresponding Kronos 2220 pigmented coatings. Despite this the CO₂ evolution rate results showed pigmentation with Tronox R-KB-4 to provide better protection against polymer photo-oxidation than the Kronos 2220 pigment. Figure 7.10 shows that the Tronox R-KB-4 TiO₂ provided a far higher degree of shielding against UV wavelength light and therefore photo-oxidation of the PVC than the Kronos 2220 pigment.

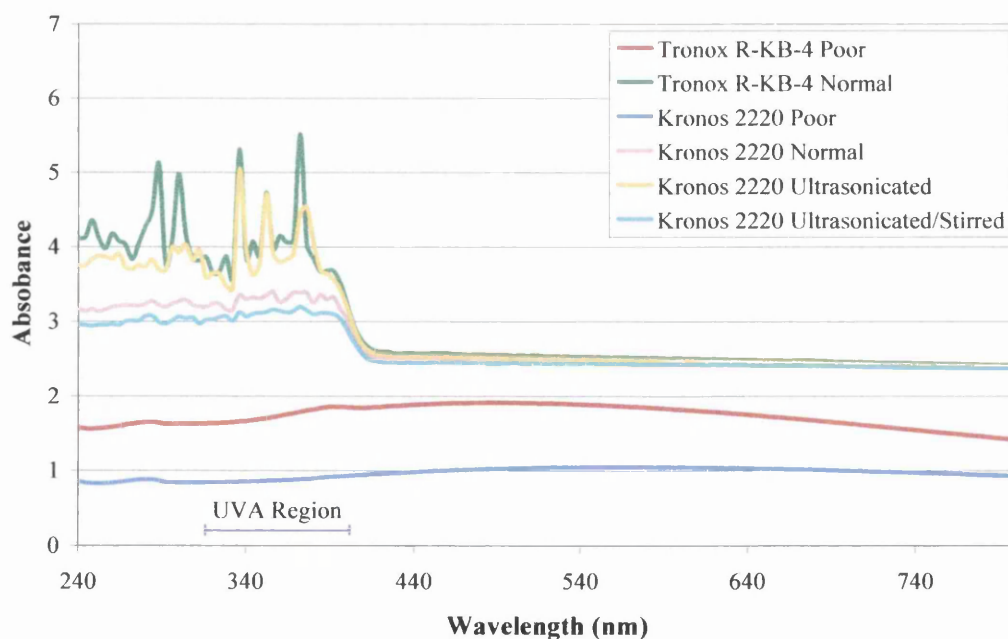


Figure 7.10 – UV/Vis Spectra of Pigmented PVC Coatings

Table 7.1 showed that ultrasonication of the pigmented coating did increase the number of discrete particles and the surface area coverage by these particles. This was further confirmed by the increase in absorbance shown by the coating compared to that containing the normally dispersed pigment. The significant increase in CO₂ evolution rate shown by this coating was due to cavitation damage to the stabilising coating on the titania particles during ultrasonication.

The decrease in the rate of CO₂ evolved by the ultrasonicated coating following stirring was most likely due to the change in absorbance characteristics caused by a difference in dispersion. SEM analysis of the coating following stirring showed a decrease in the number of discrete particles and their surface area coverage compared to the coatings cast immediately following ultrasonication. Figure 7.10 showed the ultrasonicated coating to have a higher absorbance spectrum, particularly in the UV region compared to the same coating following stirring. This increased absorbance resulted in a higher incidence of photoactivation of the de-stabilised pigment and therefore an increase in the rate of photo-oxidation.

7.4 Conclusions

This work has shown that pigment dispersion does affect the kinetics of coating photo-oxidation. The results have shown that for both pigments a poor dispersion of TiO₂ gave a higher rate of CO₂ evolution compared to a better pigment dispersion.

It was clear from the results that the Tronox R-KB-4 was more effective at shielding the polymeric matrix and therefore reduction photo-oxidation than the Kronos 2220 pigment. The reduction in CO₂ evolution rate compared to un-pigmented PVC for the normal dispersion of Tronox R-KB-4 was twice that of Kronos 2220. This was further verified by both the normal and poor dispersions of the Tronox R-KB-4 decreasing the rate of CO₂ evolution rate compared to the un-pigmented PVC, while the Kronos 2220 only effected a reduction at normal dispersion.

The coating containing the poor dispersion of Kronos 2220 TiO₂ exhibited a slight increase in CO₂ evolution rate compared to that of the coating containing the normal pigment dispersion. This showed that for the same pigment loading agglomeration of the TiO₂ particles causes an increase in coating photo-oxidation. Compared to discrete individual particles at the same pigment loading, large

agglomerations of pigment provide a decreased level of shielding to the polymer leaving the coating more susceptible to penetration by ultraviolet (UV) light.

The coating containing a poor dispersion of Tronox R-KB-4 did not show an increase in CO₂ evolution compared to the un-pigmented PVC. Like the Kronos 2220, the coating containing the poor dispersion of Tronox R-KB-4 pigment showed a reduction in shielding and increase in CO₂ evolution compared to the coating containing the normal pigment dispersion. It is clear from the results that the Tronox R-KB-4 was more effective at scattering the incident UV light and that the stabilising coating was more effective at reducing photoactivation than that on the Kronos 2220.

The increase in CO₂ evolution rate in the ultrasonicated coatings was a result of cavitation damage to the stabilising coating, which reduced pigment photostability. The decrease in CO₂ evolution for the coating following stirring was a result of a decrease in UV absorbance compared to that cast directly following ultrasonication was a result of different dispersion characteristics. Despite the reduction in CO₂ evolution rate, the high rate of CO₂ evolution compared to the coatings which had not been subjected to ultrasonication showed that the cavitation damage to the stabilising coating was irreversible.

It has been shown that optimising pigment dispersion reduces photoactivity however it should be ensured that stabilising coating is not damaged in the process, which can result in a significant increase in photoactivity. Further work should be carried out to investigate whether similar effects occur during multiple milling, which is often employed for difficult pigment combinations in coloured systems and could have a seriously damaging effect on durability.

7.5 References

1. Kronos International Inc, *Kronos Titanium Dioxide in Plastics*. 1993: Leverkusen, Germany.
2. Kronos Worldwide Inc, *Application Fields for Kronos TiO₂ Grades (Plastics)*. (Cited 28th February 2008). Available from: <http://www.kronostio2.com/>.
3. Kronos International Inc, *More than 30 Years of Reliability in PVC Profile Protection - Kronos 2220 and Kronos 2222 TiO₂*. 2002: Leverkusen, Germany.
4. Gesenhues, U., *Polymer Degradation and Stability*, 2000. **68**(2): p. 185-196.
5. Boxall, J. and Von Frauhhofer, J.A., *Concise Paint Technology*. 1977, Elek Science: London.
6. Egerton, T.A. and Tooley, I.R., *Journal of Physical Chemistry B*, 2004. **108**(16): p. 5066-5072.

7. Birkin, P.R., Eweka, E., and Owen, J.R., *Journal of Power Sources*, 1999. **81-82**: p. 833-837.
8. Suslick, K.S., Didenko, Y., Fang, M.M., Hyeon, T., Kolbeck, K.J., Mc Namara, W.B.I., Mdleleni, M.M., and Wong, M., *Philosophical Transactions of the Royal Society A*, 1999. **357**: p. 335-353.
9. Kim, K.Y., Byun, K.-T., and Kwak, H.-Y., *Chemical Engineering Journal*, 2007. **132**(1-3): p. 125-135.

Chapter 8

Conclusions and Future Work

This work has shown that measurement of evolved carbon dioxide (CO₂) provides a rapid means of evaluating coating photo-oxidation, allowing prediction of durability in significantly shorter times than QUV A or xenon arc. As a result of differences in the nature of irradiation and analysis between the testing methods slight discrepancies in the durability rankings were observed. Measurement of evolved CO₂ does, however give a measurement of the total degradation occurring within a coating as compared to changes in surface properties illustrated by changes in gloss retention.

Increased cross-linking within the polymeric matrix reduces oxygen permeation and ultraviolet (UV) penetration through the coating causing a reduction in oxidation and thus CO₂ evolution below the surface. In these circumstances incident UV is reflected back to the surface, as a result oxidation is concentrated in this region leading to a greater degree of degradation and therefore loss of gloss at the surface. This does not necessarily prove that the coating is unstable since increased cross-linking improves stability within the bulk polymeric matrix, however from an aesthetic point of view poor gloss retention is undesirable. It would be beneficial in future studies to analyse photo-oxidation as a function of depth into the coating using the FTIR microscope in order to investigate whether lower CO₂ evolution rates correspond to decreasing total degradation.

It was possible via measurement of evolved CO₂ to identify the occurrence of photocatalysis by photoactive titanium dioxide (TiO₂) pigment grades and to clearly distinguish between coatings of high and low stability. Discrepancies between the durability rankings occurred only between photostable TiO₂ pigments with similar photoactivity grades. The CO₂ evolution measurement apparatus would be a valuable addition to the current suite of durability tests. The primary strength of this accelerated test method is that it provides a very rapid means of screening coating durability in a much shorter time than QUV A or xenon arc. Since slight discrepancies between CO₂ evolution rate and gloss retention were observed in the more stable coatings it should not be used as a replacement for long-term commercial testing. It is advisable to use CO₂ measurement to identify the most suitable coatings for further development and testing using commercial methods.

Commercial weathering showed all coatings pigmented with Tronox R-KB-4 to have a higher stability across the range of tests than those pigmented with Kronos 2220, Kronos 2300 and Kronos 1001. Each of the grade A and B TiO₂ pigments showed good photostability and reduced coating degradation compared to Kronos

1001. Addition of the photoactive Kronos 1001 TiO₂ grade resulted in significant photocatalysis of coating degradation and produced a coating with poor durability.

Despite its classification as a grade A photostable pigment Kronos 2220 showed poor durability compared to the Tronox R-KB-4 due to the fact that Kronos 2220 is designed specifically for use in PVC. The surfactant coating applied to the pigment was incompatible with the polyurethane and polyester-melamine resins. This resulted in an unstable dispersion of the pigment near the coating surface which increased degradation and therefore gloss loss. Further investigations should be carried out on different TiO₂ grades in polyurethanes in order to characterise the effects of pigment coatings on dispersion within the resin and therefore overall durability.

Changes to the polymer resin in an attempt to improve coating durability did not provide the consistent improvements anticipated. In both polyurethane and polyester-melamine coatings changing the polyester polyol caused a general decrease in surface durability resulting in a higher photoactivity ranking. The polyurethane based on the HDI/IPDI polyisocyanate was the most durable resin and combination of this with Tronox R-KB-4 produced the most durable coating of all tested. This coating retained the highest percentage of initial gloss following xenon arc weathering and also had the lowest CO₂ evolution rate of all coatings tested in the flat panel irradiation apparatus. It is recommended from this work that polyurethane coatings developed for external high durability applications should be based on the HDI/IPDI based polyurethane pigmented with Tronox R-KB-4.

It was found that in all cases the addition of single secondary coloured pigments affected coating photo-oxidation. The organic pigments stabilised the coating against oxidation and the effects of acid catalysis in comparison with the standard white coating. This suggested attack on the organic pigments themselves, which ultimately could cause colour change to the coating. In the majority of cases the addition of inorganic secondary pigments resulted in an increase in photo-oxidation, these pigments also caused a general increase in the acid catalysis ratio.

This was most likely due to the organic pigment itself being attacked and thus reducing degradation of the PVC coating whilst the inorganic pigments were not attacked and thus oxidation was focussed on the polymer. Further work should be carried out into this using colour measurement. It is anticipated that increased attack on the pigment would cause a greater change in colour of the coating. This would also

be advantageous to investigate whether the increased colour stability of inorganic pigment compared to organics is detrimental to the protection it provides to the polymer. Once again, the technique of FTIR spectroscopy combined with techniques for surface porosity measurement such as impedance spectroscopy could be used to evaluate the influence of coating pigmentation and additives such as matting agents.

It was clear that ternary and quaternary pigment additions accelerate photo-oxidation. This could be due to charge percolation by the carbon black however this should be investigated further by changing single components of the pigmentation blend. The addition of matting agent also appeared to have an accelerative effect of coating photo-oxidation however its differing effect on different colours should be investigated further. Further investigations into the activity of different coloured pigments should be carried out, particularly with regard to ternary and quaternary additions. A combination of FTIR and UV/Vis spectroscopy could be used to investigate the effect of coloured pigmentation on the absorbance characteristics of the coating and consequently, photo-oxidation.

This work has highlighted the level of caution needed when formulating paints with numerous components. Even small changes to the resin, matting agent or changing pigments can significantly affect the coating and these effects should be studied in more detail in the future.

The decrease in CO₂ evolution for the coating following stirring was a result of a decrease in UV absorbance compared to that cast directly following ultrasonication was a result of different dispersion characteristics. Compared to discrete individual particles at the same pigment loading, large agglomerations of pigment provide a decreased level of shielding to the polymer leaving the coating more susceptible to penetration by UV light. It has been shown that optimising pigment dispersion reduces coating photo-oxidation however care should be taken to ensure that the stabilising coating is not damaged. The high rate of CO₂ evolution compared to the coatings which had not been subjected to ultrasonication showed that the cavitation damage to the stabilising coating was irreversible. Further work should be carried out to investigate whether similar effects occur during multiple milling.

Addition of polyamide beads resulted in a significant increase in photo-oxidation. It is likely that the majority of photo-oxidation occurring within the textured coatings was due to increased oxygen permeation at the interface between the coating and the beads. Despite differences in basic resin stability the textured coatings

exhibited similar durability. The increased CO₂ evolution rates given by the HDI/IPDI coating containing the polyamide bead additions indicated that the HDI/IPDI based polyurethane had a greater reaction with the resin than the HDI polyurethane.

It should be noted that this testing regime was focused on model coatings and did not investigate the effects of commercial additives such as UV stabilisers. Further investigations should be carried out on fully formulated coatings in order to assess whether the HDI/IPDI based polyisocyanate could provide a significant improvement to the durability of polyurethane coated products.